

*Supercritical fluid extraction and analysis
of indigenous medicinal plants for uterotonic activity*

by

VIKASH SEWRAM

Submitted in partial fulfillment of the requirements
for the degree of

DOCTOR OF PHILOSOPHY

in the

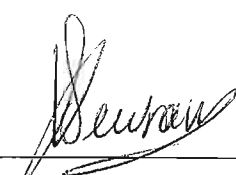
Department of Chemistry and Applied Chemistry,
University of Natal, Durban, South Africa

1997


Preface


The experimental work described in this thesis was carried out in the Department of Chemistry & Applied Chemistry and the Department of Physiology, University of Natal, Durban, under the supervision of Professor M.W. Raynor (Applied Chemistry), Professor D.A. Mulholland (Chemistry) and Doctor D.M. Raidoo (Physiology).

These studies represent original work by the author and have not been submitted in any form to another university. Where use was made of the work of others, it has been duly acknowledged in the text.

SIGNED: 
Vikash Sewram

We hereby certify that the above statement is correct.

SIGNED: 
Professor M.W. Raynor

SIGNED: 
Professor D.A. Mulholland

SIGNED: 
Doctor D.M. Raidoo

Department of Chemistry and Applied Chemistry
University of Natal
Durban

Acknowledgements

I would like to express my sincere thanks and appreciation to the following for their contribution to this thesis:

- Professor M.W. Raynor, Professor D.A. Mulholland, and Doctor D.M. Raidoo, for their expert guidance and constant encouragement throughout the course of this project.
- Doctor B.S. Martincigh for allowing the use of the preparative HPLC instrument.
- Mr S. Peterson and Mrs S. Naidoo for their assistance in the Applied Chemistry department.
- Mr D. Jagjivan for obtaining NMR spectra of all the isolated compounds.
- Mr B. Parel for his assistance in the organic research laboratory whenever required.
- Mr R. Naicker and Mr K Perumal of the Department of Physiology who assisted with the biological assays and in the construction of the organ baths for on-line bioassays.
- Mr M. Wagner of the Analytical unit, Department of Physiology, for allowing the use of the GC-MS and HPLC instruments.
- Doctor P. Boshoff of the Cape Technikon for his assistance in obtaining mass spectra and high resolution mass measurements of the isolated compounds.
- Mrs J. Govender and Mr R. Suchipersad for the administrative aspects related to this work.
- All my colleagues in the Department of Physiology and Department of Chemistry and Applied Chemistry especially Mr N. Naidoo and Miss K. Kowlaser who made my working environment a pleasant and cheerful one.
- The FRD and University of Natal for providing financial assistance for these studies.
- My parents Mr and Mrs S. Girdhari for their love and support throughout my years of study.

Abstract

Ingestion of extracts prepared from various medicinal plants to induce or augment labour is common amongst Black South African women during the late stages of pregnancy. This applies particularly to the rural areas where modern health care facilities are often lacking. Many of these plants have not been investigated scientifically and one needs to substantiate claims of quality, safety and efficacy. Furthermore, it is believed that the consumption of these plant extracts can result in foetal meconium staining at delivery.

An investigation into the uterotonic properties of three plants viz. *Ekebergia capensis* Sparrm. *Clivia miniata* (Lindl.) Regel. and *Grewia occidentalis* L. were carried out using guinea pig uterine smooth muscle *in vitro*. Supercritical fluid extraction was performed with water modified supercritical carbon dioxide to extract the uterotonic components. An attempt was also made to couple supercritical fluid extraction directly on-line to the bioassay so that on line screening of crude plant extracts could be performed within short periods of time. The effects of supercritical CO₂ decompression on temperature and pH of the muscle bathing solution were considered since these factors affect muscle contractility. The direct effects of excess CO₂ on intracellular mechanisms were eliminated by constructing a CO₂ reduction interface together with passage of carbogen which aided in the rapid displacement of excess CO₂. As samples of these extracts were found to induce muscle contraction, supercritical fluid fractionation (SFF) was performed by sequentially increasing the fluid density. Extracted fractions were obtained by sequentially increasing the pressure at constant temperature and modifier concentration in an attempt to identify the active fractions. Extractions were performed at 200 atm, 300 atm and 400 atm respectively. Subsequent testing of these fractions enabled the detection of active and inactive fractions as well as a fraction that had a spasmolytic effect on uterine muscle. The 400 atm extracts of *E. capensis* and *C. miniata* displayed maximum activity while only the 300 atm extract of *G. occidentalis* induced uterine muscle contraction. Subsequent analysis of the sequentially extracted fractions, by high

performance liquid chromatography and micellar electrokinetic capillary chromatography revealed that certain compounds present in the fractions that stimulated muscle contraction, were sensitive to the extraction pressure hence making it possible to determine the compounds that were likely to be active. Column chromatography followed by various spectroscopic techniques were performed in an attempt to isolate and elucidate the structures of the compounds that were present in the plant extracts. The extract of *Ekebergia capensis* yielded five known compounds (β -sitosterol, oleanonic acid, 3-epioleanolic acid, 2,3,22,23-tetrahydroxy-2,6,10,15,19,23-hexamethyl-6,10,14,18-tetracosatetrene and 7-hydroxy-6-methoxy coumarin. The extract of *Clivia miniata* yielded linoleic acid and 5-hydroxymethyl-2-furancarboxaldehyde while the extract of *Grewia occidentalis* yielded 3-(4-hydroxy-3-methoxyphenyl)-2-propenal, a novel compound 2,2',6,6'-tetramethoxy-4'-al-4-(ω -oxo-*E*-propenyl)-biphenyl and oleanonic acid. The pure compounds were further evaluated pharmacologically to identify the active components and assess the physiological mode of action by the use of various receptor blockers. Oleanonic acid, 3-epioleanolic acid, linoleic acid and 5-hydroxymethyl-2-furancarboxaldehyde and 3-(4-hydroxy-3-methoxyphenyl)-2-propenal were found to induce an agonistic muscle response. All these compounds were observed to mediate their effects through the cholinergic receptors. The results obtained in this study supports the claim of these plants possessing uterotonic properties.

Publications and Conference Presentations

Selected results from this thesis have been published in scientific journals and presented at various conferences.

1. D.A. Mulholland, S. Iourine, V. Sewram, M.W. Raynor, D. Raidoo, Novel compounds from South African *Ekebergia* species, *Planta Med.*, **62** (1996), 125.
2. V. Sewram, M. W. Raynor, D.A. Mulholland, D.M. Raidoo, Coupling SFE to uterotonic bioassay: The on-line approach to analyzing medicinal plants, *J. Pharm Biomed. Anal.*, in press.
3. V. Sewram, M.W. Raynor, D.A. Mulholland, D.M. Raidoo, On-line SFE-bioassay of uterotonic active fractions from Indigenous Medicinal Plants. (Oral presentation), 2nd International Symposium on Natural Drugs, Maratea, Italy, 28 September - 1 October 1997.
4. V. Sewram, D.M. Raidoo, M.W. Raynor, D.A. Mulholland, Interfacing SFE with uterotonic bioassay: A novel approach to drug discovery. (Oral Presentation), 25th Annual Congress of the Physiological Society of Southern Africa and 2nd International Congress of the African Association of Physiological Sciences, International Convention Centre, Durban, 21 - 24 September 1997.
5. V. Sewram, M.W. Raynor, D.A. Mulholland, D.M. Raidoo, Coupling SFE to uterotonic bioassay: The on-line approach to analyzing medicinal plants. (Oral presentation), 6th Frank Warren National Organic Chemistry Conference, Mtunzini, KwaZulu-Natal, 29 June - 1 July 1997.

6. V. Sewram, M.W. Raynor, D.M. Raidoo, D.A. Mulholland, "On-line SFE-bioassay with MECC of uterotonic active fractions from Medicinal Plants." (Poster presentation), 19th International Symposium on Capillary Chromatography and Electrophoresis, Wintergreen, Virginia, USA, 18 - 22 May 1997.
7. V.Sewram, M.W. Raynor, D.A. Mulholland, D. Raidoo, "Off-line Supercritical fluid Extraction (SFE) - Micellar Electrokinetic Capillary Chromatography (MECC) of Utero-tonic Compounds from an Indigenous Medicinal Plant, *Ekebergia capensis* Sparrm. (Poster presentation), 18th International Symposium on Capillary Chromatography, Riva del Garda, Italy, May 1996.
8. V.Sewram, M.W. Raynor, D.A. Mulholland, D. Raidoo, "Off-line Supercritical fluid Extraction (SFE) - Bioassay - Micellar Electrokinetic Capillary Chromatography (MECC) of Utero-tonic Compounds from *Ekebergia capensis* Sparrm. (Poster presentation), Chromatography and Mass Spectrometry conference, Vaal Spa, Christiana, 25 - 29 August 1996 (**PRIZE FOR BEST POSTER ON METHOD DEVELOPMENT IN SEPARATION SCIENCE**)
8. V.Sewram, M.W. Raynor, D.A. Mulholland, D. Raidoo, "Supercritical fluid extraction and analysis of an Indigenous medicinal plant, *Ekebergia capensis* Sparrm. for Utero-tonic activity. (Poster presentation), International Symposium on Supercritical Fluid Chromatography and Extraction, Indianapolis Indiana, USA, March 1996.
9. V. Sewram, M.W. Raynor, D.A. Mulholland, D. Raidoo, "Supercritical fluid Extraction and Analysis of utero-tonic compounds from *Ekebergia Capensis* Sparrm. (Poster presentation), Conference proceedings, 33rd Annual Convention of the South African Chemical Institute, University of Cape Town, Cape Town, January 1996.

10. V. Sewram, M.W. Raynor, D.A. Mulholland, D.M. Raidoo, Supercritical fluid extraction and analysis of indigenous medicinal plants for tocolytic activity. (Oral presentation), Research Colloquium, Department of Physiology, Faculty of Medicine, December 1995.

11. V. Sewram, M.W. Raynor, D.A. Mulholland, D.M. Raidoo, Supercritical Fluid Extraction and analysis of indigenous medicinal plants for tocolytic activity. (Oral presentation) Conference proceedings, 2nd Annual Symposium of the Centre for Indigenous Plant Use Research (CIPUR), University of Natal, November 1995.

Awards received

Recipient of the 1995 Analytica Award from the Analytical Division of the South African Chemical Institute for past and present research involving Analytical techniques.

Award for best poster on Method Development in Separation Science exhibited at the Chromatography and Mass Spectrometry conference in Vaal Spa, Christiana, August 1996.

Recipient of the 1997 Sasol Postgraduate Medal

Table of contents

	Page
Preface	ii
Acknowledgements	iii
Abstract	iv
Publications and conference presentations	vi
List of Figures	xvii
List of Tables	xxvi
List of Schemes	xxvii
List of Abbreviations and Units	xxvii
1 Introduction and Aims	1
References	4
2 Theory of Supercritical Fluid Extraction (SFE)	5
2.1 Definition of a supercritical fluid	5
2.2 Physical properties of supercritical fluids	6
2.3 Advantages of SFE	7
2.4 Selection of a supercritical fluid	8
2.5 Unique properties of SF-CO ₂	12
2.6 Generalized method and instrumentation requirements for SFE	13
2.7 Selection of SFE conditions	16
2.8 Use of modifiers in SFE	17
2.8.1 Methods of adding modifiers	18
2.9 Modes of SFE	23
2.10 Kinetics of SFE	24
2.11 Physical matrix effects	26

2.12	Impact of matrix on extraction kinetics	26
2.13	Class-selective SFE	30
	References	31
3	Application of SFE to natural products: A literature review	34
3.1	Introduction	34
3.2	Alkaloids	36
3.3	Steroids	42
3.4	Flavour and Fragrance Compounds	44
3.5	Carotenoids	48
3.6	Lipid materials	50
3.7	Miscellaneous applications	51
	References	53
4	Separation techniques	58
4.1	Introduction	58
4.2	Theory of Chromatography	58
	4.2.1 Column Efficiency	61
	4.2.2 Selectivity	62
	4.2.3 Resolution	62
	4.2.4 The van Deemter equation in Chromatography	63
4.3	Theory of electrophoretic separation	65
	4.3.1 Background electrolyte	66
	4.3.2 Instrumentation	67
	4.3.3 Electrophoresis	68
	4.3.4 Electroosmosis and the electrical double layer	69
	4.3.5 Efficiency	71
	4.3.6 Flow Profile	71
	4.3.7 Modes of capillary electrophoresis.	73
	4.3.7.1 Micellar Electrokinetic Capillary Chromatography	73

	4.3.7.2 Principles of separation in MECC	73
	4.3.7.3 Theory of MECC	75
	References	76
5	Experimental	78
	5.1 Introduction	78
	5.2 Plant material	78
	5.3 Preparation of crude aqueous extracts	78
	5.4 Off-line supercritical fluid extraction of plant components.	79
	5.4.1 Pump	79
	5.4.2 Plumbing	81
	5.4.3 Extraction vessels	81
	5.4.4 Extraction parameters	82
	5.5 Uterotonic bioassay	83
	5.6 On-line SFE-Bioassay.	85
	5.7 Muscle bath construction.	89
	5.7.1 Muscle bath A	89
	5.7.2 Muscle bath B	90
	5.8 Tapered restrictor fabrication.	91
	5.9 pH measurements of Tyrodes solution.	92
	5.10 Isolation and structural elucidation of plant components	92
	5.10.1 Column Chromatography	92
	5.10.2 Thin layer chromatography	92
	5.11 Spectroscopic techniques	93
	5.11.1 ^1H and ^{13}C NMR spectroscopy	93
	5.11.2 Infrared Spectroscopy	93
	5.11.3 High Resolution Mass Spectrometry	93
	5.11.4 Acetylation of compound 4	94
	5.12 Chromatographic and electrophoretic analysis of the plant extracts	94
	5.12.1 HPLC analysis.	94

5.12.2	Capillary electrophoresis	95
5.12.2.1	Buffer preparation	97
5.12.2.2	Sample preparation and injection	97
5.12.3	Supercritical fluid chromatography	99
5.13	Column packing	101
5.14	Preparation of porous ceramic frits	103
5.15	GC-MS Analysis of <i>Clivia miniata</i> L.	103
5.16	Esterification of fatty acid mixture	104
5.17	Identification of active components and assessment of mode of action	104
5.18	Extractives from <i>Ekebergia capensis</i>	105
5.18.1	Physical data of compound 1	105
5.18.2	Physical data of compound 2	105
5.18.3	Physical data of compound 3	106
5.18.4	Physical data of compound 4	107
5.18.5	Physical data of compound 5	108
5.19	Extractives from <i>Clivia miniata</i>	108
5.19.1	Physical data of compound 6	108
5.19.2	Physical data of compound 7	108
5.20	Extractives from <i>Grewia occidentalis</i>	109
5.20.1	Physical data of compound 8	109
5.20.2	Physical data of compound 9	110
5.20.3	Physical data of compound 10	110
	References	111
6	SFE optimization by application of dynamic extraction model for the extraction of plant components	112
6.1	Introduction	112
6.2	The Extraction Model	113
6.3	Selection of extraction temperature	114
6.4	Selection of extraction pressure	115

6.5	Selection of dynamic extraction time	116
6.6	Supercritical fluid extraction of <i>Ekebergia capensis</i>	116
6.7	Supercritical fluid extraction of <i>Grewia occidentalis</i>	119
6.8	Supercritical fluid extraction of <i>Clivia miniata</i>	121
6.9	Conclusion	123
	References	124
7	The role of bioassays in medicinal plant analysis and a preliminary investigation of the plant extracts for uterotonic activity	126
7.1	Introduction	126
7.2	Selection of bioassays	127
7.3	The uterotonic bioassay	127
7.4	Theory of smooth muscle contraction	129
7.5	The effect of acetylcholine (ACh) on smooth muscle	132
7.6	Analysis of extracts of <i>Ekebergia capensis</i> Sparrm.	134
	7.6.1 Aqueous extract	134
	7.6.2 SFE extracts	136
	7.6.3 Supercritical fluid fractionation of <i>Ekebergia</i> extracts	138
7.7	Analysis of extracts of <i>Clivia miniata</i> (Lindl.) Regel	142
	7.7.1 Aqueous extract	142
	7.7.2 SFE extract	143
7.8	Analysis of <i>Grewia occidentalis</i> L.	144
	7.8.1 Aqueous extract	144
	7.8.2 SFE extract	145
7.9	Conclusion	145
	References	146

8	Coupling SFE to uterotonic bioassay: An on-line approach to analysing Medicinal Plants	148
8.1	Introduction	148
8.2	Results and Discussion	150
8.2.1	Temperature effects	150
8.2.2	pH effects	152
8.2.3	Evaluation of Extracts	157
8.2.3.1	Analysis of <i>Ekebergia capensis</i>	157
8.2.3.2	Analysis of <i>Grewia occidentalis</i>	160
8.2.3.3	Analysis of <i>Clivia miniata</i>	162
8.3	Conclusions	164
	References	164
9	Extractives from <i>Ekebergia capensis</i> Sparrm.	166
9.1	The Genus <i>Ekebergia</i>	166
9.2	Structure elucidation of compounds isolated	173
9.2.1	Compound 1	173
9.2.2	Compound 2	175
9.2.3	Compound 3	177
9.2.4	Compound 4	179
9.2.5	Compound 5	182
	References	186
10	Extractives from <i>Clivia miniata</i> (Lindl.) Regel.	188
10.1	The genus <i>Clivia</i>	188
10.2	Structural elucidation of compounds isolated from <i>Clivia miniata</i>	191
10.2.1	Compound 6	191
10.2.2	Compound 7	195
	References	197

11.	Extractives from <i>Grewia occidentalis</i>	198
11.1	The genus <i>Grewia</i>	198
11.2	Structural elucidation of compounds isolated from <i>Grewia occidentalis</i>	200
11.2.1	Compound 8	200
11.2.2	Compound 9	203
11.2.3	Compound 10	206
	References	206
12	<i>In vitro</i> screens and functional assays of isolated compounds	207
12.1	Introduction	207
12.2	Receptors and biological response	207
12.3	The role of chemical bonding	209
12.4	Analysis of compounds from <i>Ekebergia capensis</i>	211
12.4.1	Compound 2	211
12.4.2	Compound 3	212
12.5	Analysis of compounds from <i>Clivia miniata</i>	214
12.5.1	Compound 6	214
12.5.2	Compound 7	216
12.6	Analysis of compounds form <i>Grewia occidentalis</i>	217
12.6.1	Compound 8	217
12.7	Assessment of mode of action through receptor binding assays	218
12.7.1	Compound 3 from <i>Ekebergia capensis</i>	218
12.7.2	Compound 7 from <i>Clivia miniata</i>	220
12.7.3	Compound 8 from <i>Grewia occidentalis</i>	221
12.8	Conclusion	222
	References	222

13	Chromatographic and electrophoretic analysis of the plant extracts	223
13.1	Introduction	223
13.2	Reverse-phase HPLC	223
13.2.1	Analysis of extracts from <i>Ekebergia capensis</i>	223
13.2.2	Analysis of extracts from <i>Clivia miniata</i>	228
13.2.3	Analysis of extracts from <i>Grewia occidentalis</i>	231
13.3	Capillary electrophoresis	235
13.3.1	Analysis of extracts from <i>Ekebergia capensis</i>	236
13.3.1.1	Buffer selection	236
13.3.1.2	Optimization of surfactant concentration	236
13.3.1.3	pH optimization	240
13.3.1.4	Variation of applied voltage	243
13.3.1.5	Separation of components under optimised conditions	243
13.3.2	Analysis of extracts from <i>Clivia miniata</i>	248
13.3.3	Analysis of extracts from <i>Grewia occidentalis</i>	251
13.4	Packed capillary column SFC	255
13.4.1	SFC with CO ₂	255
13.4.2	SFC with hydrofluorocarbon	258
13.5	Conclusion	258
	References	259
14	Overview and concluding remarks	261
	APPENDIX 1	263
	APPENDIX 2	265

List of Figures

		Page
Figure 2.1	Pressure/temperature phase diagram of a substance.	5
Figure 2.2	Effect of temperature and pressure on the Hildebrand solubility parameter for supercritical CO ₂ . (14)	9
Figure 2.3	Effect of pressure changes on density of supercritical CO ₂ at different temperatures.	12
Figure 2.4	Schematic diagram of an SFE setup for off-line recovery of analytes.	14
Figure 2.5	Typical extraction cells used in analytical SFE.	15
Figure 2.6	Schematic diagram of modifier delivery system for SFE.	19
Figure 2.7	Schematic diagram of device used to modify supercritical CO ₂ (22). Arrows indicate direction of flow. Components: A = four port valve; B = "Parker" or "Swagelok" brand "tee" tubing fitting (1/16 × 1/16 × 1/4 inch stainless steel); C = 1/4 inch normal pipe thread × 1/4 inch tubing stub fitting welded into D; D = modifier chamber; E = 1/16 inch o.d. stainless steel tubing; F = heating coil; G = extraction cell; H = heater; I = restrictor; J = collection vial.	21
Figure 2.8	Relationship between the critical temperature, pressure and mole fraction of CO ₂ -methanol mixtures according to Saito and Nitta. (23)	22
Figure 2.9	Generalised extraction curve of percent solute extracted as a function of volume of extraction fluid or time of extraction.	24
Figure 2.10	Mass transport steps for the SFE of an analyte from a porous matrix particle.	27
Figure 2.11	Plot of $\ln (m/m_0)$ against extraction time for the supercritical fluid extraction of camphor from rosemary.	29
Figure 3.1	Capillary GC/FID pattern of <i>Senecio inaequidens</i> pyrrolizidine alkaloid fraction extracted by off-line SFE. (16) 1, senecivernine; 2, senecionine; 3, seneciphylline; 4, integerrimine; 5, retrorsine; 6, usaramine; 7, desacetyl doronine; 8, doronine.	38

Figure 3.2	Capillary GC/FID pattern of <i>Senecio cordatus</i> pyrrolizidine alkaloid fraction extracted by off-line SFE. (16) 1, seneciverine; 2, senecionine; 3, seneciphylline; 4, spartiodine; 5, integerrimine; 6, jacobine; 7, jacozone.	38
Figure 3.3	Influence of water on the extraction curves of thebaine at constant mass flow-rate (12). SFE was performed at 20 MPa and 40.5 °C using CO ₂ :methanol: water mixtures of the following w:w:w compositions: ◊ 50:32:18; ▲ 50:36:14; ■ 50:40:10; ◆ 50:44:6; ● 50:46:4; □ 50:49:1; ○ 50:49.5:0.5; △ 50:50:0	39
Figure 3.4	The dependence of extraction yield on CO ₂ consumption at 50 °C. (18)	40
Figure 3.5	Comparison of chromatograms generated by (A) SFE-GC-FID analysis of rosemary and by (C) Standard on-column injection of a methylene chloride extract. Chromatogram (B) shows the result of a second SFE-GC-FID analysis of the same sample. (35)	45
Figure 4.1	A chromatogram with its characteristic features.	60
Figure 4.2	van Deemter plot Change in H versus linear mobile phase velocity u . $H_{\min} = A + (2BC)^{1/2}$; $u_{\text{opt}} = (B/C)^{1/2}$	64
Figure 4.3	Basic Scheme of a CE instrument C = separation capillary; E = electrolyte reservoirs with platinum electrodes S = sample vial D = detector R = signal recorder	67
Figure 4.4	Double layer structure at a silica wall.	70
Figure 4.5	Velocity profiles of liquid flowing in a capillary under the action of (a) electroosmosis and (b) hydrostatic pressure.	72
Figure 4.6	Schematic representation of the separation principle of MECC.	74
Figure 4.7	Schematic representation of the zone separation in MECC.	75

Figure 5.1	Photograph of the home assembled SFE system.	79
Figure 5.2	Schematic diagram of a syringe pump	80
Figure 5.3	A diagram of a commercially available stainless steel extraction vessel with fingertight end caps. (1)	82
Figure 5.4	Schematic diagram of the uterotonic bioassay setup used to monitor muscle activity.	84
Figure 5.5	Schematic diagram of the on-line SFE-bioassay setup.	86
Figure 5.6	Plumbing schematic of the multiport valve used for switching between static and dynamic modes of extraction.	87
Figure 5.7	Polypropylene muscle bath designed for horizontal flow of CO ₂ with direct introduction into the muscle bath.	89
Figure 5.8	Polypropylene muscle bath designed for vertical flow of CO ₂ with direct introduction into a CO ₂ reduction interface.	90
Figure 5.9	Schematic steps showing the preparation of a tapered capillary restrictor. (1) a micro-Bunsen burner is used for localized heating of the capillary. (2) tension is applied and the capillary pulled to a hair like taper. (3) polyimide resin is applied to the taper which is subsequently positioned with a capillary sleeve. (4) the resin cures and glues the taper to part of the inner wall of the sleeve.	91
Figure 5.10	Interior of the Capillary Cartridge. (3)	96
Figure 5.11	Assembly for sample injection in the microliter scale.	98
Figure 5.12	Schematic diagram of injection valve for SFC.	99
Figure 5.13	Schematic diagram of butt-connection of column to restrictor	100
Figure 5.14	Schematic diagram of the supercritical fluid CO ₂ packing system. (4)	102
Figure 6.1	Generalized solubility isotherm as a function of pressure at constant temperature.(9)	115
Figure 6.2	Extraction curve of mass extracted from <i>Ekeberia capensis</i> Sparrm. as a function of extraction time (min).	118
Figure 6.3	Plot of $\ln (m/m_0)$ against extraction time (min) for the supercritical fluid extraction of <i>Ekebegia capensis</i> Sparrm.	118

Figure 6.4	Extraction curve of mass extracted from <i>Grewia occidentalis</i> L. as a function of extraction time (min).	120
Figure 6.5	Plot of $\ln (m/m_0)$ against extraction time (min) for the supercritical fluid extraction of <i>Grewia occidentalis</i> L.	120
Figure 6.6	Extraction curve of mass extracted from <i>Clivia miniata</i> L. as a function of extraction time (min).	122
Figure 6.7	Plot of $\ln (m/m_0)$ against extraction time (min) for the supercritical fluid extraction of <i>Clivia miniata</i> L.	123
Figure 7.1	The pharmacokinetic influences on a biologically active agent.	128
Figure 7.2	Diagram of the mechanism of activation of smooth muscle contraction by Ca^{2+} .	131
Figure 7.3	Biosynthesis of Acetylcholine.	132
Figure 7.4	Electrical recording of Guinea Pig uterine smooth muscle contraction induced by 1 μg <i>O</i> -Acetylcholine hydrochloride (ACh).	133
Figure 7.5	Electrical recording of non pregnant guinea pig uterine smooth muscle contraction induced by (a) 588 μg of the aqueous extract of milled wood of <i>Ekebergia capensis</i> and (b) 700 μg of the aqueous extract after administration of mepyramine. w = muscle wash	135
Figure 7.6	Electrical recording of contractions induced by the SFE extract of <i>Ekebergia capensis</i> .on a non-pregnant uterus.	137
Figure 7.7	Electrical recording of contractions induced by the SFE extract of <i>Ekerbergia capensis</i> .on a pregnant uterus.	138
Figure 7.8	Electrical recording of non pregnant guinea pig uterine smooth muscle contraction induced by the sequentially fractionated extract of <i>Ekebergia capensis</i> at 400 atm.	139
Figure 7.9	Electrical recording of non pregnant guinea pig uterine smooth muscle contraction induced by the sequentially fractionated extract of <i>Ekebergia capensis</i> at 350 atm.	140

Figure 7.10	Electrical recording of non pregnant guinea pig uterine smooth muscle contraction induced by the sequentially fractionated extract of <i>Ekebergia capensis</i> at 300 atm.	141
Figure 7.11	Electrical recording of pregnant guinea pig uterine smooth muscle contraction induced by the aqueous extract of <i>Clivia miniata</i> (Lindl.) Regel.	142
Figure 7.12	Electrical recording of pregnant guinea pig uterine smooth muscle contraction induced by the SFE extract of <i>Clivia miniata</i> (Lindl.) Regel.	143
Figure 7.13	Electrical recording of pregnant guinea pig uterine smooth muscle contraction induced by the aqueous extract of <i>Grewia occidentalis</i> L.	144
Figure 7.14	Electrical recording of pregnant guinea pig uterine smooth muscle contraction induced by the SFE extract of <i>Grewia occidentalis</i> L.	145
Figure 8.1	The effect of CO ₂ decompression on temperature of Tyrodes solution. CO ₂ was decompressed from an internal pressure of 400 atm through a 25 μm i.d. tapered restrictor (■) and a linear restrictor (◆)	151
Figure 8.2	The effect of CO ₂ decompression on pH of modified (0.2 mM Na ₂ HPO ₄ , 0.2mM NaH ₂ PO ₄) and original Tyrodes solution (0.4 mM NaH ₂ PO ₄). CO ₂ was decompressed from an internal pressure of 400 atm through a 25 μm i.d. tapered restrictor; CO ₂ flow was measured at 150 atm after decompression and found to be 18 ml/min.	153
Figure 8.3	The direct effect of CO ₂ on muscle contractility. Muscle activity was inhibited following a blank extraction with CO ₂ at 400 atm and 80°C.	154
Figure 8.4	The effect of SFE extract of <i>E. capensis</i> on Guinea Pig uterine smooth muscle. a) total 400 atm extract, b) sequentially fractionated extract obtained at 200 atm, c)300 atm and d) 400 atm demonstrating that the 400 atm extract was most potent.	159

↑ point at which contents of the extract collection chamber was transferred to the muscle bath; **W** = muscle wash with Tyrodes solution.



Figure 8.5	The effect of SFE extract of <i>G. occidentalis</i> on Guinea Pig uterine smooth muscle. a) total 400 atm extract, b) sequentially fractionated extract obtained at 200 atm, c) 300 atm and d) 400 atm demonstrating that the 300 atm extract was most potent.  point at which contents of the extract collection chamber was transferred to the muscle bath; W = muscle wash with Tyrodes solution.	161
Figure 8.6	The effect of SFE extract of <i>C. miniata</i> on Guinea Pig uterine smooth muscle. a) total 400 atm extract, b) sequential extract at 200 atm, c) 300 atm d) 400 atm demonstrating that the 400 atm extract was most potent.  point at which contents of the extract collection chamber was transferred to the muscle bath; W = muscle wash with Tyrodes solution.	163
Figure 10.1	GC-MS total ion chromatogram of esterified fatty acid mixture showing linoleic acid methyl ester as the major component.	192
Figure 10.2	EI mass spectrum for linoleic acid methyl ester with the matching spectrum from the Wiley library confirming the identity of linoleic acid.	193
Figure 12.1	Illustration of the different conformations of drug molecules and their ability to bind to the receptor surface (7).	208
Figure 12.2	Illustration of various drug-receptor bonds.	210
Figure 12.3	Electrical recording of contractions induced by compound 2 of <i>Ekebergia capensis</i> on a non-pregnant uterus.	211
Figure 12.4	Electrical recording of contractions induced by compound 3 of <i>Ekebergia capensis</i> on a non-pregnant uterus.	212
Figure 12.5	Electrical recording of pregnant guinea pig uterine smooth muscle contraction induced by compound 6 of <i>Clivia miniata</i> (Lindl.) Regel.	215

Figure 12.6	Electrical recording of pregnant guinea pig uterine smooth muscle contraction induced by compound 7 of <i>Clivia miniata</i> (Lindl.) Regel.	216
Figure 12.7	Electrical recording of pregnant guinea pig uterine smooth muscle contraction induced by compound 8 of <i>Grewia occidentalis</i> L.	217
Figure 12.8	Receptor binding assays of compound 3 from <i>E. capensis</i> .	219
Figure 12.9	Receptor binding assays of compound 7 from <i>C. miniata</i> .	220
Figure 12.10	Receptor binding assays of compound 8 from <i>G. occidentalis</i> .	221
Figure 13.1	Reverse-phase HPLC chromatogram of total SFE extract of <i>E. capensis</i> wood obtained at 400 atm and 80 °C. Conditions: Bondclone-10 C18 reverse phase column; gradient elution (methanol/water); column temperature 40 °C; UV detection at 280 nm.	225
Figure 13.2	Reverse-phase HPLC chromatogram of sequentially extracted SFE fractions of <i>E. capensis</i> wood. Conditions: Bondclone-10 C18 reverse phase column; gradient elution (methanol/water); column temperature 40 °C; UV detection at 280 nm.	226
Figure 13.3	Reverse-phase HPLC chromatogram of first batch of SFE extract of <i>E. capensis</i> wood showing the variation of chemical composition with seasonal changes. Conditions: Bondclone-10 C18 reverse phase column; gradient elution (methanol/water); column temperature 40 °C; UV detection at 280 nm.	227
Figure 13.4	Reverse-phase HPLC chromatogram of total SFE extract of <i>C. miniata</i> root obtained at 400 atm and 80 °C. Conditions: Bondclone-10 C18 reverse phase column; gradient elution (methanol/water); column temperature 40 °C; UV detection at 280 nm.	228
Figure 13.5	Reverse-phase HPLC chromatogram of sequentially extracted SFE fractions of <i>C. miniata</i> root. Conditions: Bondclone-10 C18 reverse phase column; gradient elution (methanol/water); column temperature 40 °C; UV detection at 280 nm.	229

- Figure 13.6 Reverse-phase HPLC chromatogram of total 400 atm SFE extracts of *C. minata* root showing the variation of chemical composition with seasonal changes. (A) second batch of plant material obtained during spring
(B) first batch of plant material obtained during autumn
Conditions: Bondclone-10 C18 reverse phase column; gradient elution (methanol/water); column temperature 40 °C; UV detection at 280 nm. 230
- Figure 13.7 Reverse-phase HPLC chromatogram of total SFE extract of *G. occidentalis* wood obtained at 400 atm and 80 °C.
Conditions: Bondclone-10 C18 reverse phase column; gradient elution (methanol/water); column temperature 40 °C; UV detection at 254 nm. 232
- Figure 13.8 Reverse-phase HPLC chromatogram of sequentially extracted SFE fractions of *G. occidentalis* root.
Conditions: Bondclone-10 C18 reverse phase column; gradient elution (methanol/water); column temperature 40 °C; UV detection at 254 nm. 233
- Figure 13.9 Reverse-phase HPLC chromatogram of total 400 atm SFE extracts of *G. occidentalis* wood showing the variation of chemical composition with seasonal changes.
(A) second batch of plant material obtained during spring
(B) first batch of plant material obtained during autumn
Conditions: Bondclone-10 C18 reverse phase column; gradient elution (methanol/water); column temperature 40 °C; UV detection at 254 nm. 234
- Figure 13.10 Electropherogram of total 400 atm extract of *E. capensis* wood obtained with 20 mM $\text{Na}_2\text{B}_4\text{O}_7 \cdot 10\text{H}_2\text{O}$ and (A) 30 mM SDS and (B) 60 mM SDS, pressure injection for 1 sec, UV detection at 280 nm. 237
- Figure 13.11 Variation of migration time as a function of sodium cholate concentration. (▲ oleanonic acid, ◆ scopoletin, ■ 3-epioleanolic acid) 238
- Figure 13.12 Structure of Bile salts 239

- Figure 13.13 Variation of migration time of the *Ekebergia* components as a function of buffer pH. Run buffer: 20 mM Na₂B₄O₇·10H₂O with 120 mM sodium cholate. (▲ oleanonic acid, ◆ scopoletin, ■ 3-epioleanolic acid) 241
- Figure 13.14 Electropherogram of total 400 atm extract of *E. capensis* wood obtained at pH 9.70. 242
- Figure 13.15 Variation of migration time of *Ekebergia* components as a function of applied voltage. 245
- Figure 13.16 Electropherogram of total 400 atm extract of *E. capensis* wood obtained under optimised pH conditions 246
Conditions: 20 mM Na₂B₄O₇·10H₂O with 120 mM sodium cholate at pH 9.70, pressure injection for 1 sec, UV detection at 280 nm.
- Figure 13.17 Electropherograms of sequentially extracted fractions of *E. capensis* wood obtained under optimised pH conditions 247
Conditions: 20 mM Na₂B₄O₇·10H₂O with 120 mM sodium cholate at pH 9.70, pressure injection for 1 sec, UV detection at 280 nm.
- Figure 13.18 Electropherograms of sequentially extracted fractions of *C. miniata* root. 249
Conditions: 30 mM Na₂HPO₄, 30 mM NaH₂PO₄, 120 mM sodium cholate, pH 6.95, applied voltage of 20 kV, pressure injection for 1 sec, UV detection at 280 nm.
- Figure 13.19 Electropherograms of (A) SFE and (B) aqueous extracts of *C. miniata* root showing the presence of 5-hydroxymethyl-2-furancarboxaldehyde in both extracts. 250
Conditions: 30 mM Na₂HPO₄, 30 mM NaH₂PO₄, 120 mM sodium cholate, pH 6.95, applied voltage of 20 kV, pressure injection for 1 sec, UV detection at 280 nm.
- Figure 13.20 Variation of migration time as a function of pH for the components of *G. occidentalis* obtained at 400 atm. (■ oleanonic acid, ◆ coniferaldehyde, ▲ 2,2',6,6'-tetramethoxy-4'-al-4-(ω-oxo-*E*-propenyl)-biphenyl) 251

Figure 13.21	Electropherogram of total 400 atm extract of <i>G. occidentalis</i> wood obtained under optimised conditions Conditions: 20 mM Na ₂ B ₄ O ₇ ·10H ₂ O with 100 mM sodium cholate at pH 9.80, pressure injection for 1 sec, UV detection at 254 nm.	252
Figure 13.22	Electropherograms of sequentially extracted fractions of <i>G. occidentalis</i> wood. Conditions: 30 mM Na ₂ HPO ₄ , 30 mM NaH ₂ PO ₄ , 120 mM sodium cholate, pH 6.95, applied voltage of 20 kV, pressure injection for 1 sec, UV detection at 280 nm.	254
Figure 13.23	Packed capillary SFC of 5 mg/ml naphthalene standard Conditions: 300 atm, 50 °C, 30 cm × 100 µm i.d. column packed with ODS2, UV detection at 254 nm	256
Figure 13.24	Possible interaction of chlorosilanes and carbonyl compounds with residual silanols. (42)	257
Figure 13.25	Formation of “bifurcated” hydrogen bond.	257

List of Tables

Table 1.1	Selected examples of important bioactive substances from natural sources.	3
Table 2.1	Comparison of physical properties of gases, liquids and supercritical fluids.	6
Table 2.2	Critical conditions of common SFE solvents.	11
Table 2.3	Examples of commonly-used modifiers in SFE applications.	18
Table 4.1	Commonly used buffers in CE	66
Table 5.1	Gradient elution programme employed to separate the plant components.	95
Table 6.1	Data used to obtain m_o for <i>Ekebergia capensis</i> Sparrm.	117
Table 6.2	Data used to obtain kinetic plot for the extraction of <i>Ekebergia capensis</i> Sparrm.	117
Table 6.3	Data used to obtain m_o for <i>Grewia occidentalis</i> L.	119
Table 6.4	Data used to obtain kinetic plot for the extraction of <i>Grewia occidentalis</i> L.	119
Table 6.5	Data used to obtain m_o for <i>Clivia miniata</i> L.	121
Table 6.6	Data used to obtain kinetic plot for the extraction of <i>Clivia miniata</i> L.	122

List of Schemes

Scheme 9.1	Oxidation of side chain.	166
Scheme 9.2	Furan ring formation.	167
Scheme 9.3	Biosynthesis of scopoletin.	185

List of Abbreviations and Units

ACh	acetylcholine
ADP	adenosine diphosphate
α	alpha
atm	atmospheres
ATP	adenosine triphosphate
ATPase	adenosine triphosphatase
β	beta
bs	broad singlet
CE	capillary electrophoresis
CGE	capillary gel electrophoresis
CIEF	capillary isoelectric focusing
CITP	capillary isotachophoresis
CMC	critical micelle concentration
CO ₂	carbon dioxide
COSY	correlated spectroscopy
CZE	capillary zone electrophoresis
δ	chemical shift
d	doublet
dd	double doublet

DEPT	distortionless enhancement by polarization transfer
DMSO	dimethyl sulphoxide
EOF	electroosmotic flow
FID	flame ionization detector
FTIR	fourier transform infrared
FTNMR	fourier transform nuclear magnetic resonance
GC	gas chromatography
GC-MS	gas chromatography-mass spectrometry
HEPES	N-2-hydroxyethylpiperazine-N'-2-ethanesulphonic acid
HETCOR	heteronuclear chemical shift correlation
HPLC	high performance liquid chromatography
Hz	Hertz
i.d.	internal diameter
KBr	potassium bromide
LC/MS	liquid chromatography/mass spectrometry
m	multiplet
MECC	micellar electrokinetic capillary chromatography
MES	2-(N-morpholino)ethane sulphonic acid
MLC	myosin light chain
MLCK	myosin light chain kinase
MPa	megapascal
MS	mass spectrometry
<i>m/z</i>	mass to charge ratio
NOE	nuclear overhauser effect
o.d.	outer diameter
ODS	Octadecylsilyl

P_c	critical pressure
%	percent
PAHs	polyaromatic hydrocarbons
PCBs	polychlorinated biphenyls
PEEK	polyetheretherketone
PIPES	piperazine-N,N'-bis(2-ethane)sulphonic acid
PTFE	polytetrafluoroethylene
s	singlet
SC-CO ₂	supercritical carbon dioxide
SDS	sodium dodecyl sulphate
SF	supercritical fluid
SFC	supercritical fluid chromatography
SFE	supercritical fluid extraction
SFF	supercritical fluid fractionation
T_c	critical temperature
TLC	thin layer chromatography
Tricine	N-[tris(hydroxymethyl)-methyl]glycine
Tris	tris(hydroxymethyl-aminomethane)
UV	ultraviolet
viz.	namely
°C	degree celcius
cm	centimeter
cm ⁻¹	wavenumber
kV	kilovolt
min	minute
mg	milligram

ml	millilitre
ml/min	millilitre per minute
ng	nanogram
µg	microgram
µl	microlitre
µm	micrometer

CHAPTER 1

Introduction and Aims

Despite the dramatic advances made in orthodox medicine over the past 100 years, there has been an increasing interest in complimentary systems (1). About 80 % of the world's population relies on traditional medicines, and governments of Third-World countries, unable to sustain a complete coverage of modern drugs, have encouraged the rational development of traditional treatments. Furthermore, the services and advice of indigenous practitioners are valued because they are offered in terms that patients can understand and in the context of cultural values and practices that are shared by both patients and healers alike.

The plant kingdom constitutes an abundant source of new chemical products which may be important due to their biological properties and in particular because of their potential use in medicine (2). Many plants produce secondary metabolites which have extensive drug effects. Table 1.1 outlines a few examples of important constituents produced by plants. This outline also shows some of the important constituents besides drugs, such as the essential oils which are used for foods etc.

Traditional medicine used during pregnancy currently still plays an integral part in the lives of most black South African women. This applies particularly to the rural areas where modern health care facilities are often lacking. Fertility is a dominant theme as it ensures the preservation and propagation of the tribe. Children are regarded as an insurance against loneliness and poverty in old age and, as a result, a sterile woman is treated with contempt and pity (4, 5). Pregnancy is an event of great importance and many traditions and taboos are upheld to ensure a successful confinement and the birth of a healthy child. Traditional medicine recognises the value of antenatal medication and, as a result, the ingestion of plant extracts during pregnancy is common and as many as fifty seven

different plants are used (6). Different concoctions known as 'isishilambezo' are consumed by women as antenatal remedies or, more specifically, to induce or augment labour. Many of these plants have not been investigated scientifically and one needs to substantiate claims of quality, safety and efficacy. Hence, investigation of components contained in these medicinal preparations is important as the utilization of the whole plant or other crude preparations for therapeutic purposes can have several drawbacks. These include:

1. Variation in the concentration of the active constituents with topography, season, as well as with climatic and ecological conditions.
2. Co-occurrence of undesirable compounds causing antagonistic, synergistic, or other undesirable, and possibly unpredictable, modulations of the bioactivity.
3. Losses of bioactivity due to variability in collection, storage, and preparation of the raw material.

Furthermore, it is believed that the consumption of these concoctions can result in foetal meconium staining at delivery. Meconium is a heterogenous substance found in foetal intestine and contains a number of pigments. Passage of meconium into the amniotic fluid followed by aspiration into the foetus can result in foetal distress. A study undertaken by Mĩtri *et al.* (7) has revealed a high incidence of foetal meconium passage in babies whose mothers had a history of consuming isishilambezo mixtures. Hence identification and isolation of these biologically active compounds is necessary since pure compounds can be administered in reproducible, accurate doses, with obvious benefits from an experimental or therapeutic point of view. Secondly, it permits the structural determination of bioactive compounds that may enable the production of synthetic material, incorporation of structural modifications, and a rationalization of mechanisms of action. This, in turn, will enable investigations of structure/activity relationships, facilitating the developments of new compounds with similar or more desirable bioactivities. Hence this study is aimed at making an important contribution to the welfare of black South Africans.

Table 1.1 Selected examples of important bioactive substances from natural sources (3).

Biochemical class	Botanical source	Biological activity
1. Glycoside		
*Anthraquinones	<i>Rhamnus purshiana</i>	Cathartic
Barbaloin	<i>Aloe barbadensis</i>	Cathartic
2. Steroids		
Diosgenin	<i>Dioscorea spp.</i>	**Oral contraceptives, corticosteroids
Digitoxin	<i>Digitalis spp.</i>	Cardenolides
3. Alkaloids		
Atropine	<i>Atropa belladonna</i>	Parasympatholytics
Colchicine	<i>Colchicum autumnale</i>	Antigout
Vincristine	<i>Catharanthus roseus</i>	Anticancer
Morphine	<i>Papaver somniferum</i>	Analgesic
Quinine	<i>Cinchona spp.</i>	Antimalarial
Reserpine	<i>Rauwolfia serpentina</i>	Hypotensive
Artemisinin	<i>Artemisia annua</i>	Antimalarial
4. Limonoid		
Azadirachtin	<i>Azadirachta indica</i>	Antifeedant pesticide

* Active as the glycoside

** After chemical modification

This project is a multidisciplinary approach to the analysis of medicinal plants consumed during pregnancy in an attempt to validate the physiological properties these plants are said to manifest as well as document any toxic effects. The preparation of plant extracts for scientific analysis is currently usually still performed by classical liquid solvent extractions in a Soxhlet apparatus. Unfortunately, liquid solvent extractions often require several hours or even days to perform, result in dilute extracts (which must be concentrated for trace analysis), and may not result in quantitative recovery of target

analytes. Furthermore, concerns regarding the hazardous nature of many commonly used solvents together with the cost and environmental dangers of waste solvent disposal has given support to the development of alternative sample extraction methods. The limitations of conventional methods have fueled interest in the development of supercritical fluid extraction (SFE) as an alternative to extractions using liquid solvents.

The aims and objectives of this work were to investigate the possibility of using supercritical carbon dioxide to extract the uterotonic components from three selected plants and to isolate and elucidate the structures of the biologically active compounds by various chromatographic and spectroscopic techniques. An attempt was also made to couple SFE directly on-line to a bioassay using guinea pig uterine smooth muscle *in vitro* so that on line screening of crude plant extracts could be performed within short periods of time. Further, a pharmacological evaluation of the isolated compounds was undertaken. The thesis ends with an overview of this investigation and the main conclusions which have been drawn from this study.

References

1. W.C. Evans, *Trease & Evan's Pharmacognosy*, 13th Ed., Alden Press, Oxford, UK (1989), p.617.
2. G.B. Marini-Bettolo, M. Nicoletti, M. Patamia, C. Galeffi and I. Messana, *J. Chromatogr.*, **213** (1981) 113.
3. A. Der Marderosian and L.E. Liberti, *Natural products medicine*, G. F. Stickley Co., Philadelphia, USA (1988), p.17.
4. M. Brindley, *S. A. Journal of Ethnology*, **8** (1985), 98.
5. M.V. Gumedi, *SAMJ*, **53** (1978), 823.
6. D.J.H. Veale, K.I. Furman and D.W. Oliver, *J. Ethnopharm.*, **36** (1992) 185.
7. F. Mitri, G.J. Hofmeyer and C.J. Van Gelderen, *SAMJ*, **71** (1987), 431.

CHAPTER 2

Theory of Supercritical Fluid Extraction (SFE)

The solubility of solids in supercritical fluids was first discovered by Hannay and Hogarth in 1879 (1). Since then, the application of supercritical fluid extraction as an alternative to distillation and conventional solvent extraction has been considered by a number of industries including the food, polymer, petroleum and pharmaceutical industries (2-5). This technique offers the analyst an alternative for preparing samples prior to analysis that is rapid and environmentally less hazardous. This chapter describes the basic principles involved in applying the technique to sample preparation.

2.1 Definition of a supercritical fluid

In order to define a supercritical fluid (SF), one needs to consider the phase diagram illustrated in Figure 2.1.

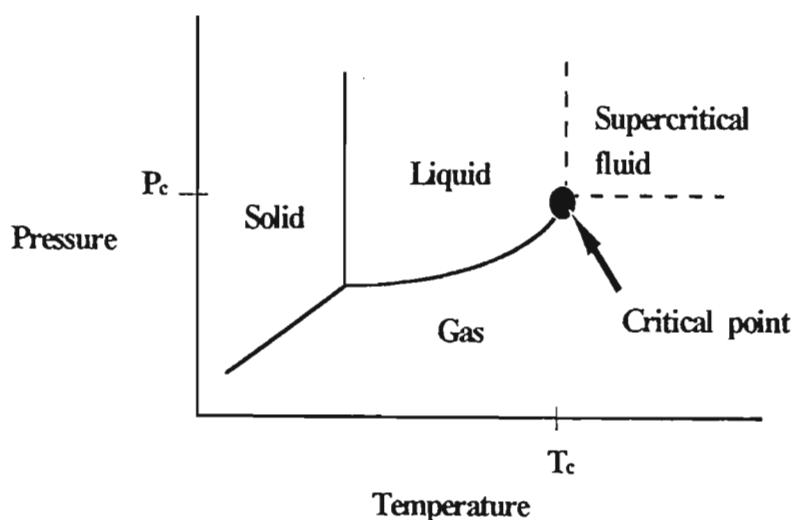


Figure 2.1 Pressure/temperature phase diagram of a substance.

If a liquid and a gas are in equilibrium and one moves along the gas-liquid coexistence curve towards the critical point, by increasing both the temperature and pressure, the liquid becomes less dense because of thermal expansion and the gas becomes more dense as the pressure increases. At the critical point, the densities of the two phases become identical and the distinction between the gas and liquid disappears. The substance becomes a supercritical fluid and is characterized by a critical temperature and pressure (T_c and P_c). The region of interest for SFE is the area above the critical point where densities, solubilities, viscosities and diffusivities are intermediate between those of typical gases and liquids.

2.2 Physical properties of supercritical fluids

Supercritical fluids offer a convenient means to achieve solvating properties which have gas and liquid-like characteristics without actually changing chemical structure. By selective control of pressure and temperature one can access a significant range of physicochemical properties (density, diffusivity, dielectric constant, etc.) without ever passing through a phase boundary, e.g. changing from gas to liquid form. A supercritical fluid can therefore be considered a continuously adjustable solvent. Table 2.1 illustrates how supercritical fluids compare to gases and liquids in terms of the important physicochemical properties of each.

Table 2.1 Comparison of physical properties of gases, liquids and supercritical fluids (6).

	Gas ^a	Liquid ^a	SF ^b
Density (g/cm ³)	0.6 - 2×10^{-3}	0.6 - 1.6	0.2 - 0.9
Diffusion rates (cm ² /s)	0.1 - 0.4	0.2 - 2×10^{-5}	0.1 - 4×10^{-3}
Viscosity (g/cm.s)	1 - 3×10^{-4}	0.2 - 3×10^{-2}	1 - 9×10^{-4}

^a at 25 °C and 1 atm

^b at T_c and P_c to $4 \times P_c$

These favourable physical properties of SFs are advantageous for extraction applications.

2.3 Advantages of SFE

SFE has several potential advantages over classical liquid extraction methods.

Speed: Mass transfer is faster in a supercritical fluid than in liquid solvents because supercritical fluids have lower viscosities and higher solute diffusivities. The low viscosities provide favourable flow properties. This permits supercritical fluids to penetrate matrices with low permeability more readily than conventional solvents. The higher solute diffusivity is a significant property as rates of extraction are ultimately limited by the speed with which analyte molecules are transported by diffusion from the sample matrix into the bulk fluid. Hence SFE can usually be completed within a short period of time, compared to several hours for liquid solvent extractions.

Variable solvent strength: The solvent strength of a supercritical fluid is a function of its density (7), which, in turn, is a function of temperature and pressure. The relationship between pressure, temperature and density may be described by an equation of state, a number of which have been developed by various workers (8, 9, 10). The general trend is for higher pressures (at a given temperature) to increase density and solvating power, while increasing temperature at a constant pressure will result in a reduction in density and hence solvent strength. These parameters (density, pressure, temperature) are, therefore, of prime importance in controlling the extraction process. This allows SFE parameters to be optimized for a target analyte, and provides a method to achieve class-selective extractions from a single sample by simply extracting the sample at two different pressures with the same supercritical fluid.

Reduction of liquid solvent usage: The large volumes of liquid solvents used for conventional extractions have caused recent concern because of their potential toxic nature and rapidly increasing disposal costs. Since most commonly-used supercritical

fluids such as CO₂ are gases at ambient conditions and SFE effluents are typically collected in small volumes of liquid solvents (or no liquid solvent for on-line SFE methods), the need for liquid solvents is dramatically reduced. In a similar manner, the need to concentrate extracts prior to analysis of trace analytes is also greatly reduced.

Simplified on-line coupling with chromatographic techniques: The gaseous nature (at ambient conditions) of most supercritical fluids also facilitates the direct coupling of SFE with GC and SFC.

Analyte crystallization: Solid compounds may be crystallized from supercritical fluids and the size of the crystals manipulated by changing process pressures and temperatures. The ability to make small crystals is of interest to the pharmaceutical industry, where product morphology can be critical to drug uptake rates, and where mechanical fragmentation procedures may be unacceptable, owing to thermal instability or contamination risks (11).

2.4 Selection of a supercritical fluid

The critical pressure and temperature are two important parameters that need consideration when selecting a supercritical fluid. The analyst should strive to select a fluid that exhibits the best compromise in solubilizing the solutes of interest as well as mass transfer characteristics required to rapidly effect the extraction of the analytes. Qualitatively, the solvent strength of an eluent may be described by the solubility parameter introduced by Hildebrand and Scott (12). They stated that the solubility parameters of the solvent and the solute should be similar to achieve dissolution of the solute. This condition can be approximated if the solubility parameter of the analyte is known and if certain correlations are used, such as one proposed by Giddings *et al.* (13):

$$\delta_{sol} = 1.25 P_c^{1/2} \frac{\rho}{\rho(liq)} \quad (2.1)$$

where δ_{sol} is the Hildebrand solubility parameter, P_c is the critical pressure of the fluid, ρ is the density of the supercritical fluid, and $\rho_{(liq)}$ is the density of the fluid in its liquid state. Optimization of pressure and temperature will assure a high flux rate of the analyte into the extracting medium, thereby saving consumption of fluid, while assuring rapid sample processing. Figure 2.2 shows the dependence of the Hildebrand solubility parameter on temperature and pressure for supercritical CO₂.

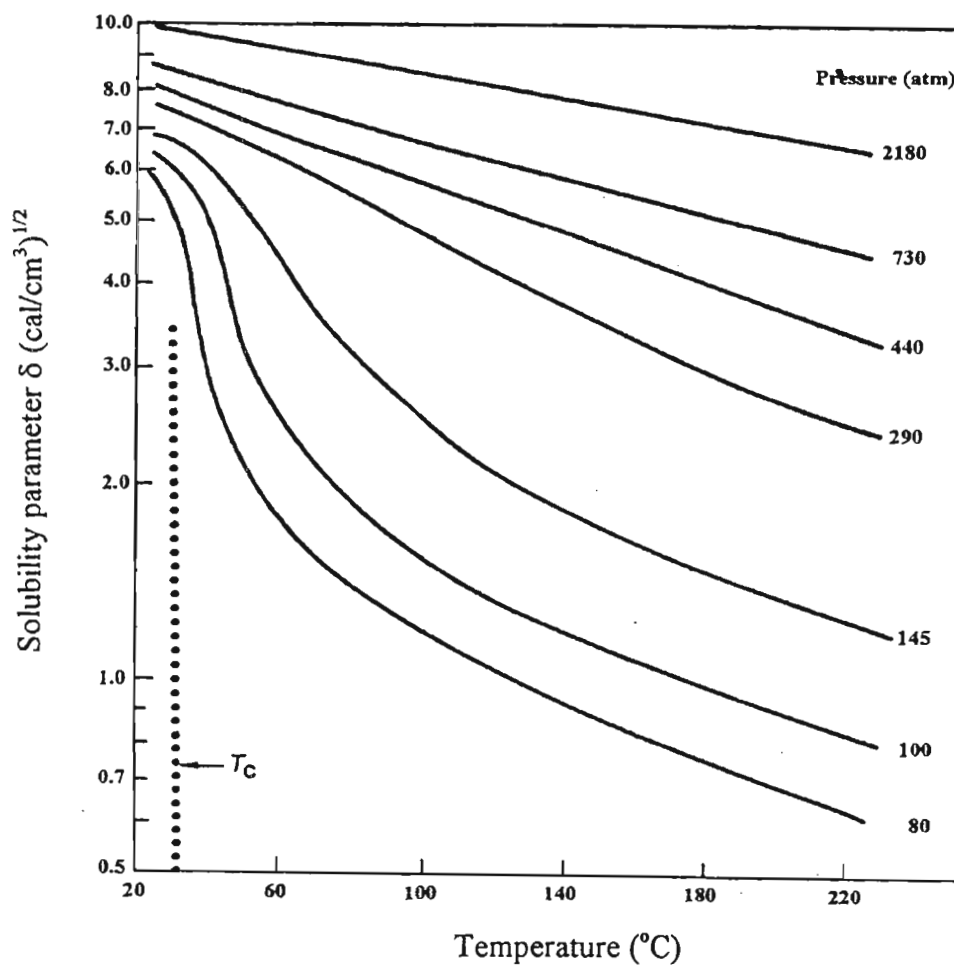


Figure 2.2 Effect of temperature and pressure on the Hildebrand solubility parameter for supercritical CO₂. (14)

The critical pressure, to a first approximation, determines the magnitude of the fluid's solvent power in the condensed state and can therefore be used as a crude guide to match the fluid with the anticipated polarity of the compounds to be extracted. For example, ethane has a lower critical pressure than carbon dioxide as shown in Table 2.2. Based on this criterion, ethane would not dissolve a moderately polar solute to the same extent as carbon dioxide. Likewise, fluids which exhibit higher critical pressures than carbon dioxide, are known to solubilise polar compounds at higher concentrations in the fluid phase than supercritical CO₂.

The critical temperature of the fluid is also important when one considers the effect of extraction temperature on the thermal stability of target analytes. Fluids which are characterized by high critical temperatures require elevated extraction temperatures in order to effect extraction in the supercritical state.

Table 2.2 Critical conditions of SFE solvents. (15)

Compound	Critical temperature (°C)	Critical pressure (atm)	Critical density (g/cm ³)	Acentric factor (ω)	Dipole moment (D)
Ethylene	9.9	50.5	0.23	-	-
Chlorotrifluoromethane	28.8	38.2	0.58	0.198	0.5
Carbon dioxide	31.0	72.9	0.47	0.239	0.0
Ethane	32.2	48.2	0.20	0.099	0.0
Tetrafluoroethylene	33.3	38.9	0.58	-	-
Nitrous oxide	36.5	71.7	0.46	0.165	0.2
Methyl fluoride	44.6	58.0	0.31	-	-
Sulfur hexafluoride	45.6	37.1	0.75	0.286	0.0
Chlorodifluoromethane	96.4	48.5	0.52	0.221	1.4
Propane	96.7	42.0	0.22	0.153	0.0
Carbon disulfide	104.8	65.0	0.45	0.109	0.0
Dichlorodifluoromethane	111.7	39.4	0.56	-	-
Dimethyl ether	126.9	52.6	0.26	-	-
Ammonia	132.3	111.3	0.24	0.250	1.5
Sulfur dioxide	157.5	77.7	0.53	-	-
Nitrogen dioxide	157.8	100.0	0.56	-	-
Methyl ethyl ether	164.7	43.4	0.27	-	-
Diethyl ether	193.6	36.3	0.27	-	-
n-Pentane	196.6	33.3	0.23	0.251	0.0
Isopropanol	235.3	47.0	0.27	0.665	1.7
Acetone	235.9	47.0	0.28	0.304	2.9
Methanol	240.3	78.9	0.27	0.556	1.7
Ethanol	243.4	63.0	0.28	0.644	1.7
Chloroform	263.4	54.0	0.58	0.218	1.1
n-Heptane	267.0	27.0	0.24	0.349	0.0
Water	374.0	218.0	0.32	0.344	1.8

2.5 Unique properties of SF-CO₂

Supercritical carbon dioxide has been the fluid of choice in many SFE studies. This fluid has the added advantage over other supercritical solvents because it is non-toxic, non-flammable, environmentally acceptable, inexpensive, and leaves no solvent residue. In addition, the critical temperature is low (31°C), thus extractions can be performed at moderate temperatures hence preventing the degradation of thermally labile compounds. Modest compression of CO₂ produces a substantial change in its fluid density due to the high non-ideality exhibited by this fluid as seen from the pressure-density isotherm (Figure 2.3). Even though supercritical CO₂ preferentially extracts non-polar compounds, it can exhibit an induced dipole moment, which enhances the extraction of moderately polar solutes into the fluid phase (16).

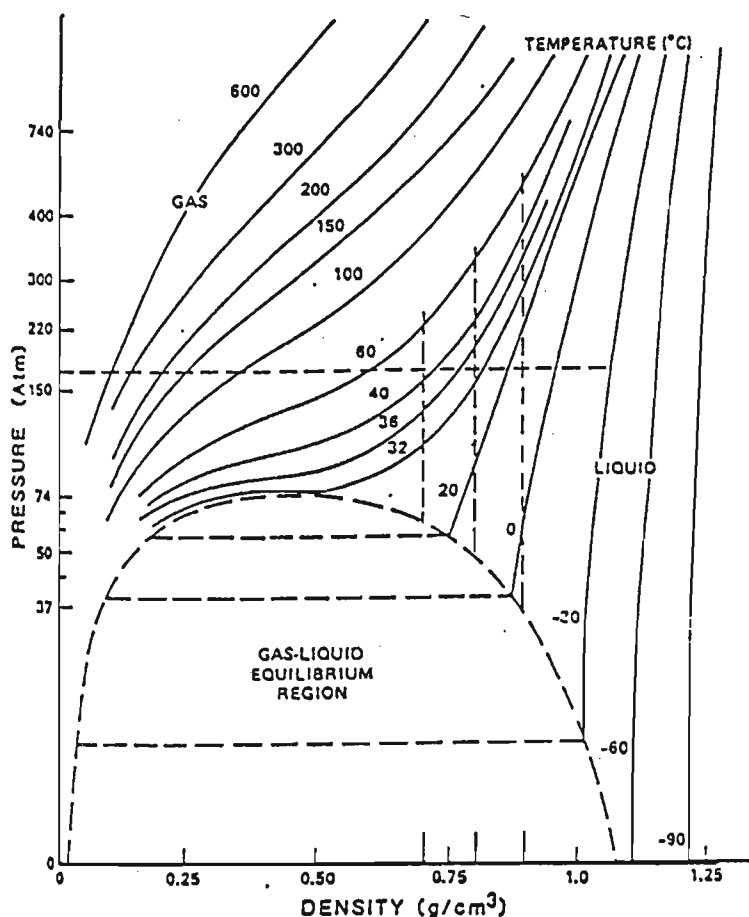


Figure 2.3 Effect of pressure changes on density of supercritical CO₂ at different temperatures. (17)

2.6 Generalized method and instrumentation requirements for SFE

The essential equipment needed to perform SFE is shown in Figure 2.4. A high pressure pump is used to provide pressurized fluid (at a constant pressure) to the sample which is contained in the extraction vessel or sample cell. The extraction vessel is housed in an oven to maintain the temperature above the critical temperature of the extraction fluid. The extraction fluid is pumped through the extraction vessel, the analytes are partitioned into the supercritical fluid, and the analytes are collected after depressurization of the supercritical fluid. The depressurization step and the flow control is achieved by using a back pressure regulator or a length of fused silica tubing (typically 10 to 50 μm i.d.).

Extracted analytes are most often collected in a small volume of liquid solvent (off-line SFE) or the analytes transferred directly to a chromatographic system (on-line SFE) like SFC or GC. Alternate methods such as cryogenic trapping (18, 19) or collection onto a sorbent cartridge have also been used (20).

The pump is usually a syringe or reciprocating type and requires an external cooling source to assure liquefaction of the fluid. If necessary, the modifier component can be added by methods discussed in section 2.8.1.

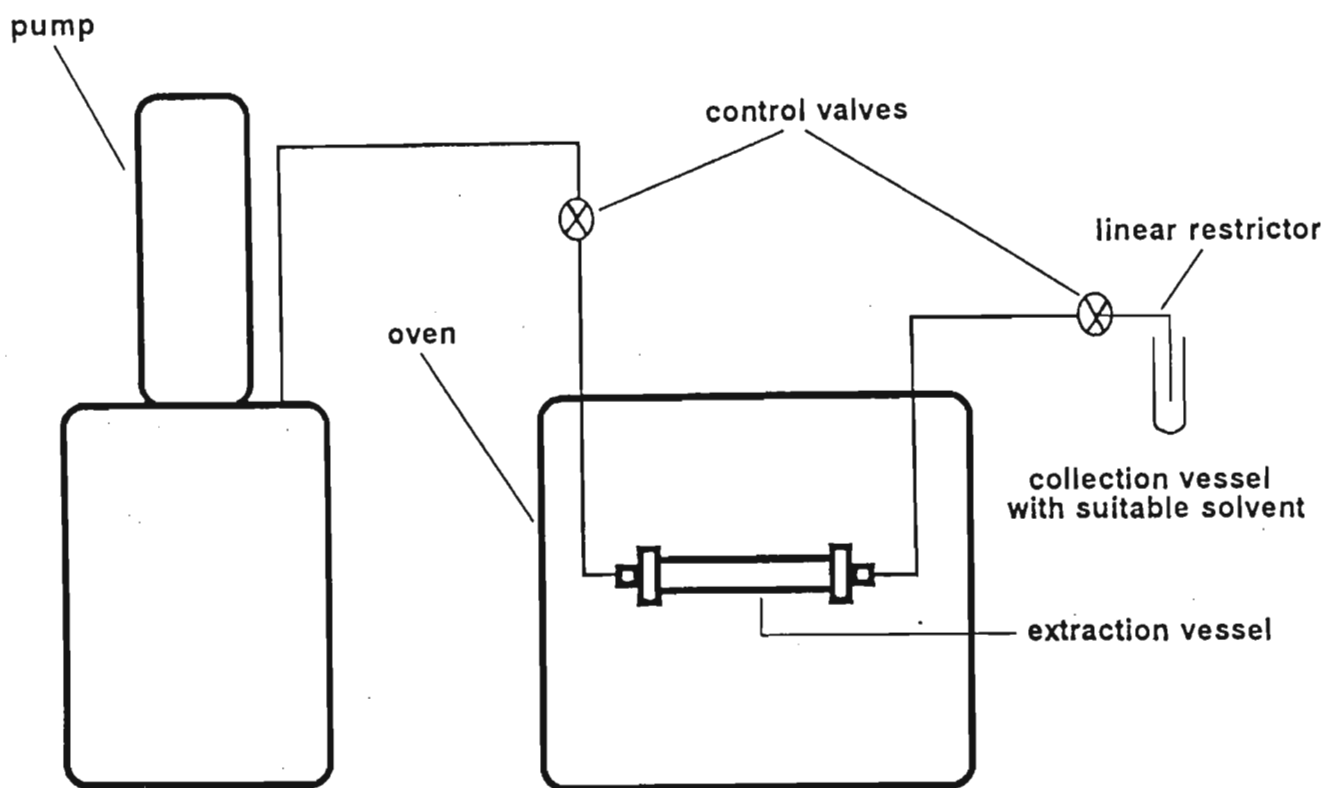


Figure 2.4 Schematic diagram of an SFE setup for off-line recovery of analytes.

Extraction cells have been fabricated out of a variety of materials appropriately suited to pressures to be used, but most cells consist of a tubular metal cavity with associated compression fittings. In the past, many investigators have utilised tube fittings or HPLC columns as extraction cells (21), but recently, commercially available extraction cells with finger-tight fittings have become available. Figure 2.5 shows typical vessels currently employed in SFE.

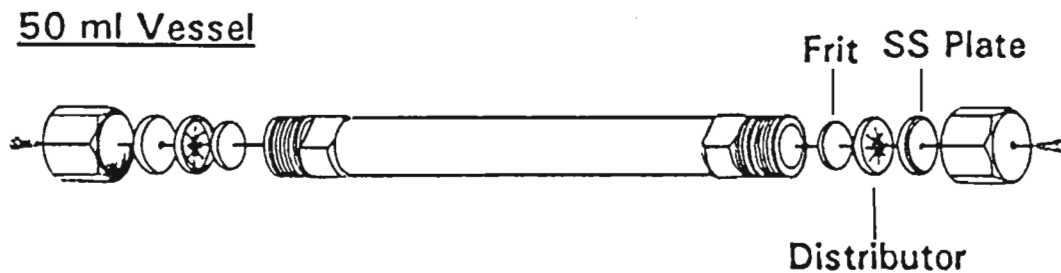
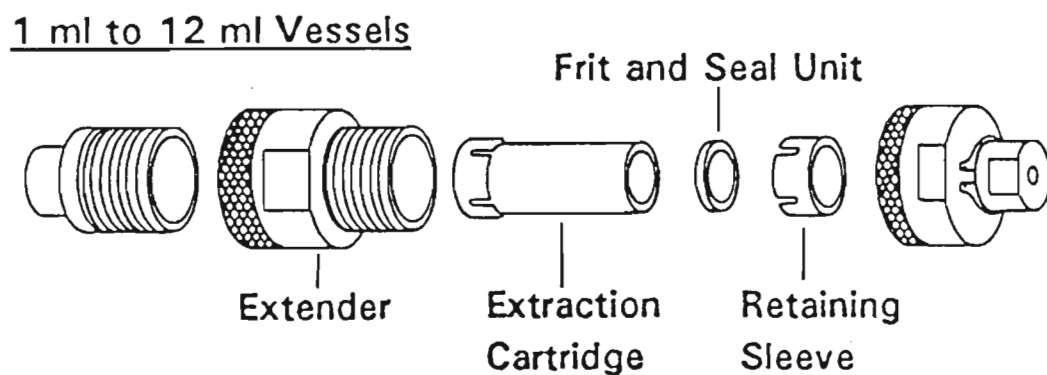
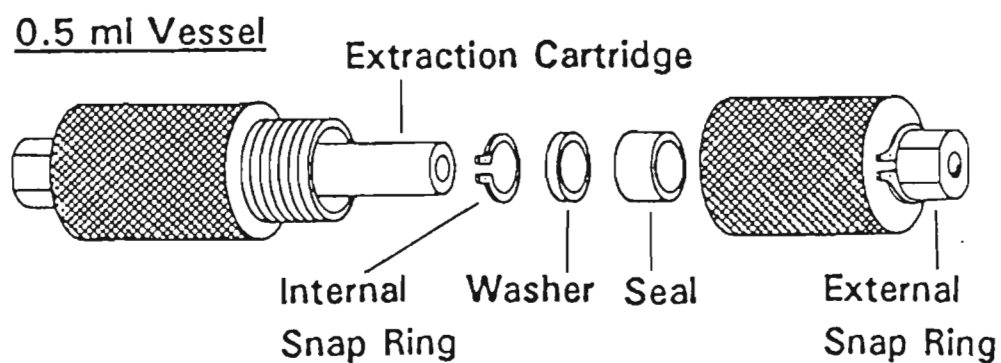


Figure 2.5 Typical extraction cells used in analytical SFE.

2.7 Selection of SFE conditions

As stated earlier, the density, pressure and temperature are of prime importance in controlling the extraction process and, although some relationships between them and solubility have been developed (22), it is generally not possible to predict ideal extraction conditions on a purely physicochemical basis. However, it is often possible to predict the overall feasibility of an extraction or initial extraction condition. In SFE, the solvent strength of a given fluid is primarily dependent upon its density. However it is much easier to measure directly and control the pressure (and temperature) than to measure directly and control the fluid density. It is possible, however, at a specific temperature, to relate fluid pressure to density, thus allowing measurement and control of the density by measuring and controlling the pressure. For low density gases, this is easily done with the ideal gas law, $PV/RT = 1$. (The molar volume, V , is the reciprocal of the molar density. Knowledge of the gas's molar mass, M , makes conversion from molar density to mass density trivial: mass density, ρ , is M/V). At high densities, which are frequently encountered in SFE, the ideal gas law is no longer valid. The work by Pitzer (23, 24), however, allows the ideal gas law to be extended by adding another term, called the compressibility factor, which is a function of the pressure, temperature, and molecular identity of the fluid. With this extension, the gas law becomes $PV/RT = z$, where z is the compressibility factor. Pitzer was able to reduce the molecular identity terms of z to a single number, called the acentric factor, ω . This factor attempts to account for both the molecular size and shape. The value of the acentric factor (refer to Table 2.2) was taken to be the ratio of the vapour pressure of the substance at 70% of its critical temperature to that at its critical temperature. Thus, at a given temperature, pressure, and known acentric factor, z can be determined (25). This allows V to be determined from the gas law ($V = zRT/P$) and thus the mass density to be determined if the molar mass of the fluid is known.

The same principle described for pressure to density conversion of a single fluid can be used for binary fluids as well. When two fluids are mixed, critical parameters can be calculated based on the physical-chemical properties and the mole fraction of each fluid in the mixture (26).

2.8 Use of modifiers in SFE

Difficulties are experienced when fairly polar analytes need to be quantitatively extracted, as these analytes display a reduced solubility in the supercritical CO₂ phase. In these cases a fluid with a higher solvent strength should be chosen, but the use of more polar fluids is severely limited by practical considerations. Supercritical ammonia would be very attractive from a solvent strength point of view, but it is difficult to pump as ammonia is chemically reactive (dissolves pump seals) and is likely to be too dangerous for routine use. Supercritical methanol is also an excellent solvent but is less attractive because of its high critical temperature and because it is a liquid at ambient conditions, which complicates sample concentrations after extractions. Despite its excellent characteristics as an SFE fluid, the routine use of CHClF₂ is also not likely because of negative environmental effects. Hence CO₂ still remains the fluid of choice in many applications. In the case of polar analytes, it becomes desirable to add a polar co-solvent to the supercritical fluid to enhance the solubility of an analyte in the extracting medium. Such co-solvents (also called modifiers or entrainers) are usually organic solvents that are added to the source of compressed fluid. Table 2.3 lists examples of commonly-used modifiers in SFE applications.

Table 2.3 Examples of commonly-used modifiers in SFE applications. (26)

Modifier	T _c (°C)	P _c (atm)	Molar mass g/mol	Dielectric constant at 20 °C
Methanol	239.4	79.9	32.04	32.70
Ethanol	243.0	63.0	46.07	24.30
Propan-1-ol	263.5	51.0	60.10	20.33
Propan-2-ol	235.1	47.0	60.10	19.30
Hexan-1-ol	336.8	40.0	102.18	13.30
2-Methoxyethanol	302.0	52.2	76.10	16.93
Tetrahydrofuran	267.0	51.2	72.11	7.58
1,4-dioxane	314.0	51.4	88.11	2.25
Acetonitrile	275.0	47.7	41.05	37.50
Dichloromethane	237.0	60.0	84.93	8.93
Chloroform	263.2	54.2	119.38	4.81
Carbon disulphide	279.0	78.0	76.13	2.64
Water	374.1	217.6	18.01	80.1

2.8.1. Methods of adding modifiers

There are a number of ways in which modifiers can be added to primary supercritical fluids (27-30). Premixed cylinders can be purchased from commercial sources. These cylinders have a discrete concentration level of a specific modifier in CO₂ for example. The cylinder is directly connected to the supply pump, which then delivers premixed modified fluid to the SFE vessel. One disadvantage of this technique is that, to obtain different percentages of modifier, different cylinders with a range of concentrations of modifier are necessary. Also, it has been experimentally observed that, as material is drawn from the cylinder, a shift in the vapour-liquid equilibrium results, leading to a change in the concentration of

the modifier in the liquid phase (31). As the liquid phase is drawn, CO₂, being the more volatile component, vapourises disproportionately occupying the liberated volume. As a result, the concentration of the modifier in the liquid phase increases. Such behaviour has been found to give rise to reproducibility problems in extraction efficiency (32).

Modifiers can also be added to CO₂ by using two separate supply pumps. One pump is used primarily for CO₂ delivery and the second pump is used for modifier delivery. Downstream of both these pumps is a mixing tee where the modifier is equilibrated with either liquid or supercritical CO₂ in a thermostatted zone. A schematic diagram is shown in Figure 2.6. The mixed fluid is then delivered to the extraction vessel.

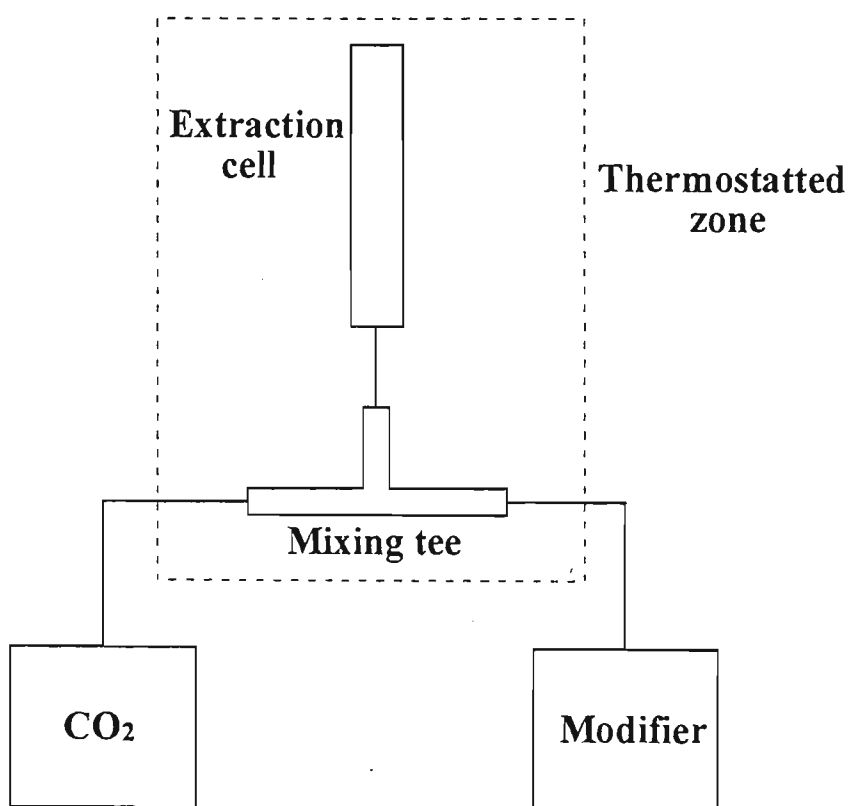


Figure 2.6 Schematic diagram of modifier delivery system for SFE.

Unlike the first method of introducing modifiers, in this case the compressibility of the fluids must be taken into account otherwise pumping of the modifier into the CO₂ pump can occur.

The next and perhaps the most effective way (if matrix-analyte interactions are strong) of delivering a modifier for SFE is by directly adding the modifier to the sample matrix prior to extraction. In this respect, the highest concentration of modifier is delivered to the matrix. Moreover, one can screen a number of modifiers and modifier concentrations in a relatively rapid fashion without purging the entire system between experimental runs. Ashraf-Khorassani and Taylor compared the extraction efficiency of PCBs from river sediment using two different methods for incorporation of modifier into the SFE system (33). They found that off-line addition of modifier to the SFE vessel prior to extraction was more effective in promoting extraction efficiency of PCBs than using in-line modifier addition. Also, direct spiking of the matrix required less modifier than the in-line approach for achieving the same level of recovery.

Hawthorne *et al.* developed a simple saturation chamber to provide modified supercritical CO₂ and used this device (Figure 2.7) for the extraction of linear alkylbenzenesulfonates from soil, sediment and municipal wastewater treatment sludge (34). Reproducible and quantitative recoveries (>90%) were achieved.

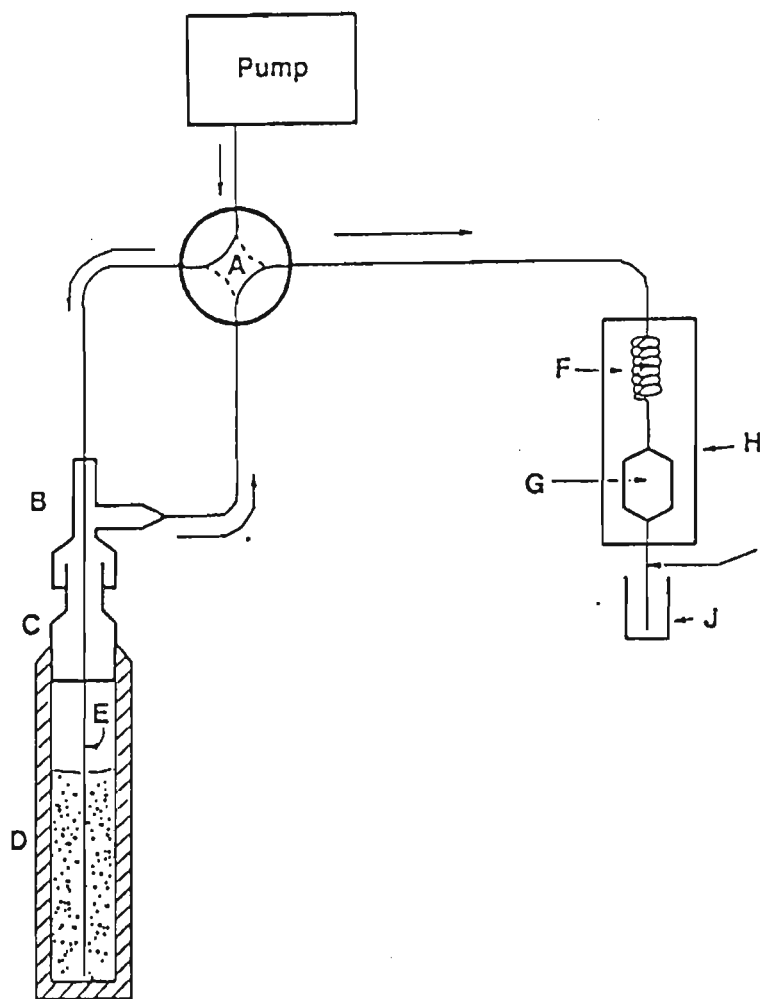


Figure 2.7 Schematic diagram of device used to modify supercritical CO₂ (34).

Arrows indicate direction of flow. Components: A = four port valve; B = ‘Parker’ or ‘Swagelok’ brand ‘tee’ tubing fitting (1/16 × 1/16 × 1/4 inch stainless steel); C = 1/4 inch normal pipe thread × 1/4 inch tubing stub fitting welded into D; D = modifier chamber; E = 1/16 inch o.d. stainless steel tubing; F = heating coil; G = extraction cell; H = heater; I = restrictor; J = collection vial.

With any method of adding modifiers to the primary fluid, it must be remembered that the addition of modifiers changes the critical point of the mixture from one recorded for the pure fluid. The critical temperature of the mixed solution is higher than that of the pure fluid, and therefore the extraction temperature should be raised to ensure that a single phase supercritical fluid is present during SFE to avoid possible solute partitioning between the two phases that might coexist. Hence it is important to recognise the magnitude of this change so as to adjust the experimental parameters accordingly. The solubility of the co-solvent in the supercritical fluid is also determined by the extraction pressure, therefore the quantity of the cosolvent that can be added to the fluid phase must be regulated. For example, Figure 2.8 shows the relationship between the critical temperature, pressure and mole fraction of a CO₂-methanol mixture. Clearly, if a methanol mole fraction of 0.2 in CO₂ was required for extraction, it would be necessary to operate above 150 bar (15 MPa) and 80 °C in order to maintain a homogenous supercritical fluid (23). Water is also scarcely soluble in liquid carbon dioxide (around 0.1% m/m at 20 °C); its solubility increases in fluid CO₂ with increasing temperature (around 0.3% m/m at 50°C)

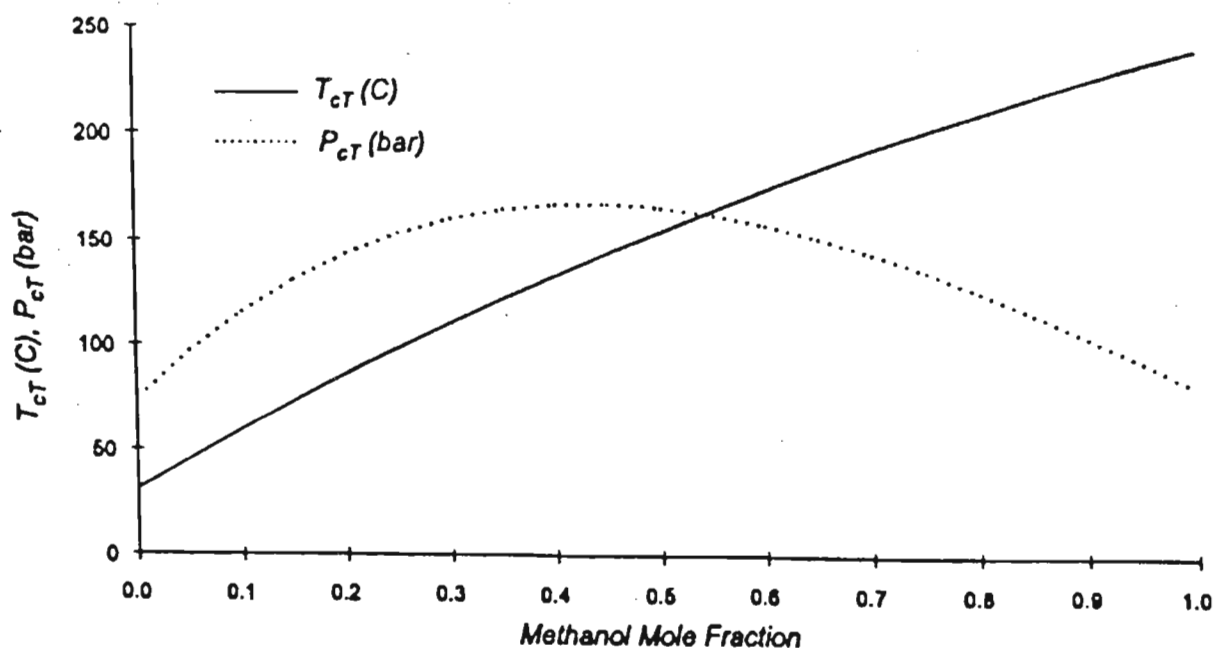


Figure 2.8 Relationship between the critical temperature, pressure and mole fraction of CO₂-methanol mixtures according to Saito and Nitta. (35)

Furthermore, depending upon the modifier identity, the nature of the analytes of interest, as well as the type of sample matrix, there is a need to apply an equilibration period when using modifiers in SFE. If the modifier has not reached a level of equilibration with the supercritical fluid (i.e. existing as a one phase system) as well as the sample matrix, there could be situations where the enhancement of the extraction efficiencies using modifiers are not seen. In these cases, what happens is that the modifier is displaced out of the extraction vessel into the collection vial without achieving an interactive extraction. In most situations, when a modifier is required to enhance SFE efficiencies, a static equilibration period is recommended.

2.9 Modes of SFE

Two common modes are used for SFE; dynamic and static. For dynamic SFE, the sample is constantly swept with fresh supercritical fluid at a flow rate determined by the extraction pressure and the dimensions of the outlet restrictor. Dynamic SFE continually provides new fluid to the sample, and is more effective when the supercritical fluid is likely to become saturated with the target analytes.

For static SFE, the extraction vessel is pressurised with the fluid and the sample is extracted with no outflow of the supercritical fluid. After the extraction is thought to be completed, a valve is opened at the outlet of the cell to allow the analytes to be swept from the cell into the collection vial. Typically, a static extraction is followed by several minutes of dynamic extraction to recover the analytes. Static extraction has the advantages that less fluid is used and that liquid polarity modifiers can be used by simply adding them to the cell prior to pressurisation. However, in a static mode, extraction times may be longer because the movement of components must rely on diffusion as opposed to the mass action of the carrier in dynamic systems.

2.10 Kinetics of SFE

It is important to understand the kinetics of SFE. Extraction by a supercritical fluid is never complete in finite time. It is relatively rapid initially, but then there follows a long tail in the curve of percent extracted versus time as illustrated in Figure 2.9. In a typical situation, 50% is extracted in ten minutes, but it may be a hundred minutes before approximately 99% is extracted. It is not correct, therefore, to assume that extraction is essentially complete if it has been carried out for two consecutive equal periods of time and the second period produces only a fraction of the compound extracted in the first period.

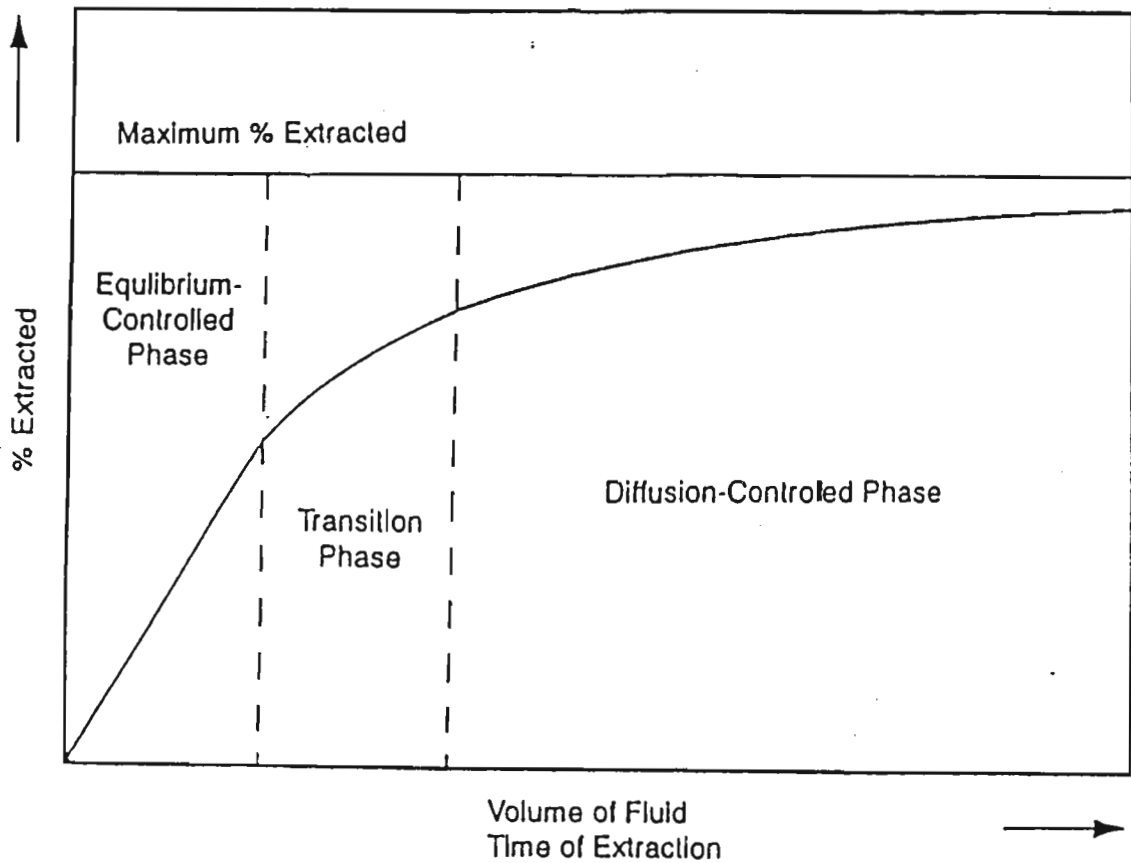
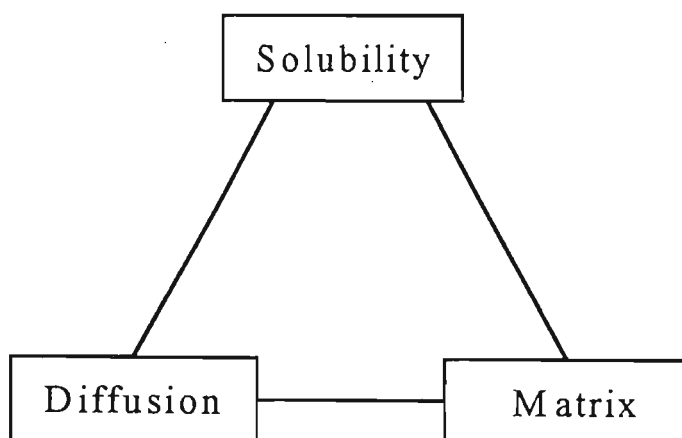


Figure 2.9 Generalised extraction curve of percent solute extracted as a function of volume of extraction fluid or time of extraction.

As shown in the above figure, the initial portion of the extraction curve is linear, indicating that quasi-equilibrium conditions are governing the partition of the solute into the mobile dense fluid phase. After a finite time, the yield curve starts to become convex with respect to the time axis as the extraction experiences a transition from equilibrium to diffusion controlled kinetics. In the final stage of the extraction, the kinetics are dominated by diffusive mechanisms which may be quite complex, depending on the morphology of the substrate being extracted. For the case of the solid substrate, factors such as the degree of swelling of the substrate can have a profound effect on the yield curve.

Three interrelated factors influence recovery as shown in the SFE triangle below.



For extraction to be successful, the analytes must firstly be sufficiently soluble in supercritical fluid. This factor is especially important at the beginning of extraction, when extraction is occurring at a higher rate.

Secondly, the solute must be transported sufficiently by 'diffusion' from the interior of the matrix in which it is contained. The 'diffusion' process may be normal diffusion of the

solute, or it may involve diffusion of the fluid into the matrix and perhaps subsequent replacement of solute by solvent molecules on surface sites.

The third factor is that of the matrix. Even though a particular compound may be soluble in a supercritical fluid, not all of it may be necessarily extracted from the matrix due to adsorption effects.

2.11 Physical matrix effects

The physical morphology of the substrate undergoing SFE can have a pronounced influence on the efficiency of the extraction and the rate at which it is conducted. In general, the smaller the particle size of the substrate, the more rapid and complete the extraction will be. This effect is largely due to the shorter internal diffusional path lengths over which the extracted solutes must travel to reach the bulk fluid phase. Synder *et al.* have carried out studies and shown that the geometric size of the matrix particles can influence the speed and completeness with which SFE can be conducted (36). As in solid-liquid extraction, an increase in the matrix's porosity will generally promote a more efficient and rapid SFE.

2.12 Impact of matrix on extraction kinetics

The rate of removal of a solute from a matrix using SFE is a function of its solubility in the fluid media and the rate of mass transport of the solute out of the sample matrix. Rate limiting kinetics can adversely impact on the rapid extraction of an analyte despite favourable solubility characteristics in the supercritical fluid medium. As shown in Figure 2.10, there are four major mass transport mechanisms to consider:

1. analyte diffusion through the internal volume of the sample,
2. surface desorption of the analyte,
3. diffusion of the analyte through a surface boundary layer, and
4. transport in the bulk supercritical fluid phase.

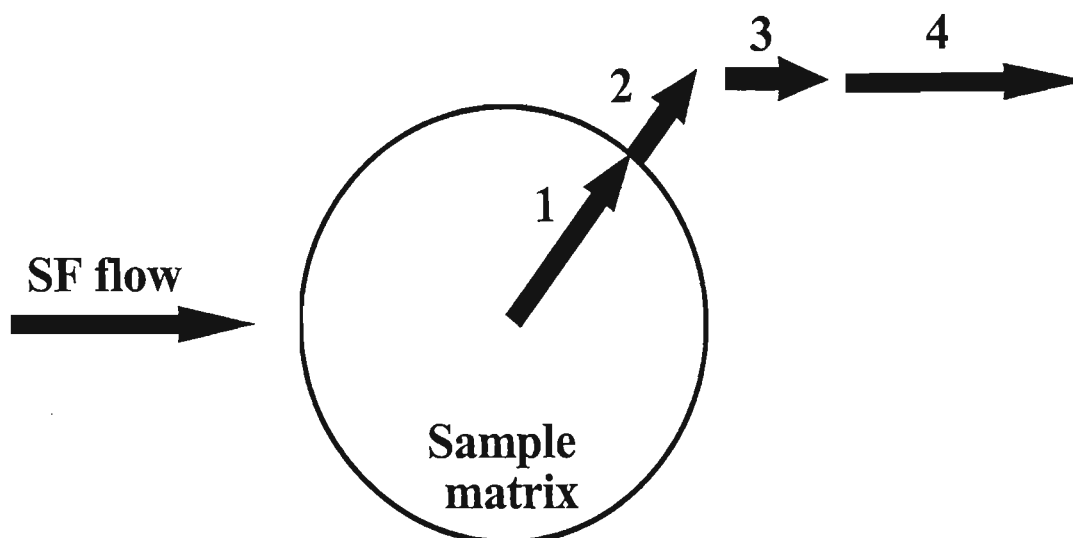


Figure 2.10 Mass transport steps for the SFE of an analyte from a porous matrix particle.

If the rate determining step is intraparticle diffusion, then the rate of extraction will be a function of the particle size of the sample matrix. It should be recognised however, that some sample matrices when exposed to supercritical fluids swell, thereby facilitating the mass transport of the analyte from within a sample matrix (37). An excellent example of this principle is the observation that polymeric films are plasticized by supercritical gases (38). This undoubtedly contributes to the success in applying SFE for the analysis of additives in plastics (39).

Surface desorption of an analyte by a supercritical fluid (step 2) is an important step in SFE for many sample types. For certain analyte-matrix combinations, the solvating power of the supercritical fluid alone will not suffice to assure a complete or rapid extraction. The use of a modifier will frequently accelerate the desorption of an analyte from the surface of the sample matrix. Wheeler and McNally have shown that the extraction efficiencies of herbicides from soil can be increased by direct addition of microlitre quantities of ethanol or methanol to the sample before commencement of extraction (40).

Diffusion of the analyte through a surface boundary layer (step 3) may also kinetically influence analyte extraction. As noted by King (41) and Porcher (42), many solid samples will promote condensation of a surface layer of the dense extraction fluid at the fluid-solid interface. The density of the adsorbed surface film will partly depend on the pressure applied to the supercritical fluid and the affinity of the sample matrix for the fluid. The development of a condensed fluid film at the surface of the sample matrix can aid in the recovery of certain analytes through competitive adsorption at the sample interface (41) as well as inhibit the transport of the analyte into the fluid phase. The kinetics of transport through a rate limiting surface film will primarily depend on the thickness of the surface film and the total surface area of the sample matrix.

The final step (step 4) depicted in Figure 2.10 is the transport of the analyte in the bulk fluid phase. Such transport is governed primarily by the diffusion coefficients of the analyte in the fluid medium and is independent of the sample matrix.

Various models for SFE, mostly based on mass balance, have been proposed (43, 44, 45, 46). However, as most models proposed require matrix characteristics which, in the case of natural products, are difficult to understand, and, since samples are never spherical and vary in particle size, it is not possible to model an extraction exactly. In many cases, the simple first order extraction rate law or hot ball model applies (43). The model describes a solid sphere of radius r with a uniform initial concentration of material that is immersed in a fluid in which the concentration of extracted material is zero. If the mass of the solute is m_0 initially and m after a given time period, then a plot of $\ln (m/m_0)$ against time has the form shown in Figure 2.11. The initial steep fall represents the extraction of the majority of the material. The exponential behaviour of the extraction after this initial period means that extrapolation may be used to obtain the actual mass of the analyte without exhaustively extracting the sample. If the extraction is carried out to obtain an extracted mass m_1 , followed by two subsequent time periods to obtain masses m_2 and m_3 , then it can be shown that the total mass of sample is

$$m_o = m_1 + \frac{m_2^2}{m_2 - m_3} \quad (2.2)$$

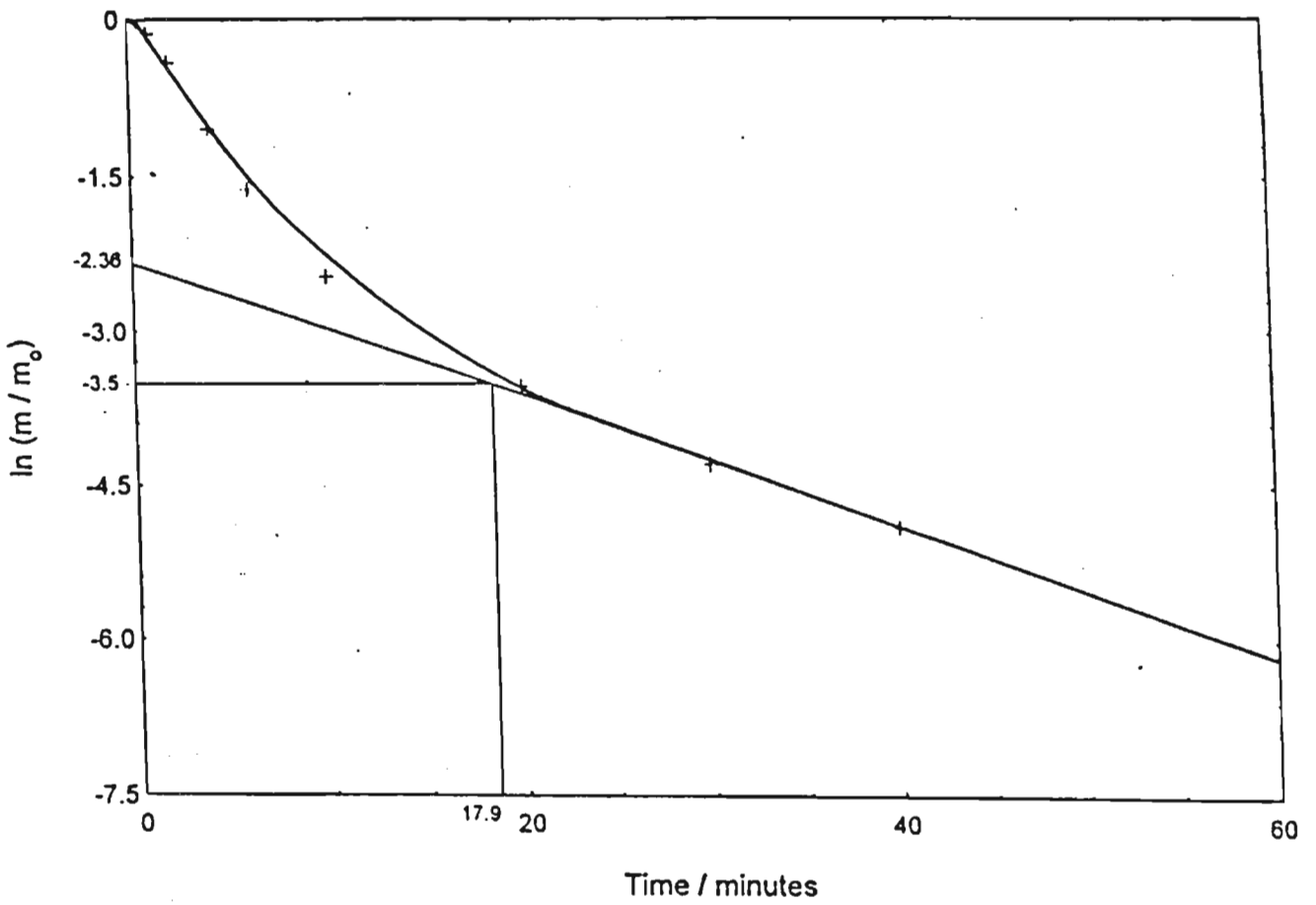


Figure 2.11 Plot of $\ln(m/m_o)$ against extraction time for the supercritical fluid extraction of camphor from rosemary.(47)

2.13 Class-selective SFE

The coextraction of unwanted solutes along with target analytes frequently occurs in analytical SFE, whether conducted in the off-line or on-line mode. As discussed earlier, one of the potential advantages of SFE over liquid solvent extraction is that the solvent strength of a SF can be changed by simply changing its density. Thus, the potential to achieve class-selective extractions exists by extracting the same sample at different pressures with the same fluid. Although obtaining a pure analyte from complex matrices using SFE is unlikely, sequential extractions of different compound classes have been demonstrated. For example, alkanes can be extracted from urban air particulates with CO₂ at 75 atm (45 °C) whereas the polyaromatic hydrocarbons (PAHs) remain unextracted until the pressure is raised to 300 atm. By sequentially extracting the air particulates at these two pressures, 85-90% selectivities can be achieved (48). Class selective SFE has also been applied to the extraction of target analytes from a bulk matrix (e.g., fat) which is itself soluble in supercritical CO₂ under most conditions. Even though fat components are highly soluble above pressures of ca. 120 atm, selective extracts of non-polar analytes have been achieved by extracting the samples at lower pressures. King has used this approach and achieved quantitative recovery of pesticides from fat samples, yet the extracts were sufficiently fat-free to allow direct GC analysis (49). Selective extraction of lactones from milk fat triglycerides has also been reported (50). A single extraction concentrated the lactones by 20 to 50 times, while a two step extraction yielded a concentration factor of ca. 500 times. Class selective extractions have also been achieved by depositing the analytes onto a sorbent column, then eluting them with SFs in SFC mode. Such approaches have been used to achieve rapid fractionation of alkanes, alkenes, and aromatics from gasoline (51, 52) and fractionation of saturates, aromatics and asphaltenes from crude oil (53). These favourable extraction properties of supercritical fluids makes this technique appropriate for a wide variety of applications and there is no doubt that SFE will continue to find use in the analytical laboratory.

References

1. K.A. Larson and M.L. King, *Biotechnol. Prog.*, **2** (1986), 73.
2. G.R. List, J.P. Friedrich and J. Pominski, *J. Am. Oil Chem. Soc.*, **61** (1984), 1847.
3. J.R. Bradley, *J. Dairy Sci.*, **72** (1989), 2834.
4. S.A. Liebman, E.J. Levy, S. Lurcott, S. O'Neil, J. Guthrie, T. Ryan and S. Yochlovich, *J. Chromatogr. Sci.*, **27** (1989), 118.
5. D.F. Williams, *Chem. Eng. Sci.*, **36** (1981), 1769.
6. S.R. Wallenborg, *PhD thesis*, Uppsala University (1997), p.3.
7. G.M. Schneider, *Angew Chem. Int. Ed.*, **17** (1978), 716.
8. D.Y. Peng and D.B. Robinson, *Ind. Eng. Chem. Fundam.*, **15** (1976), 59.
9. K.D. Bartle, A.A. Clifford and G.F. Shilstone, *J. Supercritical Fluids*, **5** (1992), 220.
10. R. Dohrn, *J. Supercritical Fluids*, **5** (1992), 81.
11. T.W. Randolph, *Tibtech*, **8** (1990), 78.
12. J.H. Hildebrand and R.L. Scott, *The Solubility of Nonelectrolytes*, New York, USA (1950), p.53.
13. J.C. Giddings, M.N. Myers, L. McLaren and R.A. Keller, *Science*, **162** (1968), 67.
14. R.A. Allada, *Ind. Eng. Chem. Process Des. Dev.*, **23** (1984), 344.
15. R.C. Reid, J.M. Prausnitz and B.E. Poling, *The Properties of Gases and Liquids*, 4th Ed., McGraw-Hill, New York, USA (1987), p.122.
16. C.T. Lira, In: *Supercritical Fluid Extraction and Chromatography*, B.A. Charpentier and M.R. Sevenants (Eds.), American Chemical Society, Washington DC, USA (1988), p.1.
17. D. Leyendecker, In: *Supercritical Fluid Chromatography*, R.M. Smith (Ed.), The Royal Society of Chemistry, London, UK (1988), p.53.
18. J.M. Levy, R.M. Ravey, R.K. Houck and M. Ashraf-Khorassani, *Fresenius J. Anal. Chem.*, **344** (1992), 517.
19. Q.L. Xie, K.E. Markides and M.L. Lee, *J. Chromatogr. Sci.*, **27** (1989), 365.

20. R.J. Maxwell, A.R. Lightfield and A.A.M. Stolker, *J. High Resol. Chromatogr.*, **18** (1995), 231
21. T.P. Zhuze, G.N. Jushkevich and J.E. Gekker, *Maslo-Zhir. Promst.*, **24** (1958), 34.
22. J.W. King and J.P. Friedrich, *J. Chromatogr.*, **517** (1990), 449.
23. K.S. Pitzer, *J. Am. Chem. Soc.*, **77** (1955), 3427.
24. K.S. Pitzer, D.Z. Lippmann, R.F. Curl Jr., C.M. Huggins and D. E. Petersen, *J. Am. Chem. Soc.*, **77** (1955), 3433.
25. J.C. Fjeldsted, W.P. Jackson, P.A. Peaden and M.L. Lee, *J. Chrom. Sci.*, **21** (1983), 222.
26. M.L. Lee and K.E. Markides (Eds.), *Analytical Supercritical Fluid Chromatography and Extraction*, Chromatography Conferences, Inc., Provo, Utah, USA (1990), p.100.
27. T.A. Berger, J.F. Dye, M. Ashraf-Khorassani and L.T. Taylor, *J. Chromatogr. Sci.*, **27** (1989), 105.
28. D.R. Gere, R. Board and D. McManigill, *Anal. Chem.*, **54** (1984), 736.
29. J. M. Levy, A.C. Roselli, D.S. Boyer and K. Cross, *J. High Resol. Chromatogr.*, **13** (1990), 416.
30. J.M. Levy, E. Storozyński and M. Ashraf-Khorassani, *Supercritical Fluid Technology*, ACS Symposium Series, **488** (1992), 338.
31. F.K. Schweighardt and P.M. Mathias, *J. Chromatogr. Sci.*, **31** (1993), 207.
32. J. Via, L.T. Taylor and F.K. Schweighardt, *Anal. Chem.*, **61** (1994) 1459.
33. M. Ashraf-Khorassani and L.T. Taylor, *Int. Lab.*, March 1986, 16.
34. S.B. Hawthorne, D.J. Miller, D.D. Walker, D. E. Whittington and B.L. Moore, *J. Chromatogr.*, **541** (1991), 185.
35. M. Saito and T. Nitta, In: *Fractionation by Packed Column SFC and SFE*, M. Saito, Y. Yamauchi and T. Okuyama (Eds.), VCH Publishers, New York, USA (1994), p.27.
36. J.M. Snyder, J.P. Friedrich and D.D. Christianson, *J. Am. Oil. Chem. Soc.*, **61** (1984), 5475.

37. J. W. King, *Personal Communication*, 7th International Symposium on SFC and SFE, Indianapolis, USA (1996).
38. J.S. Chiou, J.W. Barlow and D.R. Paul, *J. Appl. Polym. Sci.*, **30** (1985), 3911.
39. J. Nicholas, K.D. Bartle and A.A. Clifford, In: *Proceedings - 11th International Symposium on Capillary Chromatography*, P. Sandra and G. Redant (Eds.), Huthig, Heidelberg (1990), p.665.
40. J.R. Wheeler and M.E. McNally, *J. Chromatogr. Sci.*, **27** (1989), 534.
41. J.W. King, In: *Supercritical Fluids: Chemical and Engineering Principles and Applications*, T.G. Squires and M.E. Paulaitis (Eds.), American Chemical Society, Washington D.C., USA (1987), p.150.
42. J. Porcher and J.R. Strubinger, *J. Chromatogr.*, **479** (1989), 251.
43. K.D. Bartle, A.A. Clifford, S.B. Hawthorne, J.J. Langenfeld, D.J. Miller and R. Robinson, *J. Supercrit. Fluids*, **3** (1990), 143.
44. J. Pawliszyn, *J. Chromatogr. Sci.*, **31** (1993), 31.
45. H. Sovova, *Proc. 3rd Int. Symp. Supercrit. Fluids*, Strasbourg, France, **2** (1994) p.131.
46. E. Reverchon & L. Sesti Osseo, *Proc. 3rd Int. Symp. Supercrit. Fluids*, Strasbourg, France, **2** (1994), p.189.
47. D.F. G. Walker, K.D. Bartle, D. G.P.A. Breen, A.A. Clifford and S. Costiou, *Analyst*, **119** (1994), 2789.
48. S.B. Hawthorne and D.J. Miller, *J. Chromatogr. Sci.*, **24** (1986), 258.
49. J.W. King, *J. Chromatogr. Sci.*, **27** (1989), 355.
50. A.B. de Haan, J. de Graauw, J.E. Schaap and H.T. Badings, *J. Supercritical Fluids*, **3** (1990), 15.
51. J.M. Levy, R.A. Cavalier, T.N. Bosch, A.M. Rynaski and W.E. Huhack, *J. Chromatogr. Sci.*, **27** (1989), 341.
52. J.M. Levy and J.P. Guzowski, *Fresenius Z. Anal. Chem.*, **330** (1989), 207.
53. H. Skaar, H.R. Noli, E. Lundanes and T. Greibrokk, *J. Microcol. Sep.*, **2** (1990), 222.

CHAPTER 3

Application of SFE to natural products:

A literature review

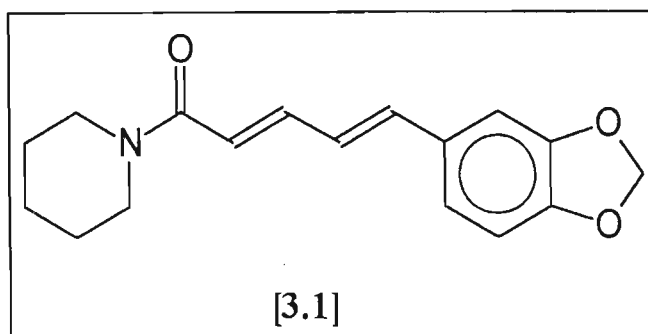
3.1 Introduction

Supercritical fluids were used as a mobile phase in a chromatographic separation as early as 1962 by Klesper *et al.* (1). Despite the report of this application, the advantages of supercritical fluids in the extraction and chromatography of natural products have only been properly realised recently (2). SFE is being increasingly used as a sample preparation method for the analysis of solutes in solid and liquid matrices. Traditionally SFE was used for many years for preparative scale isolation of compounds from plant matrices. Currently, commercialized industrial scale processes such as the decaffeination of coffee and the extraction of hops, spices and tobacco exist.

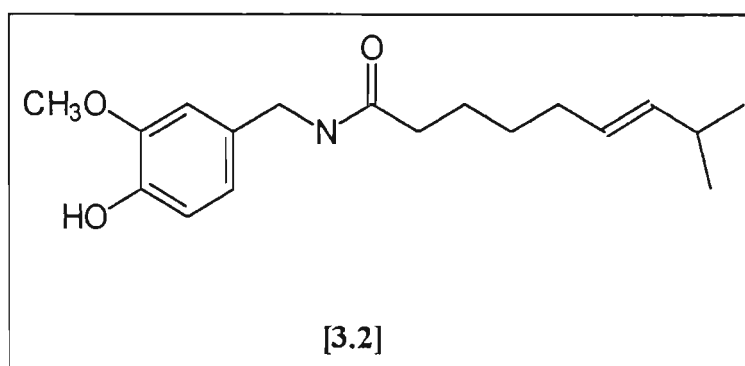
The extraction of caffeine from green coffee beans is achieved by soaking the beans in water and then extracting them in the pressure range of 160 to 220 bar and at temperatures between 70 to 90 °C. Under these conditions, the extraction is extremely selective and the caffeine content can be reduced from 0.7-3% to 0.02%. (3). The caffeine is food grade and is incorporated into beverages such as cola.

Extraction of hops is an important development in the brewing industry. The valuable constituents of the hop resins give the characteristic bitter taste of the beer. Both are unsaturated acids containing about 25 carbon atoms together with hydroxy and keto groups. With supercritical CO₂, almost 99% extraction of the humulones is achieved, well above the required minimum of 95% (4).

Spice extraction has also become a commercial operation. Many spices are extracted, usually with dichloromethane and, of these, extractions with supercritical CO₂ have been reported for black pepper, nutmeg and chillies. Piperine [3.1], makes up 98% of the hot principle of pepper.



Extraction of ground black pepper, followed by transfer of the supercritical phase to a vessel held at below supercritical temperature and pressure, produced a yellow pasty extract containing nearly 98% of the piperine. Similarly, extraction of ground chillies gave a red oil containing 97% of the main alkaloid, capsaicine [3.2] (5).



Tobacco differs as a starting material in that it is the extraction residue, the treated tobacco, that is wanted, whereas the extracted nicotine is of secondary interest. Since tobacco treated with organic solvents often acquires a rubbery texture, special processes have to be considered to avoid this, as it is disadvantageous to further processing.

Extraction with SC-CO₂ is one possible means, though it causes some expansion of the tobacco.

Many other applications involving process scale SFE have been documented (6,7). These include refining of triglycerides and fatty acids, the production of essential oil extracts from natural products, and the production of low fat and low cholesterol foods. Apart from these processes, current trends are towards the application of SFE as an analytical extraction method (8) and numerous analytical scale SFE procedures have been published. These procedures are concerned more with the extraction of analytes of interest from a bulk matrix as a sample preparation technique prior to their characterisation by other analytical methods such as chromatographic, spectrometric, spectroscopic and gravimetric techniques. It is therefore potentially very useful for the extraction of natural products prior to structural characterisation.

This chapter reviews the use of SFs for the analytical scale extraction of natural products. Different classes of compounds have been discussed and each highlights the applications where SFE was shown to be advantageous.

3.2. Alkaloids

Alkaloids are structurally the most diverse class of secondary metabolites encountered, most commonly, in the plant kingdom, but representatives have been isolated from fungi and mammals (9). Their manifold pharmacological activities have always excited man's interest. The most common alkaloid which has been extracted by SFE is caffeine. Sugiyama *et al.* (10) demonstrated the extraction and analysis of caffeine from roasted coffee beans by direct coupling of SFE-SFC. The extraction conditions such as pressure, temperature, water content and extraction times were initially investigated by off-line SFE-SFC. SFE was performed with CO₂ at 20 MPa; 20% added water and 48 °C for 60 minutes. A JASCO Fine Pak SIL C18 HPLC column was used with a methanol-water (55:45) mobile phase at a flow rate of 1.2 ml per minute. UV detection was performed at 272 nm.

Ndiomu and Simpson (11) compared SFE with liquid extraction for the isolation of caffeine from kolanuts. Low SFE recoveries of 53.7% were obtained while liquid extraction with tetrahydrofuran and methanol yielded 97,0% and 99,4% respectively. The SFE recoveries were attributed to two factors. Firstly, the extraction was carried out at a comparatively low density although the system was operated at its maximum pressure, and secondly the kolanuts were dried before extraction. The presence of water in the sample is known to enhance the solubility power of the SF and this has been demonstrated by Janicot *et al.* (12) for the extraction of alkaloids thebaine, codeine and morphine from poppy straw. Elizabeth *et al.* (13) also isolated caffeine from coffee powder and performed structural confirmation by FTIR and FTNMR.

The extraction of monocrotaline, a hepatotoxic pyrrolizidine alkaloid, from the seeds of *Crotalaria spectabilis* was successfully performed by Schaeffer *et al.* (14). Supercritical CO₂ with 5-10 mol percent ethanol was employed at a pressure of 10.34 MPa and 22.15 MPa and 35-55 °C. However, the presence of highly soluble lipid material in the seeds resulted in low monocrotaline percentage (approximately 24% m/m) in the extracts. A cation-exchange resin trap was incorporated to selectively trap the alkaloids after SFE, in preference to the co-extracted lipid material (15). The reported yield of monocrotaline increased to 95% m/m.

The pyrrolizidine alkaloid fraction of two *Senecio* species (*Senecio inaequidens* and *S. cordatus*) was extracted by off-line SFE and analysed by capillary GC (16). SFE was carried out with a home-assembled apparatus, using methanol/CO₂ as the extracting medium, at 55 °C and 15 MPa. This technique was found to produce cleaner extracts and higher recoveries. Figures 3.1 and 3.2 show the capillary GC/FID pattern of the extracts from *S. inaequidens* and *S. cordates* respectively. SFE required a smaller amount of sample, gave a quicker extraction, a simplified fraction clean-up and a higher recovery.

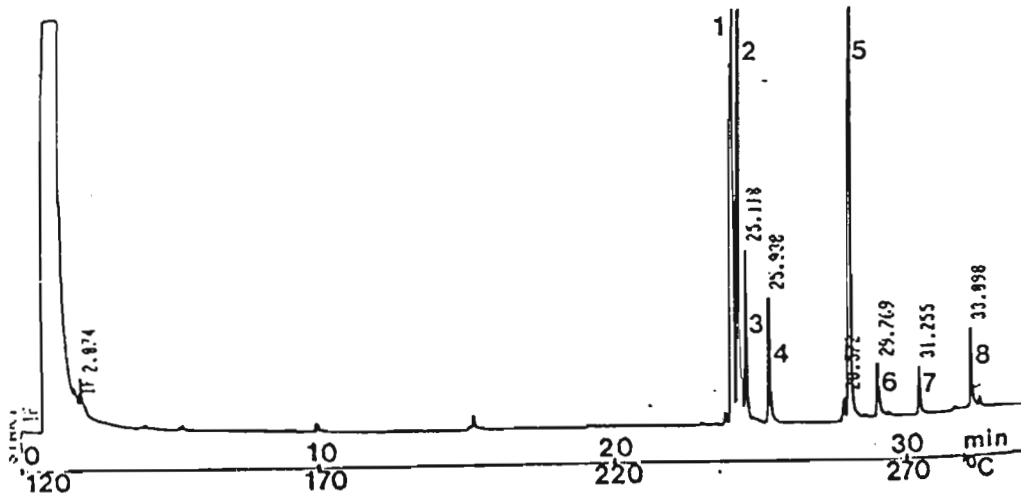


Figure 3.1. Capillary GC/FID pattern of *Senecio inaequidens* pyrrolizidine alkaloid fraction extracted by off-line SFE. (16)
 1, senecivernine; 2, senecionine; 3, seneciophylline; 4, integerrimine;
 5, retrorsine; 6, usaramine; 7, desacetyl doronine; 8, doronine.

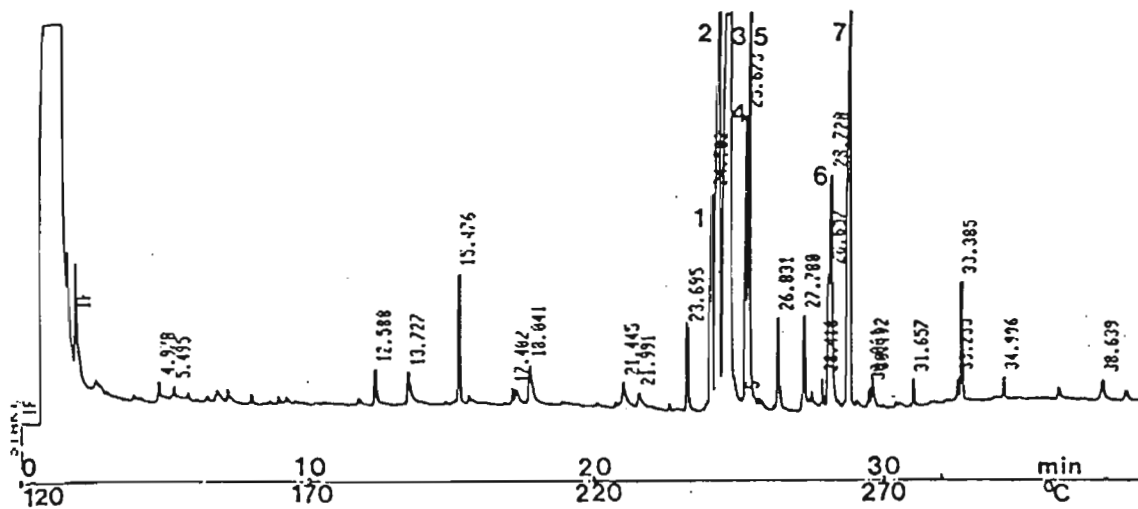


Figure 3.2. Capillary GC/FID pattern of *Senecio cordatus* pyrrolizidine alkaloid fraction extracted by off-line SFE. (16)
 1, senecivernine; 2, senecionine; 3, seneciophylline; 4, spartiodine;
 5, integerrimine; 6, jacobine; 7, jacozone.

The extraction of alkaloids thebaine, codeine and morphine from poppy straw was also investigated.(12). Extraction with pure SC-CO₂ at 20 MPa and 40.5 °C was unsuccessful, hence the influence of various polarity modifiers were considered. It was found that 50 % methanol in CO₂ was necessary in order to achieve quantitative extraction yields for morphine. A mixture of 25% methanol, 0.22% methylamine and 0.34% water produced the same effect as 50 % methanol in CO₂. The methylamine:water mixture, however, had a major drawback in that morphine in the presence of the amine degraded in the presence of light. Hence, CO₂:methanol:water mixtures were investigated and it was observed that by increasing the water content in the extraction fluid, the extraction rate for thebaine was dramatically enhanced (Figure 3.3).

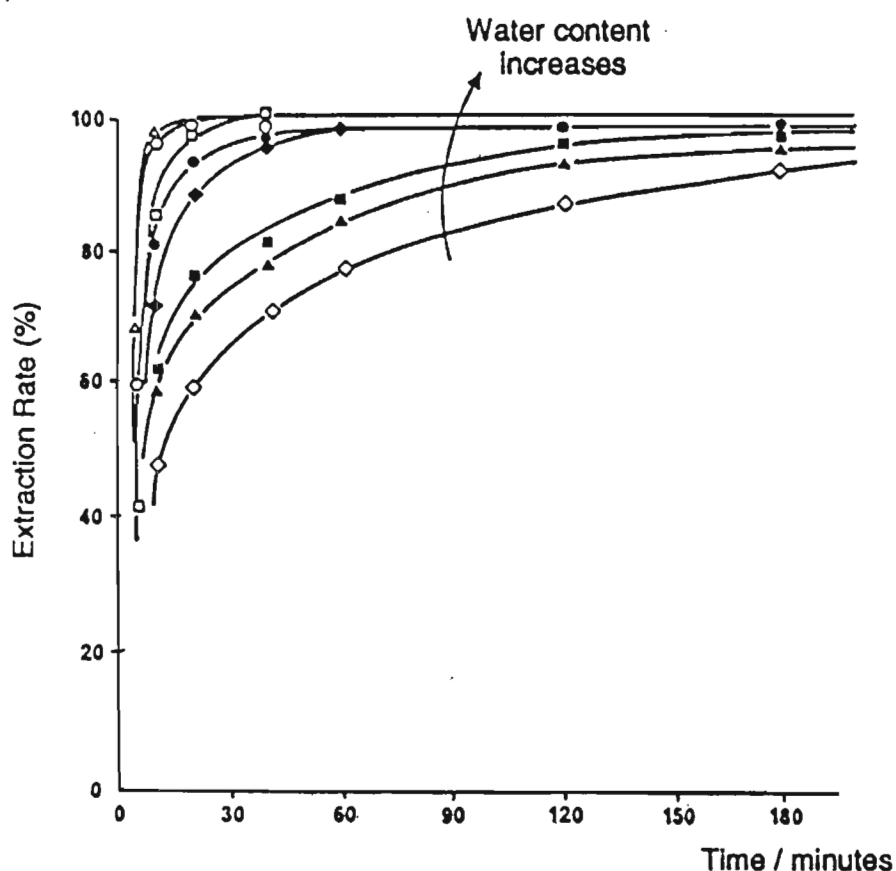


Figure 3.3. Influence of water on the extraction curves of thebaine at constant mass flow-rate (12). SFE was performed at 20 MPa and 40.5 °C using CO₂:methanol:water mixtures of the following w:w:w compositions:
 ◇ 50:32:18; ▲ 50:36:14; ■ 50:40:10; ◆ 50:44:6; ● 50:46:4;
 □ 50:49:1; ○ 50:49.5:0.5; △ 50:50:0

Sharma *et al.* investigated the use of SC-CO₂ for the extraction of moist snuff (17). Pure and methanol modified SC-CO₂ was used at 54.4 MPa and 60 °C over a 20 min period. Methanol modified CO₂ extracted compounds such as benzyl alcohol, benzothiazole and cotinine which were not present in the extracts obtained using pure CO₂.

The extraction of vindoline, an indole alkaloid from *Catheranthus roseus* was investigated by Kyu-Min *et al.* (18). Vindoline is the biosynthetic precursor of the dimeric alkaloids, vinblastine and vincristine. These two dimeric alkaloids have been used in chemotherapy for the treatment of Hodgkin's disease and acute leukemia (19,20). The extraction was carried out using pure CO₂ at various temperature and pressure conditions and the resulting extracts analysed by LC/MS. Figure 3.4. illustrates the dependence of extraction yield on CO₂ consumption at various pressures and constant temperature (50 °C). Extraction of the leaves at 300 bar and 70 °C was found to produce the highest yield of vindoline.

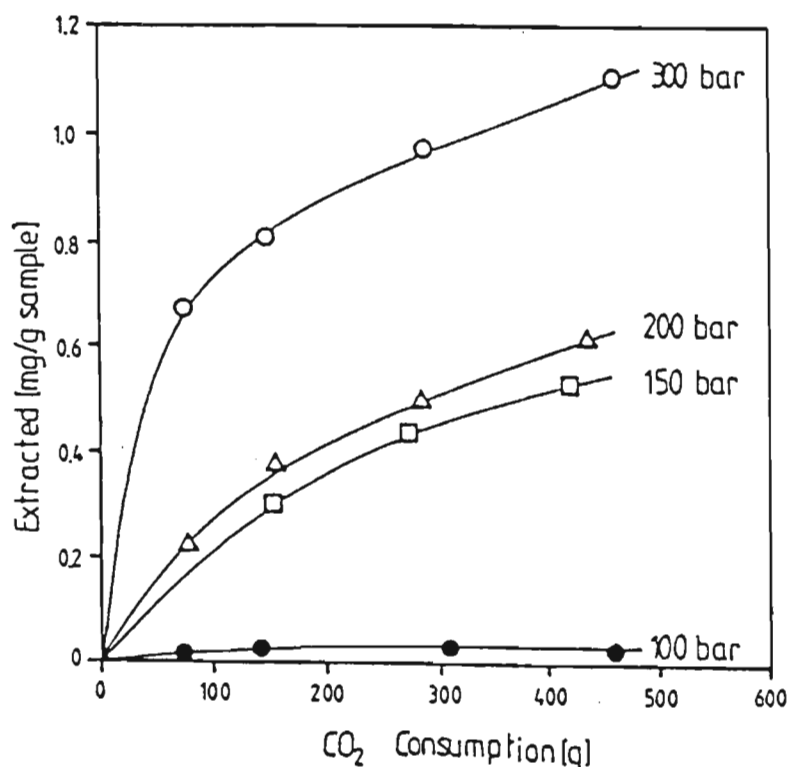


Figure 3.4. The dependence of extraction yield on CO₂ consumption at 50 °C. (18)

Bugatti *et al.* used SC-CO₂ in the extraction of isoquinoline alkaloids, *O*-methylcariachine, protopine, α -allocryptopine, escolzine, californidine, sanguinorine and chelerythine from the aerial parts of *Eschscholtzia californica* (Papaveraceae) (21). Extractions were performed at 40 °C using pressures from 8 to 30 MPa and analysis performed by reversed phase HPLC with UV photodiode array detection.

A study was also undertaken to investigate SFE as an alternative method for the selective recovery of drugs of abuse, specifically cocaine, from hair (22). While urine analysis can detect only relatively recent drug exposure, hair analysis has potential for providing long-term information about drug usage. A variety of CO₂-modifier mixtures were investigated as extractants. Modifier was added directly to the sample by injection into the CO₂ stream upon initiation of a static extraction step. Quantitative analysis of the SFE extracts was performed using capillary GC with nitrogen-phosphorous detection (GC - NPD). The most efficient recoveries of cocaine were obtained using CO₂ modified with 100 μ l water/triethylamine (TEA) (85:15 v/v) or with 100 μ l methanol / water / TEA (76:10:14 v/v) and extracting the hair sample at 40 MPa and 110 °C for 10 min statically, followed by a 15 minute dynamic extraction period.

Supercritical fluid extraction has also been investigated to isolate some of the major oxindole alkaloids of *Uncaria tormentosa* (23). *U. tormentosa* is a woody vine and is used for the treatment of gastritis, ulcers, cancer, arthritis, etc (24). Pure and methanol modified SC-CO₂ were used to generate the extracts that were subsequently analysed by both GC/MS and HPLC/MS. The extractions were first performed with pure CO₂ at 250 atm at 60 °C for 30 minutes in dynamic mode to yield fraction 1. The extraction was then performed with 10% methanol modified CO₂ for 60 minutes to yield fraction 2. Fraction 1 was found to contain two isomers of mitraphylline while fraction 2 contained 5 isomers of mitraphylline and two isomers of rhynchophylline. The average SFE yield (3 determinations) was 82,6% (with a coefficient of variation of 17.8%) for mitraphylline and 99.5% (coefficient of variation of 6.2%) for rhynchophylline.

3.3 Steroids

The steroids are a subclass of the triterpenoids and are known for their outstanding chemical, biological and medical importance. Analytical SFE has been investigated on moderately polar compounds such as cholesterol, stigmasterol, testosterone, cortisone and the anabolic steroid trebolone. Solubility data for cholesterol, stigmasterol and ergosterol in SC-CO₂ was obtained by Wong and Johnstone (25). The solubility of cholesterol in pure CO₂ was found to be approximately three times greater than that of stigmasterol, and fifty times that of ergosterol although these sterols have similar structures. Furthermore, the addition of methanol or ethanol to CO₂ increased the solubility of the sterols by up to two orders of magnitude. In studies using ascending pressure profile extraction, milk fat was stripped of 90% of its cholesterol using pure SC-CO₂ (26). The efficiency of separation was measured on each fraction collected at each pressure interval and cholesterol assayed using an AOAC procedure and GC. The extraction of cholesterol from egg yolk and blood serum was also carried out by Ong *et al.* (27;28). Pure SC-CO₂ at 45 °C and 17.7 MPa was used and the extraction carried out for about 60 min. The result obtained were comparable to classical methods for cholesterol analysis.

Polar SFs such as Freon-22 have also been used for the extraction of estrone, testosterone, estriol, cortisone, methyl testosterone and hydro-cortisone from spiked glass wool (29). Li *et al.* compared the results obtained using Freon-22 with those using pure CO₂. Extractions were performed with CO₂ at 50 °C for 30 min and with Freon-22 at 100 °C for 15 min using pressures up to 18 MPa. The extraction efficiency with Freon-22 was significantly better than that with CO₂. However, Freons are not recommended as extraction fluids owing to their adverse environmental effects.

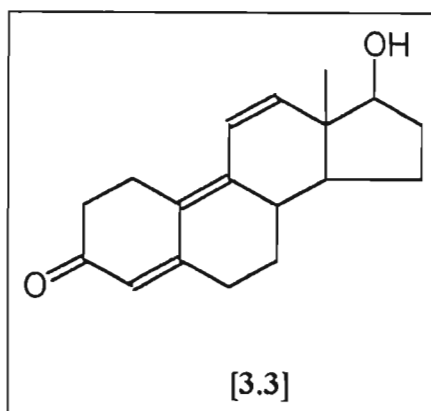
SFE was also investigated as a fast laboratory method to determine the levels of fungal infection in foodstuffs (30). The extraction of ergosterol (a fungal metabolite) from flour, mouldy bread and mushroom caps was performed using CO₂ at 40 °C and a density of 0.90 g/ml. Analyte trapping was performed using an octadecylsilyl (ODS) material. The analyte, after being washed off with methanol, was subsequently analysed by packed

column SFC on a Spherisorb amino column (3 μm) using CO_2 with 10% methanol, and employing UV detection at 282 nm. The observed levels of ergosterol ranged from 0.08 $\mu\text{g/g}$ in cake flour to 14,3 mg/g in freeze-dried mushroom caps.

Ouabain is a steroid-derived polar compound with eight hydroxyl groups. It belongs to a group of drugs known as digitalis cardioglycosides, which are derived from plants and used in the treatment of heart failure. These drugs are used at very low concentrations, that is in the 1-20 ng/ml range. On-line SFE-SFC with fraction collection was performed on this compound and important information pertaining to solute elution density, efficiency of extraction, solute trapping, and chromatography was obtained (31). The cell was packed with an adsorbent containing the sample of interest and extraction carried out with CO_2 at 400 atm, 80 $^\circ\text{C}$ for 30 min. Solute trapping was performed in a deactivated capillary solute concentrator within a cryogenic trap. The capillary solute concentrator was directly connected to the SFC column (3m X 50 μm i.d. SB-Methyl 100) and chromatography performed by density programming.

The SFE extract of the bark of *Cedrela toona* (Meliaceae) was also analysed by Modey *et al.* (32). SFE was performed with CO_2 at 40 $^\circ\text{C}$ and 39 MPa for 50 min (25 min static extraction followed by 25 min dynamic extraction). GC-MS analysis of the extract revealed the presence of stigmasterol and the 22,23-dihydro- derivative of stigmasterol.

Synthetic anabolic steroids such as trenbolone [3.3] speed muscle development in animals but are known to be hazardous to man.



Administration of anabolic steroids to food-producing animals has been prohibited in the UK since 1986, but on-going monitoring is clearly necessary. SFE was evaluated for the quantitative extraction of trenbolone from beef (33). Experiments on beef spiked with trenbolone suggested that SFE is best carried out on freeze-dried samples. The presence of methanol modifier was necessary to increase solubility and reduce matrix interaction. Extraction was near-complete (98 % recovery) within 60 min at 75 °C and 400 atm using 0.1 methanol mole fraction in CO₂. Under these conditions, extraction of fats and other endogenous materials is minimised. However, the authors stated that these results could not be used to illustrate the extraction behaviour from naturally contaminated samples, as in naturally contaminated samples, the trenbolone may, for example, be exposed to different active sites and a greater fraction of it encapsulated within cells. Despite these and other possible differences, this study does provide a useful prediction for the extraction conditions that might be required.

3.4 Flavour and Fragrance Compounds

The extraction of flavour and fragrance compounds from plants has been successfully achieved using supercritical CO₂. The sesquiterpenoid bitter principals, calamus, acorone and isoacorone present in *Acorus calamus* are thermally unstable and partially decompose using steam distillation. SFE was carried out at 9 MPa and 40 °C to successfully extract these components (34). The yield of the bitter principle improved and the decomposition problems were eliminated.

On line extraction and analysis of flavour and fragrance compounds was performed by Hawthorne *et al.* (35). Extracted components were transferred directly from the extraction cell onto the GC column via an on-column injector. A variety of samples including herbs, spices, orange peel and spruce needles were analysed to demonstrate the potential of this technique. As shown in Figure 3.5, the on-line SFE-GC results were comparable to the off-line analysis of a variety of SFE extracts which were injected manually into the GC. Cryogenic trapping at -30 °C was employed during the extraction

of thyme and compounds such as borneol, thymol and carvacrol were identified by mass spectrometry.

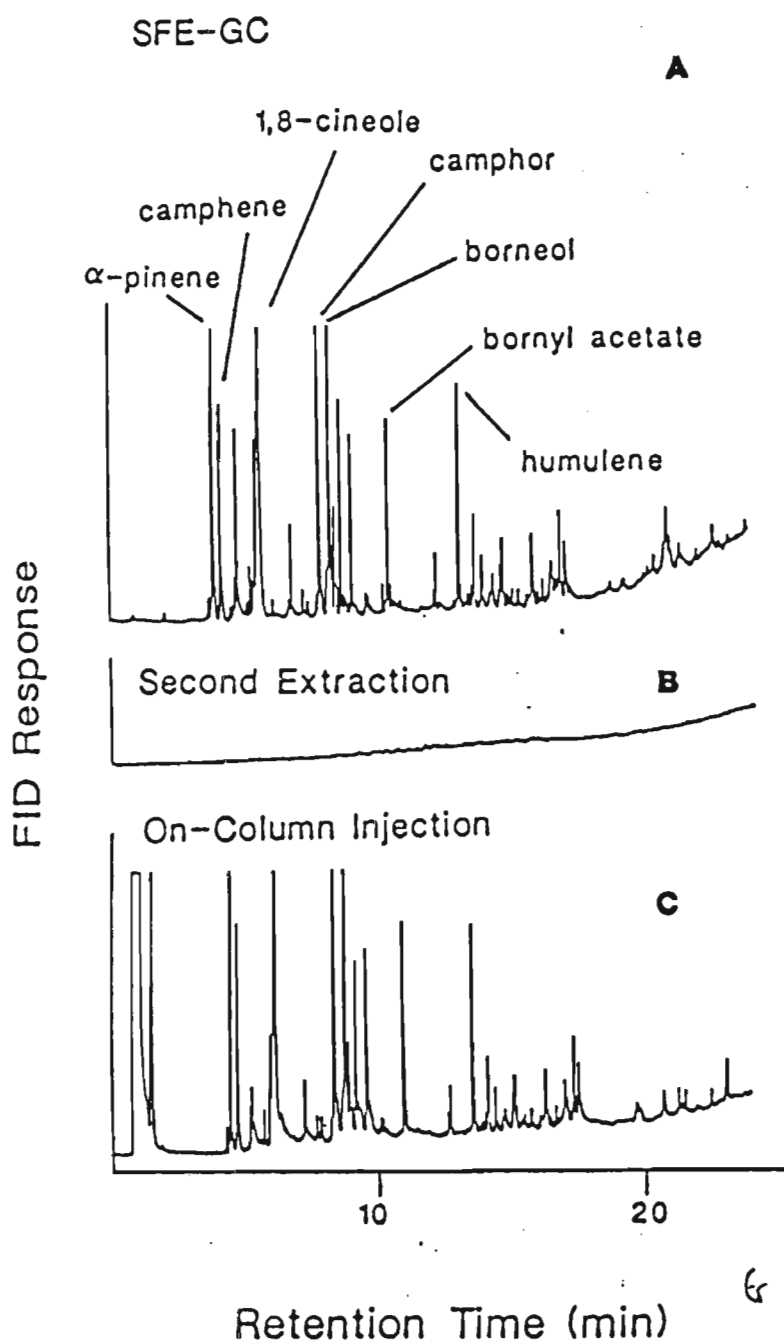


Figure 3.5. Comparison of chromatograms generated by (A) SFE-GC-FID analysis of rosemary and by (C) Standard on-column injection of a methylene chloride extract. Chromatogram (B) shows the result of a second SFE-GC-FID analysis of the same sample. (35)

The extraction of a number of herbs used in herbal remedies have also been carried out using SFE. In 1991, Ma and coworkers (36) extracted and analysed three kinds of herbs used in traditional Chinese medicine viz. frankincense, myrrh and *Evodia rutaecarpa*. SFE with CO₂ was performed at 20 MPa and 50 °C followed by GC-MS analysis. Large amounts of sesquiterpenes were found to be present in the extract of myrrh while the *Evodia* extract was found to contain monoterpenes, sesquiterpenes, diterpenes and aliphatic hydrocarbons. The study revealed the potential of SFE as an analytical tool for the study of medicinal plants.

The medicinal herb, feverfew, *Tanacetum parthenium*, was also analysed for the presence of the sesquiterpene lactone, porthenolide by GC (37, 38). Extraction was first performed using SC-CO₂ at 25 MPa and 45 °C and the analyte trapped in a cryogenically cooled flask at 17 °C using liquid nitrogen. The addition of methanol or acetonitrile as a modifier increased yields of porthenolide.

Work was performed on tumeric, the ground rhizome of the plant *Curcuma longa*, a species of the Zingiberaceae family which is native to Southern Asia (39). It is valued for its yellow-colouring components and its use as a spice, as well as being an ingredient in traditional medicines and cosmetics. SFE employing pure CO₂ at 25 MPa and 60 °C was used initially to remove low polarity components. However, CO₂ modified with 20% methanol was required to extract the more polar curcuminoids and under optimized conditions, gave more than 90% recovery of curcumin.

The plant *Zingiber zerumbet* also belongs to the Zingiberaceae family. The rhizome of this species is an important ingredient for the famous Indonesian traditional medicine, Jamu. Supercritical CO₂ at 60 °C and 20 MPa was used to extract the non-polar components of the dried rhizome of this plant (40) and analysis carried out by GC. SFE of *Z. zerumbet* was performed initially using pure CO₂ at 60 °C, and the sample was extracted sequentially at 10 MPa and then at 20 MPa. The combined SFE extracts gave a 1.92% yield compared to the dichloromethane extract which gave a 1.98% yield of the

dried plant material. The extracts were examined by capillary GC and the peaks were identified by GC-electron ionization MS and coinjection with authentic samples. Comparison of the SFE extracts with the dichloromethane extract by capillary GC showed that similar components were extracted and the composition of the SFE extracts were comparable to that of the dichloromethane extract.

Barton *et al.* (41) extracted volatile compounds from *Mentha piperita*. The flavour and fragrance of the CO₂ mint extracts were closer in quality to actual mint leaves compared with mint oils extracted by conventional steam distillation. The extraction conditions were CO₂, 6-18 MPa, 24 - 43 °C and 4-9 hours.

Simandi *et al.* (42) also reported on SFE of the leaves of *M. piperita* and found the extract to contain more of the fragrance characteristic compound menthofuran than the distilled oil. In addition, these workers extracted the flavours of *Lavandula intermedia* using a step-wise pressure programme. Unlike the SFE extract, the distilled oil contained high levels of linalool resulting from the hydrolysis of linalyl acetate once again illustrating the disadvantages of steam distillation. The results indicate that the most natural and true-tasting extracts are obtained by techniques which utilize low temperature and avoid degradative heat processes and reactive solvents. Moyler (6) has reviewed the published literature pertaining to the extraction of forty two natural botanical extracts.

SFE has also been utilized for the selective extraction of the essential oils myrcene, caryophyllene, humulene and the α - and β - bitter acids of hops, *Humulus lupulus* (43). At a density of 0.2 g/ml and a temperature of 50 °C, 98% myrcene, 91% humulene and 95% β -caryophyllene were extracted. The bitter acids only became soluble in CO₂ at 0.25 g/ml and were completely extracted at about 0.9 g/ml. The essential oils were analysed by capillary GC and the bitter acids by micro-LC and MECC.

A procedure to extract free aroma terpenic components in musts and wines was also presented by Carro *et al.* (44). Due to the high number of variables that potentially affect

SFE, experimental designs were used to simultaneously optimize the operational parameters and to establish their possible interactions. Plackett Burman Factorial designs were applied on a synthetic hydroalcoholic model solution of five terpenic compounds, linalool, α -terpineol, citronellol, nerol, and geraniol. The following experimental variables were optimized: SC-CO₂ density and flow, static and dynamic extraction times, extraction cell and trap temperatures. Best results were obtained at 0.9 g/ml at 54 °C after a static extraction time of 5 minutes followed by dynamic extraction of 40 minutes. The trap temperature was maintained at 10 °C and a CO₂ flow of 2ml/min.

The extraction of aroma compounds in fruits has also been investigated. Kerrola *et al.* (45) used on-line SFE-GC in the analysis of carvone and limonene in caraway fruits of various origins. Extractions were performed at 9.7 MPa and 50 °C. Fractionation of lemon peel oil by SFE-preparative SFC was also investigated (46,47). The SFE results indicated that CO₂ extracts were similar in composition to cold-pressed oil, but contained less limonene, 10 times the concentration of alcohols, and three to five times the concentration of linalyl acetate.

3.5 Carotenoids

The high degree of unsaturation in carotenoids has rendered them heat and light sensitive making carotenoids the most experimentally demanding group of terpenes. The polyene chain is responsible for the intense colour of the carotenoids, which are pigments that occur in many plant and animal sources (47). Many SFE studies have focused on carotenoid compounds, firstly because of their possible role in reducing the incidence of certain cancers in humans, secondly because of the provitamin A activity of β -carotene and thirdly because of the anti-oxidant activity of β -carotene.

Favati *et al.* (48) investigated SC-CO₂ for the extraction of carotene and lutein from alfalfa leaf protein concentrate (LPC). Over 90% of the carotene contained in LPC was removed at extraction pressures in excess of 30 MPa. However, the removal of lutein from the LPC required higher extraction pressures (70 MPa) to attain 70% recovery.

Extractions were performed on 45-50 gram samples of LPC and chromatographic analysis was performed using HPLC. SFE provided the possibility of obtaining a selective extraction of natural colourants free of solvent residuals for food dyes.

The SFE of carotenoids from algae has also been investigated (49, 50). Extractions from a mediterranean brown alga were conducted by applying a controlled stagewise pressure increase and different fractions in terms of colour and composition were obtained depending on the density of the extracting fluid. The pressure was stepped from 8 to 10, to 15, 20 and 25 MPa at temperatures of 35, 45 and 55 °C. Subsequent analysis of the extracts by TLC and HPLC showed the presence of β -carotene amongst many other unidentified components.

The extraction of carotenoids from foodstuffs, specifically tomato paste, canned pumpkin, spinach, red palm oil, butter and cheese was also carried out with SC-CO₂ and various modifiers (51). Static and dynamic extractions were investigated using CO₂ modified with 1% methanol, ethanol or isopropanol at pressures of 13,6-68 MPa and temperatures of 40, 55 and 70 °C. HPLC was used to confirm the presence of specific carotenoids including lycopene. A poor yield (24%) was reported for tomato paste however the yield increased to 78% when modified CO₂ was employed.

The extraction of α -carotene from sweet potatoes has also been reported (52). Supercritical CO₂ was employed at 41.4 MPa and 41 °C. The extract was found to contain about 94% α -carotene, but the yield varied depending on the moisture content of the sample, the method of sample dehydration and the particle size. Marsilli and Callahan (53) compared SFE using CO₂ with classical solvent extraction using ethanol:pentane for the extraction of carotenes from a number of vegetable samples. The SFE method proved favourable in terms of both extraction yield and speed.

3.6 Lipid materials

Pure and modified CO₂ has been successfully applied to the extraction of many lipid materials such as vegetable oils, fatty acids, fatty acid esters, phospholipids and tocopherols. Many reports have outlined the use of SC-CO₂ for large-scale (54-56) and analytical-scale (57, 58) extraction of oilseeds. Dry milled corn-germ was also extracted using supercritical CO₂ at 34-54 MPa and 50 °C (59). The oil was found to be lower in free fatty acids and refining loss and was lighter in colour compared with commercial expeller-milled oil.

Friedrich *et al.* (60) also extracted oil from soyabeans using pure SC-CO₂ at 50 °C and pressure of 68 MPa. The oil was found to be lighter in colour and to contain less iron and about one-tenth the phosphorous content as was obtained by hexane extractions on the same sample.

Tocopherols in wheat germ have also been studied extensively (61, 62). SFE was used in tandem with SFC for on-line separation of the tocopherols. SFE was performed with pure SC-CO₂ at 25 MPa and 40 °C. 0,03% tocopherol and 10% oil by weight was extracted. SFC was performed with ethanol modified CO₂ and the eluent monitored with a multiwavelength UV detector.

Prostaglandins were also selectively analysed without derivatization using SFE and open tubular column SFC (63). These C₂₀ polyunsaturated fatty acids containing a substituted cyclopentane ring, possess a strongly diversified physiological activity and are potent at sub - ppm levels. Aqueous prostaglandin samples were extracted from adsorbents onto which the samples had been loaded, using CO₂ at a density of 0,800 g/ml and at 35-50 °C. The extract was then trapped in a solute trap cooled with liquid CO₂ prior to SFC analysis. Eleven prostaglandin standards were separated in thirty five minutes using this method.

Supercritical CO₂ has shown advantages for the extraction of oils from grape seeds (64). A 3 hour extraction with CO₂ at 35 MPa and 40 °C gave similar yields to a 20 hour Soxhlet extraction with hexane. The SFE extract had a lower percentage of free fatty acids and unsaponifiables than the solvent extract and did not require degumming or alkali refining. Further, extraction with CO₂ at low temperature enabled the seed proteins to be recovered. These are normally denatured on extraction with hot organic solvents.

The extraction of polar phospholipids from soyabeans has also been investigated (65). A two step extraction sequence was performed. Initial extraction aided in the removal of the soyabean oil while the second extraction with ethanol modified CO₂ was undertaken to isolate the phospholipid enriched fractions. Analysis were performed by HPLC. It was observed that at methanol mole fraction of 0.52, the recovery of phospholipids was very low, however recoveries increased considerably to around 10 g/kg of soyabean using 0.102 and 0.162 mole fractions of ethanol respectively.

The quantitative extraction of pecan oil was undertaken by Maness *et al.* (66) employing CO₂ as the extraction solvent, and chilled hexane as the trapping solvent. The fatty acid composition for the total lipid fraction of oils extracted as well as the total oil content obtained with SFE was the same as for oils extracted with organic solvents. Extraction was carried out at 69 MPa and 75 °C with a 250 ml/min restrictor for specified durations.

The extraction of fatty and waxy material from rice bran was also investigated with SC-CO₂ at pressures up to 28 MPa and temperatures between 40 and 70 °C (67). Although the yields obtained with SF were only 16-60% of those obtained by Soxhlet extraction with hexane, the extract was lighter in colour and richer in wax content and long chain fatty acids C₂₀-C₃₄.

3.7 Miscellaneous applications

SFE has been employed for the extraction of taxanes. SFE of taxicin from the dried needles of the English yew tree, *Taxus baccata* was carried out at 400 atm and 50 °C with

pure CO₂ (68). Extraction times varied between 15 and 105 minutes and restrictor temperatures were between 100 and 175 °C. Subsequent analysis by SFC and proton NMR confirmed the identity and purity of taxicin. SFC was performed on 10 m × 50 μm i.d. SB-Biphenyl-30 (30% biphenyl-substituted polydimethylsiloxane) or carbowax column. Pure CO₂ was used as the mobile phase, the oven temperature was 120 °C and sample introduction was via a 50 nl timed-split injection valve. The extraction efficiency of SFE was comparable with that obtained using liquid solvents.

Furanocoumarins are representatives of the compounds commonly present in higher plants from the Umbelliferae and Rutaceae families. Linear furanocoumarins have been found to exhibit a pronounced photosensitizing activity and have thus been used in clinical treatment of skin lesions (psoriasis and vitiligo) (69, 70). The fruit of *Archangelica off. Hoffm.* constitute one of the richest sources of furanocoumarins. SFE has been successfully employed in the extraction of these compounds. Fractionating SFE was performed by varying both the temperature and pressure of CO₂. Under optimal conditions, the overall SFE recoveries of the compounds extracted were close to those obtained by soxhlet extraction (71).

The isolation of sulfonamides from chicken eggs has also been carried out using SFE (72). Sulfonamides are routinely used in veterinary medicine in raising cattle and poultry because of their broad range of activity against gram-positive and gram-negative bacteria. Whole egg was mixed with hydromatrix and the sample extracted at 40 °C with SC-CO₂ at 680 bar. The sulfonamides were trapped in-line on an alumina sorbent bed and eluted with phosphate buffer and methanol for subsequent analysis by HPLC.

From this literature review, it has become quite evident that SFE has a wide application area and is capable of extracting a wide range of diverse compounds from a variety of sample matrices. Although SFE does not provide the solution to every problem, the use of SFE in other areas of natural products still await investigation.

References

1. E. Klesper, A.H. Corwin and D.A. Turner, *J. Org. Chem.*, **27** (1962), 700.
2. C.D. Bevan and P.S. Marshall, *Nat. Prod. Rep.*, **11** (1994), 451.
3. H. Engelhardt and A. Gross, *Trends in Analytical Chemistry*, **10** (1991), 64.
4. P. Hubet and O.G. Vitzthum, *Angew. Chem. Int. Ed.*, **17** (1978), 710.
5. D.F. Williams, *Chemical Engineering Science*, **36** (1981), 1769.
6. D.A. Moyer, In: *Extraction of Natural products using Near-critical Solvents*, M.B. King and T.R. Bott, (Eds.). Blackie, Glasgow, UK (1993), p.149.
7. S.S.H. Rizvi, *Supercritical Fluid Processing of Food and Biomaterials*, Blackie, Glasgow, UK (1994), p.12.
8. S.R. Sargenti and F.M. Lancas, *J. High Resol. Chromatogr.*, **20** (1997), 511.
9. J. Mann, R.S. Davidson, J.B. Hobbs, D.V. Banthorpe and J.B. Harborne, *Natural Products, their Chemistry and Biological Significance*, Longman Group, London, UK (1994), p.389.
10. K. Sugiyama, M. Saitto, T. Hando and M. Senda, *J. Chromatogr.*, **332** (1985), 107.
11. D.P. Ndiomu and C.F. Simpson, *Anal. Chim. Acta.*, **213**, (1988), 237.
12. J.L. Janicot, M. Cauder and R. Rosset, *J. Chromatogr.*, **505** (1990), 247.
13. P. Elizabeth, M. Yoshioka, Y. Yamauchi and M. Saito, *Anal. Sci.*, **7** (1991), 427.
14. S.T. Schaeffer, L.H. Zalkow and A.S. Teja, *AIChE Journal*, **34** (1988), 1740.
15. S.T. Schaeffer, L.H. Zalkow and A.S. Teja, *Ind. Eng. Chem. Res.*, **28** (1989), 1017.
16. C. Bicchi, P. Rubiolo, C. Frattini; P. Sandra and F. David, *J. Nat. Prod.*, **54** (1991), 941.
17. A.K. Sharma, B. Prokopczyk and D. Hoffmann, *J. Agric. Food Chem.*, **39** (1991), 508.

18. S. Kyu-Min, Y, Ji-Ho, L. Huen, H. Won-Hi and Y. Seung-Man. *Biochemical Engineering 2001, Proceedings of the Asian-Pacific Biochemical Engineering Conference* (1992), p.566.
19. G.B. Boder, M.Gorman, I.S. Johnson and P.J. Simpson, *Lloydia*, **27** (1964) 328.
20. Y. Miura, K. Hirata, N. Kurando, K. Miyamoto and K. Uchida, *Planta Med.*, **54** (1988), 18.
21. C. Bugatti, M.L. Colombo and A. Mossa, *Planta Med.*, **59** (1993), A626.
22. J.F. Morrison and W.A. MacCrehon, *Proc. 5th Int. Symp. Supercrit. fluid Chromatogr. Extr.*, Baltimore, MA., USA (1994), p.F16.
23. V. Lopez-Avila, J. Benedicto and D. Robaugh, *J. High. Resol. Chromatogr.*, **20** (1997), 231.
24. H. Stuppner, S. Sturm and G. Konwalinka, *Chromatographia*, **34** (1992), 597.
25. J.M. Wong and K.P. Johnstone, *Biotechnol. Prog.*, **2** (1986), 29.
26. R.L. Bradley Jr., *J. Dairy Sc.*, **72** (1989), 2834.
27. C.P. Ong, H.L. Lee and S.F.Y. Li, *J. Chromatogr.*, **515** (1990); 509.
28. C.P. Ong, H.L. Lee and S.Y.F. Li, *J. Microcol. Sep.*, **2** (1990) 69.
29. S.F.Y. Li, C.P. Ong, M.L. Lee and H.K. Lee, *J. Chromatogr.*, **515** (1990), 515.
30. J.C. Young and D.E. Games, *J. Agric. Food Chem.*, **41** (1993), 577.
31. Q.L. Xie, K.E. Markides and M.L. Lee, *J. Chromatogr. Sci.*, **27** (1989), 365.
32. W.K. Modey, D.A. Mulholland, H. Mahomed and M.W. Raynor, *J. Microcol. Sep.*, **8** (1996), 67.
33. N. Din; K. D. Bartle and A.A. Clifford, *J. High Resol. Chromatogr.*, **19** (1996), 465.
34. E. Stahl and K. Keller, *Planta Med.*, **47** (1983), 75.
35. S. B. Hawthorne, M. S. Krieger and D. J. Miller, *Anal. Chem.*, **60** (1988), 472.
36. X, Ma, X. Yu, Z. Zheng and J. Mao, *Chromatographia*, **32** (1991), 40.
37. R. M. Smith and M. D. Burford, *J. Chromatogr.*, **627** (1992), 255.
38. R. M. Smith and M. D. Burford, *J. Chromatogr.*, **600** (1992), 175.

39. M. M. Sanagi, U. K. Ahmad and R. M. Smith, *J. Chromatogr. Sci.*, **31** (1993), 20.
40. U. K. Ahmad, H. M. Sirat, M. M. Sanagi and R. M. Smith, *J. Microcol. Sep.*, **6** (1994), 27.
41. P. Barton, R.E. Hughes, Jr. and M. M. Hussein, *J. Supercrit. Fluids*, **5** (1992), 157.
42. B. Simandi, A. Kery, E. Lemberkovics, M. Oszagyan and E. Hethelyi, *Planta Med.*, **59** (1993), A626.
43. M. Verschuere, P. Sandra and F. David, *J. Chromatogr. Sci.*, **30** (1992), 388.
44. N. Carro, C. M. Garcia and R. Cela, *J. Microcolumn Sep.*, **8** (1996), 453.
45. K. Kerrola, P. Alhonmaki and H. Kallio, *Proc. 5th Int. Symp. Supercrit. Fluid Chromatogr. Extr.*, Baltimore, MA, USA (1994), p.E2.
46. Y. Yamauchi and M Saito, In: *Fractionation by Packed column SFC and SFE*, M. Saito, Y. Yamauchi & T. Okuyama (Eds.), VCH publishers, New York, USA (1994), p.69.
47. R. Ramage in *Chemistry of Terpenes and Terpenoids*, A. A. Newman (Ed.), Academic Press Inc., London (1972), p.288.
48. F. Favati, J.W. King, J. P. Friedrich and K. Eskins, *J. Food Sci.*, **53** (1988), 1532.
49. T. Lorenzo, S.J. Schwartz and P. K. Kilpatrick, In: *Proc. Int. Symp. Supercrit. Fluids*, M. A. Mchugh (Ed.), (1991), p.297.
50. P. Subra and P. Boissinot, *J. Chromatogr.*, **543** (1991), 413.
51. L. H. Tonucci and G. R. Beecher, *Proc. 4th Int. Symp. Supercrit. Fluid Chromatogr. Extr.*, Cincinnati; OH, USA (1992), p.119.
52. G. A. Spanos, H. Chem and S. J. Schwartz, *J. Food Sci.*, **58** (1993), 817.
53. R. Marsilli and D. Callahan, *J. Chromatogr. Sci.*, **31** (1993), 422.
54. D.D. Christianson, J. P. Friedrich, E.B. Bagley and G. E. Inglett, In: *Maize: Recent Progress in Chemistry and Technology*, G.E. Inglett (Ed.), Academic Press, New York, USA (1982), p.231.

55. G. R. List, J. P. Friedrich and J. Pominski, *J. Am. Oil. Chem. Soc.*, **61** (1984), 1847.
56. C. A. Passey and N. D. Patil, in *Proceedings of the 2nd International Conference on Separations Science and Technology*, M. H. I. Baird & S. Vijayan (Ed.), Canadian Society for Chemical Engineering, Ottawa, Canada (1989), p.57.
57. S. L. Taylor, J. W. King and G. R. List, *J. Am. Oil. Chem. Soc.*, **70** (1993), 437.
58. J. W. King and J. H. Johnson, in *Proc. 5th Int. Symp. Supercrit. Fluid Chromatogr. Extr.*, Cahnes Publishing, Des Plaines (1994), p.13.
59. D. D. Christianson, J. P. Friedrich, G. R. List, K. Warner, E. B. Bagley, A.C. Stringfellow and G.E. Inglett, *J. Food Sci.*, **49** (1984), 229.
60. J.P. Friedrich, G.R. List and A.J. Heakin, *J. Am. Oil Chem. Soc.*, **59** (1982), 288.
61. M. Saito, T. Hondo and Y. Yamauchi, *In: Supercritical Fluid Chromatography*, R.M. Smith (Ed.), Royal Society of Chemistry, London, UK (1988), p.203.
62. M. Saito, Y. Yamauchi, K. Inomata and W. Kottkamp, *J. Chromatogr. Sci.*, **27** (1989), 79.
63. I.J. Koski, B.A. Jansson, K.E. Markides and M.L. Lee, *J. Pharm. Biomed. Anal.*, **9** (1991), 281.
64. A. Molero Gomez, W.Huber, C. Pereyra Lopez and E. Martinez la Ossa, *Proc. 3rd Int Symp. Supercrit. Fluids.*, Strasourg, France (1994), p.413.
65. L.Montanori, J.W. King, G.R. List and K.A. Rennick, *Proc 3rd Int. Symp. Supercrit. Fluids.*, Strasbourg, France (1994), p.497.
66. N.O. Maness, D. Chrz, T. Pierce and G.H. Brusewitz, *J. Am. Oil Chem. Soc.*, **72** (1995), 665.
67. A. Garcia, A. de Lucas, J. Rincon, A. Alvorez, I. Gracia and M.A. Garcia, *J. Am.Oil Chem. Soc.*, **73** (1996), 1127.
68. D.M. Heaton, K.D. Bartle, C.M. Rayner and A.A. Clifford, *J. High Resolut. Chromatogr.*, **16** (1993), 666.
69. J. Willis and D.E.R. Harris, *Arch. Dermat.*, **107** (1973), 358.
70. V. Wolf, T.B. Fitzportick and J.A. Parrish, *Arch Dermat.*, **112** (1976), 943.

71. J. Gawdzik, S. Kawka, M. Mardarowicz, Z. Suprynowicz and T. Wolski, *J. High Resol. Chromatogr.*, **18** (1995) 781.
72. J.W. Pensabene, W. Fiddler and O.W. Parks, *J. Chromatogr. Sci.*, **35** (1997) 270.

CHAPTER 4

Separation techniques

4.1 Introduction

Plant extract analysis for phytoremediation and the development of phytochemicals for medicinal applications requires the characterisation of a wide variety of compounds. Analysing the extracts of plants involves matrices that are unavoidably complex and often requires manipulation of a mixture of components with varying solubilities and volatilities present in different proportions. Many different chromatographic techniques have been applied to the separation and identification of individual components from these matrices (1-3) depending on the requirements to be fulfilled in order to achieve an effective separation. More recently, capillary electrophoretic techniques have also found use in the analysis of plant extracts (4-6). This chapter outlines the basic conditions and theory of the chromatographic and capillary electrophoretic processes used in the characterisation of plant extracts. The general equations applicable to gas chromatography (GC), supercritical fluid chromatography (SFC), liquid chromatography (LC) and capillary electrophoresis (CE) are discussed.

4.2 Theory of Chromatography

Chromatography is defined as a separation method whereby individual chemical compounds which were originally present in a mixture are resolved from each other by the selective process of distribution between two heterogeneous (immiscible) phases. The distribution of chemical species to be separated occurs in a dynamic process between the mobile and the stationary phase (7). The stationary phase is a dispersed medium, which usually has a relatively large surface area, through which the mobile phase is allowed to flow. The chemical nature of the stationary phase exercises the primary control over the separation process (8). The greater the affinity of a particular solute for the stationary medium, the longer it will be retained in the system. The mobile phase can be either gas,

liquid or supercritical fluid hence the name gas, liquid or supercritical fluid chromatography. Each technique has its own niche. For example, GC is most useful for small volatile molecules that are thermally stable whereas SFC is often applied to thermally labile compounds and those which are too involatile to be analysed by GC. HPLC is usually used to separate polar and high molecular weight compounds and is the technique which is most appropriate for the majority of sample types which are not amenable to GC or SFC.

All chromatographic separations are based upon differences in the extent to which solutes are partitioned between the mobile and the stationary phase. The equilibrium involved can be described quantitatively by means of a partition coefficient K_i , for each solute (i) in the sample which for chromatography is defined as

$$K_i = \frac{C_{i,s}}{C_{i,m}} \quad (4.1)$$

Here, $C_{i,s}$ and $C_{i,m}$ are the concentrations of a solute in the stationary phase and mobile phases respectively.

The distribution of each solute between the stationary and mobile phase is described by the capacity factor (k')

$$k' = \frac{x_{i,s}}{x_{i,m}} = \left(\frac{C_{i,s}}{C_{i,m}} \right) \left(\frac{V_s}{V_m} \right) = \frac{K_i}{\beta} \quad (4.2)$$

where x represents the masses of components i (in each phase), V_s and V_m are the volumes of the stationary and mobile phases, respectively, and β is the phase ratio of the column, that is,

$$\frac{V_m}{V_s}$$

Figure 4.1 shows a typical chromatogram and its characteristic features.

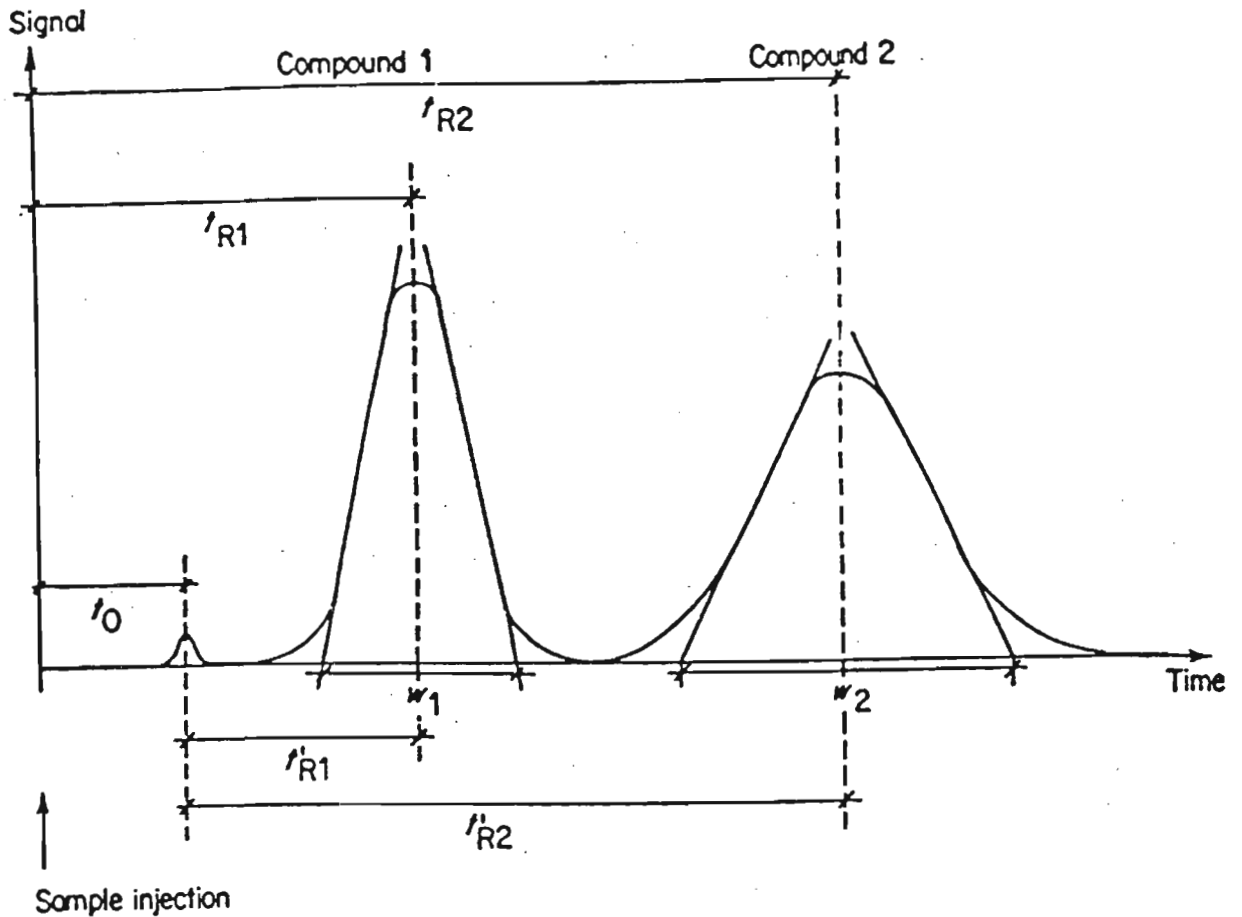


Figure 4.1 A chromatogram with its characteristic features.

Here w is the peak width at the baseline and t_0 is the dead time or retention time of an unretained solute (i.e. the time required by the mobile phase to pass through the columns). Hence the average linear flow velocity, \bar{u} can be calculated as

$$\bar{u} = \frac{L}{t_0} \quad (4.3)$$

where L is the column length. The retention time t_r is the period between sample injection and recording of the peak maximum while t'_r is the net retention time. Two compounds can be separated if they have different retention times. Figure 4.1 shows that

$$t_r = t_0 + t'_r. \quad (4.4)$$

The retention time of a solute is a function of mobile phase flow velocity and column length. If the mobile phase is flowing slowly or if the column is long, then t_o is large and hence so is t_r . Therefore t_r is not suitable for characterising a compound and instead, the capacity factor, also known as the k' value is preferred:

$$k' = \frac{t'_r}{t_o} = \frac{t_r - t_o}{t_o} \quad (4.5)$$

The capacity factor is independent of the column length and mobile phase flow-rate (provided that \bar{u} does not exceed 5 cm s^{-1})

4.2.1 Column Efficiency

Efficiency is used to describe the potential separation capabilities of the chromatographic system. The results are expressed in terms of theoretical plates (n), which can be thought of as a certain number of separation stages. The more stages in a given separation, the higher the column efficiency (n). There are several ways to calculate n from the chromatogram. The most simple approach utilizes the retention time (t_r) and the baseline width (w).

$$n = 16 \left(\frac{t_r}{w} \right)^2 \quad (4.6)$$

As the column length (L) increases, n increases. In order to compare the efficiencies of columns of different lengths, the height equivalent to a theoretical plate, *HETP*, is used instead of n :

$$HETP = \frac{L}{n} \quad (4.7)$$

4.2.2 Selectivity

The ease of separating two different components on a column is given by the selectivity, α . It is calculated from the ratio of k' values and is always expressed as a number greater than 1.

$$\alpha = \frac{k'_2}{k'_1} \quad (4.8.)$$

where k'_1 , and k'_2 are the capacity factors of each component and k'_2 is the capacity factor of the later eluting component. Conceptually, α represents the spacing between peak maxima. With a large α (wide spacing), components separate and as α approaches unity, the peaks fuse.

In GC, selectivity is a result of the vapour pressure of the solute and intermolecular force interactions with the stationary phase. In LC and SFC, the selectivity can also be affected by interactions between solutes and the mobile phase. The interactions can either be by dispersion, dipole-dipole or dipole-induced dipole. Dispersion interactions account for separations based on differences in solute boiling points and sizes. Dipole-dipole interactions account for separations of polar compounds on a polar stationary phase and dipole-induced dipole interactions occur when dipolar solute molecules act as an electron donor or electron acceptor.

4.2.3 Resolution

The basic equation defining the resolution (R), between any two compounds is:

$$R = \frac{2\Delta t}{(w_{b1} + w_{b2})} \quad (4.9)$$

In terms of the column efficiency, n , the selectivity, α , and the capacity factor, k' , R is given by:

$$R = \frac{n^{1/2}}{4} \left(\frac{\alpha - 1}{\alpha} \right) \left(\frac{k_2}{1 + k_2} \right) \quad (4.10)$$

4.2.4 The van Deemter equation in Chromatography

A number of valuable concepts are embraced by the van Deemter equation (7), which permits evaluation of the relative importance of a series of parameters on column efficiency and relates H to the average mobile phase linear velocity \bar{u} .

For packed columns

$$H = 2\lambda d_p + \frac{2D_m}{\bar{u}} + \frac{d_p^2 (1 + 6k' + 11k'^2) \bar{u}}{24D_m (1 + k')^2} \quad (4.11)$$

where d_p is the column packing particle diameter and λ is the eddy diffusion coefficient. D_m is the diffusion coefficient of the solute in the mobile phase.

Simplifying the equation becomes

$$H = A + \frac{B}{\bar{u}} + C\bar{u} \quad (4.12)$$

The A term includes packing and multi-flowpath factors, B is the longitudinal diffusion term and C is the resistance to mass transfer term. The A term can be influenced by particle size, geometry and tightness of packing of the stationary phase in a packed column while the B term arises from the tendency of molecules to migrate from the concentrated central part of a band towards more dilute regions on either side and is directly proportional to the rate of diffusion of the solute in the mobile phase and inversely proportional to the linear velocity of the mobile phase. The above equation can also be represented graphically in Figure 4.2 which shows the effect of H with changes in mobile phase linear velocity. Equation 4.12 represents a hyperbola that has a minimum at linear velocity (u_{opt})

$$u_{opt} = \frac{B^{1/2}}{C} \quad (4.13)$$

and a minimum H value (H_{min}) at $A + 2(BC)^{1/2}$. The constants may be graphically calculated from an experimental plot of H versus mobile phase linear velocity as shown in Figure 4.2. From this figure it can be seen that the A term ($2\lambda d_p$) is independent of mobile phase linear velocity. The second term is a measure of the effect of molecular diffusion on zone spreading and becomes significant at very low flow rates. The third term accounts for resistance to mass transfer and this term becomes significant at higher mobile phase linear velocities.

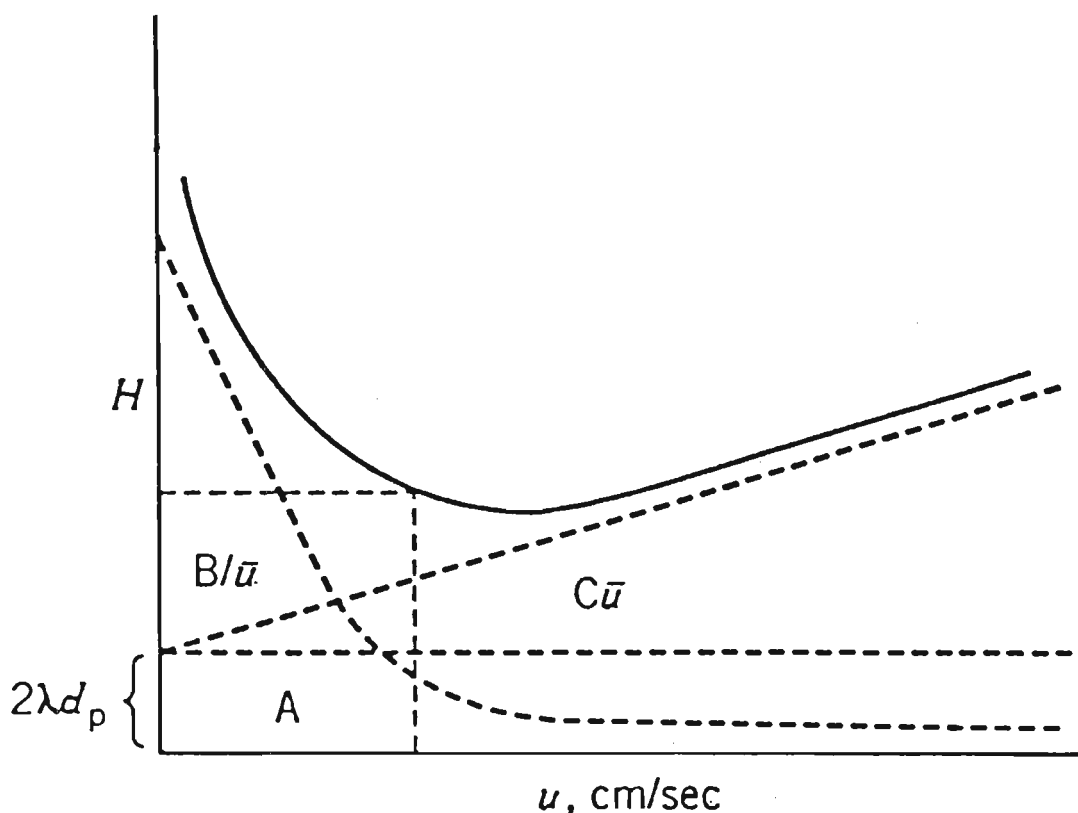


Figure 4.2 van Deemter plot

Change in H versus linear mobile phase velocity u .

$$H_{min} = A + (2BC)^{1/2}, \quad u_{opt} = (B/C)^{1/2}$$

Open tubular columns contain no packing and the A term becomes zero, reducing the van Deemter equation to a form known as the Golay equation (8):

$$H = \frac{2D_m}{u} + \frac{d_c^2 (1 + 6k' + 11k'^2) \bar{u}}{96D_m (1+k')^2} + \frac{2k'd_f^2 \bar{u}}{3(1+k')^2 2D_s} \quad (4.14)$$

where d_f is the stationary phase film thickness, d_c is the column internal diameter and D_s is the diffusion coefficient of the solute in the stationary phase. Simplifying, the equation becomes:

$$H = \frac{B}{\bar{u}} + C_m \bar{u} + C_s \bar{u} \quad (4.15)$$

The C term results because of laminar flow through the open tube which gives rise to the characteristic parabolic velocity profile over the tube cross section. Solutes in the centre of the flow move faster than solutes near the wall. Failure of the solute to rapidly diffuse in a radial direction tends to keep the solute distributed on streamlines of differing velocity, thus broadening the peak. The C_s term is usually negligible if thin films are used but can become appreciable if thick films are used. By differentiation of equation 4.15, it can be seen that the optimum mobile phase velocity (i.e. the velocity that produces a minimum value for H and maximum value for n) is:

$$u_{opt} = \frac{B^{1/2}}{C} = \frac{4.2D_m}{d_c} \quad (4.16.)$$

4.3 Theory of electrophoretic separation

Another technique receiving attention for the analysis of natural products is capillary electrophoresis. It is a separation technique that has rapidly developed over the past few years and has been widely applied to the analysis of macromolecules, amino acids, chiral drugs, vitamins, inorganic acids, proteins and peptides (9).

Electrophoresis is defined as the differential movement of charged species by attraction or repulsion in an electric field hence CE permits the rapid and efficient separations of charged components present in small volumes. Separations are based on the differences in electrophoretic mobilities of ions in electrophoretic media inside small capillaries.

4.3.1 Background electrolyte

The electrophoresis buffer is of key importance in CE because its composition fundamentally determines the migration behaviour of the analytes. A suitable electrolyte must ensure the correct electrophoretic behaviour of all individual solutes, the overall stability of the system and satisfactory separation of the analytes. A wide variety of electrolyte systems have been used in CE to effect the required separations. The majority of these are aqueous buffers. Table 4.1 lists some commonly used buffers in CE.

Table 4.1 Commonly used buffers in CE (4).

* See list of abbreviations

Buffer	Useful pH range
Borate	8.24 - 10.24
Phosphate	1.12 - 3.12
Acetate	3.75 - 5.75
Phosphate	6.21 - 8.21
* Zwitterionic buffers	
MES	5.15 - 7.15
PIPES	5.80 - 7.80
HEPES	6.55 - 8.55
Tricine	7.15 - 9.15
Tris	7.30 - 9.30

The choice of the electrolyte system in a CE separation involves consideration of many factors, such as the solubility and stability of the analytes in the electrolyte, the degree of ionization of the analytes, the influence of the anions and cations present in the electrolyte on the electromigration of the solutes, the effect of pH, the effects of organic modifiers and other additives, and the dissipation of heat generated in the electrolyte during the passage of the current.

4.3.2 Instrumentation

The equipment consists of five units: the anode and the cathode reservoirs with the corresponding electrodes, the separation capillary, the injection system and the detector. The basic instrumental setup to accomplish capillary electrophoresis is depicted in Figure 4.3.

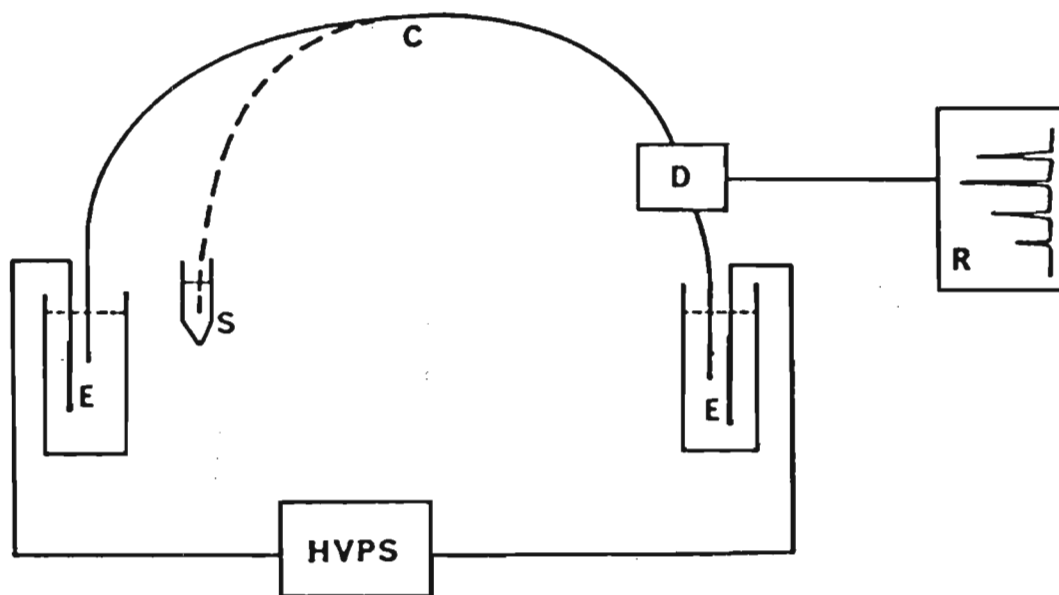


Figure 4.3 Basic Scheme of a CE instrument

- C = separation capillary;
- E = electrolyte reservoirs with platinum electrodes
- S = sample vial
- D = detector
- R = signal recorder

A capillary tube filled with the buffer solution is placed between two buffer reservoirs. The electric field is applied by means of a high voltage power supply which can generate voltages up to 30 kV. Injection of the sample is performed by replacing one buffer reservoir with the sample vial and a defined sample volume is introduced into the capillary by either hydrodynamic flow or electromigration. An on-column ultraviolet absorbance detector is located at the end of the capillary which is opposite to the injection side. If an uncoated open-tube fused silica capillary is used as the separation chamber, two electrokinetic actions occur under the influence of the electric field. First electrophoresis of the ions takes place, secondly, electroosmosis, which takes place due to the immovable charge of the capillary walls being effective from the basic to the weak acid pH range. Separation, however, is based solely on electrophoresis while electroosmosis causes a liquid transport analogous to a mechanical pump. Because the electroosmosis flow in aqueous solution is mostly directed toward the cathode, the sample is injected at the anode. The sample components migrate with different migration velocities, depending on their charge densities, towards the corresponding electrodes. They are all carried through the detection system by the electroosmotic flow (EOF), which is higher than the migration velocities of the ions.

4.3.3 Electrophoresis

Electrophoresis is the movement of charged particles in response to the applied field. Upon the application of a constant electric field E ($E = V/L$ where V is the voltage applied across the capillary of length L), ionic species undergo an electrostatic force, F_e , which is proportional to the electric field strength and the charge (q) of the particular ion. This electric force can be given by:

$$F_e = qE \quad (4.17)$$

This force causes the acceleration of ions toward the oppositely charge electrode. As the velocity of the ions increases, the counteracting frictional force (F_f) caused by the surrounding solution slows down the species. The frictional force (assuming a spherical ion) can be expressed in terms of Stokes law as:

$$F_f = 6\pi\eta r v \quad (4.18)$$

where η is the solution viscosity; r , the ion radius and v is the ion velocity.

After reaching a steady state, the ions move with a constant velocity (v) which is proportional to the applied electric field and is given by

$$v = \mu_e E \quad (4.19)$$

where μ_e is the electrophoretic mobility and is a characteristic property of a given medium at a given temperature.

During electrophoresis: $F_e = F_f$

(4.20)

hence: $qE = 6\pi\eta r v$ (4.21)

Solving for velocity:

$$v = \frac{qE}{6\pi\eta r} \quad (4.22)$$

and substituting equation 4.22 into equation 4.19 yields an equation that describes the electrophoretic mobility in terms of physical parameters:

$$\mu_e = \frac{q}{6\pi\eta r} \quad (\text{cm}^2\text{V}^{-1}\text{s}^{-1}) \quad (4.23)$$

Hence small, highly charged species have high mobilities whereas large, minimally charged species have low mobilities.

4.3.4 Electroosmosis and the electrical double layer

Electroosmosis of ions is an important phenomenon in CE and originates from the negative charges on the innerwall of the capillary tube. In uncoated fused silica capillaries, an electric double layer is formed from the ionization of silanol groups present on the surface of the capillary. The double layer (Figure 4.4) is generally explained using the Gouy-Chapman model (11-14). According to this treatment, the double layer consists of a fixed layer of negative charges and a positive part formed by a net excess of positive

ions in the background electrolyte. The cations are arranged in two layers, a fixed layer (Stern layer) and a diffuse layer, and at a position just outside of the compact-diffuse layer interface a plane of shear is established.

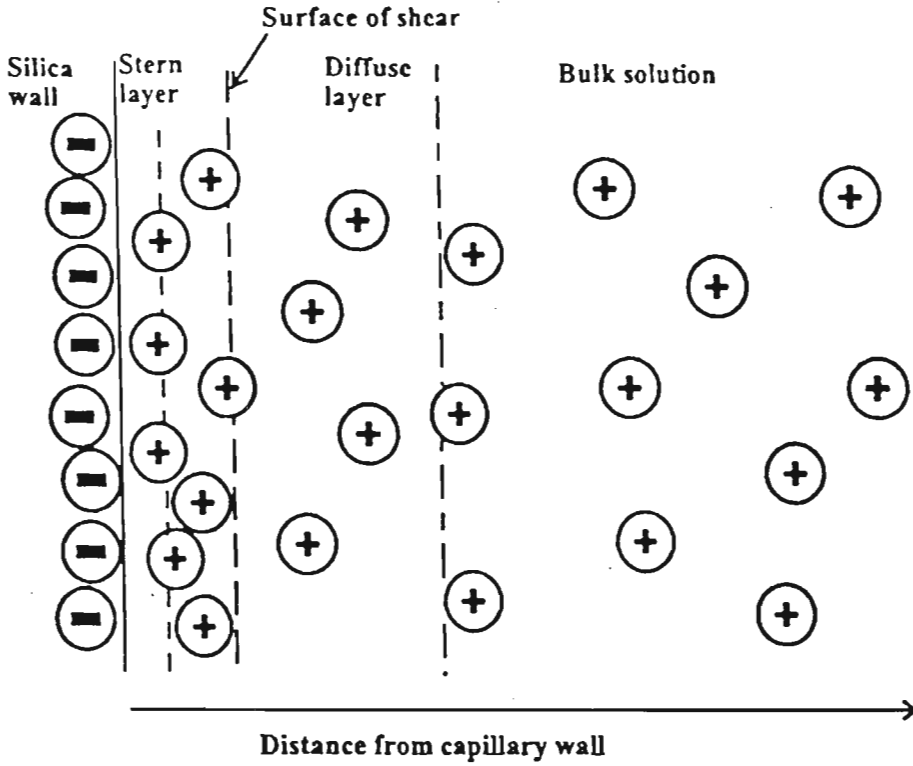


Figure 4.4 Double layer structure at a silica wall.

The potential at this boundary is known as the zeta potential, ζ . The potential in the diffuse layer falls exponentially to zero. The negative charge on the capillary surface is balanced by the positively charged layer of hydrated cations. Upon application of the electric field, this layer begins to move toward the cathode and, owing to viscous drag, transports the bulk liquid inside the capillary. The zeta potential (ζ), is given by the Helmholtz equation:

$$\zeta = \frac{4\pi\eta\mu e}{\epsilon} \quad (4.24)$$

where η is the viscosity, ϵ is the dielectric constant of the solution, and μ_e is the electrophoretic mobility. The linear velocity, v , of the electroosmotic flow is given by

$$v = \frac{\epsilon}{4\pi\eta} E\zeta \quad (4.25.)$$

The double layer is typically a very thin layer (up to several hundred nanometers) relative to the radius of the capillary (typically 50-100 μm). Therefore, the electroosmotic flow may be considered to originate at the walls of the capillary.

The magnitude of the zeta potential is determined by the surface charge on the capillary wall. This charge is pH dependent; thus the magnitude of EOF varies with pH. At high pH, the silanol groups are predominantly deprotonated and the EOF is much greater than at low pH where the silanol groups become protonated. The EOF can vary by more than an order of magnitude between pH 2 and 12. The pH and applied voltage have been found to increase flow linearly. The zeta potential is also dependent on the ionic strength of the buffer. Increased ionic strength leads to double layer compression, decreased zeta potential and reduced EOF.

4.3.5 Efficiency

Efficiency is gauged by the number of theoretical plates generated by the column. In CE, the number of theoretical plates is not dependent on the length of the column as in HPLC or GC but rather on the applied voltage as expressed in equation 4.26.

$$N = \frac{\mu V}{2D_m} \quad (4.26)$$

where μ is the mobility and V is the applied voltage.

4.3.6 Flow Profile

An important feature of the electroosmotic flow is its velocity flow profile. In an electrically driven system, the liquid flow caused by electroosmosis shows a plug profile

driving force is uniformly distributed along the capillary. Consequently, a uniform flow velocity vector across the tube occurs. Unlike in pressure-driven flow system such as HPLC, frictional forces at the liquid-solid boundaries cause a strong pressure drop across the capillary. These forces result in a laminar or parabolic flow profile. As a consequence, a cross-sectional velocity gradient occurs within the capillary resulting in a velocity profile such that the velocity vector is highest in the middle of the tube and goes toward zero approaching the walls. Hence zone broadening caused by the laminar flow profile in HPLC is therefore negligible in CE. Figure 4.5 illustrates the velocity profiles of liquid flowing in a capillary under the action of (a) electroosmosis and (b) hydrostatic pressure.

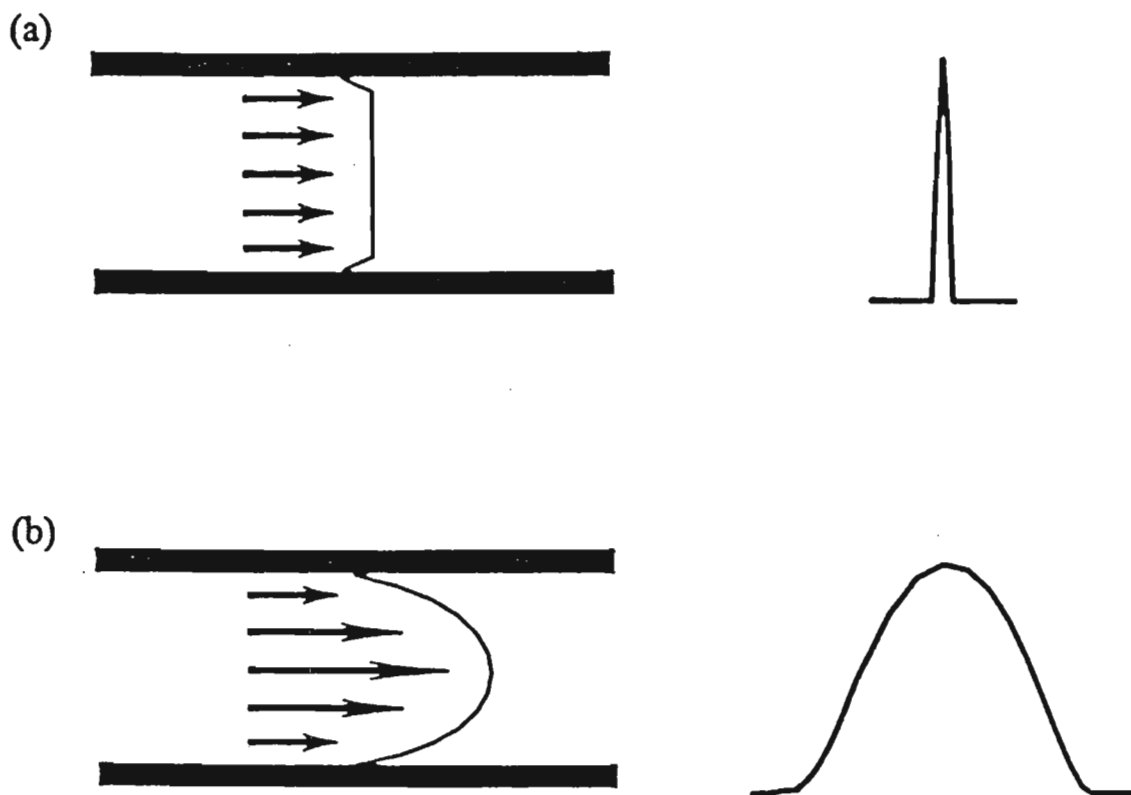


Figure 4.5 Velocity profiles of liquid flowing in a capillary under the action of (a) electroosmosis and (b) hydrostatic pressure.

4.3.7 Modes of capillary electrophoresis.

The versatility of CE is partially derived from its numerous modes of operation. The separation mechanisms of each mode are different and thus can offer orthogonal and complementary information. The basic methods encompassed by CE include capillary zone electrophoresis (CZE), micellar electrokinetic capillary chromatography (MECC), capillary gel electrophoresis (CGE), capillary isoelectric focusing (CIEF), and capillary isotachopheresis (CITP). In this study MECC was used in the separation of the plant extracts as a complementary technique to the other chromatographic methods employed and is hence the only mode that is discussed further.

4.3.7.1 Micellar Electrokinetic Capillary Chromatography

Micellar electrokinetic chromatography (MECC) is a mode of CE in which surfactants are added to the buffer solution. Surfactants are molecules which exhibit both hydrophobic and hydrophilic character. They have polar “head” groups that can be cationic, anionic, neutral, or zwitterionic and they have nonpolar, hydrocarbon tails. The formation of micelles or “micellization” is a direct consequence of the “hydrophobic effect.” The surfactant molecules can self-aggregate if the surfactant concentration exceeds a certain *critical micelle concentration* (CMC). The hydrocarbon tails will then be oriented toward the center of the aggregated molecules, whereas the polar head groups point outward. Micellar solutions may solubilize hydrophobic compounds which otherwise would be insoluble in water. Every surfactant has a characteristic *CMC* and aggregation number, i.e., the number of surfactant molecules making up a micelle. The size of the micelles is in the range of 3 to 6 nm in diameter; therefore, micellar solutions exhibit properties of homogeneous solutions.

4.3.7.2 Principles of separation in MECC

The separation principle of MECC is based on the differential partition of the solute between the micelle and water. Figure 4.6 shows a schematic representation of the principle of MECC.

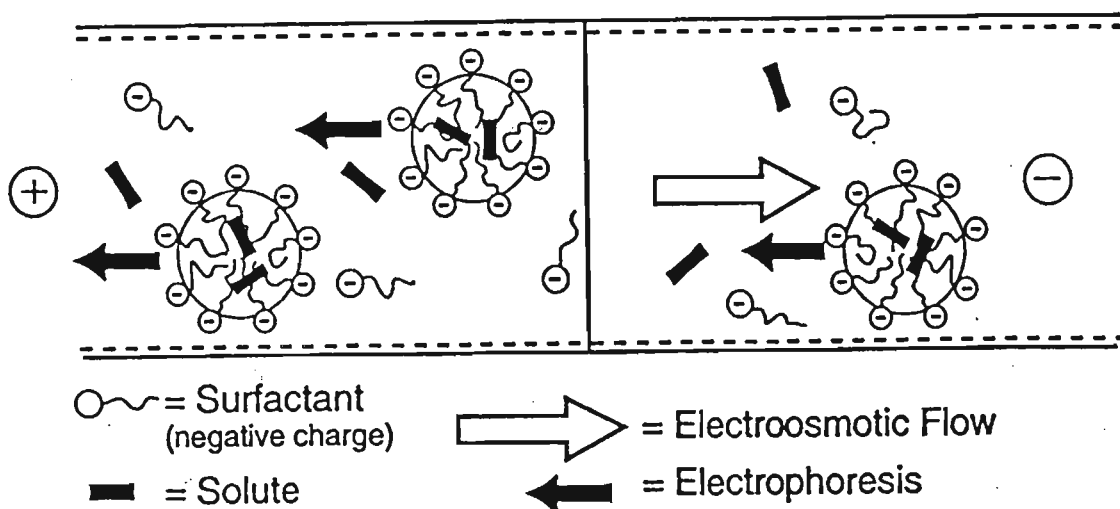


Figure 4.6 Schematic representation of the separation principle of MECC.

When an anionic surfactant such as sodium dodecyl sulfate (SDS) is employed, the micelle migrates toward the positive electrode by electrophoresis. The electroosmotic flow transports the bulk solution toward the negative electrode due to the negative charge on the surface of fused silica. The electroosmotic flow (EOF) is normally stronger than the electrophoretic migration of the micelle under neutral or alkaline conditions and, therefore, the anionic micelle also travels towards the negative electrode at a retarded velocity. When a neutral analyte is injected into the micelle solution, a fraction of it is incorporated into the micelle and it migrates at the velocity of the micelle. The remaining fraction of the analyte remains free from the micelle and migrates at the electroosmotic velocity. The migration velocity of the analyte thus depends on the distribution coefficient between the micelle and the non-micellar (aqueous) phase. The greater the percentage of analyte that is distributed into the micelle, the slower it migrates. The analyte must migrate at a velocity between the electroosmotic velocity and the velocity of the micelle, provided the analyte is electrically neutral. In other words, the migration time of the analyte, t_r , is

limited between the migration time of the bulk solution, t_o , and that of the micelle, t_{mc} . This is often referred to in the literature as the migration time window in MECC and is illustrated clearly in Figure 4.7. This technique, originally introduced by Terabe *et al.* in 1984, has been well applied to the separation of both neutral and ionic molecules present in natural product matrices (15-19).

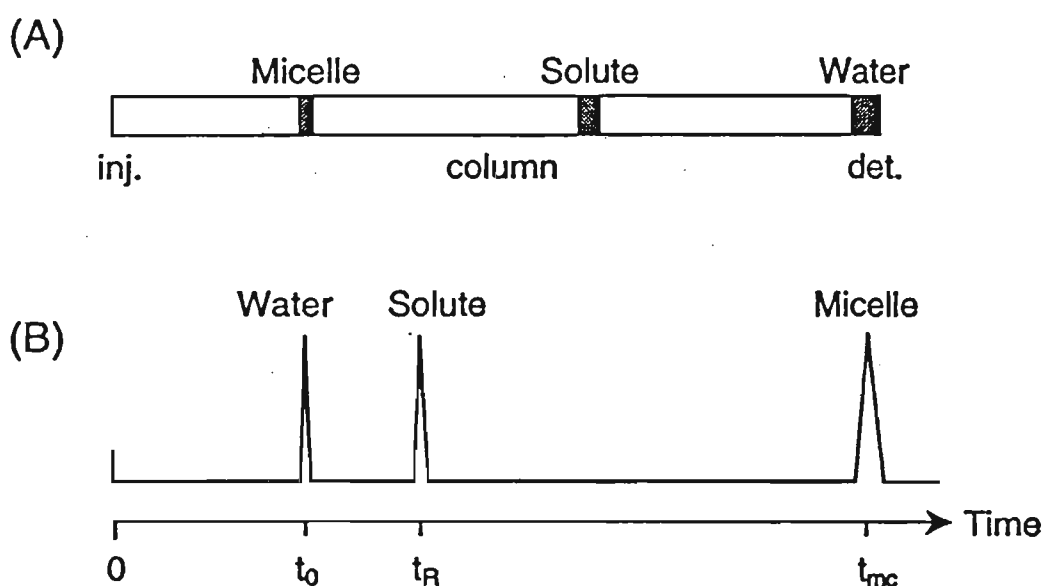


Figure 4.7 Schematic representation of the zone separation in MECC.

4.3.7.3 Theory of MECC

In the previous chromatographic techniques described, the capacity factor is obtained by the use of equation 4.5. However in MECC, k' can be obtained by the following equation (20):

$$k' = \frac{t_m - t_o}{t_o (1 - t_r/t_{mc})} \quad (4.27)$$

As t_{mc} becomes infinite (micellar phase becomes stationary), equation 4.27 reduces to the analogous equations for conventional chromatography. The parameters t_o and t_{mc} are

experimentally determined by injecting methanol, which is assumed not to interact with the micelles, and Sudan III, which is assumed to be fully solubilised.

Resolution in MECC is given by (21):

$$R = \frac{N^{1/2}}{4} \frac{\alpha - 1}{\alpha} \frac{k'_2}{k'_2 + 1} \frac{1 - t_0/t_{mc}}{1 + (t_0/t_{mc}) k'_1} \quad (4.28)$$

Efficiency Selectivity Retention

where α is the separation factor given by k'_2/k'_1 . The differences between MECC and conventional chromatography are accounted for in the last term of the equation. As t_{mc} becomes infinite, the latter term equates to unity and results in an expression for resolution that is identical to that of conventional chromatography.

In MECC fast efficient separations can be obtained because of three important phenomena. First, the flat flow profile of the EOF does not require mass transfer in the mobile phase across the capillary diameter. Secondly, fused silica capillaries dissipate heat efficiently, thereby minimizing thermal effects. Thirdly, micelles are dynamic structures, allowing for fast solute entrance/exit kinetics.

References

1. V. Sewram, J.J. Nair, D.A. Mulholland and M.W. Raynor, *J. High Resolut. Chromatogr.*, **18** (1995), 363.
2. A.A. Elujoba, A.F. Fell and P.A. Linley, *J. Pharm. Biomed. Anal.*, **9** (1991), 711.
3. W.K. Modey, D.A. Mulholland, H. Mohamed and M.W. Raynor, *J. Microcol. Sep.*, **8** (1996), 67.
4. S-J, Sheu and C-F Lu, *J. High Resolut. Chromatogr.*, **19** (1996), 409.
5. C-T Chen and S-J. Sheu, *J. Chromatogr. A.*, **710** (1995), 323.

4. S-J, Sheu and C-F Lu, *J. High Resolut. Chromatogr.*, **19** (1996), 409.
5. C-T Chen and S-J. Sheu, *J. Chromatogr. A.*, **710** (1995), 323.
6. M.I. Gil, F. Ferreres and F.A. Tomás-Barberán, *J. Liq. Chromatogr.*, **18** (1995), 3007.
7. J.J. van Deemter, F.J. Zuiderweg & A. Klinkenberg, *Chem. Eng. Sci.*, **5** (1956), 271.
8. M.J.E. Golay, In: *Gas Chromatography*, D.H. Desty (Ed.), Butterworths, London, UK (1958), p.35.
9. D.N. Heiger, *High Performance Capillary Electrophoresis*, Hewlett Packard Company, Waldbronn, Germany (1992), p.7.
4. D. N. Heiger, *High Performance Capillary Electrophoresis- An Introduction*, Hewlett Packard, Waldbronn, Germany (1992), p.15.
11. T.S. Stevens & H.J. Cortes, *Anal. Chem.*, **55** (1983), 1365.
12. D.J. Shaw, *Electrophoresis*, Academic Press, London, UK (1969) p.29.
13. F. Foret and P. Bocek, *Adv. Electrophoresis*, **3** (1990), 272.
14. K. Solomon, D.S. Burgi and J.C. Helmer, *J. Chromatogr.*, **559** (1991), 69.
15. S-J. Sheu and C-F Lu, *J. High Resolut. Chromatogr.*, **19** (1996), 409.
16. M-W. Hsiao and S-T. Lin, *J. Chromatogr. Sci.*, **35** (1997), 259.
17. M.I. Gil, F. Ferreres and F.A. Tomás-Barberán, *J. Liquid. Chromatogr.*, **18** (1995), 3007.
18. K-L. Li and S-J. Sheu, *Anal. Chim. Acta*, **313** (1995), 113.
19. C-T. Shen and S-J. Sheu, *J. Chromatogr.*, **710** (1995), 323.
20. S. Terabe, K. Otsuka, K. Ichikawa, A. Tsuchiya and T. Ando, *Anal. Chem.*, **56** (1984), 111.
21. S. Terabe, K. Otsuka and T. Ando, *Anal. Chem.*, **57** (1985), 834.

CHAPTER 5

Experimental techniques

5.1 Introduction

This chapter describes the experimental details of the techniques employed for the extraction and analysis of the plant extracts from *Ekebergia capensis*, *Clivia miniata* and *Grewia occidentalis* and the individual components isolated. Both the off-line and on-line bioassay techniques are discussed as well as the various chromatographic and spectroscopic techniques used.

5.2 Plant material

Initially, when this project was initiated, fresh plant material of *Ekebergia capensis* Sparrm. was obtained from a patient attending the ante-natal clinic at King Edward VIII hospital in May 1995. The identity of this plant was authenticated by comparison with a reference specimen at the Natal Herbarium. Plant material of *Grewia occidentalis* L. and *Clivia miniata* L. was obtained from the Silverglen Medicinal Plant Nursery (KwaZulu-Natal, SA). Thereafter, for further analysis, a second batch of all three plants was obtained from the Medicinal Plant Nursery in November 1995. The wood of *E. capensis*, *G. occidentalis* and *C. miniata* was debarked, finely ground and left to air dry for 72 hours. Due to the high moisture content of *C. miniata* the roots were initially dried and then ground into a fine powder.

5.3 Preparation of crude aqueous extracts

Aqueous extracts of the plants were prepared by heating 6.0 g of milled plant material in 50 ml distilled water for 30 minutes. The resulting decoction was filtered through a fluted Whatman 542 filter paper (Whatman International Ltd, Maidstone, England, UK) and freeze dried.

5.4 Off-line supercritical fluid extraction of plant components.

Initial SFE studies were performed on a home assembled SFE system. The SFE apparatus comprised of a Lee Scientific Series 501 syringe pump (Dionex, Sunnyvale, CA, USA) controlled by Lee Scientific software and a Perkin-Elmer Sigma chromatographic oven (Perkin Elmer, Norwalk, Connecticut, USA) to house the extraction cell (Figure 5.1). A simple schematic diagram is shown in Figure 2.4.



Figure 5.1 Photograph of the home assembled SFE system.

5.4.1 Pump

The syringe pump (Figure 5.2) had a cylinder capacity of 150 ml and could deliver a fluid up to 400 atm in pressure. An electronically-actuated valve within the pump was switched so as to connect the pump cylinder with either the gas cylinder or the extraction vessel. Direct introduction of a liquid from a high pressure tank into a cooled pump cylinder head was the recommended method for filling the pump with CO₂. It is usually necessary to cool the pump head when working with eluents that are gaseous at ambient temperatures.

Cooling reduces the tendency of the liquid eluent to undergo gasification in the pump head and also enhances the pumping efficiency. As an added advantage, cooling results in a maximum fill of the pump cylinder. The pump cylinder jacket was therefore cooled by circulating cold water at 5 °C around it. This cold water was generated by a cooling unit (Grant Inst., Cambridge, UK). A piece of rubber tubing was connected from the outlet of the water bath to the 1/4 inch brass bulkhead fitting on the pump labelled coolant inlet. Another piece of rubber tubing was connected from the coolant outlet bulkhead fitting on the pump back to the inlet of the water bath to ensure the constant flow of the cooling solvent around the pump cylinder jacket. Both the pump cylinder jacket and the coolant transfer lines were insulated using a cut-to-fit polymer foam material. This step was essential to prevent excessive air moisture condensation and loss of cooling efficiency.

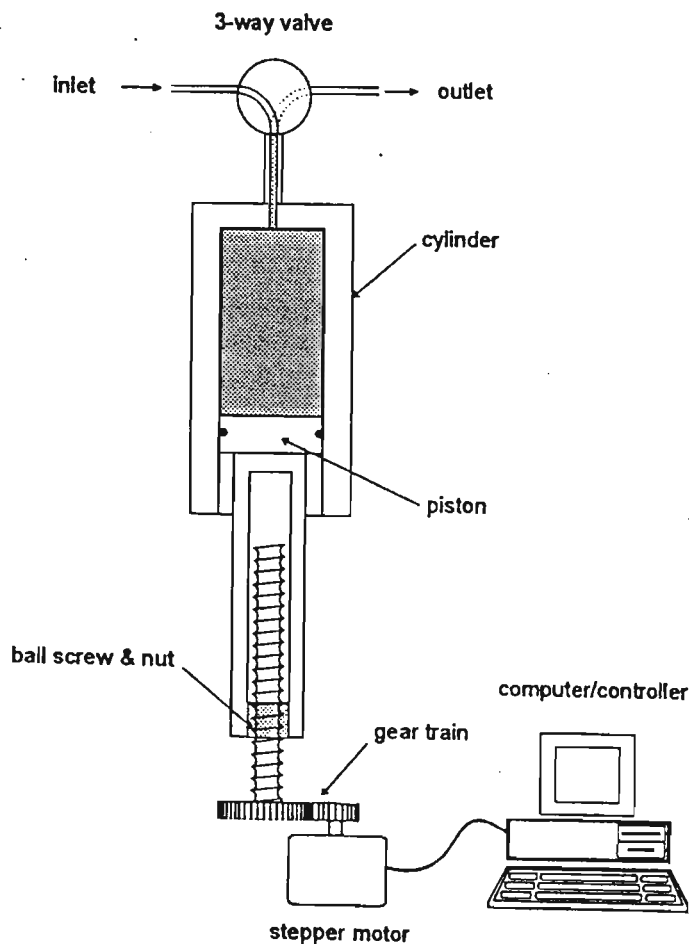


Figure 5.2 Schematic diagram of a syringe pump (1).

5.4.2 Plumbing

The plumbing was accomplished as follows: A 1.5 m × 1/16 inch o.d. stainless steel tube soldered onto a 10 cm × 1/8 inch o.d. tubing was used to connect the high pressure tank containing SFE/SFC grade liquid CO₂ (Air products and Chemicals Inc., Allentown, PA USA) to the 1/16 inch bulkhead fitting labelled gas source at the back of the series 501 pump. The ends of the stainless steel tubing were pushed through (A) a 1/16 inch swagelok nut and a 1/16 inch stainless steel Swagelok ferrule (Swagelok Co., Solon, OH, USA) at the end for connection to the pump, and (B) a 1/8 inch swagelok nut and a 1/8 inch brass swagelok ferrule at the end to the high pressure CO₂ tank. Both ends were connected to the pump and tank respectively. A piece of 1/16 inch o.d. stainless steel tubing with 1/16 inch nuts and ferrules fitted at both ends were connected from the 1/16 inch bulkhead on the pump labelled carrier fluid to a 4-port valve (Valco Inst., TX, USA) fixed outside the GC oven. This served as an on/off valve to control the entry of the fluid into the extraction vessel. A short piece of 1/16 inch o.d. stainless steel tubing was again connected from the 4-port valve to the extraction vessel housed in the GC oven. Finally, the outlet of the extraction vessel was connected to a high pressure 2-way valve (Supelco, Bellefonte, PA, USA) placed outside the oven. This served to control extractions either in the static or dynamic mode. A 20 cm × 50 μm i.d. deactivated fused silica capillary (SGE, Australia) was placed on the outlet of the 2-way high pressure valve for fluid decompression and also as a back pressure regulator. One end of the capillary was threaded through a short 1/16 inch o.d. polyetheretherketone (PEEK) sleeve (Upchurch Scientific, Washington, USA) which was pushed through a 1/16 inch nut and stainless steel ferrule in that order before connecting that 2-way pressure valve. The end of the capillary restrictor was immersed into 15 ml methanol (BDH Laboratory Supplies, Poole, England) contained in a round bottom flask for trapping of the extracted analytes.

5.4.3 Extraction vessels

Two stainless steel commercially available extraction vessels (Keystone Scientific, Bellefonte, PA, USA) were used in this study. One vessel had a volume of 24 ml while the other a volume of 10 ml. Figure 5.3 below shows a diagram of a 24 ml vessel with

high pressure end caps. Both end caps were fitted and sealed manually and housed a 5 μm bed support and a spring-loaded polytetrafluoroethylene (PTFE) cap seals. The vessels had a maximum pressure rating of 666 atm (10 000 psi).

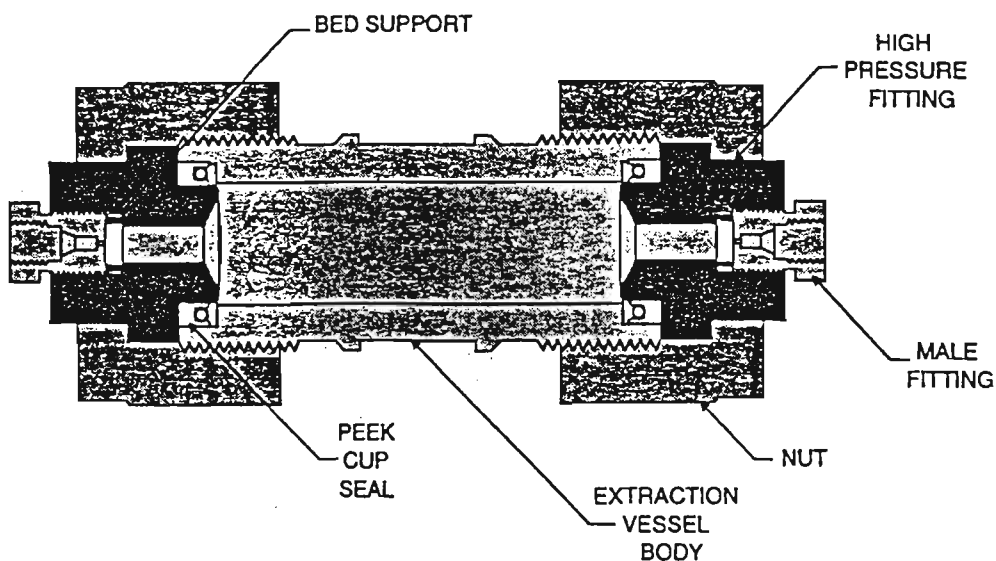


Figure 5.3 A diagram of a commercially available stainless steel extraction vessel with fingertight end caps. (2)

5.4.4 Extraction parameters

Total extractions were performed on the dry milled samples at 400 atm and 80 °C. The samples were spiked with 2 mol % H₂O as modifier to increase the solvating power of supercritical CO₂. The plant samples were packed tightly into the extraction vessel to reduce the vessel void volume. The masses of the plant samples varied due to the particle size of the material and will hence be given in the later chapters when discussed individually. The vessel was placed horizontally in the oven and the extraction performed for 50 minutes static period followed by a 20 minute dynamic extraction period. Although this orientation of the vessel is generally not recommended, it was not possible to keep the the vessel vertical due to the dimensions of the oven. Supercritical fluid fractionation was also performed to decrease the complexity of the total extract. Sequential extracts were thus obtained by simply increasing the pressure at constant temperature while performing extractions on the same sample.

5.5 Uterotonic bioassay

A schematic diagram of the bioassay setup is seen in Figure 5.4. Mature non-pregnant guinea pigs were obtained from the Biomedical Resource Centre, University of Durban-Westville (KwaZulu-Natal, RSA). 20% pentobarbitone (Maybaker, Port Elizabeth, RSA) was administered intramuscularly as an anaesthetic, at a dose of 0.2 g/kg. The uterus was removed by a midline incision into the lower abdominal cavity and washed immediately in Tyrodes solution at 4°C. The bioassay was performed by placing a 2 cm longitudinal strip of uterine muscle into the muscle bath containing 10 ml Tyrodes solution maintained at 37°C. The lower end of the muscle was fixed to a glass capillary tube while the upper end was suspended by a thread attached to a Harvard 386 smooth muscle isotonic transducer (Harvard Apparatus Company, Inc., Massachusetts, USA) which transformed the change in muscle length into a proportional electrical signal. A continuous supply of 95% O₂ and 5% CO₂ (MG Fedgas, Durban, RSA) was administered through the glass capillary tube at a flow rate of 60 ml/min to provide tissue oxygenation and act as a suitable buffer. This signal was recorded using an electrically driven Beckmann R511A chart recorder (Beckman, Inc., Illinois, USA) at a chart speed of 0.05 mm/sec. Caution was exercised in ensuring that the lumen of the uterus remained open at both ends during the assay. *O*-Acetylcholine hydrochloride (ACh) (BDH Chemicals, England, UK) was used as a standard smooth muscle stimulant at a concentration of 1 µg/100 µl. The extracts were dissolved in 0.9% sodium chloride (Sabax Ltd, Johannesburg, RSA) at known concentrations and dispensed into the muscle bath using Eppendorf pipets. Physiological fluid (Tyrodes solution) was prepared by dissolving 2.70 mmol KCl, 1.05 mmol MgCl₂·6H₂O, 0.40 mmol NaH₂PO₄, 1.80 mmol CaCl₂, 137.00 mmol NaCl, 11.90 mmol NaHCO₃ and 5.60 mmol D-glucose in distilled water.

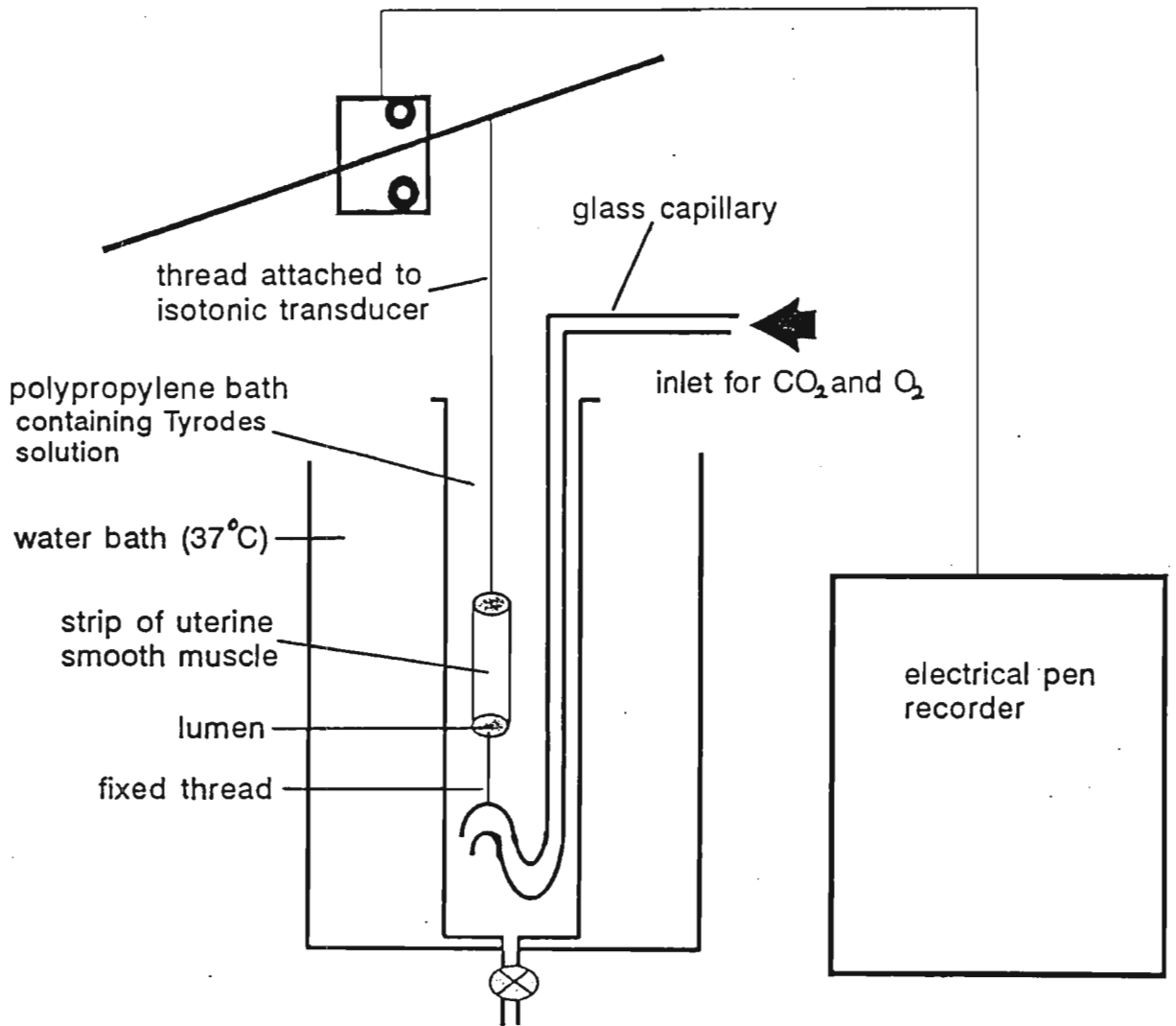


Figure 5.4 Schematic diagram of the uterotonic bioassay setup used to monitor muscle activity.

5.6 On-line SFE-Bioassay.

The schematic diagram of the on-line SFE-bioassay setup is shown in Figure 5.5. SFE was performed using a Lee Scientific series 600 SFC pump (Dionex, Sunnyvale, CA, USA) to deliver the SFE fluid, and the series 600 SFC/GC oven to house the extraction vessel. A 24 ml stainless steel extraction vessel (Keystone Scientific; Bellefonte, PA) was housed vertically in the oven maintained at 80 °C. A Lee Scientific supercritical fluid extraction injection accessory controlled the passage of CO₂ to and from the extraction vessel. This consisted of a temperature controlled block maintained at the same temperature as the oven and a multiport valve which enabled switching between dynamic and static modes of extraction. As shown by the schematic diagram of the system in Figure 5.6, fluid from the pump was initially allowed to pass through *on/off* valve V1 into the extraction vessel, while keeping the vent valve at position 10 closed, and the multiport valve in the static mode. This allowed the vessel to pressurise to the required pressure, hence allowing static extraction to proceed for 50 minutes. The multiport valve was thereafter switched from position 9 to position 8 thereby linking ports 1 and 2 to facilitate dynamic extraction. The ¹/₁₆ inch stainless steel tubing connected to port 2 was redirected back into the oven in an attempt to maintain constant temperature during transport of the extracted analytes. Upon exit from the oven, the fluid passed through a 50 µm tapered restrictor (SGE; Australia) and decompressed into the muscle bath at a flow of 18 ml/min at 150 atm (Figure 5.5).

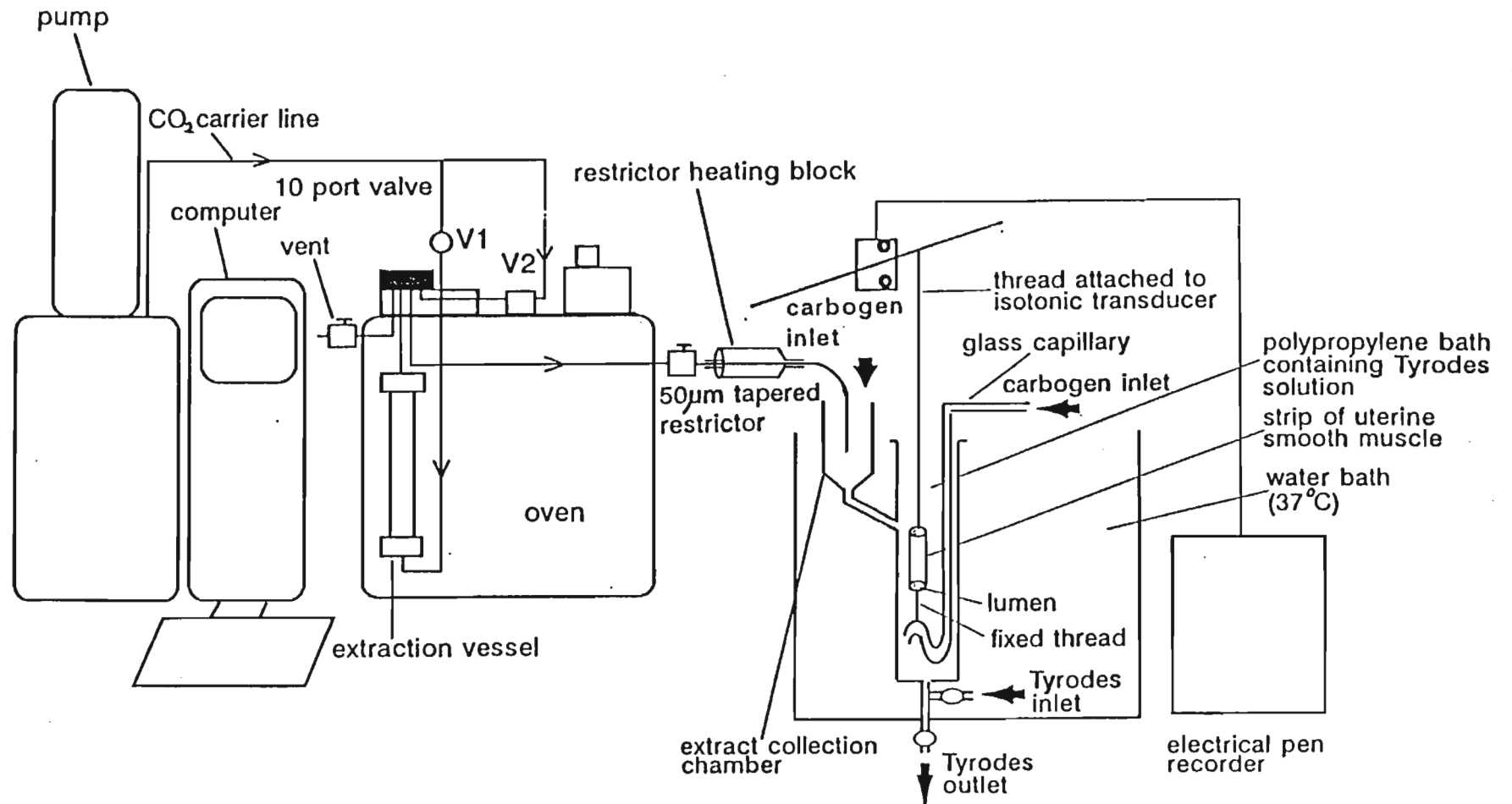


Figure 5.5 Schematic diagram of the on-line SFE-bioassay setup

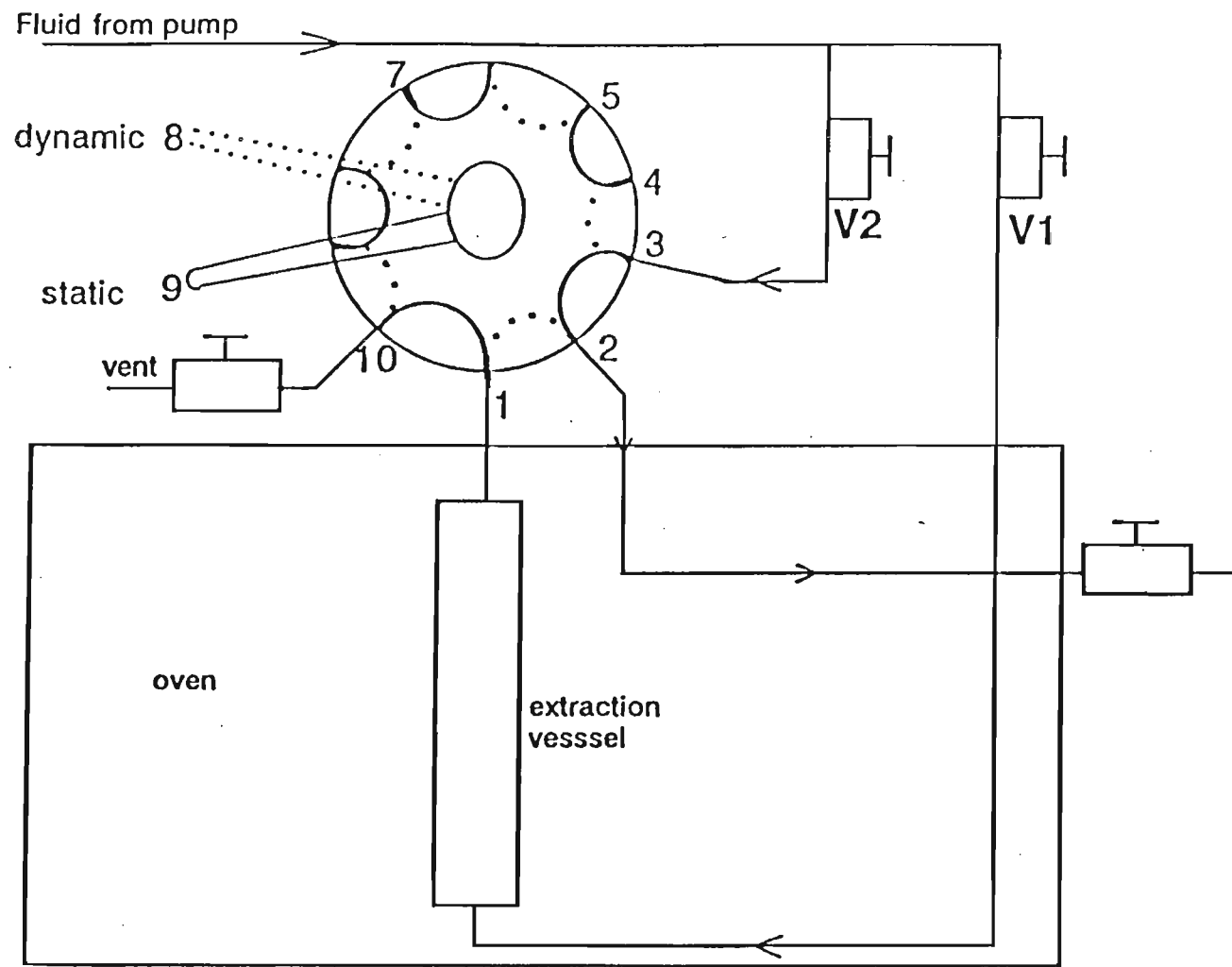


Figure 5.6 Plumbing schematic of the multiport valve used for switching between static and dynamic modes of extraction.

SFC grade CO₂ (Air products and Chemicals; Allentown, PA) was used as the extraction fluid. Each plant sample was tightly packed into the extraction vessel and 200 µl H₂O added to the matrix. Extraction was carried out at 400 atm and 80 °C for 50 minutes static followed by a 20 minute dynamic extraction period. Further, SFE fractions were obtained by sequentially increasing the pressure at constant temperature and modifier concentration. Extractions were performed at 200, 300 and 400 atm respectively. After the 20 minute dynamic extraction period for each sample, the multiport valve was switched back to the static mode (port 9) followed by closure of valve V1 (Figure 5.5). Valve V2 was thereafter opened allowing pure CO₂ of the same density as the extracting fluid, to flow through ports 3 and 2. This procedure enabled flushing and cleansing of the 1/16 inch transfer line as well as the tapered restrictor, thereby eliminating the possibility of memory effects during analysis. The vessel was simultaneously vented through port 10. The bioassay was performed as described in section 5.4, however modifications to the Tyrodes solution as well as the muscle bath were carried out to alleviate the side effects of excess CO₂. These are discussed in chapter 8.

5.7 Muscle bath construction.

5.7.1 Muscle bath A

Muscle baths were constructed in house from 10 ml polypropylene syringes (Terumo Corporation, Tokyo, Japan). The first bath was designed for horizontal flow of CO₂ directly into the muscle bath. This was accomplished by attaching a 10 cm length of PEEK tubing (Upchurch Scientific, Washington, USA) from the wall of the polypropylene syringe to the wall of the Perspex water bath (Figure 5.7). The restrictor passed through the PEEK tubing until it protuded into the muscle bath.

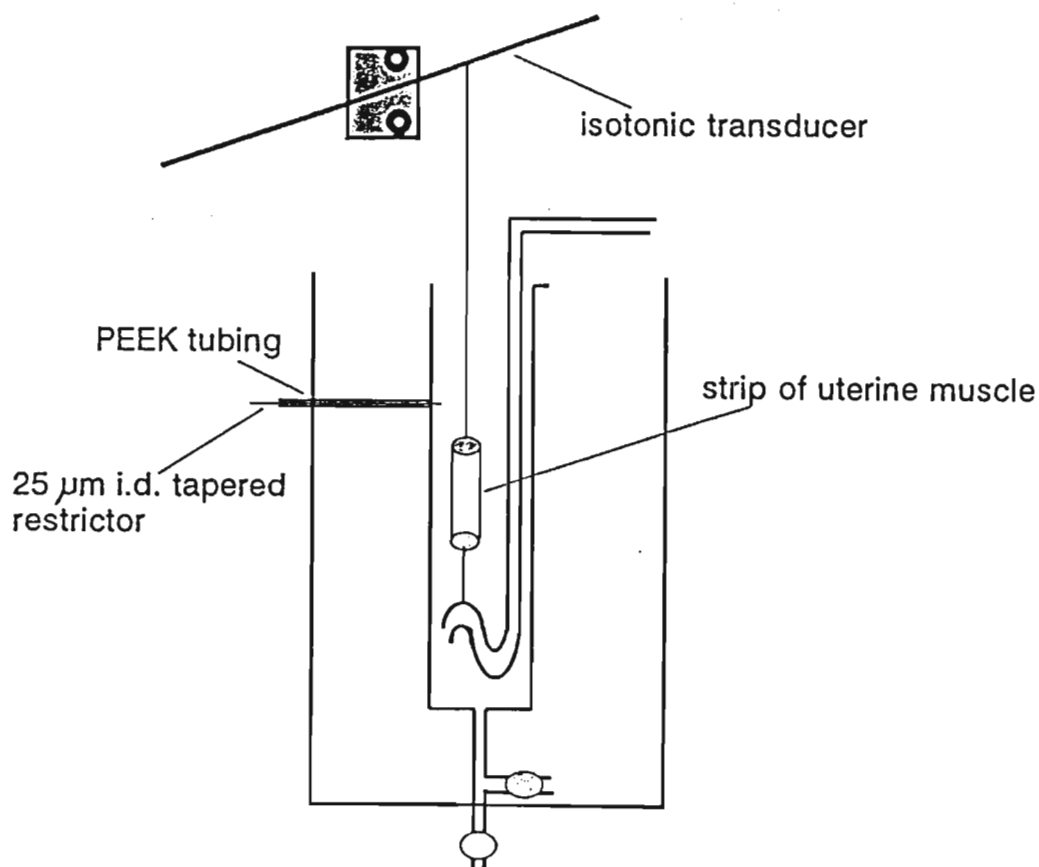


Figure 5.7 Polypropylene muscle bath designed for horizontal flow of CO₂ with direct introduction into the muscle bath.

5.7.2 Muscle bath B

A second bath was designed for vertical flow of CO_2 due to failure of the first horizontal flow bath to perform efficiently. The reasons for this are discussed in Chapter 8. This second bath consisted of a second chamber of 6 ml capacity called the extract collection chamber, linked via a detachable side arm to the muscle bath (Figure 5.8). The extract collection chamber functioned as a CO_2 reduction interface with extractions performed directly into this chamber while the muscle remained in the muscle bath. The muscle bath was filled with Tyrodes solution by upward displacement until the level of Tyrodes in the extract collection chamber had reached a volume of 4 ml.

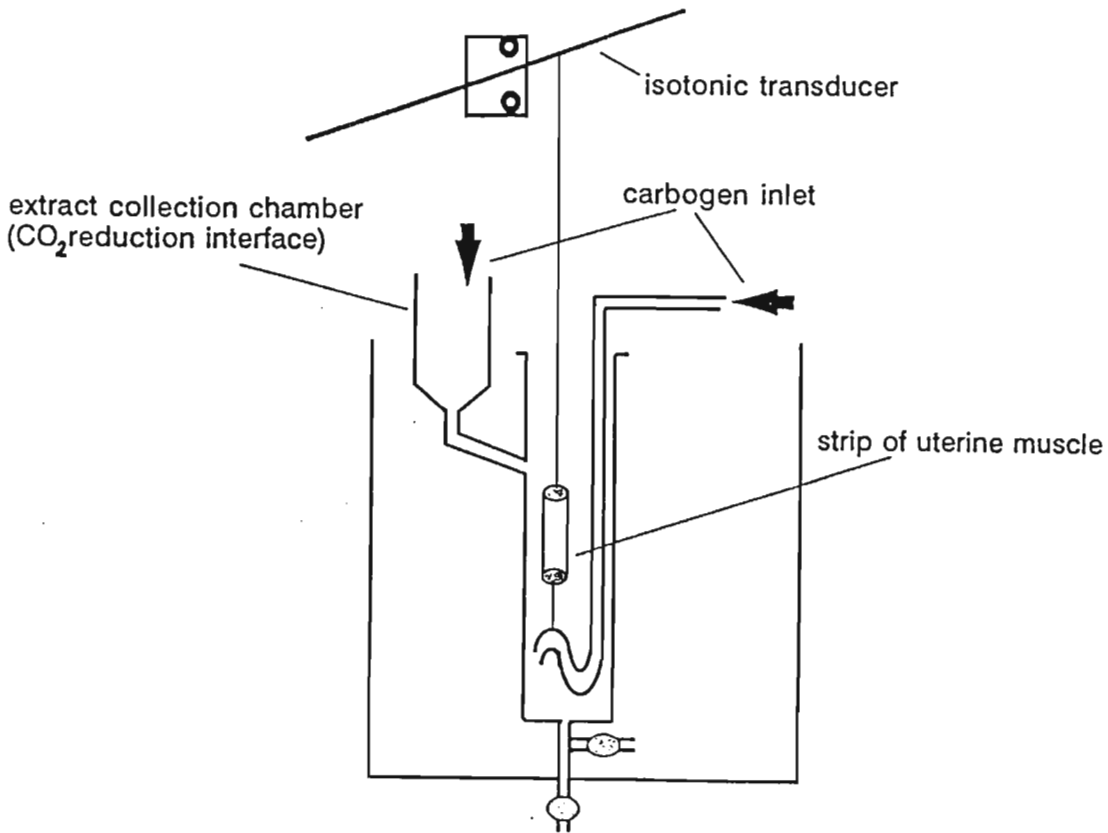


Figure 5.8 Polypropylene muscle bath designed for vertical flow of CO_2 with direct introduction into a CO_2 reduction interface.

5.8 Tapered restrictor fabrication.

The end of a length of 25 μm and 50 μm i.d. deactivated capillary tubing (SGE; Australia) was held in the tip of a bunsen burner flame. Tension was applied by hand on both sides of the heated area. As the fused silica melted, the capillary was pulled to a hair like taper and removed from the flame (Figure 5.9). The restrictor orifice was thereafter adjusted by cutting back the taper and measuring the gaseous flow rate at room temperature and at a pressure of 150 atm (3).

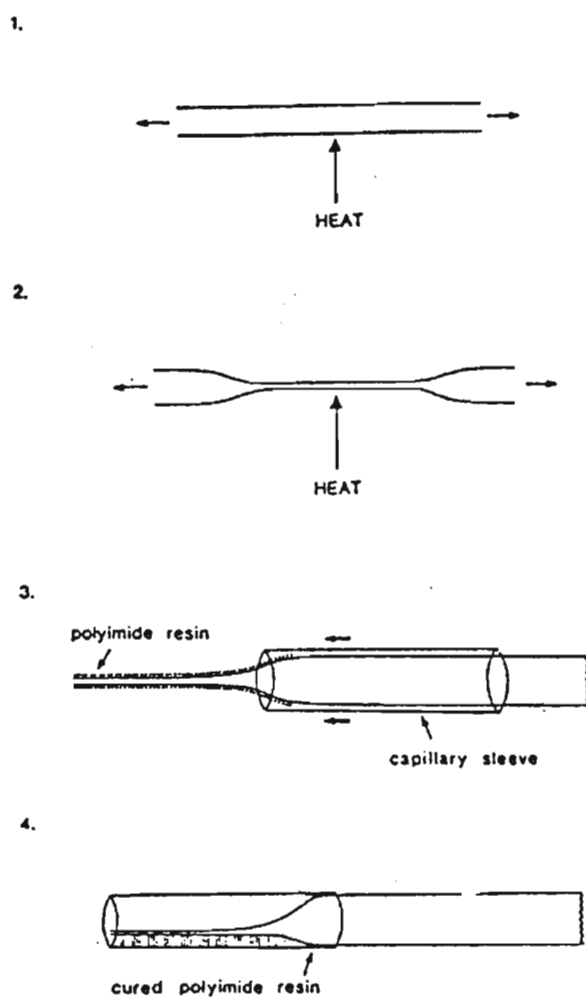


Figure 5.9 Schematic steps showing the preparation of a tapered capillary restrictor.

- (1) a micro-Bunsen burner is used for localized heating of the capillary.
- (2) tension is applied and the capillary pulled to a hair like taper.
- (3) polyimide resin is applied to the taper which is subsequently positioned with a capillary sleeve.
- (4) the resin cures and glues the taper to part of the inner wall of the sleeve.(3)

5.9 pH measurements of Tyrodes solution.

The effects of CO₂ on the pH of Tyrodes solution was monitored by using the pH meter 300 (Zeiss, W. Germany) with a combination pH electrode (Beckmann Instr. CA, USA). The instrument was calibrated with pH 7 and pH 4 buffer solutions supplied by Beckman Instruments (Fullerton, CA, USA).

5.10 Isolation and structural elucidation of plant components

5.10.1 Column Chromatography

Exhaustive supercritical fluid extractions of the plant samples were performed into methanol using the 24 ml extraction vessel until subsequent extractions yielded no further extractables. Column chromatography was thereafter performed repeatedly in order to separate and purify the compounds present in the extracts. The length and diameter of the columns as well as the particle size of the stationary phase had to be varied in order to optimize resolution of the compounds.

Initially, use was made of a 50 cm × 5 cm i.d. glass column packed with silica gel 60 (0,2-0,5 mm particle size, 35-20 mesh ASTM, Merck Art 7734, Merck Chemicals, Darmstadt, Germany), with gravity elution. This was followed by the use of gravity columns (50 cm × 3.5 cm) packed with silica gel 60 (0,040-0,053 mm particle size 230-400 mesh ASTM, Merck Art. 9385, Merck Chemicals, Darmstadt, Germany). In certain cases, flash chromatography was found useful for the speedy separation of mixtures. The latter technique involved the use of pressure in order to elute the various fractions from the column. The flow rate was maintained at approximately 60 ml/min for flash chromatography.

5.10.2 Thin layer chromatography

Thin layer chromatography was conducted on the crude extracts and the various fractions collected, using pre-coated 0,2 mm thick aluminium-backed silica gel 60 TLC plate (Merck Art 5553, Merck Chemicals, Darmstadt, Germany). The spots on the plates were visualised by spraying with a reagent comprising anisaldehyde (Fluka Chemicals; Buchs,

Switzerland), concentrated sulphuric acid (BDH Chemicals, England, UK) and methanol (Polychem Supplies, Durban, RSA) in the ratio 1.25 : 2.5 : 96.25. Coloured spots were observed after heating the plates with a heatgun.

5.11. Spectroscopic techniques

5.11.1 ^1H and ^{13}C NMR spectroscopy

All ^1H NMR, ^{13}C NMR and 2-dimensional NMR spectra were recorded at room temperature on a Varian Gemini 300 MHz spectrometer (Varian Instruments, Palo Alto, California, USA). The solvents used were deuteriochloroform (CDCl_3) and deuteriomethanol (Merck Chemicals, Darmstadt, Germany) and all δ values were relative to TMS.

5.11.2 Infrared Spectroscopy

The samples were prepared on KBr discs and infrared spectra recorded on a Mattson 2020 Galaxy series FTIR spectrophotometer (Mattson Instruments, Inc., Madison, USA). The samples were dissolved in dichloromethane (Saarchem Holpro, Krugersdorp, RSA) and added dropwise onto the surface of the KBr disk (FTIR grade, Sigma-Aldrich S.A. (Pty) Ltd, Midrand, RSA). The solvent was allowed to evaporate off, leaving a thin film of sample on the disk for analysis. The data was acquired using the Mattson software (copyrighted 1989).

5.11.3 High Resolution Mass Spectrometry

High resolution mass spectra at the recorded at the Cape Technikon on VG 70E WRM spectrometer while mass measurements were performed on a Kratos High Resolution MS 9/50 mass spectrometer by Dr P. Boshoff. The voltage of the ion source was maintained at 70 eV.

5.11.4 Acetylation of compound 4 from *Ekebergia capensis* Sparrm.

Compound 4 (2 mg) was dissolved in pyridine (1 ml) (Holpro Analytics, Midrand, RSA) and the solution gently warmed on a steam bath. Acetic anhydride (1 ml) (Saarchem (Pty). Ltd, Muldersdrift, RSA) was then added to the solution, which was stirred and left to stand overnight at room temperature. Thereafter methanol (10 ml) was added to hydrolyse the residual anhydride. Two portions of toluene (each 10 ml) (BDH Chemicals Ltd, Poole, England) were then added to the mixture and successively removed under reduced pressure in order to remove traces of pyridine. The residual toluene was removed under reduced pressure by the addition of aliquots of methanol (each 10 ml).

5.12 Chromatographic and electrophoretic analysis of the plant extracts

5.12.1 High performance liquid chromatography.

HPLC was carried out using a Hewlett Packard HP 1090 liquid chromatograph equipped with dual pumps, a Model 7010 sample injection valve, an automatic injector capable of injecting up to 25 μ l and a UV photodiode array detector (Hewlett Packard, Waldbronn, Germany). A 50 μ l aliquot of a solution of the extract dissolved into methanol was injected onto a Bondclone-10 C18 reverse phase column packed with 5 μ m particles (300 \times 3.9 mm i.d., Phenomenex, Torrance, CA, USA). A 70 \times 3.9 mm guard column packed with 5 μ m C18 packing (Phenomenex, Torrance, CA, USA) was inserted between the solvent delivery system and the column to increase column lifetime and ensure that contaminants did not interfere with analyses. Solvents were made up from HPLC grade solvents and Milli-Q⁵⁰ water and filtered through Millipore 0.45 μ m HV organic-aqueous compatible filters. All solvents were degassed with helium prior to use. Columns were washed with methanol after runs and stored in methanol. All injections were performed through the automatic injector.

A UV photodiode array (PDA) detector was used and the absorbance measured at 280 nm. The PDA detector was used to scan the entire UV wavelength region and 280 nm was found to be the optimum wavelength at which most of the eluting compounds were detected. The mobile phase was composed of both water (A) and methanol (B) at varied

compositions as gradient elution was employed in order to separate the components. The elution programme is given in Table 5.1.

Table 5.1. Gradient elution programme employed to separate the plant components.

time (min)	Eluent A (water) % v/v	Eluent B (methanol) % v/v	gradient
0	100	0	-
5	80	20	linear
10	60	40	linear
15	40	60	linear
20	20	80	linear
25	0	100	linear

5.12.2 Capillary electrophoresis

A Beckmann 2200 P/ACE electrophoresis system (Beckmann Instruments, Inc., Fullerton, CA, USA) was used. In the instrument, a fused-silica capillary, which is contained within a temperature controlled cartridge, bridges two electrolyte vials located on an autosampler. The autosampler trays rotate until the vials containing the necessary fluids for specific operations are in position beneath the ends of the capillary. The vials are then pneumatically raised so that the ends of the capillary are immersed in the fluid in the vials. Also immersed in one of these vials is a positive electrode (anode) while a negative electrode (cathode) is immersed in the other. The P/ACE instrument was controlled automatically via an IBM-compatible personal computer with the Beckman System Gold Software.

The column used was a 85 cm × 50 µm i.d fused silica capillary (SGE, Australia) inserted into a specially constructed cartridge. Within the cartridge, the capillary was wound

around a mandrel a number of times depending on its length (Figure 5.10). The effective length of the column was 75 cm and the polyimide coating was removed by heating over a bunsen flame leaving an optically transparent window. This window was fastened to an aperture and to the housing itself so that it was permanently aligned with an opening in the housing for use with the detector optics. P/ACE capillary cartridge coolant (a fluoroorganic fluid) flowed through the cartridge via two openings in the bottom of the housing (located between the ends of the capillary). This fluid circulated around the capillary within the cartridge and maintained a preset temperature (25°C) through convective heat removal. The cartridge was inserted into the rear of the autosampler. A variable wavelength detector was used to monitor the complexity of the extracts. Components from *Ekebergia capensis* and *Clivia miniata* were monitored at 280 nm while that of *Grewia occidentalis* monitored at 254 nm. Other detection wavelengths could be obtained by changing the filter.

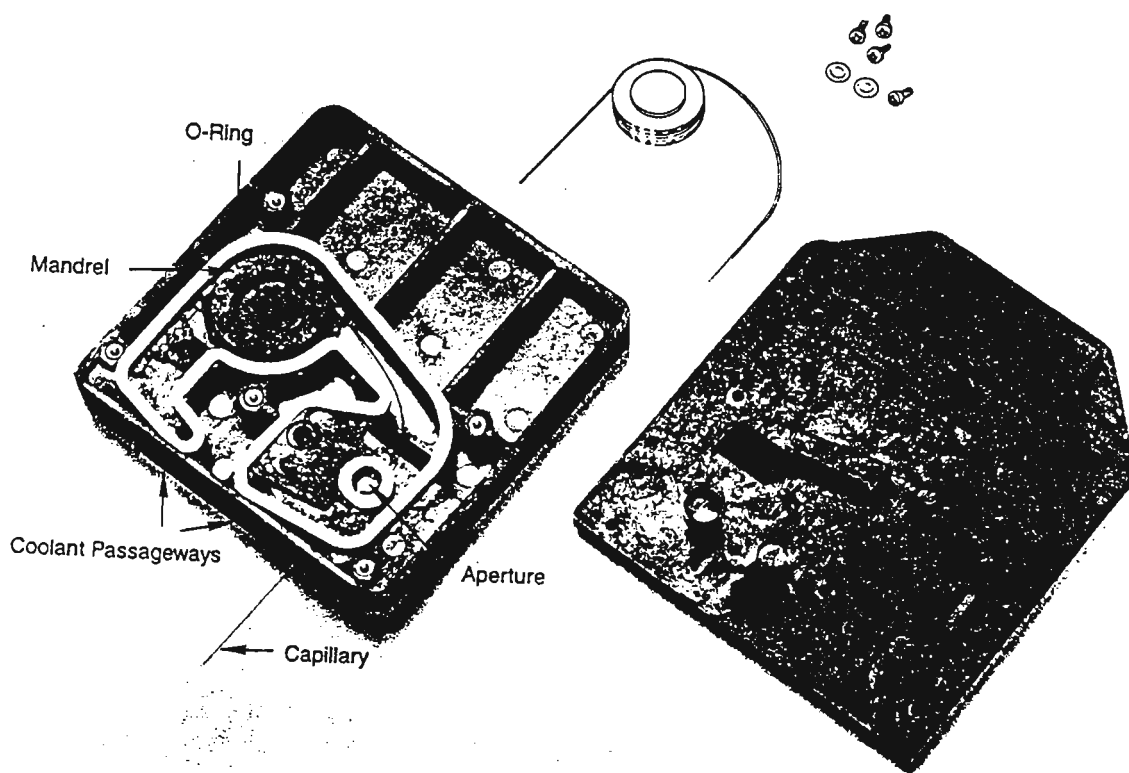


Figure 5.10 Interior of the capillary cartridge. (4)

The column was pressure rinsed with 0.1 M NaOH for 1 minute before being rinsed with the running buffer for another minute. Samples were prepared in methanol and introduced onto the column by pressure injection for 1 second. The column ends were then automatically placed back into the buffer vials and a voltage of 20 kV was applied. The run time was set at 40 minutes but could be stopped manually when necessary. At the end of each day the column was first pressure rinsed with 0.1 M NaOH followed by a rinse with water for 5 minutes each respectively. This ensured that there was no buffer present in the capillary which could crystallize out and hence block the capillary column.

5.12.2.1 Buffer preparation

The analysis of *E. capensis* was performed using 20 mM Na₂B₄O₇·10H₂O (BDH Chemicals Ltd, Poole, England, UK) and 120 mM sodium cholate (Sigma Chemicals, St. Louis, MO, USA). Extracts of *G. occidentalis* were analysed with 20 mM Na₂B₄O₇·10H₂O (BDH Chemicals Ltd, Poole, England, UK) and 100 mM sodium cholate (Sigma Chemicals, St. Louis, MO, USA). The extracts of *C. miniata* were analysed using 30 mM *di*-sodium phosphate buffer (BDH Chemicals Ltd, Poole, England, UK) with 120 mM sodium cholate (Sigma Chemicals, St. Louis, MO, USA). All buffers were prepared in deionised water and ultrasonicated for 10 minutes to remove any dissolved air and then subsequently cooled to room temperature. The buffers were filtered prior to use by passage through a 0.2 mm syringe filter (Lida, Kenosha, WI, USA).

5.12.2.2. Sample preparation and injection

All samples were prepared in methanol and filtered through a syringe filter (Lida, Kenosha, WI, USA) prior to injection onto the capillary. The samples were placed in microvials (Beckmann Instruments, Inc., Fullerton, CA, USA) making possible the injection of sample in the micoliter scale (Figure 5.11).

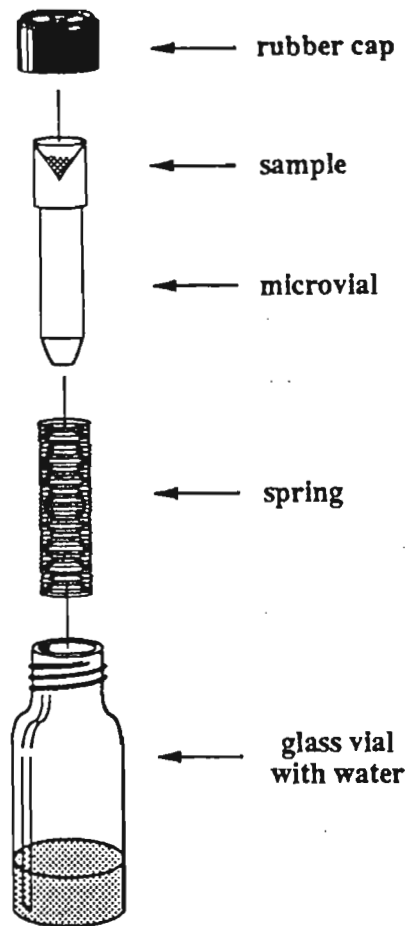


Figure 5.11 Assembly for sample injection in the microliter scale. (4)

5.12.3 Supercritical fluid Chromatography

In this work, packed capillary SFC analysis was carried out on a Lee Scientific Series 600 supercritical fluid chromatograph with a Series 600 Controller interfaced with a Varian 4270 integrator. CO₂ (Air Products and Chemicals, Allentown, PA) and HFC-134a (ICI Fluorochemicals, New Castle, USA) was evaluated as mobile phases using two separate pumps to avoid contamination of the mobile phases.

The density of the mobile phase was controlled by a 150 ml syringe pump equipped with a refrigeration unit. The pressurised fluid was delivered from the pump to a Valco C14W microvalve injector (Valco Instruments, USA) which was a pneumatically actuated timed-split injector. The injection valve was fitted with a 200 nl internal sample rotor and set up for time-split injection by installing precolumn directly into the injection valve (Figure 5.12). Initiation via an electronic signal caused the valve to be switched rapidly (in the order of milliseconds) from the load to the inject position and back again. Helium was used to power the actuator because the fast valve action requires a low viscosity gas. Due to the speed of the valve switching action, only a portion of the loop contents (~50 nL) was transferred onto the column by a mobile phase, the rest of the sample remaining in the injection loop. Therefore, injection volumes could be easily altered by increasing or decreasing the time of injection. The injector was cooled to 5 °C with a cooling jacket.

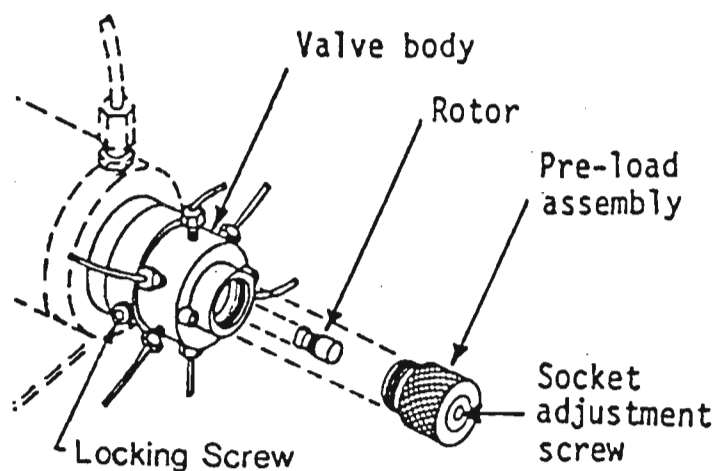


Figure 5.12 Schematic diagram of injection valve for SFC (5).

A 30 cm \times 50 μm i.d. fused silica tubing was connected between the injector and the packed column. This so called precolumn functioned as a retention gap. A 30 cm \times 100 μm i.d. column packed with 5 μm ODS-2 was used to investigate the complexity of the extracts. The column was housed inside the oven, with one end leading from the precolumn and the other end connected to a 70 cm \times 50 μm fused silica capillary. This capillary acted as a transfer line to a Spectra-Physics UV1000 variable wavelength UV detector (Spectrasystem, San Jose, CA, USA). A transparent window was formed as described in section 5.11.2 and mounted to the detector optics to facilitate detection of the compounds that they passed through the transfer line. The end of the transfer line was then connected to a 20 cm \times 10 μm i.d. linear restrictor with a flow between 1.20 and 1.50 ml/min at 150 atm at room temperature. All connections were made via a SGE minimum dead volume butt connector (SGE, Australia) which consisted of a stainless steel screw-tightened assembly (Figure 5.13). The linear restrictor was directed into the heated block (325 $^{\circ}\text{C}$) of the FID to prevent restrictor blockages.

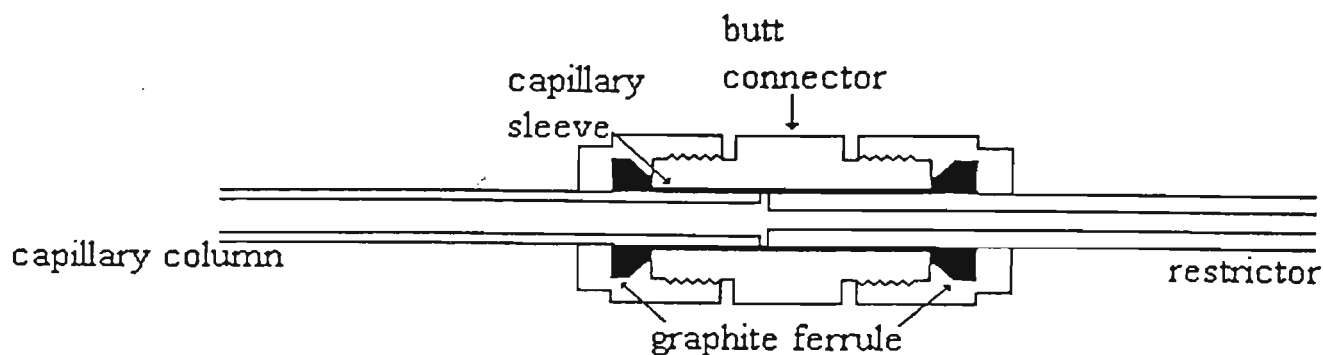


Figure 5.13 Schematic diagram of butt-connection of column to restrictor

Before use, the SFC pump was filled with CO₂ using the pump “fill” function. Once the required amount was present in the pump, the pump valve function was switched to “carrier” which directed the flow to the column. The CO₂ from one filling could easily last several days if the pump pressure was maintained when not in use. The required operating method for the analysis was programmed into the Series 600 controller. This involved setting the oven temperature, detector temperature, pump conditions and the duration of injection.

Once the system had stabilized and was ready for use, the required operating method was loaded. An excess of analyte was injected into the loop using a Unimetrics blunt-tipped 50 µl syringe, and at the electronic prompt the injector was fired and the integrator activated manually. At the end of the analysis, the SFC was returned to its original position in readiness for next analysis.

5.13 Column packing

Packed capillary columns with ODS-2 were prepared using supercritical fluid CO₂ by a method outlined by Bartle *et al.* in 1994 (6). A schematic diagram of the packing system is shown in Figure 5.14. A Lee Scientific Series 600 syringe pump was used to deliver the CO₂ to the column via the packing reservoir. The reservoir was a 6 cm × 1/8 inch stainless steel tubing with a stainless steel frit (pore size < 0.2 µm) mounted in the inlet union. The reservoir was connected to a length of fused silica capillary tubing via a reduction union. An appropriate amount of packing material depending on the length of the column was placed into the reservoir. A porous ceramic frit, as discussed in section 5.14, was made at the exit end of the column and this was connected to a linear restrictor (15 cm × 10 µm i.d. fused silica capillary). The column tubing and the restrictor were placed under water in an ultrasonic bath. Liquid carbon dioxide was introduced by opening the high pressure valves, V1 and V2. The column was sonicated during the whole packing process, and the temperature of the water was maintained at approximately 50 °C. The carbon dioxide in the reservoir and in the section of the column above the water was in the liquid state. This aided the dispersion of the packing material.

However, the carbon dioxide flowing through the section of the column beneath the water was in the supercritical fluid state with consequent faster velocity and lower viscosity than in the liquid state. Slow pressure programming was used during the packing procedure. After the packing bed in the column had grown to the required length, the packing pressure was kept constant for approximately 30 minutes at 300 atm before cessation of sonication and depressurization. Sudden depressurization was avoided, since this causes backfilling of the packing material or break up of the packed bed resulting in a significant decrease in column efficiency. The pressure was slowly reduced to 80 atm at a rate of 3 atm/min. Valves V1 and V2 were thereafter closed. The restrictor was removed once the column was taken out of the water bath. The column was left overnight so that the pressure drop across the column fell to zero. At this point, no bubbles were observed coming from the end of the column. A porous ceramic frit was finally made at the inlet of the column to hold the packing material in place.

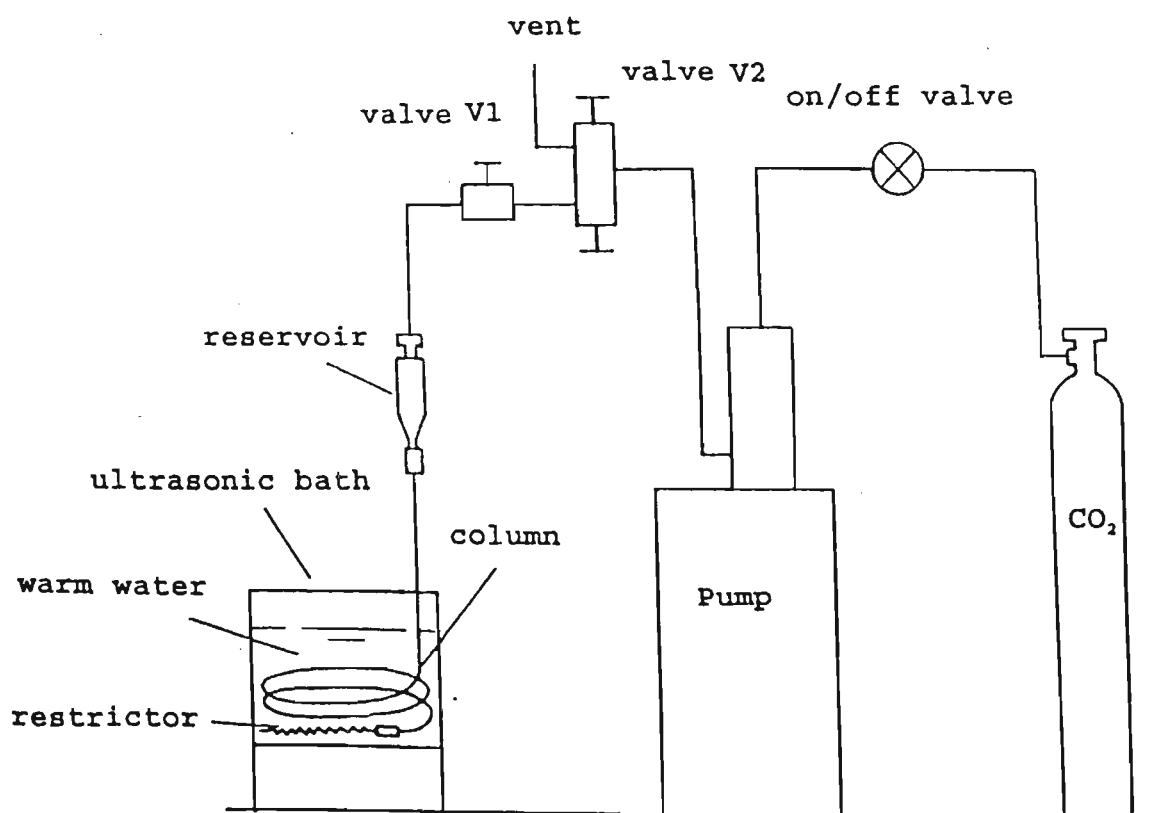


Figure 5.14 Schematic diagram of the supercritical fluid CO₂ packing system. (6)

5.14 Preparation of porous ceramic frits

Porous ceramic frits were prepared from potassium silicate. A few drops of 20 % potassium silicate was added to solid silica of 5 mm particle size to form a paste. The paste was then pressed 0.2 - 0.33 mm into the capillary. The capillary was then heated over a bunsen flame and the silica paste sintered as a result of the high temperature to form a porous frit.

5.15 GC-MS Analysis of *Clivia miniata* L.

The fatty acid fraction of *C. miniata* was analysed using a Hewlett Packard (HP) 5890 series Gas Chromatograph with an HP 5971 Series Mass selective detector (electron impact) (Hewlett Packard, Waldbronn, Germany) controlled by an HP Vectra 486/33N computer. The column used was a HP-5 M.S. (Crosslinked 5 % phenylmethyl silicone) (Hewlett Packard, Waldbronn, Germany), 25 m × 250 µm i.d. capillary column with a film thickness of 0.25 µm. All injections were performed with an SGE syringe (SGE, Australia) with the injector in the splitless mode. Helium was used as the mobile phase at a flow 0.5 ml/min (6.43 psi). The following conditions were used:

Solvent delay: 3.00 minutes

EM Voltage: 70 eV

Inlet temperature: 150 °C

Initial inlet pressure: 21.0 psi

Detector temperature: 280 °C

A temperature programme was executed as follows:

An initial oven temperature of 150 °C that was held for two minutes. Thereafter, a temperature ramp of 7 °C/min was initiated to a temperature of 180 °C. After a hold time of 10 minutes at this temperature, the ramp was continued at 7 °C/min to a final temperature of 250 °C. The final hold time was 20 minutes.

5.16 Esterification of fatty acid mixture

Since the free fatty acids are highly polar, they often have great difficulty in eluting from a GC column. Hence, the methyl esters of these fatty acids have to be formed so that analysis could be made possible. The fatty acid mixture was esterified as follows:

The esterification mixture was made by mixing methanol (10 ml), chloroform (10 ml) and concentrated sulphuric acid (0.1 ml) in a beaker. The sample (20 mg) was placed in a small test tube and to it the esterification mixture added to make the tube 3/4 full. The sample was mixed well with the reaction mixture and placed in the bomb. The bomb in turn was placed in a heatable block that was preheated to 170 °C. An empty tin was inverted and placed over the bomb to contain possible explosions. The sample was left in the heated block for 20 minutes. The bomb was thereafter removed from the heated block and allowed to cool to room temperature. The test tube was removed and the contents washed several times with water. All the washings were discarded and the chloroform solution of the methyl esters were transferred into a clean test tube. The solution was finally placed on the heated block together with the passage of air into it until the solution became clear. The solution now consisted of the methyl esters that were ready for injection into the GC (7).

5.17 Identification of active components and assessment of mode of action

The compounds isolated from the three plant extracts were further subjected to *in vitro* screening as described in section 5.5 and the uterotonic compounds identified. An assessment on the mode of action of the active compounds was carried out by the use of two receptor agonists and antagonists. Bradykinin (Sigma Chemicals, St. Louis, MO, USA) was used as the standard B₂ receptor agonist while acetylcholine (BDH Chemicals, England, UK) was used as the cholinergic receptor agonist. The biological activity of the compounds were assessed both before and after addition of the receptor blockers. HOE 140 (a peptide antagonist) (Sigma Chemicals, St. Louis, MO, USA) was used as the B₂ receptor blocker while atropine (Sigma Chemicals, St. Louis, MO, USA) was used as the cholinergic blocking agent. Bradykinin and acetylcholine were prepared to a final concentration of 30 ng/100 µl and 1 µg/100 µl respectively while HOE 140 and atropine

were made to a final concentration of 1000 µg/100 µl and 60 µg/100 µl respectively. Accurate doses were dispensed into the muscle bath using Eppendorf pipettes. The plant compounds were dissolved in 0.9% saline and in 1% DMSO solution and administered to the strips of uterine muscle accordingly as described in chapter 12.

5.18 Extractives from *Ekebergia capensis*

5.18.1 Physical data of compound 1

24-Ethylcholest-5-en-3β-ol, β-sitosterol

Yield: 5.5 mg

Mass spectrum (spectrum 1a):

EIMS m/z 414.3848 ($C_{29}H_{50}O$, req. 414.3861), 396 $[M - H_2O]^+$

Infrared spectrum (spectrum 1b):

ν_{max} (KBr): 3430 cm^{-1} (O-H stretching), 2936 cm^{-1} , 2867 cm^{-1} (saturated C-H stretching), 1049 cm^{-1} (C-O stretching), 1460 cm^{-1} , 1378 cm^{-1} (C-H deformation)

Optical rotation:

$[\alpha]_D = -34.1^\circ$ ($CHCl_3$, c 0.050), (lit value -35°) (8)

Melting point:

134-136 $^\circ C$ (lit. value 136-137 $^\circ C$) (8)

1H NMR (spectrum 1c)

δ (ppm): 0.66 (3H, *s*, H-18), 0.78 (3H, *d*, $J = 7.1$ Hz, H-27), 0.80 (3H, *d*, $J = 7.9$ Hz, H-26), 0.82 (3H, *t*, $J = 7.2$ Hz, H-29), 0.91 (3H, *d*, $J = 6,4$ Hz, H-21), 0.99 (3H, *s*, H-19), 3.50 (1H, *m*, H-3 α), 5.32 (1H, *m*, H-6)

^{13}C NMR (Table A1)

5.18.2 Physical data of compound 2

3-Oxo-12-oleanen-28-oic acid, oleanonic acid

Yield: 8.5 mg

Mass spectrum (spectrum 2a):

EIMS m/z 454.3471 ($C_{30}H_{46}O_3$, req. 454.3447), 439 $[M - CH_3]^+$, 410 $[M - CO_2]^+$

Infrared spectrum (spectrum 2b):

ν_{\max} (KBr): 3421 cm^{-1} (O-H stretching), 2922 cm^{-1} , 2850 cm^{-1} (saturated C-H stretching), 1749 cm^{-1} , 1726 cm^{-1} (C=O stretching), 1049 cm^{-1} (C-O stretching), 1462 cm^{-1} , 1377 cm^{-1} (C-H deformation), 1271 cm^{-1} (C-O stretch)

Optical rotation:

$[\alpha]_{\text{D}} = +99.4^{\circ}$ (CHCl_3 , c 0.022), (lit value $+101^{\circ}$) (9)

Melting point:

225-228 $^{\circ}\text{C}$ (lit. value 226-229 $^{\circ}\text{C}$) (9)

^1H NMR (spectrum 2c)

δ (ppm): 0.75 (3H, *s*, H-26), 0.82 (3H, *s*, H-30), 0.88 (3H, *s*, H-29), 0.98 (3H, *s*, H-24), 0.99 (3H, *s*, H-25), 1.03 (3H, *s*, H-23), 1.04 (2H, *m*, H-21), 1.06 (1H, *m*, H-15b), 1.09 (3H, *s*, H-27), 1.10 (1H, *m*, H-19b), 1.26 (1H, *m*, H-5), 1.28 (2H, *m*, H-7), 1.34 (1H, *dd*, $J_1 = 3.7$ Hz, $J_2 = 12.0$ Hz, H-1a), 1.28 (2H, *d*, $J = 5.6$ Hz, H-6), 1.57 (1H, *m*, H-19a), 1.60 (1H, *m*, H-9), 1.62 (1H, *m*, H-16a), 1.72 (2H, *dd*, $J_1 = 4.0$ Hz, $J_2 = 15.7$ Hz, H-15a), 1.81 (1H, *m*, H-1b), 1.88 (2H, *m*, H-22), 1.93 (2H, *m*, H-11), 1.99 (1H, *m*, H-16b), 2.30 (1H, *m*, H-2a), 2.50 (1H, *m*, H-2b), 2.78 (1H, *dd*, $J_1 = 3.5$ Hz, $J_2 = 12.1$ Hz, H-18), 5.24 (1H, *bs*, H-12)

^{13}C NMR (Table A1)

5.18.3 Physical data of compound 3

3 α -Hydroxy-12-oleanen-28-oic acid, 3-epioleanolic acid

Yield: 5.2 mg

Mass spectrum (spectrum 3a):

EIMS m/z 456.3590 ($\text{C}_{30}\text{H}_{48}\text{O}_3$, req. 456.3603),

Infrared spectrum (spectrum 3b):

ν_{\max} (KBr): 3404 cm^{-1} (O-H stretching), 2947 cm^{-1} , 2879 cm^{-1} (saturated C-H stretching), 1709 cm^{-1} (C=O stretching), 1444 cm^{-1} (O-H in-plane bending), 1379 cm^{-1} (C-H deformation), 1249 cm^{-1} (C-O stretch)

Optical rotation:

$[\alpha]_{\text{D}} = +69.2^{\circ}$ (CHCl_3 , c 0.013), (lit value $+68^{\circ}$) (10)

Melting point:

>250°C (lit. value 294-296 °C) (10)

¹H NMR (spectrum 3c)

δ (ppm): 0.73 (3H, *s*, H-26), 0.81 (3H, *s*, H-30), 0.88 (3H, *s*, H-29), 0.90 (6H, *s*, H-24, H-25), 0.93 (3H, *s*, H-23), 1.10 (1H, *m*, H-1a), 1.12 (3H, *s*, H-27), 1.15 (1H, *m*, H-19a), 1.30 (1H, *m*, H-1b), 1.60 (1H, *m*, H-19b), 1.66 (1H, *m*, H-2a), 1.74 (2H, *m*, H-11), 1.87 (1H, *m*, H-2b), 2.79 (1H, *dd*, $J_1 = 3.9$ Hz, $J_2 = 13.3$ Hz, H-18), 3.39 (1H, *s*, H-3β), 5.23 (1H, *m*, H-12)

¹³C NMR (Table A1)

5.18.4 Physical data of compound 4

2,3,22,23-Tetrahydroxy-2,6,10,15,19,23-hexamethyl-6,10,14,18-tetracosatetrene

Yield: 16.0 mg

Infrared spectrum (spectrum 4b):

ν_{\max} (KBr): 3437 cm^{-1} (O-H stretching), 3000 cm^{-1} - 2879 cm^{-1} (saturated C-H stretching), 1638 cm^{-1} (C=C stretching), 1459 cm^{-1} , 1381 cm^{-1} (C-H deformation), 763 cm^{-1} (C-H out-of-plane bending)

Optical rotation:

$[\alpha]_{\text{D}} = +22^\circ$ (CHCl_3 , c 0.035), (lit value $+23^\circ$) (11)

¹H NMR (spectrum 4c)

δ (ppm): 1.12 (6H, *s*, 2 × CH₃), 1.17 (6H, *s*, 2 × CH₃), 1.38 (2H, *m*, H-4a, H-21a), 1.50 (2H, *m*, H-4b, H-21b), 1.57 (6H, *s*, 2 × CH₃), 1.59 (6H, *s*, 2 × CH₃), 1.98 (8H, *m*, H-9, H-12, H-13, H-16), 2.04 (6H, *m*, H-5a, H-20a, H-8, H-17), 2.19 (2H, *m*, H-5b, H-20b), 3.32 (2H, *dd*, $J_1 = 2.0$ Hz, $J_2 = 10.3$ Hz, H-3, H-22), 5.14 (4H, *m*, H-7, H-11, H-14, H-18),

¹³C NMR (Table A1)

5.18.5 Physical data of compound 5

7-Hydroxy-6-methoxycoumarin, scopoletin

Yield: 4.2 mg

Mass spectrum (spectrum 5a):

EIMS m/z 192.0418 ($C_{10}H_8O_4$, req. 192.0422), 177 $[M - CH_3]^+$, 149 $[M - CH_3 - CO]^+$, 121 $[M - CH_3 - 2CO]^+$

Infrared spectrum (spectrum 5b):

ν_{max} (KBr): 3335 cm^{-1} (O-H stretching), 2850 cm^{-1} (symmetrical stretch of $-OCH_3$), 1706 cm^{-1} (C=O stretching), 1565 cm^{-1} , 1509 cm^{-1} (C=C stretching), 922 cm^{-1} , 860 cm^{-1} (C-H out-of-plane bending),

Melting point:

201-202°C (lit. value 204°C) (12)

1H NMR (spectrum 5c)

δ (ppm): 3.94 (3H, *s*, OCH_3), 6.10 (1H, *s*, OH), 6.24 (1H, *d*, $J_{3,4} = 9.6$ Hz, H-3), 6.83 (1H, *s*, H-5), 6.90 (1H, *s*, H-8), 7.58 (1H, *d*, $J_{3,4} = 9.6$ Hz, H-4)

5.19 Extractives from *Clivia miniata*

5.19.1 Physical data of compound 6

(Z,Z)-9,12-octadecadienoic acid, Linoleic acid

Yield: 1.0842 g

Mass spectrum of methyl linoleate (spectrum 5a):

EIMS m/z 294, 262, 150, 136, 123, 95

5.19.2 Physical data of compound 7

5-Hydroxymethyl-2-furancarboxaldehyde

Yield: 6.6 mg

Mass spectrum (spectrum 7a):

EIMS m/z 126.0307 ($C_{10}H_8O_4$, req. 126.0317), 109 $[M - OH]^+$, 97 $[M - CHO]^+$

Infrared spectrum (spectrum 7b):

ν_{\max} (KBr): 3423 cm^{-1} (O-H stretching), 2924 cm^{-1} , 2855 cm^{-1} , 1670 cm^{-1} (α,β unsaturated aldehyde C=O), 1190 cm^{-1} (C-O-C symmetric stretching), 1521 cm^{-1} (C=C stretching)

^1H NMR (spectrum 7c)

δ (ppm): 3.39 (1H, s, OH), 4.65 (2H, s, OCH₂), 6.62 (1H, d, $J_{3,4} = 3.6$ Hz, H-4), 7.42 (1H, d, $J_{3,4} = 3.6$ Hz, H-3), 9.57 (1H, s, CHO)

^{13}C NMR (Table A2)

5.20 Extractives from *Grewia occidentalis*

5.20.1 Physical data of compound 8

3-(4-hydroxy-3-methoxyphenyl)-2-propenal, coniferaldehyde

Yield: 7.5 mg

Mass spectrum (spectrum 8a):

EIMS m/z 178.0625 (C₁₀H₁₀O₃, req. 178.0630), 177 [M - H]⁺, 163 [M - CH₃]⁺, 149 [M - CHO]⁺

Infrared spectrum (spectrum 8b):

ν_{\max} (KBr): 3424 cm^{-1} (O-H stretching), 2700 cm^{-1} , 2850 cm^{-1} , 1664 cm^{-1} (α,β unsaturated aldehyde), 1587 cm^{-1} , 1514 cm^{-1} (C=C stretching), 971 cm^{-1} (C-H out-of-plane bending)

^1H NMR (spectrum 8c)

δ (ppm): 3.93 (1H, s, OCH₃), 5.95 (1H, s, OH), 6.57 (1H, dd, $J_{1,2} = 15.9$ Hz, $J_{2,3'} = 7.65$ Hz, H-2'), 6.94 (1H, d, $J_{5,6} = 8.2$ Hz, H-5), 7.05 (1H, d, $J_{2,6} = 1.8$ Hz, H-2), 7.10 (1H, dd, $J_{5,6} = 8.2$ Hz, $J_{2,6} = 1.8$ Hz, H-6), 7.38 (1H, d, $J_{1,2'} = 15.9$ Hz, H-1'), 9.63 (1H, d, $J_{2,3'} = 7.65$ Hz, CHO)

5.20.2 Physical data of compound 9

*2,2',6,6'-Tetramethoxy-4'-al-4-(ω -oxo-*E*-propenyl)-biphenyl*

Yield: 15.5 mg

Infrared spectrum (spectrum 9b):

ν_{\max} (KBr): 3418 cm^{-1} (O-H stretching), 2939 cm^{-1} , 2847 cm^{-1} , 1677 cm^{-1} (α,β unsaturated aldehyde), 1588 cm^{-1} (C=C stretching)

^1H NMR (spectrum 9c)

δ (ppm): 3.92 (6H, *s*, 2 \times OCH₃), 3.95 (6H, *s*, 2 \times OCH₃), 6.59 (57 (1H, *dd*, $J_{1',2'} = 15.9$ Hz, $J_{2',3'} = 7.65$ Hz, H-2''), 6.79 (2H, *s*, H-3, H-5), 7.13 (2H, *s*, H-3', H-5'), 7.36 (1H, *d*, $J_{1',2'} = 15.9$ Hz, H-1''), 9.64 (1H, *d*, $J_{2',3'} = 7.65$ Hz, CHO), 9.80 (1H, *s*, CHO)

^{13}C NMR (Table A2)

5.20.3 Physical data of compound 10

Data as for compound 2

References

1. M. Saito, Y. Yamauchi and T. Okuyama, *Fractionation by packed column SFC and SFE*, VCH publishers, New York, USA (1994), p.112.
2. B.S. Musser, M. Piserchio, R.A. Henry and E.L. Boone, *Proc. 5th Int. Symp. Supercritical Fluid Chromatography and Extraction*, Baltimore, Maryland, January 11-14 (1994), D5.
3. M.W. Raynor, K.D. Bartle, I.L. Davies, A.A. Clifford & A. Williams, *J. High Resolut. Chromatogr. & Chromatogr. Commun.*, **11** (1989), 289.
4. Beckmann P/ACE 5000 series instrument manual, Beckmann Instruments, Fullerton, USA (July 1993).
5. Lee Scientific series 600 supercritical fluid chromatograph instrument manual, Dionex, Sunnyvale, USA (November 1988).
6. D. Tong, K. D. Bartle & A.A. Clifford, *J. Microcol. Sep.*, **6** (1994), 249.
7. K. Devchand, M.Sc. thesis, University of Natal (1994), p.32.
8. *Dictionary of Natural Products*, J. Buckingham, F.M. Macdonald, H.M. Bradley (Eds.), Chapman & Hall Chemical database, London, UK, **5** (1994), 5258.
9. *Dictionary of Natural Products*, J. Buckingham, F.M. Macdonald, H.M. Bradley (Eds.), Chapman & Hall Chemical database, London, UK, **4** (1994), 4395.
10. *Dictionary of Natural Products*, J. Buckingham, F.M. Macdonald, H.M. Bradley (Eds.), Chapman & Hall Chemical database, London, UK, **3** (1994), 3132.
11. Y. Nishiyama, M. Moriyasu, M. Ichimaru, Y. Tachibana, A. Kato, G. Mathenge, J.N. Nganga and F. D. Juma, *Phytochemistry*, **42** (1996), 803.
12. Reference 10, p.3072.

CHAPTER 6

SFE optimization by application of dynamic extraction model for the extraction of plant components

6.1 Introduction

Optimization of conditions in any SFE experiment is important as it ensures maximum recovery of analytes. However, in natural product matrices this is sometimes difficult to achieve unless the structures of the target analytes are known prior to extraction. A knowledge of the physical and chemical properties of the solutes can be of considerable aid in establishing optimal conditions for conducting the extraction, since this will effect the time required for executing a particular extraction. Utilizing the solubility parameter theory developed by Giddings, King and Friederich (1) developed a method which permitted the quantitative estimation of solute solubility levels in dense and liquified gas media over a range of pressures and temperatures. The method incorporates the ratio of the solubility parameter of the extraction gas to that of the dissolved solute, thereby permitting correlations to be made for number of solute-gas combinations as well as solute solubilities to be estimated from a knowledge of the solute's molecular structure. However, when dealing with complex matrices of unknown chemical constituents, conditions can be optimised on the basis of total extractable material obtained per unit time (2, 3). Although the optimization would have been more meaningful if one particular important analyte was targeted, in reality this was not possible at this time because the structural elucidation was not complete and the active components not identified. It was therefore uncertain whether the active components followed an extraction profile similar to that illustrated in Figure 2.9 or whether the active components were extracted largely at a particular point within the extraction period. In order to effectively utilize SFE, the fundamental thermodynamic and kinetic parameters that impact on the distribution of the analyte between the dense fluid phase and the

substrate being extracted, needed to be evaluated. Initial extraction conditions were selected on an empirical basis.

6.2 The Extraction Model

For the extraction of uterotonic compounds from *Ekebergia capensis*, *Grewia occidentalis* and *Clivia miniata*, the “hot ball” model (4) was employed which describes the kinetics of extraction with supercritical fluids. This model, as discussed in section 2.12, requires a knowledge of the matrix characteristics, which in the case of natural products is difficult to understand due to irregular particle shapes and sizes. The model also assumes that the rate of flow of the fluid is so high that the fluid remains infinitely dilute, and also the solute is uniformly distributed throughout the matrix. It is then necessary to solve the diffusion equation for the system with appropriate boundary conditions. The problem is mathematically similar to that of the immersion of a hot sphere into a cold fluid (hence the name “hot ball” model) for which the solutions are given by Carslaw and Jaeger (5).

In a later publication, Crank (6) translated the equations into diffusion terms. Adaption of the published solutions (7, 8) leads to the following equation for the ratio of the mass, m , of extractable material that remains in the matrix sphere after extraction for time, t , to that of the initial mass of extractable material, m_o ,

$$m/m_o = (6/\pi^2) \sum_{n=1}^{\infty} (1/n^2) \exp(-n^2\pi^2Dt/r^2) \quad (6.1)$$

where n is an integer and D the diffusion coefficient of the material in the sphere. Equation 6.1 may be simplified by defining quantity t_r , which is proportional to time for any given system (and is therefore a reduced or scaled time) by the following equation:

$$t_r = \pi^2Dt/r^2 \quad (6.2)$$

In terms of the scaled time, equation 6.1 becomes

$$m/m_o = 6/\pi^2 [\exp (-t_r) + 1/4 \exp (-4t_r) + 1/9 \exp (-9t_r) + \dots] \quad (6.3)$$

The solution is therefore a sum of exponential decays, and at long times the later (more rapidly decaying) terms will decrease in importance and the first exponential term in the square brackets will become dominant. A plot of $\ln (m/m_o)$ verses time, or a quantity proportional to time, therefore becomes linear at long times as shown in Figure 2.9. The curve falls steeply initially, the rate of fall then drops and becomes approximately linear after a time corresponding to a value of t_r of around 0.5. Extrapolation of the linear portion of the curve to the $t = 0$ axis gives an intercept of approximately -0.5 [in fact $\ln (6/\pi^2) = -0.4977$]. The physical explanation of the shape of the extraction curve is that initially there is a step in concentration at the surface of the sphere and diffusion out is rapid. As the extraction continues, this step becomes eroded, but nevertheless the concentration gradient near the surface is large, and diffusion, which is proportional to the concentration gradient, continues to be at a high rate. Eventually, however, a smoother concentration profile is established over the whole sphere and diffusion loss becomes a simple exponential decay.

6.3 Selection of extraction temperature

Supercritical fluid extractions of the three plants with water modified CO₂ were performed under the following conditions: 80 °C, 400 atm, 2 mol % H₂O in a 10 ml extraction vessel. The oven temperature of 80 °C ensured that the CO₂-water mixtures were fully miscible (7), but minimised the risk of unnecessary thermal decomposition before extraction, although it was not clear whether such a temperature was effective in extracting the uterotonic components. It is important to remember that when extracting solid substrates, a knowledge of the solute melting point is critical as supercritical fluids are more effective extracting agents when the extraction is performed at a temperature above the melting point of the substrate. In this case, both mass transfer of the solute into the supercritical fluid is improved as well as solute solubility due to the weakening of the cohesive forces of the solid. Likewise, knowledge of the vapour pressure of the solute as

a function of temperature can have a profound effect on both the recorded solubility and the separation factors that are obtained in multi-component solute separation schemes (8).

6.4 Selection of extraction pressure

The fluid pressure of 400 atm gave rise to a high fluid density which usually ensures high solubility. The solubility of a substance in a supercritical fluid is primarily a function of the density of the fluid. The solubility of a substance at constant temperature is a function of pressure and in terms of mole fraction has the schematic form of Figure 6.1. In section A-B, which is at very low pressures not of concern in most extraction processes, the mole fraction (x) falls as the solute is diluted by the fluid. In section B-C there is a rapid rise in x at a so-called threshold pressure characteristic of the solute-fluid system, which is a pressure somewhat above the critical pressure of the fluid. This occurs because of the rapid rise in the density, and therefore solvating effect of the fluid at around this pressure. One must also remember that the solubility maximum is also determined by the extraction temperature since by increasing temperature the volatility of the solute also rises and eventually this effect exceeds the effect of the falling solvation and the solubility rises (11).

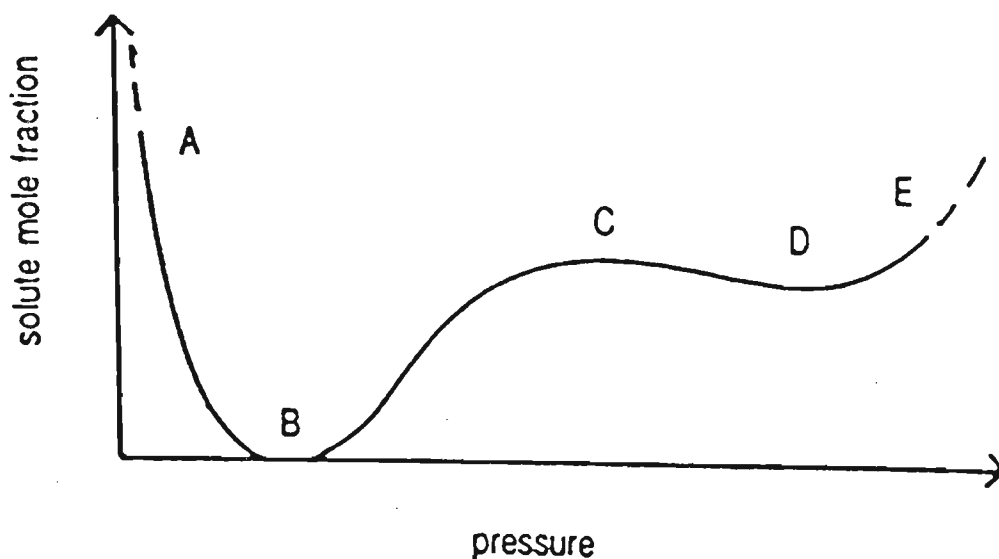


Figure 6.1 Generalized solubility isotherm as a function of pressure at constant temperature.(9)

6.5 Selection of dynamic extraction time

The optimum extraction time is dependent on the experimental pressure and temperature as well as on the flow rate of the fluid through the extraction cell. For unknown samples, the extraction time can best be found by experimentally conducting successive extractions to determine the completeness of extraction. The extraction time was determined by assessing the cumulative weight of the extract obtained from the three plants after extraction times of 10 - 80 minutes at 10 minutes intervals. These results indicate the total rates of supercritical fluid extraction of the target analytes and these analytes account for only a proportion of the total mass of the extract. It is therefore uncertain whether the extraction of these compounds follows a curve with the form of that in Figure 2.9, or whether these compounds are largely extracted at a particular point within the extraction period.

6.6 Supercritical fluid extraction of *Ekebergia capensis*

Milled wood of *E. capensis* (3.0 grams) was extracted into methanol. From Figure 6.2, it can be seen that approximately 85% of the extraction occurred within 60 minutes. Thereafter the rate of extraction dropped rapidly, the mass barely increasing after 70 minutes. The extraction was carried out for 25 minutes to obtain an extracted mass m_1 , followed by two successive extractions to obtain extracted masses m_2 and m_3 . Equation 2.2 (section 2.12) was then used to determine the total mass of the extractable material in the matrix. The results of the extraction are given in Table 6.1.

Table 6.1 Data used to obtain m_0 for *Ekebergia capensis* Sparrm.

Extraction time (min)	mass extracted (mg)
50	17.1
100	19.2
150	20.3

m_0 was calculated to be 21.51 mg and from this, the plot of $\ln (m/m_0)$ vs. time was obtained (Figure 6.3). The data used to obtain this plot is given in Table 6.2.

The curve was found to differ from the theoretical curve of Figure 2.11, in that it did not fall steeply from zero, and this is thought to be due to the effect of solubility limitation (12). Extrapolation of the linear portion of the curve to the time-zero axis, gives an intercept of -0.87 that is, $I = 0.87$, compared with a value for the sphere of 0.4977.

Table 6.2 Data used to obtain Kinetic Plot for the extraction of *Ekebergia capensis* Sparrm.

Extraction time (min)	m_e (mg)	m (mg)*	m/m_0	$\ln m/m_0$
10	4.80	16.71	0.7768	-0.2525
20	10.20	11.31	0.5258	-0.6428
30	13.80	7.71	0.3584	-1.0260
40	15.90	5.61	0.2608	-1.3440
50	17.10	4.41	0.2050	-1.5846
60	18.30	3.21	0.1492	-1.9022
70	18.60	2.91	0.1353	-2.000

* $m = m_0 - m_e$ where m_e is the mass of extract

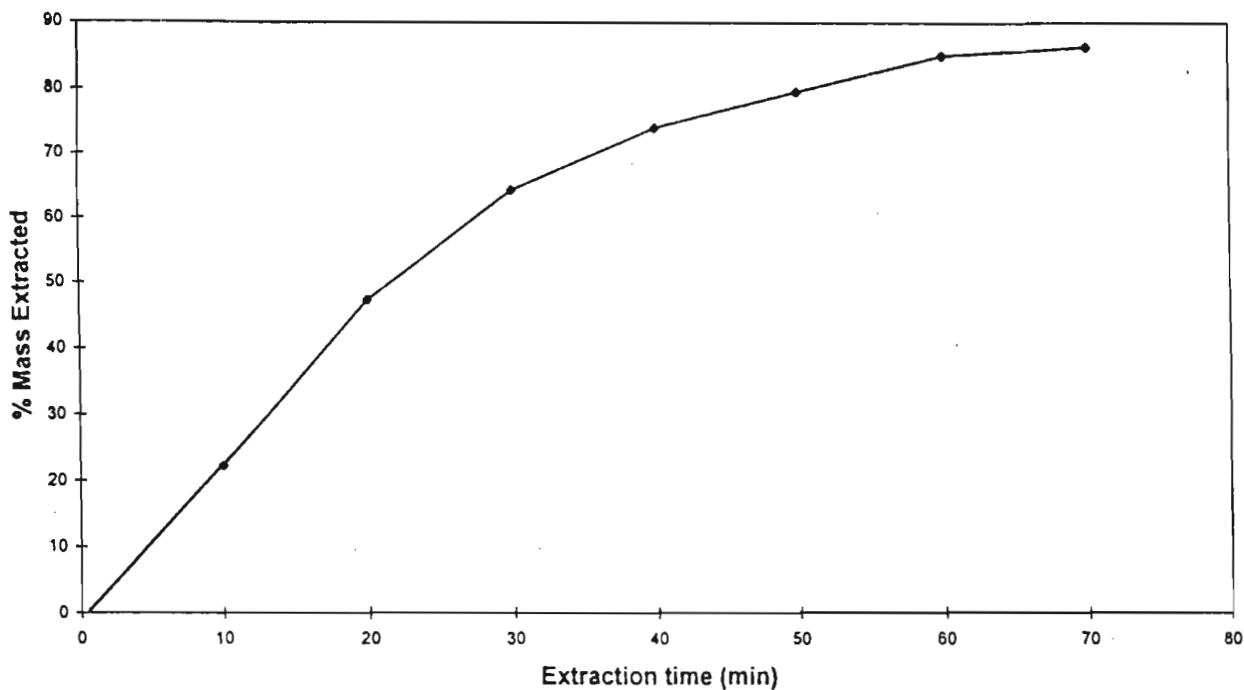


Figure 6.2 Extraction curve of mass of extract from *Ekeberia capensis* Sparrm. as a function of extraction time (min).

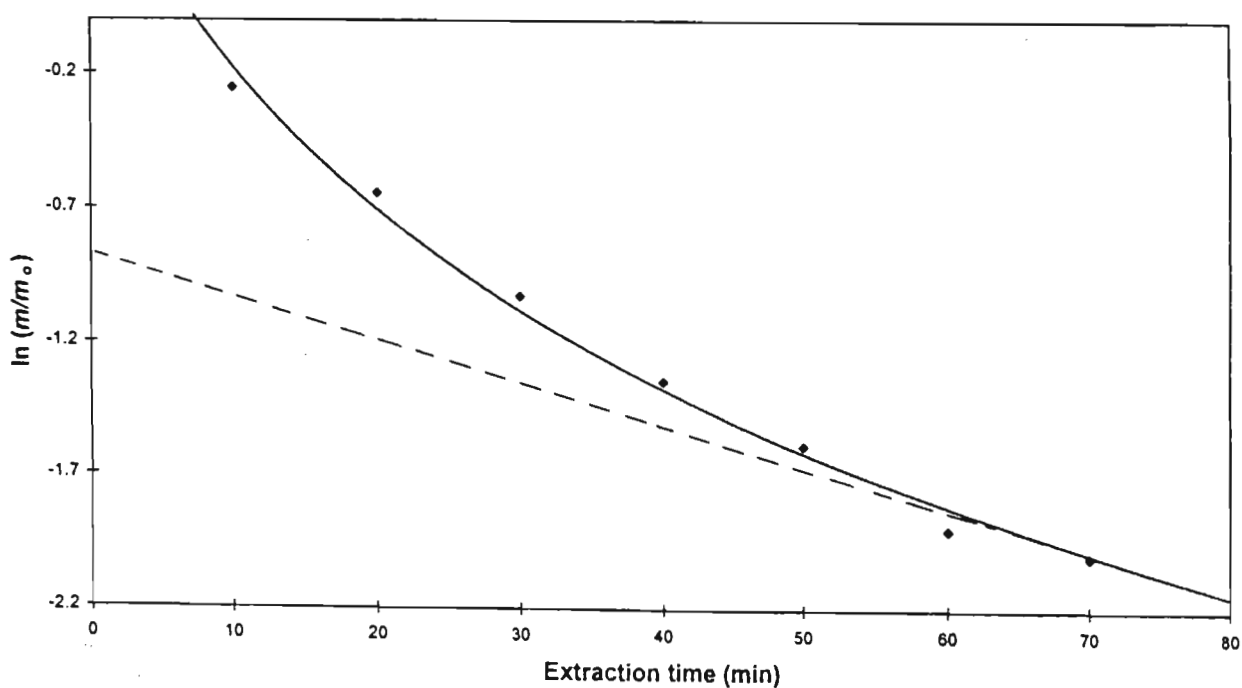


Figure 6.3 Plot of $\ln(m/m_0)$ against extraction time (min) for the supercritical fluid extraction of *Ekeberia capensis* Sparrm.

6.7 Supercritical fluid extraction of *Grewia occidentalis*

Milled wood of *G. occidentalis* (2.0 grams) was extracted. From Figure 6.4, approximately 72% was extracted within 50 minutes. The data provided in Table 6.3 below enabled calculation of m_o .

Table 6.3 Data used to obtain m_o for *Grewia occidentalis*

Extraction time (min)	mass extracted (mg)
50	6.40
100	7.90
150	8.50

m_o was calculated to be 8.90 mg. The data used to obtain the plot of $\ln (m/m_o)$ vs. extraction time is given below in Table 6.4.

Table 6.4 Data used to obtain Kinetic Plot for the extraction of *Grewia occidentalis* L.

Extraction time (min)	m_e (mg)	m (mg)	m/m_o	$\ln m/m_o$
10	1.80	7.10	0.7977	-0.2260
20	3.80	5.10	0.5730	-0.5568
30	5.00	3.90	0.4382	-0.8251
40	5.80	3.10	0.3483	-1.0546
50	6.40	2.50	0.2809	-1.2698
60	6.60	2.30	0.2584	-1.3531
70	6.80	2.10	0.2360	-1.4441

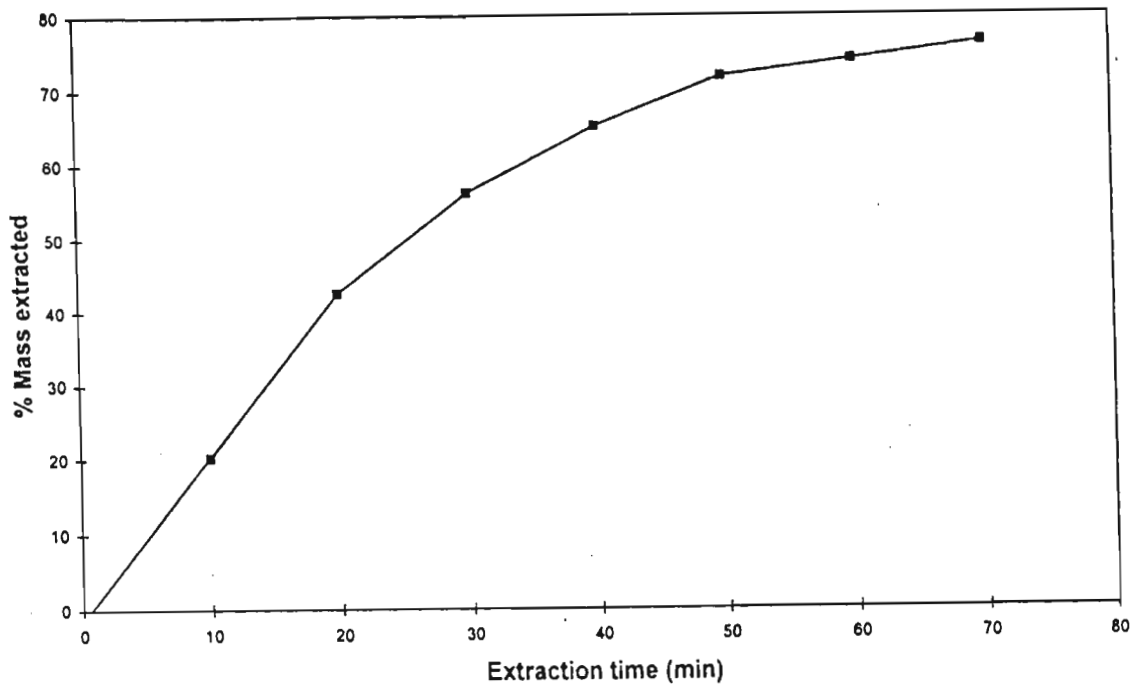


Figure 6.4 Extraction curve of mass of extract from *Grewia occidentalis* L. as a function of extraction time (min).

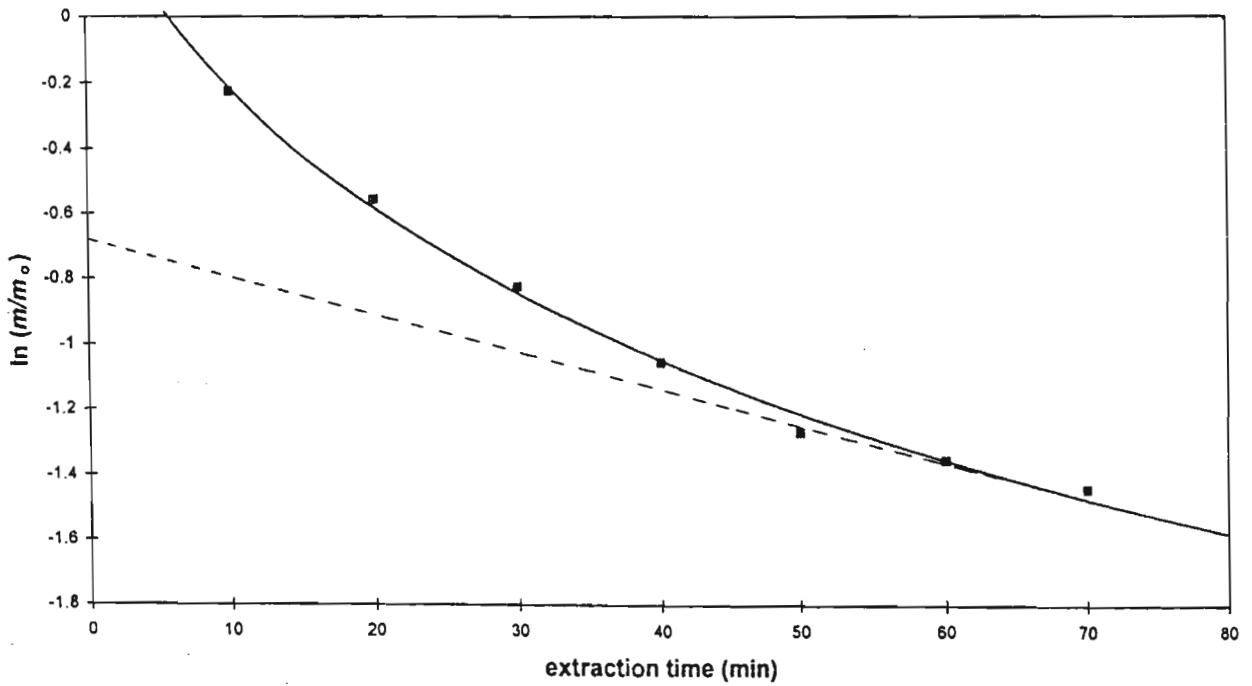


Figure 6.5 Plot of $\ln (m/m_0)$ against extraction time (min) for the supercritical fluid extraction of *Grewia occidentalis* L.

From Figure 6.5, the I intercept was extrapolated to -0.68. In the case of the spherical model, the occurrence of an intercept below that of the theoretical value indicates either non-uniform distribution of extractable compounds or irregular particle shape with a larger surface-to-volume ratio than that of the sphere. With real samples, the particles will not be exact spheres, but of irregular shape, and the concentration of extractable components in the supercritical fluid will not be zero, but often, and, especially at the beginning of the extraction, an appreciable fraction of the solubility. Furthermore, the species to be extracted may not be uniformly distributed within the matrix. Exact modelling of these more complex situations is difficult, as the parameters involved will vary and will generally not be known. The steep fall as depicted by the theoretical model is once again absent. Instead, a similar trend is seen as for *Ekebergia capensis* indicating a solubility limitation possibly due to the highly polar nature of the chemical constituents. The effect of solubility limitation is to reduce the high rate at the beginning of the extraction and also to reduce the slope of the linear portion, with the extent of these effects increasing as the pressure falls and the solubility decreases.

6.8 Supercritical fluid extraction of *Clivia miniata*

Dry milled root of *C. miniata* (2.0 grams) was extracted and from Figure 6.6, it was evident that approximately 92% of the extraction was complete within 50 minutes. The plot of $\ln (m/m_0)$ vs. time yielded an intercept of -2.00, indicative of irregular particle shape (Figure 6.7). The curve was also flattened indicating solubility limitation due to high polarity of the compounds being extracted. The kinetic data can be seen in Tables 6.5 and 6.6.

Table 6.5 Data used to obtain m_0 for *Clivia miniata* L.

Extraction time (min)	mass extracted (mg)
50	153.80
100	162.50
150	165.00

Table 6.6 Data used to obtain Kinetic Plot for the extraction of *Clivia miniata* L.

Extraction time (min)	m_e (mg)	m (mg)	m/m_o	$\ln m/m_o$
10	61.20	104.80	0.6313	-0.4599
20	104.20	61.80	0.3722	-0.9881
30	136.40	29.60	0.1783	-1.7242
40	150.20	15.80	0.0952	-2.3520
50	153.80	12.20	0.0735	-2.6106
60	155.60	10.40	0.0626	-2.7702
70	156.40	9.60	0.05783	-2.8502

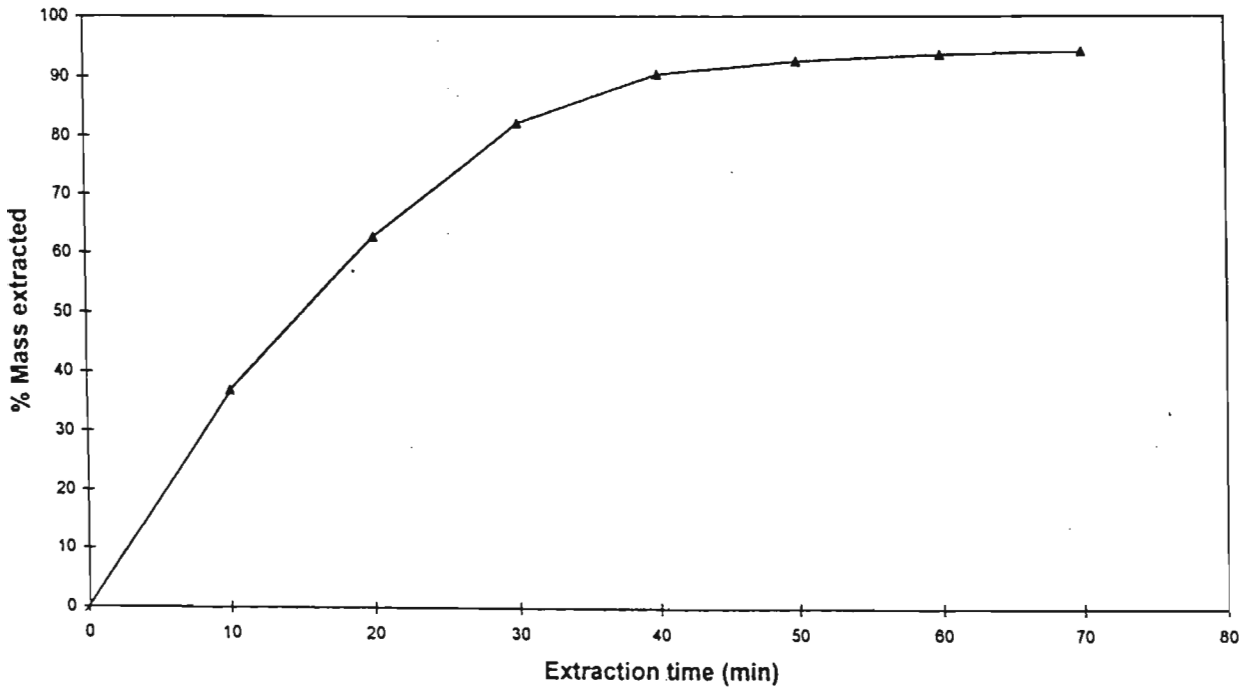


Figure 6.6 Extraction curve of mass of extract from *Clivia miniata* L. as a function of extraction time (min).

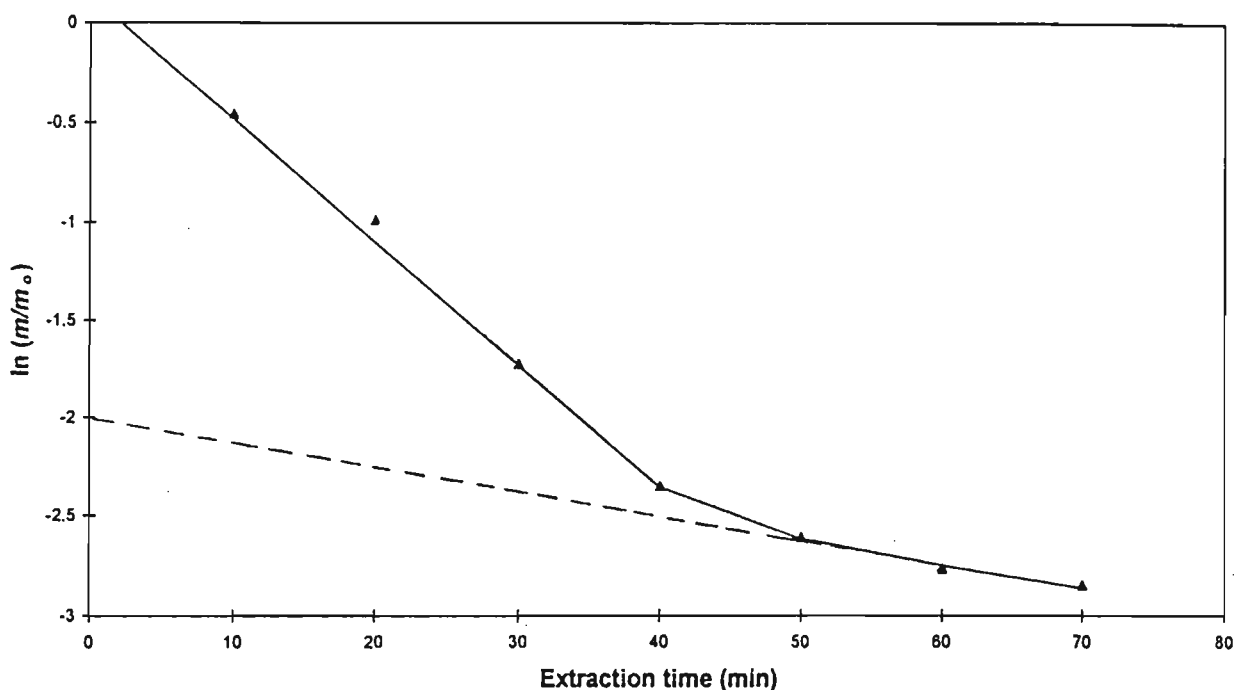


Figure 6.7 Plot of $\ln(m/m_0)$ against extraction time (min) for the supercritical fluid extraction of *Clivia miniata* L.

6.9 Conclusion

In all three cases, solubility was the controlling factor in achieving an interactive extraction. The extraction pressure could not be raised to increase the fluid density as this was a limitation of the instrument. The extraction temperature could not be lowered since water was used as the modifier and modifiers greatly increase the critical point of the fluid and it was therefore important that the temperature remained high enough to maintain a single phase region during extraction. Another reason for the solubility limitation even after adding a modifier could have been the possible displacement of the modifier out of the extraction vessel upon commencing with dynamic extraction. It was therefore necessary to include an equilibration period during extraction to prevent the modifier from being displaced in order to achieve an interactive extraction. This was accommodated for by using an initial 50 minute static extraction period followed by 20 minutes of dynamic extraction. Although the model indicated that only 43-67% of the

extractables were obtained within 20 minutes, the introduction of a static extraction period would most certainly enhance the extraction. Longer dynamic extraction times could have been employed however the total extraction time would have increased tremendously and as the final aim was to couple this technique to the uterotonic bioassay as described in Chapter 8, the extraction had to be performed within a short time together with a sufficient quantity of the extractables to induce a uterotonic response. Hence, a compromise had to be reached.

In comparison of the theoretical model with experimental extraction data, the model performed reasonably well in spite of the non-ideal nature of the samples studied. The results obtained can be explained in individual cases in terms of particle shape, solubility limitation, and non-homogeneous distribution of extractable components within the sphere. For the systems studied, the model and associated treatment appears to be a suitable basis for the analysis and discussion of kinetic extraction data. Although the model gives information about the early stages of extraction, in which the majority of material is extracted, previous considerations of solubility will be more helpful. However, the extraction of the remaining amount of extractables is vital in quantitative analytical applications and of economic importance in industrial extraction processes. For process engineering, a kinetic study and analysis of the result using this model is an important tool in designing extraction processes for maximum economic performance.

References

1. J.W King & J.P Friedrich, *J. Chromatogr.*, **517** (1990), 449.
2. D.M. Heaton, K.D. Bartle, C.M. Rayner and A.A. Clifford, *J. High Resolut. Chromatogr.*, **16** (1993), 666.
3. N.O. Maness, D. Chrz, T. Pierce and G.H. Bruswitz, *JAACS*, **27** (1995), 665.
4. K.D. Bartle, A.A. Clifford, S.B Hawthorne, J.J. Langenfeld, D.J Miller & R. Robinson, *J. Supercrit. Fluids*, **3** (1990), 143.

5. H.S. Carslaw & J.C Jaeger, *Conduction of Heat in Solids*, Clarendon, Oxford, UK (1959), p 233.
6. J. Crank, *The Mathematics of Diffusion*, Clarendon, Oxford, UK (1975), p 89.
7. A. B Newmann, *AIChE Trans.*, **27** (1931), 302.
8. G. C So & D.G McDonald, *Canadian J. Chem. Eng.*, **64** (1986), 80.
9. S.H. Page, S.R. Sumpter & M.L. Lee, *J. Microcol. Sep.*, **4** (1992), 91.
10. E. Stahl, K.W. Quirin, A. Glatz, D. Gerard & G. Rau, *Ber. Bunsenges. Phys. Chem.*, **88** (1984), 900.
11. A.A. Clifford, In: *Supercritical Fluid Extraction and its Use in Chromatographic Sample Preparation*, S.A. Westwood (Ed.), Blackie, Glasgow, UK, (1993), p.31.
12. K.D. Bartle, T. Boddington, A.A. Clifford, N.J. Corton and C.J. Dowle, *Anal. Chem.*, **63** (1991), 2371.

CHAPTER 7

The role of bioassays in medicinal plant analysis and a preliminary investigation of the plant extracts for uterotonic activity

7.1 Introduction

Once a medicinal plant has been identified, a good initial investigation is biological screening. The objectives of this screening are [1] to provide a rationale for clinical use of traditional drugs even if activity is not of an order high enough to warrant development of the active moiety as a new drug [2] to find new drugs and [3] to discover lead molecules (essentially novel chemical moieties) which can be modified through chemical means into new drugs. Furthermore, the role of bioassays on a batch to batch basis is important to confirm consistency and, hence, clinical efficacy and safety for specific case studies (1-3). A bioassay is a semi-quantitative procedure using a functional response, either *in vivo* or *in vitro*, for the determination of the amount of active substance usually against a standard calibrant. Bioassays can reflect the mode of action of a drug and the purity or potency of a product. As the composition of plant components vary from one season to another together with the co-occurrence of undesirable or perhaps toxic compounds, it becomes necessary to also evaluate the risk associated with these compounds. This might involve screens for antibiotic activity; *in vitro* inhibition tests; pharmacologic, agricultural, or veterinary screens that require diverse *in vitro* assays; and/or *in vivo* animal models and cytotoxicity testing using cells in culture. The rapid progress in the field of bioactive metabolites is due in large part to the utilization of bioassay-guided fractionation techniques. With this method most substances isolated will be those that have activity in a particular bioassay or set of bioassays, although metabolites occurring in significant quantities should not be overlooked.

7.2 Selection of bioassays

Several bioassays can be performed on plant derived products in order to identify the activities they possess. Bioassays can be selective in order to detect substances having a particular activity or broad based in order to find out if it has any exploitable potential. The cost of bioassays can be high, in terms of the animals used, labour, facilities and time. The legal requirements governing the design, safety, staffing and use of animal facilities are also becoming ever more demanding. Hence careful consideration is required for the selection of the most appropriate bioassay system for a particular purpose. It is essential to evaluate the practical elements of assay precision, ruggedness, cost and speed. The assay must then be validated, and its relevance for its intended purpose demonstrated.

7.3 The uterotonic bioassay

Isolated tissues have been used effectively in medicinal plant research to obtain information on the activity and toxicity of plant extracts. In this work selective screening was undertaken using strips of guinea pig uterine smooth muscle *in vitro* to detect uterotonic components in plant extracts. Guinea pigs were used as they are small, cheap and easily available models for certain aspects of human reproductive endocrinology. They have spontaneous ovulations with cyclic, progesterone-secreting corpora lutea of about 14 days duration (4), their uterine motility is not influenced by progesterone (5) and the placenta is steroid-secreting (4). Uterine smooth muscle *in vitro* has been used extensively for many years, not only for the purpose mentioned above but also for an understanding of the relationship between the structure and activity of biologically active peptides (6), to help with the characterization of drug receptors and the understanding of receptor mechanisms in the uterus (7, 8). An important advantage of *in vitro* analysis is the elimination, to a large extent, of pharmacokinetic variables. The response to an agonist is proportional to the concentration of that agonist and the density of its receptor sites. Unfortunately, in intact animals, this concentration is determined by many other factors besides the dose of the agent administered. Thus, a change in the response to a fixed dose might be brought about, not because the target organ has become more or less sensitive, but because a different concentration of the agent is reaching the receptor site as

a result of changes in pharmacokinetics. Although changes of a pharmacokinetic nature can occur *in vitro*, the number of variables is considerably reduced and interpretations are more direct. The pharmacokinetic influences are illustrated in Figure 7.1.

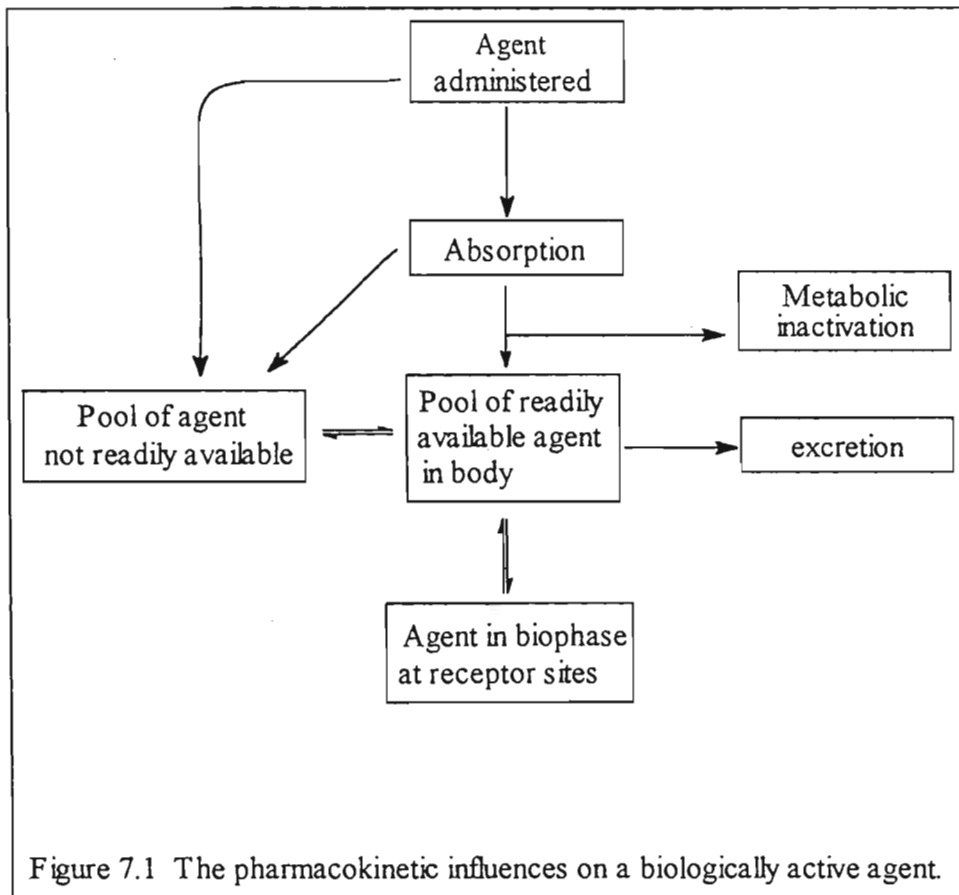


Figure 7.1 The pharmacokinetic influences on a biologically active agent.

In setting up the experiment, many factors were considered to ensure the primary requisites for isolated tissues, namely uniformity and stability. The first factor that was considered was preservation of tissue viability. Historically, pioneering work by many researchers such as Tyrode (9) and Krebs (10) has led to the definition of nutrient solutions capable of preserving isolated tissues in a viable state. Different tissues require a different milieu of ions and nutrients. Changes in ionic content and composition can affect tissue reactivity and base-line activity. For example, high osmotic pressure depresses cardiac pacemaker activity (11) while changes in levels of potassium ions (12, 13, 14) or

magnesium ions (15) can greatly modify isolated blood vessel tone and reactivity to agonists. Specific changes in ionic composition can eliminate spontaneous activity in some tissues and allow stable steady-state responses to agonists (16, 17). Tyrodes solution of constant ionic strength was therefore prepared prior to each set of experiments to provide the isolated tissues with the necessary nutrients.

Adequate delivery of oxygen to the tissue is another prime consideration. The basal activity of smooth muscle and cardiac muscle can be affected by changes in the partial pressure of oxygen (P_{O_2}) in the organ bath. For example, the contractile responsiveness of arterial smooth muscle decreases with decreasing P_{O_2} , the effects being more pronounced for thick- rather than thin-walled vessels and also for high levels of contractile stimulus (18, 19). Once the tissues were removed from the animal, they were placed immediately in cold Tyrodes together with the passage of 95 % O_2 and 5 % CO_2 at a flow rate of 60 ml/min. This ensured that the muscle remained in a viable state during the experimental period.

7.4 Theory of smooth muscle contraction

Smooth muscle is found in the walls of blood vessels, intestines, urinary and reproductive tracts. The long spindle-shaped cells associate to form a muscle in patterns appropriate to their function, such as an annular arrangement in blood vessels and a crisscross network in the bladder (20). The basic principles of contraction are the same as in striated muscle in that myosin molecules exert force on actin filaments, using ATP hydrolysis as the source of energy. Ca^{2+} is essential for smooth muscle contraction. In the head of each myosin molecule are two small polypeptides known as myosin light chains (MLC); this is in addition to the heavy myosin chains. In smooth muscle, one of these light chains (the p-light chain) inhibits the binding of the myosin head to the actin fibre, and thus prevents contraction. Ca^{2+} activates a myosin kinase that, with ATP, phosphorylates the p-light chain and abolishes its inhibitory effect, thus triggering contraction. The Ca^{2+} does not directly activate the kinase; instead it combines with a protein, calmodulin to form a calcium-calmodulin complex which induces a conformational change in the latter such that

it combines with the inactive kinase and activates it. When the Ca^{2+} level falls, the process reverses and a phosphatase dephosphorylates the myosin light chain causing muscle relaxation. The scheme is summarised in Figure 7.2. Free calcium levels are regulated by the intracellular calcium pool, by the actions of the storage vesicles and of the myometrial cell membrane. The membrane contains the calcium channels and the calcium-magnesium-stimulated ATPase system, both of which are important in the regulation of the transmembrane calcium transport.

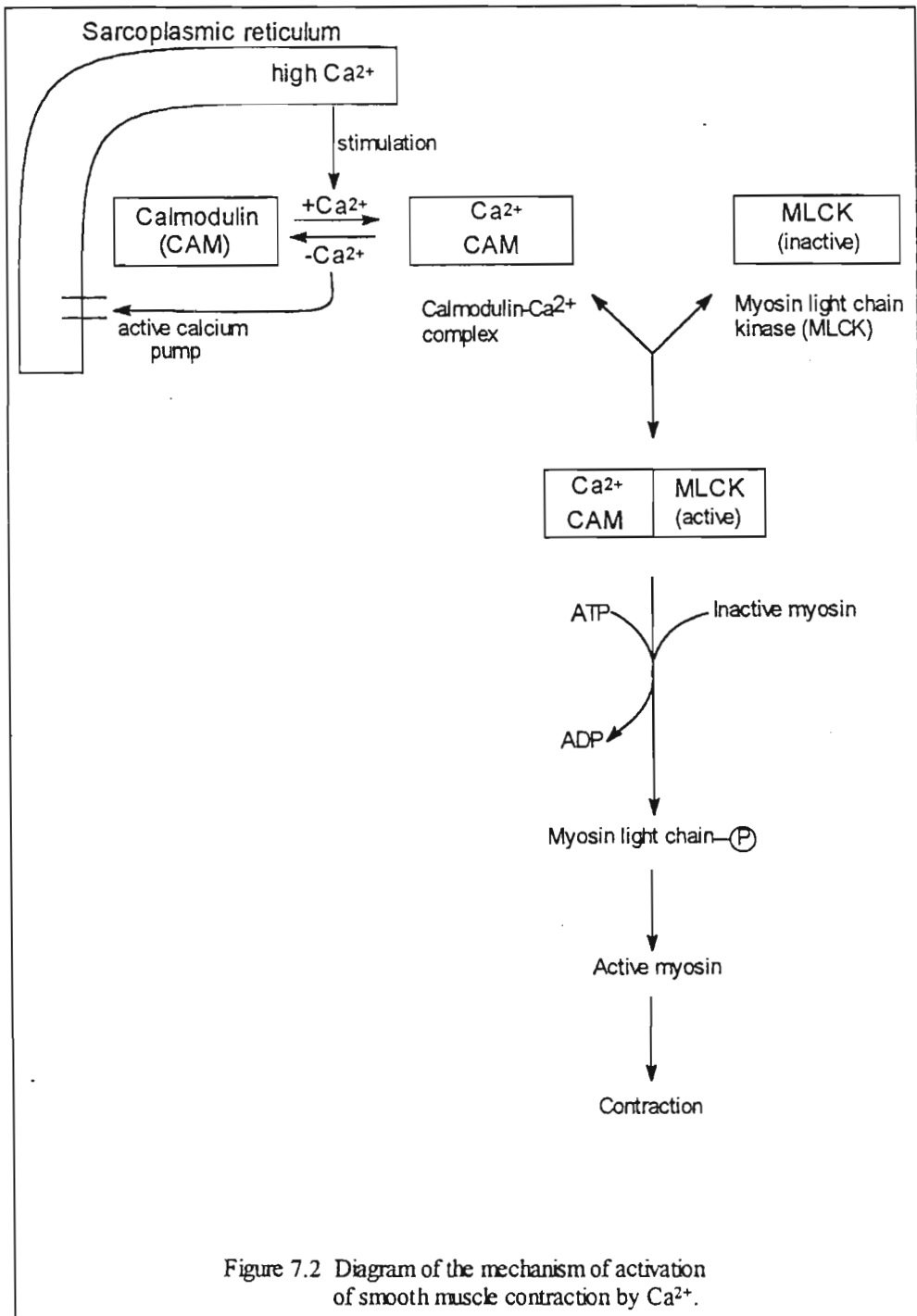
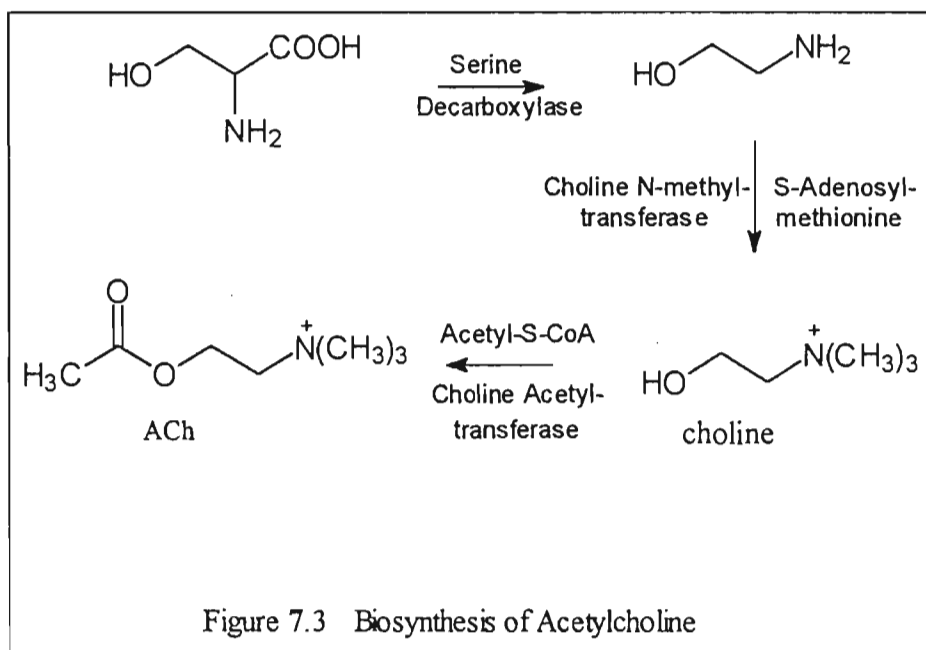


Figure 7.2 Diagram of the mechanism of activation of smooth muscle contraction by Ca^{2+} .

7.5 The effect of acetylcholine (ACh) on smooth muscle

ACh was used as the standard smooth muscle stimulant as this is the natural agonist or mediator at postganglionic parasympathetic nerve endings in the myometrium. ACh is synthesised in cholinergic neurons by the enzyme-catalysed transfer of the acetyl group from acetyl coenzyme A (acetyl CoA) to choline, a quaternary ammonium alcohol (21). The enzyme catalysing this reaction, choline acetyl transferase is also synthesised by the neuron (Figure 7.3).



Most newly biosynthesised ACh is actively transported into cytosolic storage vesicles located in the presynaptic nerve endings, where it is maintained until a release is initiated by an action potential that has been carried down the axon to the presynaptic nerve membrane. This action leads to the opening of voltage-dependent calcium channels affording an influx of Ca²⁺ and an exocytotic release of ACh into the synapse. ACh in the synapse can bind with receptors on the postsynaptic or presynaptic membranes to produce a response. Free ACh, that which is not bound to a receptor, is hydrolysed by acetylcholinesterase. This hydrolysis is the physiologic mechanism for terminating the action of ACh together with the rapid sequestering of intracellular Ca²⁺. Both applied

ACh and parasympathetic nerve stimulation have similar effects on smooth muscle. In this experiment the muscle was separated from the nerve endings hence ACh was administered directly to the muscle. Figure 7.4 displays the electrical recording of a guinea pig uterine smooth muscle contraction induced by 1 μg acetylcholine hydrochloride (ACh). Administration of this drug induced an immediate contraction. Thereafter the muscle was washed by flushing the tissue bath twice with Tyrodes solution at 37 $^{\circ}\text{C}$.

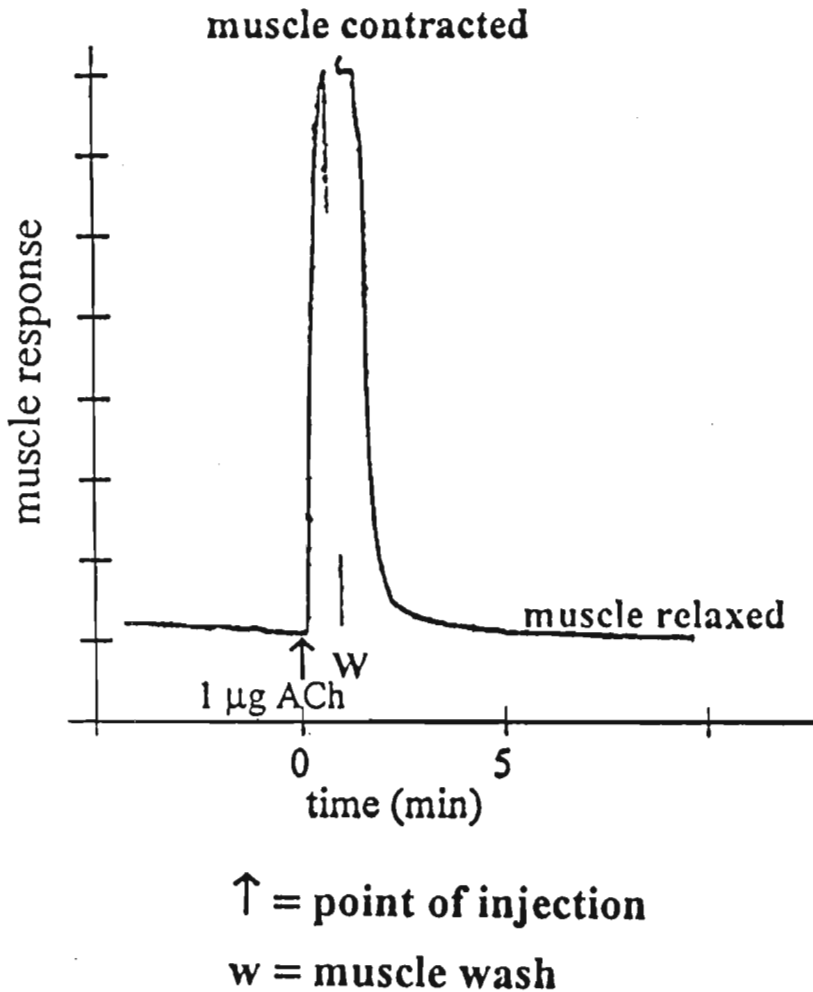


Figure 7.4 Electrical recording of Guinea Pig uterine smooth muscle contraction induced by 1 μg *O*-Acetylcholine hydrochloride (ACh).

In certain cases a higher dose of ACh was required to induce an agonistic response as a result of tissue variation. A great deal of pharmacological inference is derived from the relative sensitivity of tissues to agonists. Many factors including animal variation with respect to agonist uptake mechanisms, numbers of viable receptors, and differences in the efficiency of stimulus-response mechanisms can cause heterogeneity in sensitivity of tissues to agonists. The most common problem is animal maturity which affects receptor density and the reactivity of the isolated tissue (22).

The adsorption of drugs to the surface of the organ bath can serve as a physicochemical process of drug removal from the receptor compartment. This methodological problem has been encountered with basic antihistamines such as promethazine (23) where substantial dilution errors were introduced into experiments by use of glass containers. Adsorption to glass surfaces has been encountered with peptides such as substance P (24). Hence, to overcome surface adsorption and subsequent leaching into fresh physiological fluid, polypropylene organ baths were used as this was observed to eliminate the problem in previous experiments (25).

In this study, the uterotonic effects of three plants viz. *Clivia miniata* (Lindl.) Regel., *Ekebergia capensis* Sparrm., *Grewia occidentalis* L. were evaluated. These plants are used frequently during the late stages of pregnancy.

7.6 Analysis of extracts of *Ekebergia capensis* Sparrm.

7.6.1 Aqueous extract

The aqueous extract of *Ekebergia capensis* was prepared as outlined in section 5.3. An irreversible increase in uterine contractility was initiated 100 seconds after administration of 588 µg of the aqueous extract of *Ekebergia capensis* into the organ bath (Figure 7.5a). Attempts to reduce or stop the contractions by the addition of mepyramine, an antihistamine, were ineffective and as a result, a second strip of muscle tissue had to be prepared in order to confirm our initial findings. The second strip of muscle responded to

2 μg ACh however 12.5 μg of mepyramine was required to reduce the spontaneous contractile activity of the muscle. The muscle thereafter failed to respond adequately to up to 12 μg ACh, however when 700 μg of the aqueous extract was dispensed into the bath, a similar irreversible contractile response was initiated (Figure 7.5b). Subsequent addition of antihistamine failed to decrease the uterine contractions. Activation of H_1 receptors (histamine sites blocked by mepyramine) stimulates the contraction of smooth muscles in many organs such as gut, uterus and bronchi. Such effects are readily blocked by compounds known as H_1 antagonists (26). In this study mepyramine, an antihistamine, was used to reduce the activity induced by the extract however the results indicated that the active components stimulated muscle contraction through other receptors. Further investigations into the receptor pharmacology are discussed in a later chapter. These results however confirm that the aqueous extract of the wood of *Ekebergia capensis* is indeed uterotonnic and that the active components do not act via histamine receptors since the addition of extract after mepyramine stimulated muscle contractions and the subsequent addition of antihistamine to the organ bath after administration of the extract failed to reduce the contractile activity of the muscle.

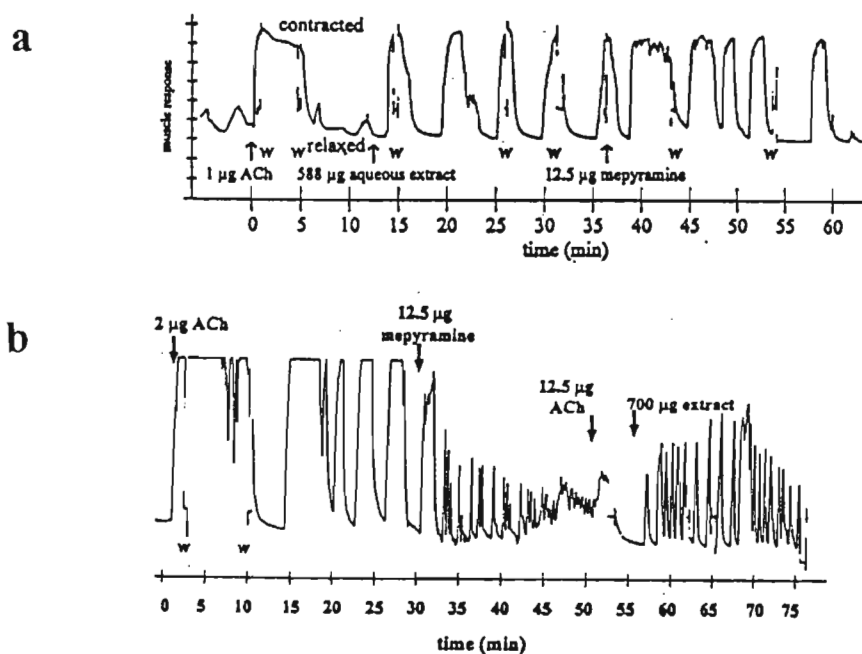


Figure 7.5 Electrical recording of non pregnant guinea pig uterine smooth muscle contraction induced by (a) 588 μg of the aqueous extract of milled wood of *Ekebergia capensis* and (b) 700 μg of the aqueous extract after administration of mepyramine. w = muscle wash

7.6.2 SFE extracts

Initial SFE extracts of the first batch of dry, milled plant material obtained at various densities of pure supercritical CO₂ were uterotically inactive probably due to the low solubility of active compounds and limited polarity or solvent strength of CO₂. The polarity of the fluid was increased by the addition of 200 µl water directly to 6.5 grams plant matrix; a common practice in SFE. The addition of modifier aided the recovery of target analytes possibly due to the enhanced solubility of the analytes in the modified fluid. The addition of modifiers has also been shown to change the morphology of the substrate that is being extracted resulting in an improved extraction flux, e.g. in the extraction of caffeine from coffee (27) and also to aid in the desorption of analytes from highly adsorptive sample matrices by displacing the analyte from the surface (28). However, modifiers greatly increase the critical point of the fluid and it was therefore important that the experimental parameters were altered to maintain a single phase region during extraction. An equilibration period was also necessary to prevent the modifier from being displaced out of the extraction vessel in order to achieve an interactive extraction. This was accommodated for by using an initial 50 minute static extraction period followed by 20 minutes of dynamic extraction. The extractables were collected into methanol which was later evaporated and weighed. Thereafter, the extracts were reconstituted in 0.9% normal saline solution at known concentrations.

The SFE extracts were subsequently evaluated. Figure 7.6 displays the muscle contractions induced by the total 400 atm SFE extract on a non pregnant uterus. The response to 760 µg of the extract was monitored for 260 seconds. Once the crest of the contraction peak was reached, the muscle was immediately washed to facilitate rapid relaxation. Thereafter a similar dose of the extract was repeated however the muscle wash was performed after the muscle had spontaneously relaxed. A third dose of 3800 µg was finally administered and on each response, an increase in the area beneath the contraction peak tracing was observed indicating that the SFE extract produced a dose response uterotonic activity. A larger dose of 7500 µg of the SFE extract was administered to the muscle and an irreversible contractile response was initiated. This

study confirms that water modified supercritical CO₂ possessed the solvating power to extract the uterotonic components.

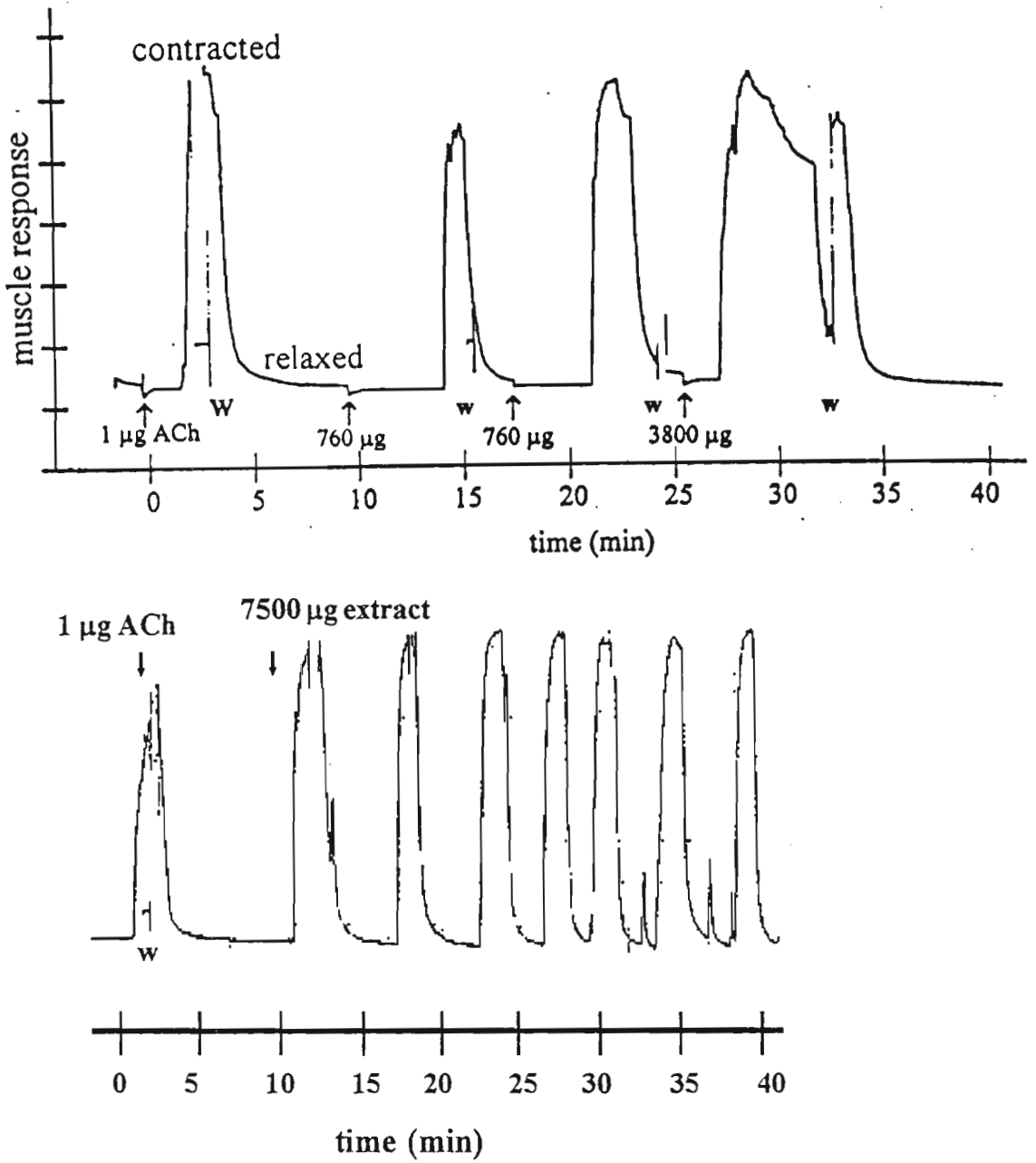


Figure 7.6 Electrical recording of contractions induced by the SFE extract of *Ekebergia capensis* on a non-pregnant uterus. w = muscle wash

When these results were compared to those obtained using a pregnant uterus, it was found that a lower dose of the extract was required to bring about a contractile response in the pregnant uterus (Figure 7.7). This may be explained due to increased sensitivity of the uterus as a result of hormonal changes during pregnancy. During pregnancy, the uterus is exposed to, and is altered by, the changing hormonal environment. Circulating estrogen and progesterone increase substantially due primarily to enhanced production of these hormones from the ovaries and placenta. There is also a substantial increase in the agonist receptors in the myometrium (29).

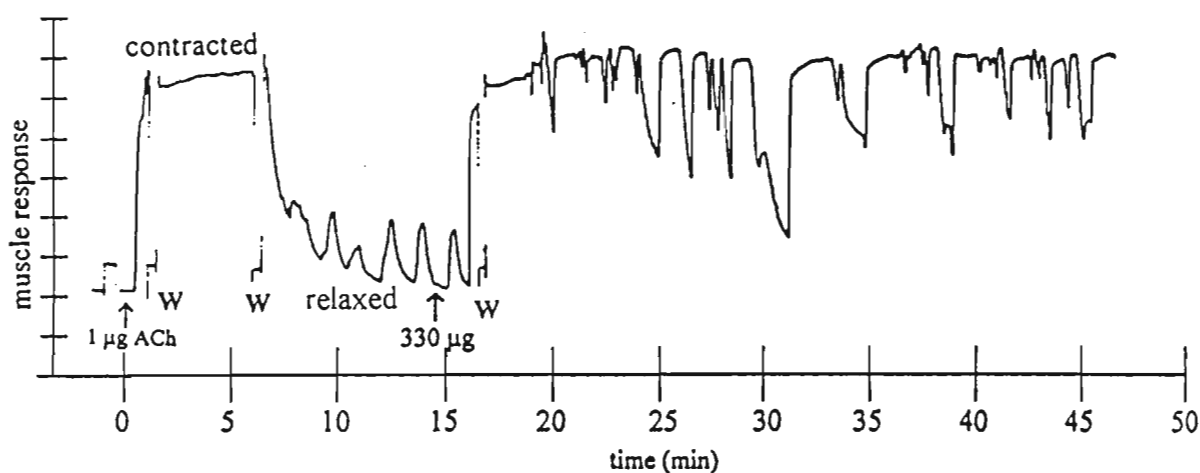


Figure 7.7 Electrical recording of contractions induced by the SFE extract of *Ekebergia capensis* on a pregnant uterus. w = muscle wash

7.6.3 Supercritical fluid fractionation of *Ekebergia* extracts

Co-extraction of unwanted solutes along with target analytes frequently occurs during extraction. Just as one can extract chemical compounds of varying polarity with solvents of different polarity, so too can one extract compounds of different classes using supercritical fluids. In an attempt to decrease the complexity of the extract, SFE fractions were obtained by sequentially increasing the pressure at constant temperature and modifier

concentration, hence changing the density of the fluid. Non polar to intermediate polarity compounds would be removed at lower pressures while the highly polar compounds were extracted at higher pressures. Subsequent physiological testing enabled active fractions to be differentiated from inactive ones as well as the detection of a fraction that was observed to have a spasmolytic effect on uterine muscle. The sequentially fractionated extract at 400 atm produced a muscle response at a dose of 315 μg (Figure 7.8). A similar response to ACh as initially observed led to the conclusion that the extract did not elicit any adverse effects on the muscle at the dose administered. A lower dose of 70 μg was administered in order to establish the lowest concentration required to bring about stimulant activity. The dose was further decreased to 35 μg at which level no activity was observed.

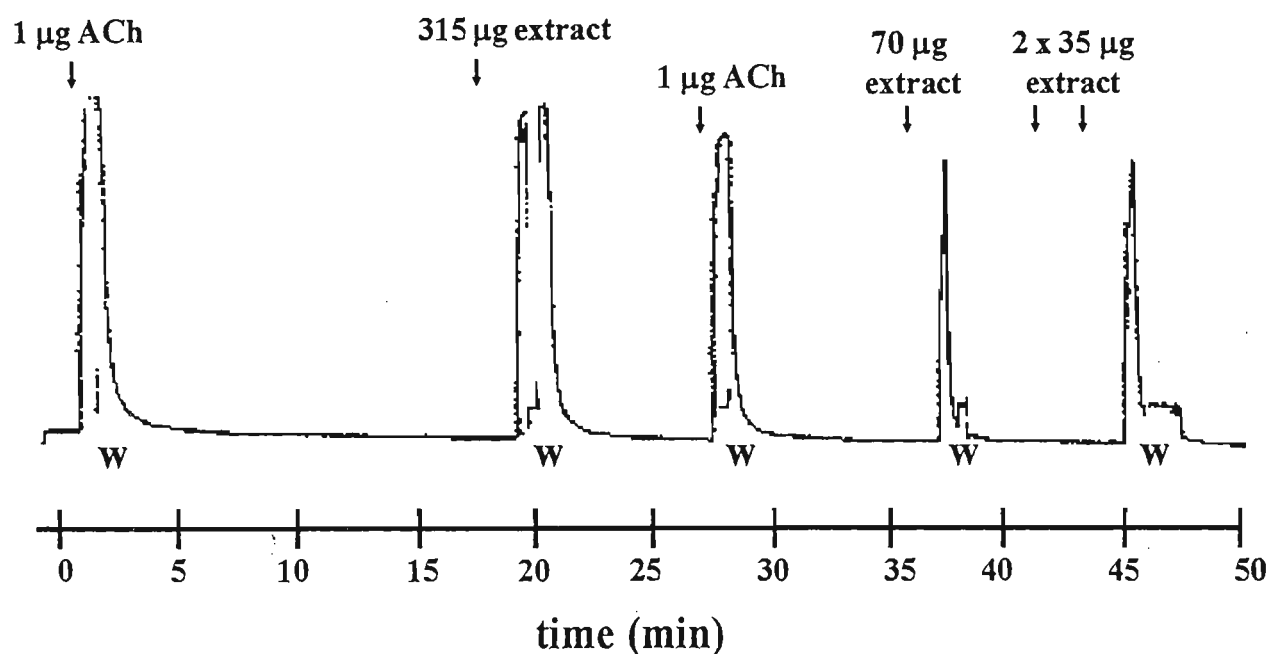


Figure 7.8 Electrical recording of non pregnant guinea pig uterine smooth muscle contraction induced by the sequentially fractionated extract of *Ekebergia capensis* at 400 atm. w = muscle wash

The extract at 350 atm also displayed stimulant activity at a dose of 317 μg . However, this was followed by a reduction in the muscle response to 1 μg ACh indicating the extract to be active as well as spasmolytic to a certain extent (Figure 7.9). Spasmolytic activity was observed by the decrease in muscle response to ACh after addition of the extract to the muscle chamber. This antagonistic behaviour of the extract would defeat its intended purpose.

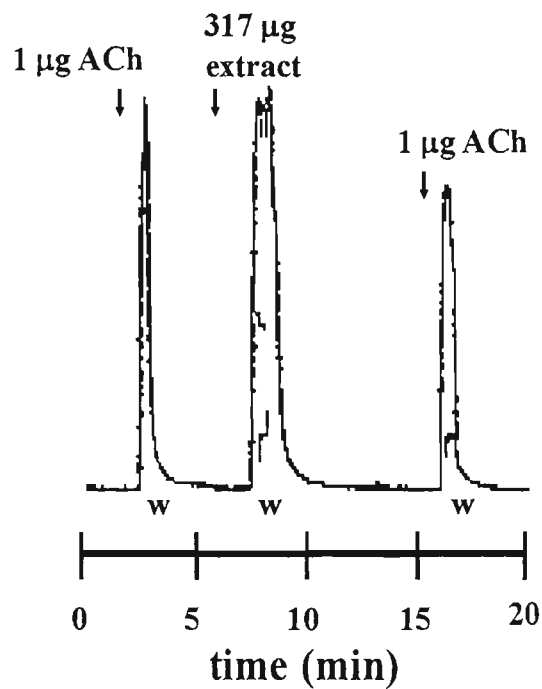


Figure 7.9 Electrical recording of non pregnant guinea pig uterine smooth muscle contraction induced by the sequentially fractionated extract of *Ekebergia capensis* at 350 atm. w = muscle wash

The 300 atm extract was inactive at all three doses, i.e 325 μg , 659 μg and 1300 μg . The ACh response decreased with each dose indicating spasmolytic activity (30) (Figure 7.10).

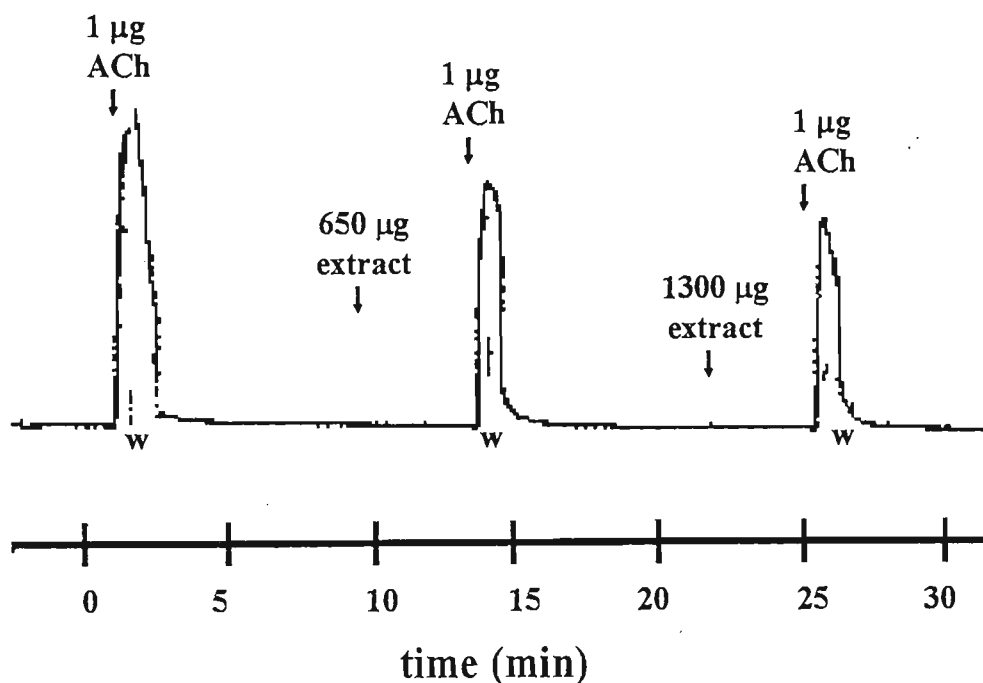


Figure 7.10 Electrical recording of non pregnant guinea pig uterine smooth muscle contraction induced by the sequentially fractionated extract of *Ekebergia capensis* at 300 atm. w = muscle wash

The extract obtained at 250 atm was non-reactive even at doses up to 2600 μg . It was difficult to evaluate the aqueous extract as opposed to the fractionated SFE extracts for toxicity due to the irreversible contractile response exerted by the aqueous extract on the muscle. Many traditional healers believe that herbal remedies are non toxic, however it is possible that due to the complex nature of the aqueous extract, the toxic effects of certain compounds are masked especially if the toxins are present at low concentrations. Supercritical fluid fractionation (SFF) has thus displayed tremendous potential in the evaluation of these extracts.

possible that due to the complex nature of the aqueous extract, the toxic effects of certain compounds are masked especially if the toxins are present at low concentrations. Supercritical fluid fractionation (SFF) has thus displayed tremendous potential in the evaluation of these extracts.

7.7 Analysis of extracts of *Clivia miniata* (Lindl.) Regel

The aqueous and SFE extracts of the root of *Clivia miniata* were screened on a pregnant guinea pig uterus.

7.7.1 Aqueous extract

The guinea pig uterine smooth muscle was observed to produce an agonistic response to 1 μg ACh. The subsequent addition of 400 μg of the aqueous extract induced a contractile response of similar amplitude as the ACh response (Figure 7.11). The contractions were observed to occur at almost equal time periods however the decrease in tension was followed by a more spasmolytic type of response. The aqueous extract of the leaves of this plant was also evaluated by Veale *et al.* (29) and found to produce concentration-dependent contractions in rat ileum and uterus. However there are no reports on the evaluation of SFE extracts nor the identification of the active components.

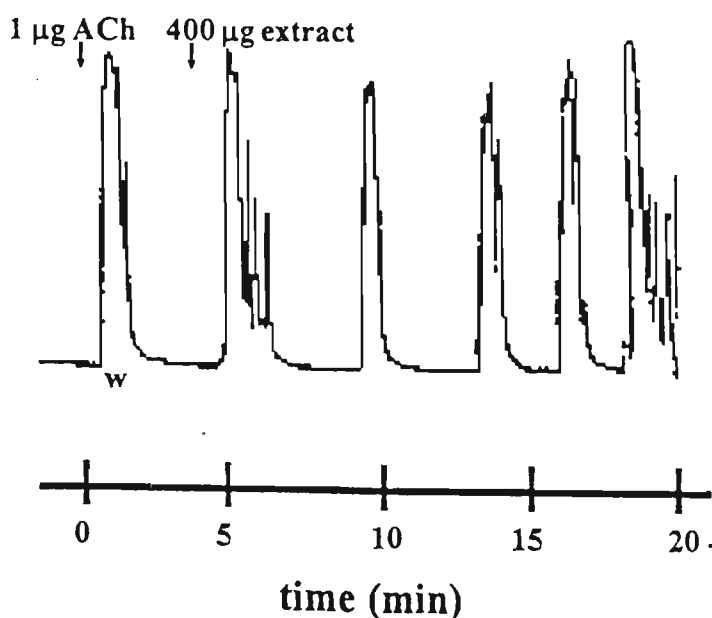


Figure 7.11 Electrical recording of pregnant guinea pig uterine smooth muscle contraction induced by the aqueous extract of *Clivia miniata* (Lindl.) Regel. w = muscle wash

7.7.2 SFE extract

After responding to a dose of 1 μg ACh, the muscle was exposed to 250 μg of the 400 atm SFE extract of *Clivia miniata*. The extract was found to elicit an immediate contractile response of high amplitude which persisted following three subsequent washes with Tyrodes solution (Figure 7.12). The muscle was monitored for a period of 45 minutes during which time there was no indication of a reduction in the contractile response. The contractions were observed to be irregular and more prolonged. Unlike the aqueous extract, a smaller dose of the SFE extract brought about a much larger effect on the muscle indicating the SFE extract to be more potent as a result of the increased selectivity of the extraction technique hence obtaining an extract with a much larger concentration of the active component.

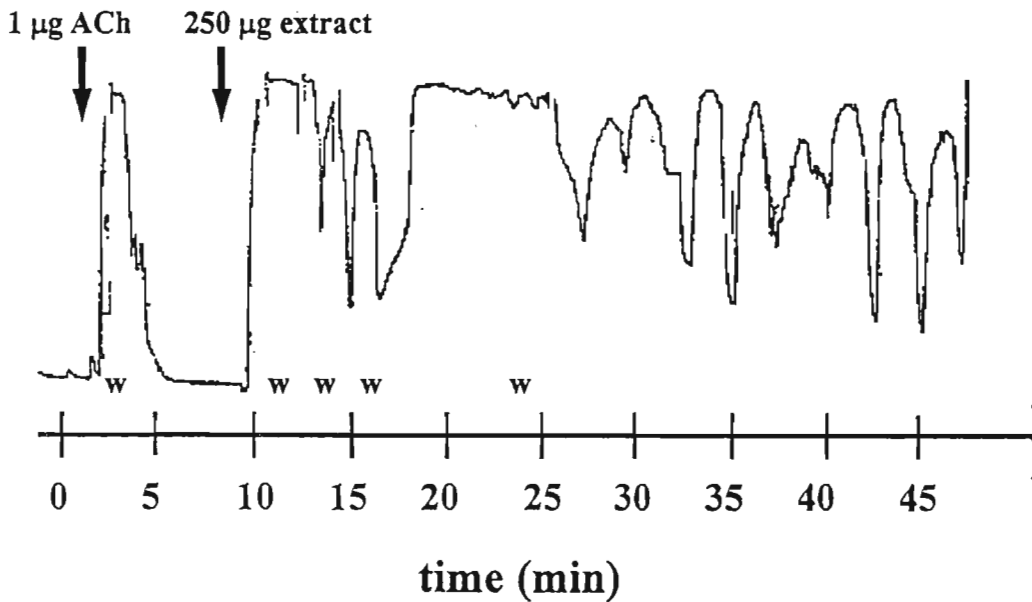


Figure 7.12 Electrical recording of pregnant guinea pig uterine smooth muscle contraction induced by the SFE extract of *Clivia miniata* (Lindl.) Regel.
w = muscle wash

7.8 Analysis of *Grewia occidentalis* L.

The aqueous and SFE extracts of the wood of *Grewia occidentalis* were screened on a pregnant uterus.

7.8.1 Aqueous extract

The aqueous extract was found to elicit a muscle response of similar amplitude as that induced by 1 μg ACh. 250 μg of the extract was administered and an immediate development in tension was observed (Figure 7.13). Upon washing the muscle with Tyrodes solution, the contractile response decreased. A subsequent addition of 200 μg of the extract to the muscle bath confirmed that the aqueous extract was uterotonic by producing a concentration dependent muscle response.

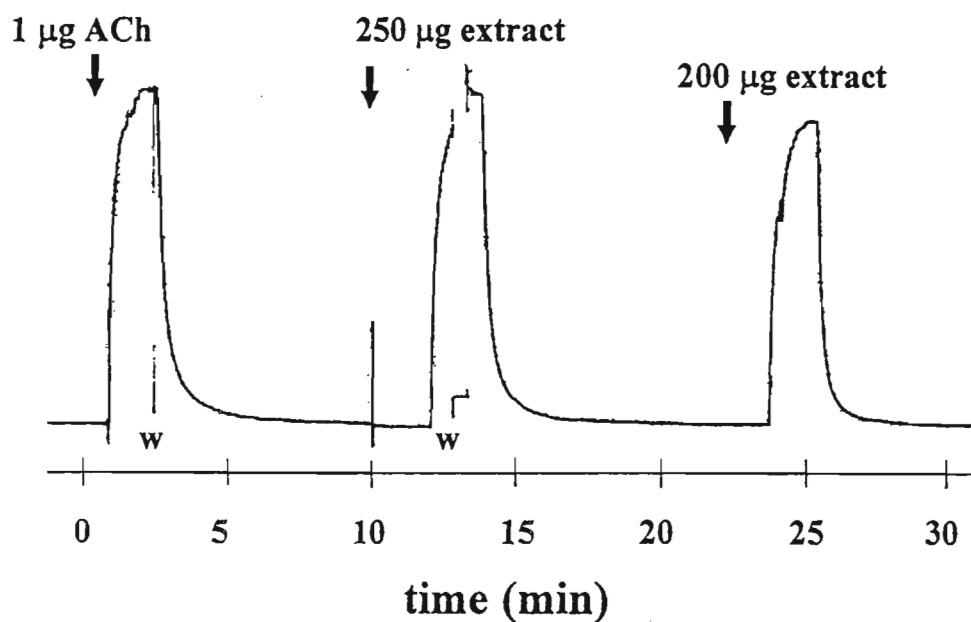


Figure 7.13 Electrical recording of pregnant guinea pig uterine smooth muscle contraction induced by the aqueous extract of *Grewia occidentalis* L.
w = muscle wash

7.8.2 SFE extract

The SFE extract was tested and found to stimulate muscle contraction although at much lower doses. Unlike the aqueous extract, only 112 μg was sufficient to induce a contractile response. The increase in tension was followed by spasmodic type behaviour however, upon washing the muscle, the response decreased (Figure 7.14). A repetition of the dose produced a similar effect as the first, confirming uterotonic activity of the SFE extract. Once again, the low doses of the SFE extract necessary can be explained due to the increased selectivity of the extraction technique and the increased sensitization of the uterus as a result of hormonal changes during pregnancy.

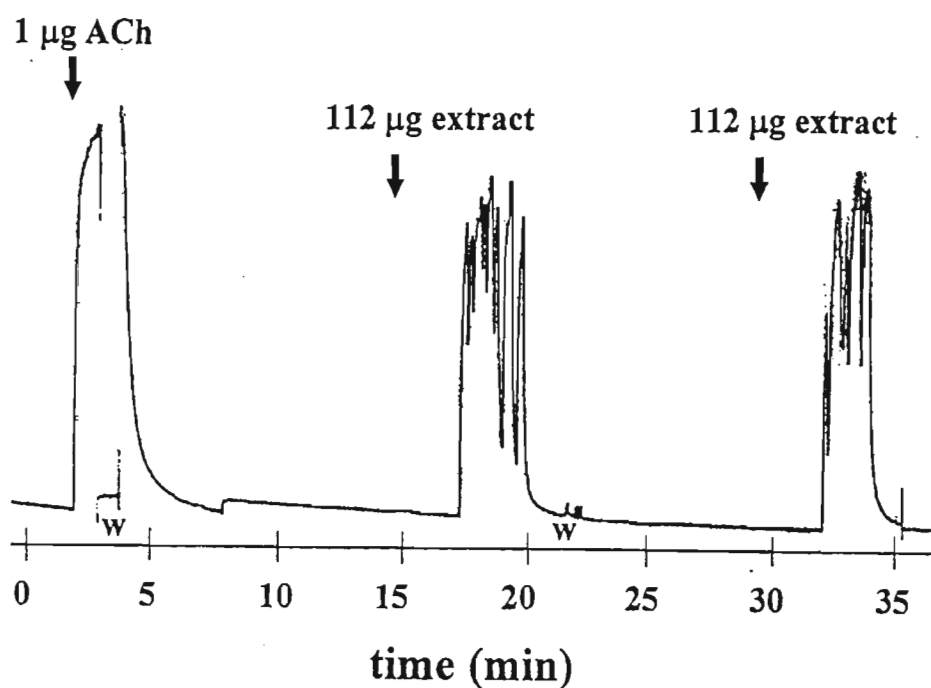


Figure 7.14 Electrical recording of pregnant guinea pig uterine smooth muscle contraction induced by the SFE extract of *Grewia occidentalis* L.
w = muscle wash

7.9 Conclusion

Supercritical fluid extraction was found to be rapid and effective in isolating target analytes that displayed distinctive results when screened for uterotonic activity. The screening technique employed also proved to be successful in evaluating the plant extracts. Having outlined the theory of muscle contraction, it can be stated that the components

contained in the plant extracts may have stimulated muscle contraction by either increasing the permeability of the cell membranes to calcium ions or by acting directly on the contractile proteins or the receptor sites. Nevertheless, this preliminary investigation warranted a further detailed study of the plant extracts in order to identify the active compounds in the hope of finding new drug leads and to study the mode of action.

References

1. S. Jeffcoate, *Trends in Biotechnology*, **14** (1996), 121.
2. D.V.M. Frank Welsch, *Teratology*, **53** (1996), 332.
3. K. Krishnan, M.L. Gargas and M.E. Andersen, *Alternative Methods in Toxicology*, **9** (1993), 185.
4. J. Hilliard, *Biol. Reprod.*, **8** (1973), 203.
5. D.G. Porter, *J. Endocrinol.*, **46** (1970), 425.
6. J. Rudinger, V. Pliska and I. Krejci, *Recent Prog. Horm. Res.*, **28** (1972), 131.
7. D.J. Crankshaw, *Eur. J. Pharmacol.*, **101** (1984), 1.
8. G.J. Moore, *Pharmacol. Ther.*, **33** (1987), 349.
9. M.V. Tyrode, *Arch. Int. Pharmacodyn. Thér.*, **20** (1910), 205.
10. H.A. Krebs, *Biochim. Biophys. Acta.*, **4** (1950), 249.
11. J. Koch-Weser, *Am. J. Physiol.*, **204** (1963), 957.
12. N. Skaug and R. Detar, *Am. J. Physiol.*, **240** (1981), H971.
13. M. Gellai and R. Detar, *Circ. Res.* **35** (1974), 681.
14. J.M. Norton and R. Detar, *Am. J. Physiol.*, **222** (1972), 474.
15. B.M. Altura and B.T. Altura, *Fed. Proc.*, **40** (1981), 2672.
16. A.S.F. Ash and H.O. Schild, *Br. J. Pharmacol. Chemother.*, **27** (1966), 427.
17. T.P. Kenakin, *J. Pharmacol. Exp. Ther.*, **223** (1982), 416.
18. A. Chang and R. Detar, *Am. J. Physiol.*, **238** (1980), H716.
19. R. Detar, *Am. J. Physiol.*, **238** (1980), H761.
20. W.H. Elliott and D.C. Elliott, *Biochemistry and Molecular Biology*, Oxford University Press, Oxford, UK (1997), p.394.

21. S. Tucek, In: *The Cholinergic Synapse, Handbook of Experimental Pharmacology*, V.P. Whittaker (Ed.), Springer-Verlag, Berlin, Heidelberg, Germany (1988), p.125.
22. T.P. Kenakin, *J. Pharmacol. Rev.* **36** (1984), 165.
23. P.B. Marshall, *Br. J. Pharmacol.*, **10** (1955), 270.
24. S.P. Watson, B.E.B. Sandberg, M.R. Hanley and L.L. Iversen, *Eur. J. Pharmacol.*, **87** (1983), 77.
25. R. Franco, M. Costa, and J.B. Furness, *Naunyn-Schmeideberg's Arch. Pharmacol.* **306** (1979), 195.
26. A.S.F. Ash and H.O. Schild, *Br. J. Pharmacol.*, **27** (1966), 427.
27. J.W. King and J.E. France, In: *Analysis with Supercritical Fluids: Extraction and Chromatography*, B. Wenclawiak (Ed.), Springer-Verlag, Berlin, Heidelberg, Germany (1992), p.32.
28. K.M. Dooley, C.P. Kao, R.P. Gambrell, and F.C. Knopf, *Ind. Eng. Chem. Res.* **26** (1987), 2058.
29. G.D. Thorburn, J.R.G. Challis, *Physiol. Rev.*, **59** (1979), 863.
30. G.K. Patnaik, K.K. Banaudha, K.A. Khan, A. Shoeb and B.N. Dhawan, *Planta Med.*, **53** (1987), 517.
31. D.J.H. Veale, D.W. Oliver, N.S. Arangies and K.I. Furman, *J. Ethnopharm.*, **27** (1989), 341.

CHAPTER 8

Coupling supercritical fluid extraction to uterotonic bioassay:

An on-line approach to analysing Medicinal Plants

8.1 Introduction

Current trends in analytical science are directed towards the analysis of the components through on-line approaches. SFE has been successfully coupled on-line to various chromatographic and spectroscopic methods. Modey *et al.* (1) used on-line SFE-GC for the analysis the limonoid cedrelone in the wood and bark of *Cedrela toona* (Meliaceae). SFE has also been successfully coupled to SFC. This approach is recommended when the sample contains thermally unstable, reactive or involatile compounds. Xie *et al.* (2) used this approach to extract and separate ouabain, a biologically active cardiac glycoside, spiked onto an inert adsorbent. SFE-HPLC has been performed by Nair and Huber (3) for the analysis of ground tablets for ibuprofen, however, the pumping of the mobile phase became difficult and erratic when gas was present in the plumbing of the HPLC system. On-line SFE-TLC has been shown to provide a rapid and simple insight into the extraction performance of compounds from various matrices (4, 5), however quantification was found to be difficult and the stability of the components on the support material or in the presence of oxygen posed a problem. For compounds showing unique regions of absorbance in the infrared region, direct coupling of the SFE effluent to an FTIR can be of great importance. The recovery and detection on n-tetracosane from a solid matrix by directly coupled SFE-FTIR was carried out by Kirschner and Taylor (6). In addition, Kalinoski *et al.* (7) used on-line SFE with chemical ionisation MS detection and collision-induced dissociation tandem MS (MS-MS) for the rapid identification of trichothecene mycotoxins. The limitation of SFE-MS is the possibility of overloading the mass spectrometer with co-extracted compounds when complex samples are analysed. Nevertheless SFE has proved to be an extremely versatile technique and we have thus exploited its potential in an attempt to couple this technique directly on-line to the

uterotonic bioassay to serve as a rapid screening tool to assess plants for uterotonic activity.

Bioassays are a common adjunct to chemical analysis. Traditionally, samples to be used for bioassay have been prepared by solvent extraction, vacuum distillation, membrane processes, lyophilization, etc (8). These techniques offer some success but also significant disadvantages. SFE has proven to be a valuable alternative method of extraction that has received tremendous attention in recent studies (9). In comparison with classical liquid-solid extraction methods, SFE offers many potential advantages as discussed in section 2.3. In addition, CO₂ provides an extraction environment free from molecular oxygen, thereby limiting potential oxidation of the extracted solutes (10). Although there have been reports of SFE coupled to immunoassay analysis, these studies have been performed using off-line collection of the extracted analytes (11, 12). On-line approaches provide potential for combined sample preparation and analysis and the ability to transfer every extracted analyte molecule to the detection system thereby increasing sensitivity. A further advantage is the elimination of sample handling prior to the bioassay hence eliminating the possibility of sample contamination.

Supercritical CO₂, unlike many liquid extraction solvents, is a nontoxic extraction medium making it appropriate for interfacing with the bioassay since the problems of artifactual solvent toxicity inherent in conventional extraction and fractionation schemes is eliminated. Unfortunately, CO₂ is not sufficiently polar to extract highly polar components. Polar compounds therefore show limited solubility in pure CO₂ and in such cases either a more polar supercritical fluid should be used or a modifier added. For our purpose, water was used as a modifier and added directly to the matrix. Although water is scarcely soluble in liquid carbon dioxide (around 0.1% m/m at 20 °C), its solubility increases with increasing temperature (around 0.3% m/m at 50 °C), and has thus proven effective in many extraction applications (13, 14).

Using the on-line system, the uterotonic effects of three plants viz. *Clivia miniata* (Lindl.) Regel., *Ekebergia capensis* Sparrm., *Grewia occidentalis* L. were evaluated. These plants are used frequently during the late stages of pregnancy. The aqueous extract of *C. miniata* was previously found to be active (15). Off-line studies have shown the aqueous and SFE extracts of *E. capensis*, *G. occidentalis* and *A. fruticosa* to stimulate uterine contractions *in vitro*. These plants were selected to demonstrate the potential of SFE linked directly to the bioassay, which could be used to rapidly screen various other plants containing uterotonic compounds.

8.2 Results and Discussion

Prior to coupling SFE to the bioassay, two factors were considered, viz. the effects of supercritical CO₂ decompression on temperature and pH of the muscle bathing solution.

8.2.1 Temperature effects

Carbon dioxide depressurises at the exit of the restrictor resulting in adiabatic cooling of the collection solvent. One of the problems with this is that the temperature of the collection solvent was not maintained and the collection solvent became so cold that samples containing water caused restrictor plugging from freezing water. Excessive cooling can also alter muscle physiological activity. Veale *et al.* (15) showed that when the organ bath temperature was reduced to 26 °C, spontaneous contractions were inhibited. However factors that interfere with spontaneous contractility may also affect agonist-induced contractility. There may also be cases where postreceptor mechanisms involved in the response of one agonist are more temperature dependent than those of another (16). For these reasons, it was decided to study muscle activity at, or near, body core temperature. Cooling experiments were performed on muscle bath A (section 5.7.1) with 25 µm i.d. fused silica capillaries. A 24.5 cm × 25 µm i.d. linear restrictor was initially used at a pump pressure of 400 atm and a reduction in the bath temperature to 35.4 °C was observed within ten minutes after commencing with dynamic extraction (Figure 8.1). Despite the problems with cooling, the linear restrictor was further evaluated during extraction of a real sample and was found to plug within 10 minutes of dynamic

extraction. This was due to decompression taking place over the entire length of the capillary resulting in the formation of analyte clusters and small particles during this process. Frit restrictors were also evaluated and were found to provide excellent temperature control due to the low flow rate of CO₂. Frit restrictors are also more resistant to plugging due to their multitude of decompression paths, however the frit failed on many accounts to withstand high pressures. A tapered restrictor of the same inner diameter as the linear restrictor was subsequently used and found to provide better temperature control and hence less cooling.

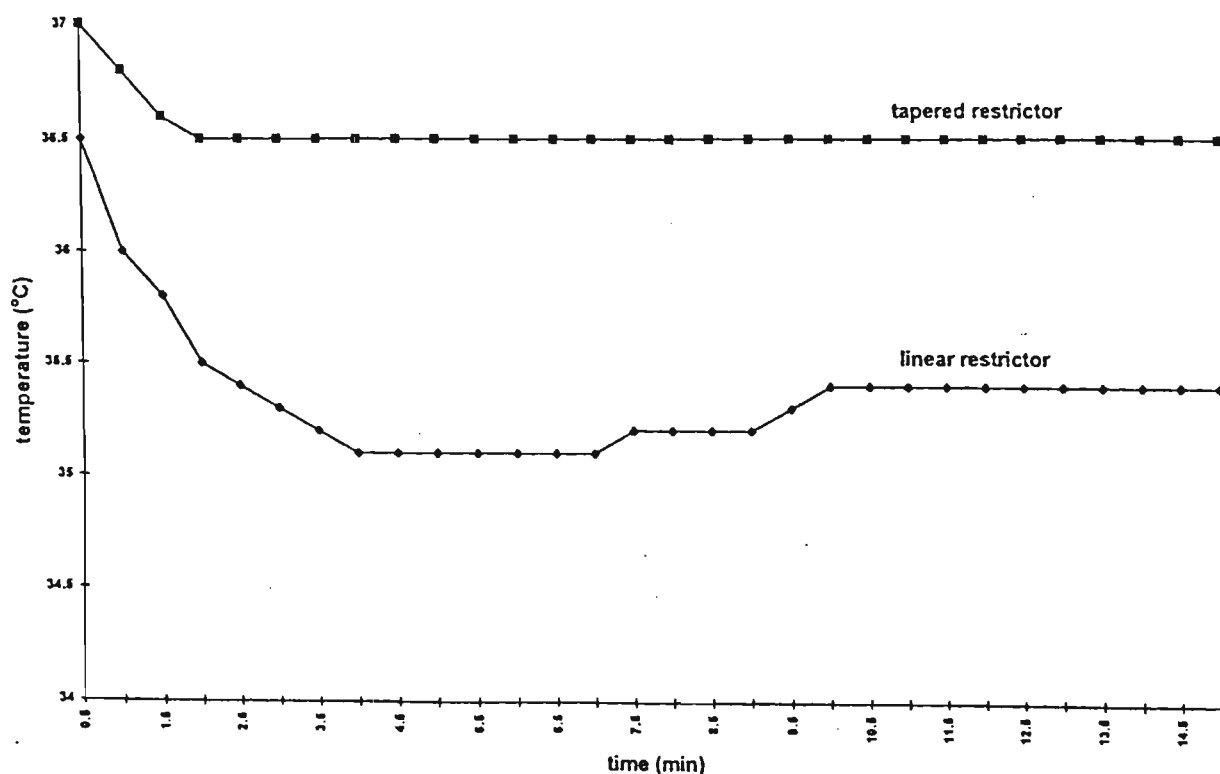


Figure 8.1 The effect of CO₂ decompression on temperature of Tyrodes solution. CO₂ was decompressed from an internal pressure of 400 atm through a 25 μm i.d. tapered restrictor (■) and a linear restrictor (◆)

The bath temperature decreased to 36.5 °C within 1.5 minutes of commencing CO₂ flow and remained constant at this temperature for the 15 minute period of the experiment. Hence it is quite apparent that the degree of cooling is controlled by the flow of CO₂ or the rate of decompression. Tapered restrictors allow for the flexibility of optimising flow rate by simply cutting back at the taper. By performing such a procedure, the inner diameter of the orifice at the end of the taper increases thereby allowing increased flow rates. Hence a compromise was reached between the rate of decompression and restrictor plugging, as low flow rates due to small inner diameters of the taper orifice would have led to blockages by the extract. A flow rate of 18 ml/min at 150 atm was found to be most appropriate and did not result in blockages. The temperature decrease was also minimized and found to be close to the desired experiment temperature.

8.2.2 pH effects

When CO₂ is introduced into water, it forms carbonic acid resulting in a decrease in pH. Some of the carbonic acid dissociates to bicarbonate and hydrogen ions. Because alteration in [H⁺] will alter cellular metabolic processes in which it is a participant, pH measurements were carried out by placing a pH electrode into the muscle bathing solution with CO₂ flow directed into the muscle bath A. As shown in Figure 8.2, within 30 seconds of commencing flow of CO₂, the pH decreased from pH 7.0 to 6.61. The rate of decrease thereafter became moderate and finally remained constant after 10 minutes at a pH of 5.75. The pH range compatible with life is about 7.8 - 6.8, however values as low as 6.0 have been reported for skeletal muscle (17). 5% CO₂ present in carbogen forms an excellent buffer with bicarbonate present in Tyrodes solution. Since the pK of the HCO₃⁻/CO₂ system is 6.1, extracellular fluid at a pH of 7.4 is not very effective in resisting changes in pH arising from changes in P_{CO₂}. Furthermore, deviations in pH may influence ionization of drugs or charged chemical groups on receptors thereby changing the moieties which interact to produce a response (18,19). Intracellular fluid, with high levels of protein and organic phosphates, is responsible for most of the buffering that occurs when P_{CO₂} changes in biological systems. Since CO₂ was used as the extracting fluid in SFE, the P_{CO₂} in extracellular fluid, intracellular fluid and Tyrodes most certainly changed. It was

therefore necessary for Tyrodes solution to exhibit buffer action even in the absence of carbogen and this was accomplished by introducing a phosphate buffer as this buffer has a pK value of 6.8. The concentration of NaH_2PO_4 originally present in Tyrodes solution was reduced from 0.4 mM to 0.2 mM together with the addition 0.2 mM Na_2HPO_4 . Subsequently, the pH over a 15 minute period decreased from pH 7.45 to 6.02 and remained constant (Figure 8.2). An improvement by 0.27 pH units was observed and this solution was used for all future assays as it provided an improved buffering capacity than the previous solution.

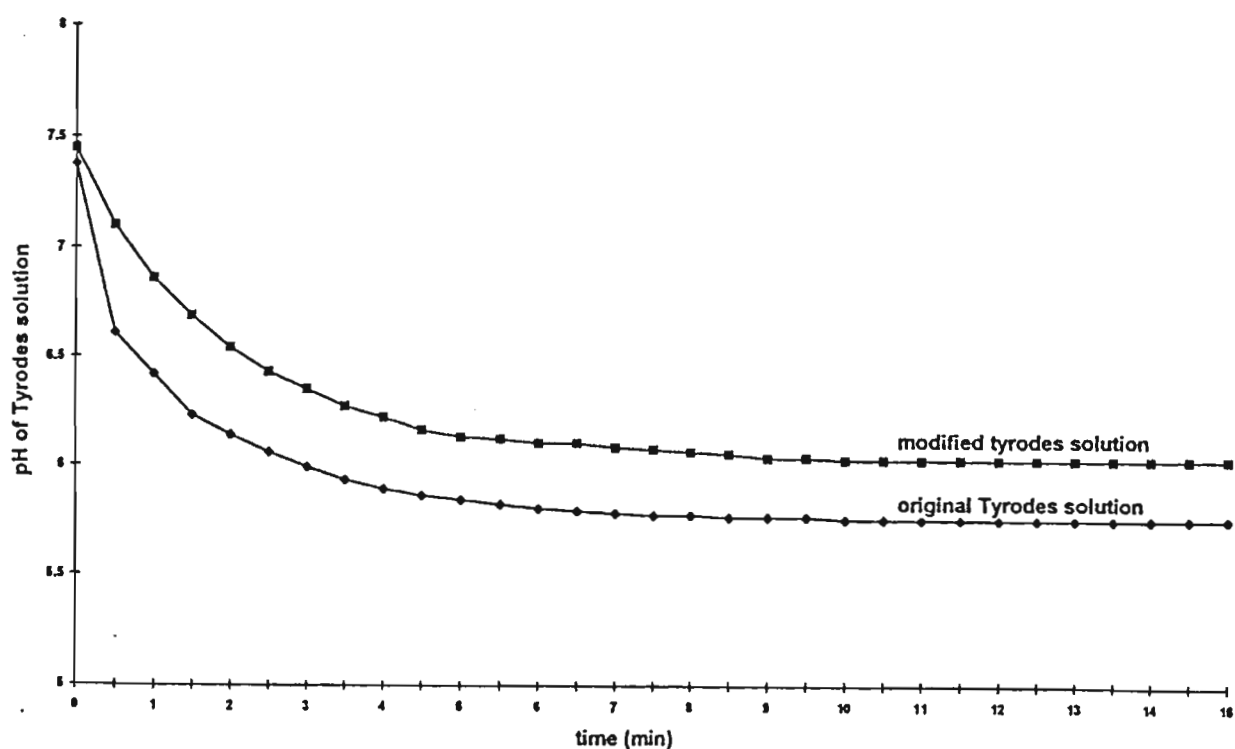


Figure 8.2 The effect of CO_2 decompression on pH of modified (0.2 mM Na_2HPO_4 , 0.2mM NaH_2PO_4) and original Tyrodes solution (0.4 mM NaH_2PO_4). CO_2 was decompressed from an internal pressure of 400 atm through a 25 μm i.d. tapered restrictor; CO_2 flow was measured at 150 atm after decompression and found to be 18 ml/min.

Tyrodes solution is a well known nutrient solution capable of preserving tissues in a viable state and although other buffers may have improved buffering capacity, changes in ionic content and composition are known to affect tissue reactivity and base line activity (20, 21). Hence minimum alterations to the recipe of Tyrodes solution were performed. The physiological activity of a strip of uterine muscle was monitored under these conditions. The muscle was allowed to develop spontaneous contractions and a dose of 1 μg ACh was administered as a standard smooth muscle stimulant (Figure 8.3a).

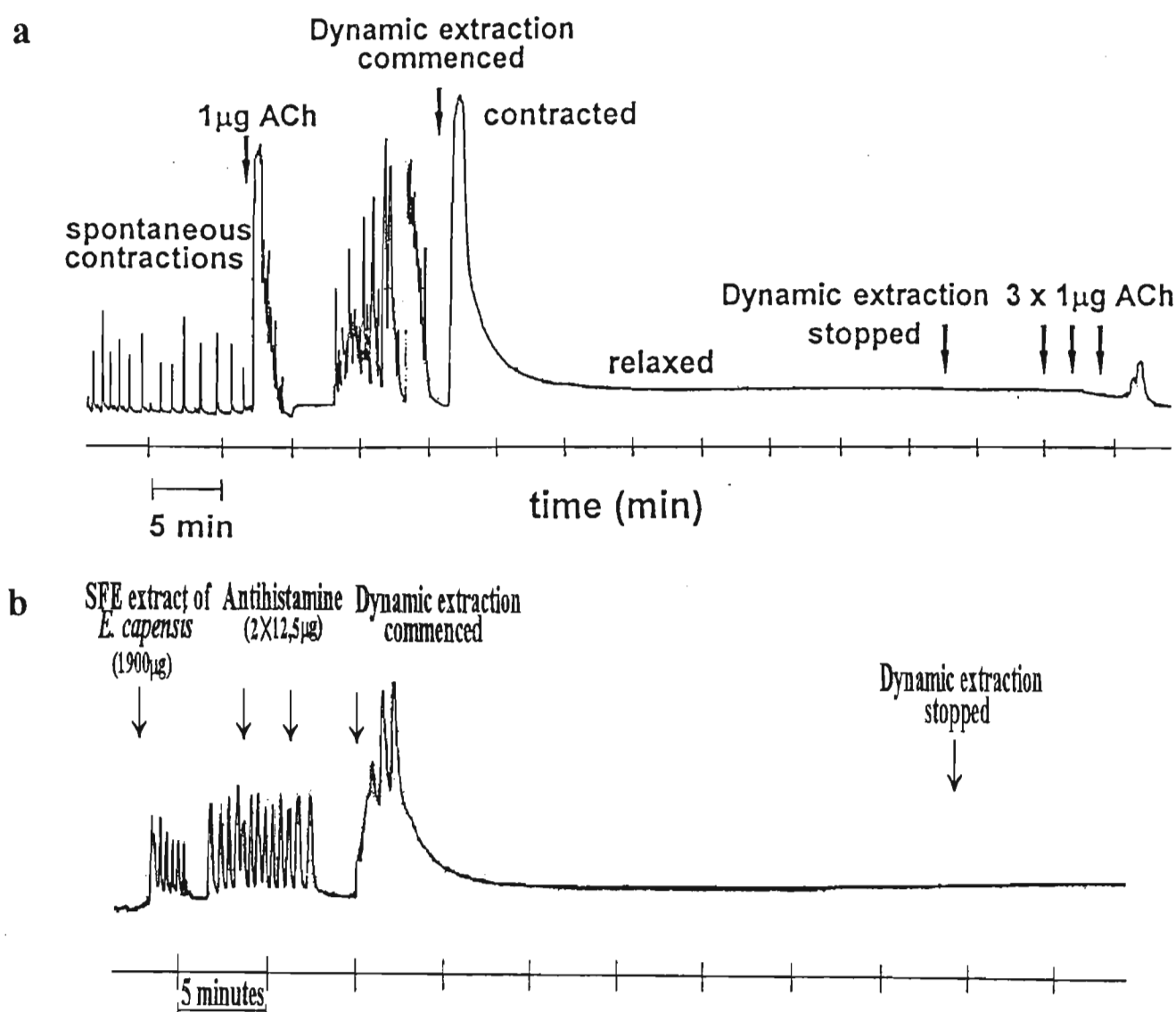


Figure 8.3 The direct effect of CO_2 on muscle contractility. Muscle activity was inhibited following a blank extraction with CO_2 at 400 atm and 80°C after (a) spontaneous muscle activity and (b) after administration of an SFE extract of *Ekebergia capensis*.

A blank extraction was performed at 400 atm and 80 °C and the CO₂ flow directed into the muscle bath via the tapered restrictor. Immediately upon commencing with the dynamic extraction, a contraction was observed. As the extraction proceeded, the muscle began to relax and a flat baseline was observed thereafter. The spontaneous contractions initially observed had ceased altogether. After 45 minutes, the extraction was stopped and this was followed by the addition of 2 × 1 µg quantities of ACh. No response was observed, however upon administering 3 µg ACh, a mild response was observed. The effects of CO₂ were further seen when an off-line extract of the wood of *E. capensis* induced muscle contractions. The contractions failed to stop even after administration of mepyramine, a (H₂) histamine receptor blocker. However when CO₂ was directed from the SFE vessel into the muscle bath, the development of tension was initially noted but this was followed by muscle relaxation and a flat baseline (Figure 8.3b). These results demonstrated that apart from the pH decrease, CO₂ was directly inhibiting spontaneous contractility of the muscle. Upon commencing with the dynamic extraction, the pH of Tyrodes solution decreased resulting in increased tension of the muscle in response to extracellular acidosis. A similar trend was observed by Cole *et al.* (22) when investigating contractile responses of isolated human ureteric smooth muscle to extracellular pH changes. However, a continuous influx of CO₂ into the organ bath resulted in the inhibition of muscle activity as CO₂ entered the cell and acidified the intracellular fluid. CO₂ is an easily diffusible gas and is able to pass through membranes and alter intracellular metabolic processes. Alterations in intracellular pH could alter smooth muscle contractility as the following physiological processes are pH sensitive:

- 1) the rate of myosin ATPase activity (23);
- 2) the sensitivity of the contractile unit to Ca²⁺ (24, 25);
- 3) transmitter release and receptor sensitivity (26);
- 4) competition at calcium binding sites (27); and
- 5) late energy production (28).

Hypoxia could also alter force development and has been shown to impair contractility in tracheal smooth muscle (25). During hypoxia there is an increase in glycolysis and a concomitant increase in intracellular lactate. Thus the reduction in force during hypoxia is

assumed to be due to a decrease in pH. Nevertheless, no matter what mechanism prevailed in altering the force development during hypercarbia, it was a reversible process. Once the flow of CO₂ ceased and the Tyrodes solution changed, the muscle regained normal physiological activity after passing carbogen through the solution for a few minutes. Having undertaken various measures to avoid temperature and pH effects, it was concluded that muscle bath A was not appropriate for on-line coupling since the muscle was in direct contact with the incoming CO₂ from the extraction vessel. The high P_{CO₂} influenced muscle activity thereby making it impossible to analyse for uterotonic activity induced by plant extracts. Since CO₂ penetrates through cell membranes easily and alters the intracellular activities, this excess had to be minimised. A second muscle bath was therefore designed to eliminate the effects of excess CO₂. It consisted of two polypropylene chambers attached via a detachable sidearm. Dynamic extraction was performed into 4 ml of Tyrodes present in the extract collection chamber while the muscle equilibrated in the 10 ml muscle bath (Figure 5.5). In this way the muscle was protected from the direct effects of high P_{CO₂}. The passage of carbogen into the extract collection chamber further assisted in the rapid displacement of CO₂. It was hypothesised that as the dynamic extraction proceeded, the concentration of the extracted material in the extract collection chamber would increase and mix with the Tyrodes solution in the muscle chamber. The carbogen flowing into the muscle chamber facilitated the rapid mixing of the plant extracts until the uterotonic components reached a sufficient concentration to induce a contractile response. If required, at the end of the dynamic extraction period, the Tyrodes solution from the extract collection chamber could be flushed into the muscle chamber to provide a higher concentration of the extract. A 50 µm i.d. tapered restrictor designed to produce the optimum flow of CO₂ was used in this setup together with the passage of carbogen into the extract collection chamber. The passage of carbogen was found to assist in maintaining the desired pH of the Tyrodes solution by rapidly displacing any excess CO₂.

8.2.3 Evaluation of Extracts

The plants used for the on-line analysis were collected during October 1995 and were hence different to the batch used for the preliminary analysis. Each plant was initially evaluated by extraction at a pressure of 400 atm and 80 °C to ascertain whether the uterotonic components were of sufficient concentration to initiate a muscle response using this new technique. Subsequent analysis was performed by sequentially extracting the components at 200, 300 and 400 atm respectively in order to decrease the complexity of the extracts and hence minimise possible antagonistic effects from interfering compounds. Fractionation also aided in determining the most potent extract of the plant which would be useful in further analysis. The response of the muscle to ACh before and after extraction of the plant components was determined for each assay.

8.2.3.1 Analysis of *Ekebergia capensis*

Following an equilibration period of 30 minutes, during which time static extraction was performed, the muscle was found to produce an adequate response to 5 µg ACh (Figure 8.4a.). Ten minutes after dynamic extraction at 400 atm commenced, the muscle was observed to develop tension. The probability of cold zone contracture was ruled out as the fluid temperature in the muscle bath during this period was found to be 37 °C. The contractile process lasted approximately 3 minutes. Once the 20 minute dynamic extraction period had lapsed and the contents of the extract collection chamber transferred to the muscle bath, the muscle developed rhythmic activity of increasing amplitude followed by a period of sustained contraction-relaxation cycles, which were observed for a period of 30 minutes. Subsequent addition of 5 µg ACh to the muscle bath produced a prolonged response of greater amplitude than the original cholinergic stimulation. A similar cholinergic response following a muscle wash with Tyrodes indicated that the extract may have sensitized the contractile mechanism thereby increasing the agonistic response of ACh.

Sequential extractions at 200, 300 and 400 atm were thereafter performed and Figure 8.4b-c displays the contractions induced by the sequentially fractionated extracts.

Approximately 6 minutes after commencing dynamic extraction at 200 atm, the muscle developed extreme tension of much larger amplitude than the ACh response (Figure 8.4b). This contraction lasted approximately 10 minutes. After completing dynamic extraction, the extract was flushed into the muscle chamber producing an increase in muscle tone. This was monitored for a 17 minute period followed by administration of ACh. Once again, in the presence of the plant extract, the muscle produced an enhanced agonistic response to ACh, however, when the muscle was washed, the response elicited was observed to be similar to the initial response. The 300 atm extract also produced a contraction approximately 15 minutes after commencing with dynamic extraction, however, when the extract was transferred to the muscle chamber, muscle activity was enhanced and a period of sustained contraction-relaxation cycles was initiated within 3 minutes (Figure 8.4c.). These contractions were monitored for approximately 20 minutes followed by the administration of ACh. Figure 8.4d displays the contractions induced by the sequentially fractionated 400 atm extract. An increase in muscle tension was observed approximately 15 minutes after commencing with the 400 atm extraction. As the extract concentration increased the muscle developed contractile activity of much larger amplitude than the 400 atm total extract indicating that the sequential extract contained a larger quantity of the active components or perhaps a smaller concentration of the interfering compounds that may have induced antagonistic effects. This extract indeed produced stimulating action followed by an increase in the frequency of contractions. The ACh response was also enhanced even after washing of the muscle with Tyrodes solution.

Upon comparison of these results with those obtained from the off-line studies, one could possibly attribute the difference in the biological activity of the sequentially fractionated extracts to seasonal changes. Seasonal changes are known to cause variation in the concentration of compounds in plants due to changes in biosynthetic conditions. Unlike the first batch of *E. capensis*, this batch did not elicit spasmolytic activity.

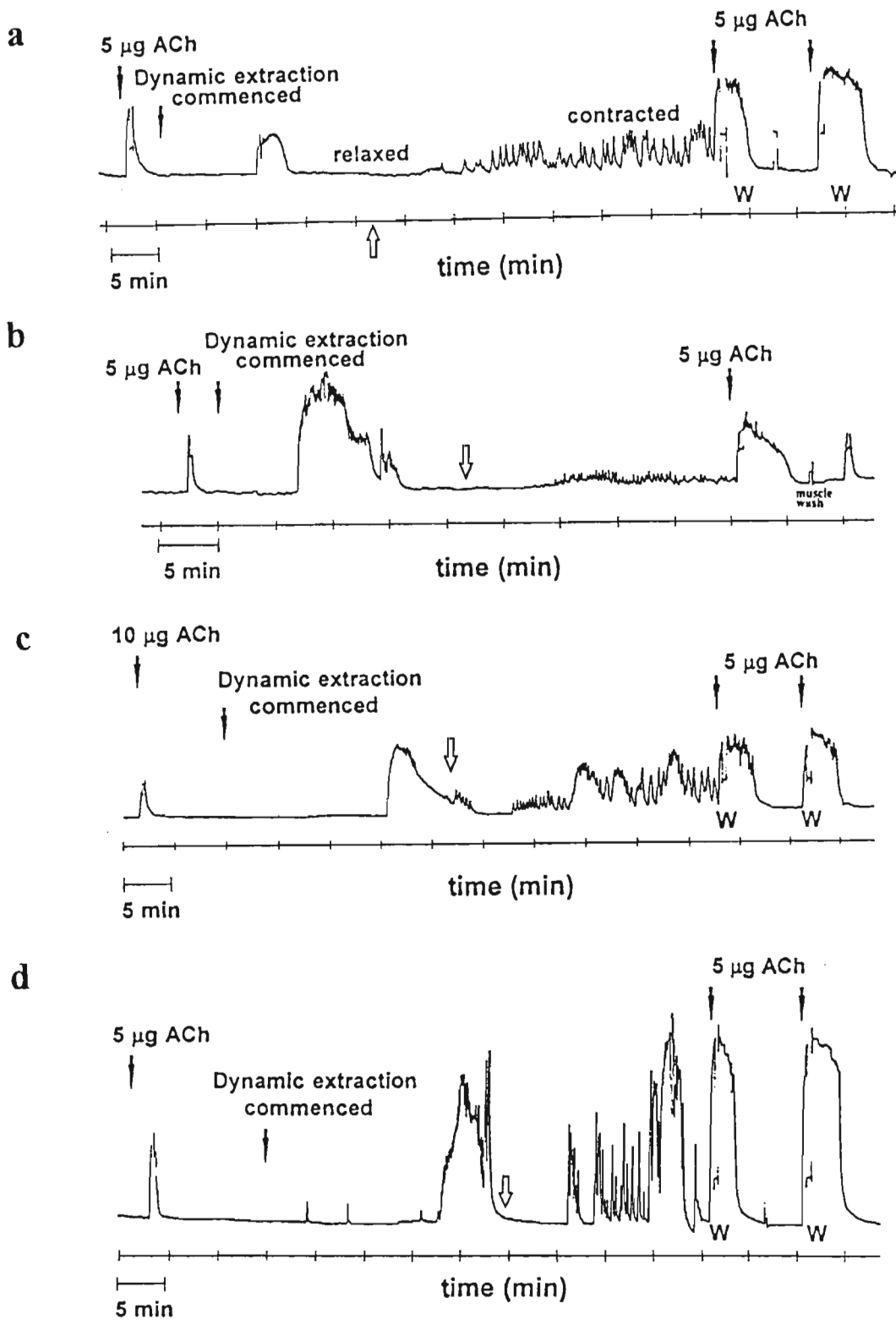


Figure 8.4 The effect of SFE extract of *E. capensis* on Guinea Pig uterine smooth muscle.

a) total 400 atm extract, b) sequentially fractionated extract obtained at 200 atm, c) 300 atm and d) 400 atm demonstrating that the 400 atm extract was most potent.

↑ point at which contents of the extract collection chamber was transferred to the muscle bath; W = muscle wash with Tyrodes solution.

8.2.3.2 Analysis of *Grewia occidentalis*

The total 400 atm extract of *G. occidentalis* produced active tension within 2 minutes of commencing dynamic extraction, however at the end of the dynamic extraction period, a tonic rhythm of extremely low amplitude was observed. This was followed by an extremely low response to ACh indicating the possibility of toxic components, however this inference remains to be confirmed (Figure 8.5a). The 200 atm sequential extract did not provide conclusive evidence of uterotonic activity although a single contraction lasting approximately 30 seconds was observed (Figure 8.5b). However, the 300 atm extract produced a well synchronised response leading to the production of regular, rhythmic contractions that were monitored for a 30 minute period (Figure 8.5c). Addition of ACh was observed to produce a contraction similar to the initial response. The 400 atm extract was also found to induce phasic contractions, however of much lower amplitude than that induced by the 300 atm extract (Figure 8.5d). This study clearly demonstrated the potential of supercritical fluid fractionation as the 300 atm sequential extract was observed to be the most potent.

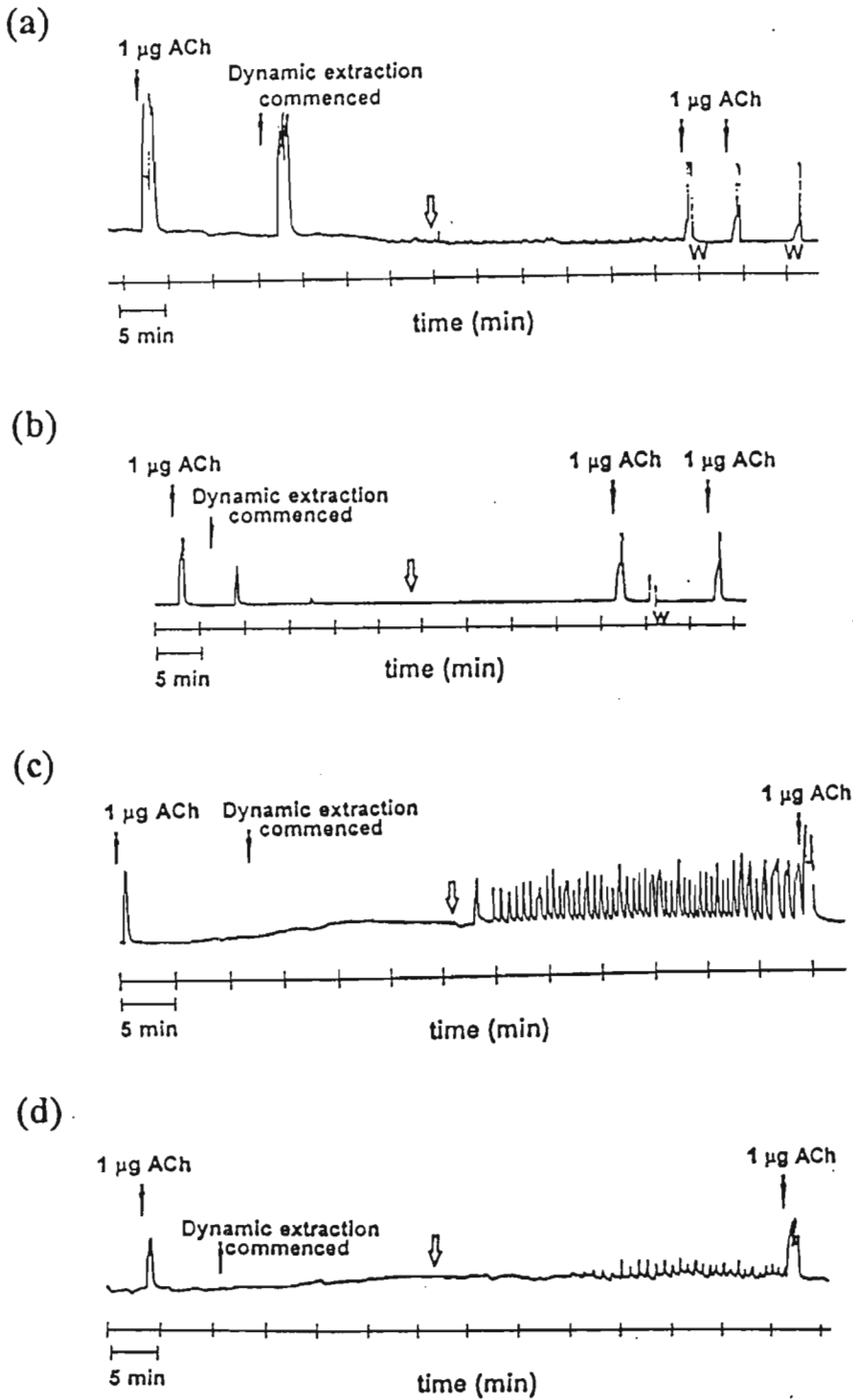


Figure 8.5 The effect of SFE extract of *G. occidentalis* on Guinea Pig uterine smooth muscle.

a) total 400 atm extract, b) sequentially fractionated extract obtained at 200 atm, c) 300 atm and d) 400 atm demonstrating that the 300 atm extract was most potent.

↑ point at which contents of the extract collection chamber was transferred to the muscle bath; W = muscle wash with Tyrodes solution.

8.2.3.3 Analysis of *Clivia miniata*

The total 400 atm extract of the roots of *C. miniata* was found to initiate contractile activity within 4 minutes of commencing with dynamic extraction. An increase in muscle tension was observed together with occasional spiking. The muscle remained in this state of contraction for approximately 8 minutes, however upon completion of dynamic extraction an intense contractile activity of high amplitude was detected (Figure 8.6a). The contractions were observed to be more irregular, more prolonged and less frequent than the contractions induced by *G. occidentalis*. The 200 atm sequential extract produced regular contractions of varied amplitude (Figure 8.6b) while the 300 atm extract was found to develop contractile activity approximately 5 minutes after stopping dynamic extraction. The contractions were observed to be phasic together with tension development (Figure 8.6c). Unlike the activity induced by the 200 atm extract, these contractions were of a greater amplitude and frequency. These contractions were monitored for a 35 minute period followed by two muscle washes in order to stop contractile activity. Addition of ACh was found to elicit a much greater response than the initial contraction and this could once again be explained by the sensitizing nature of the extract on the contractile mechanism of the uterine muscle. The 400 atm sequential extract also produced contractions which initially increased in amplitude with periods of quiescence alternating with periods of activity. The contractions were initially observed to be irregular and prolonged however with time, the amplitude decreased, followed by an increase in the frequency of contractions (Figure 8.6d). The decrease in amplitude of the contractions could be attributed to muscle fatigue.

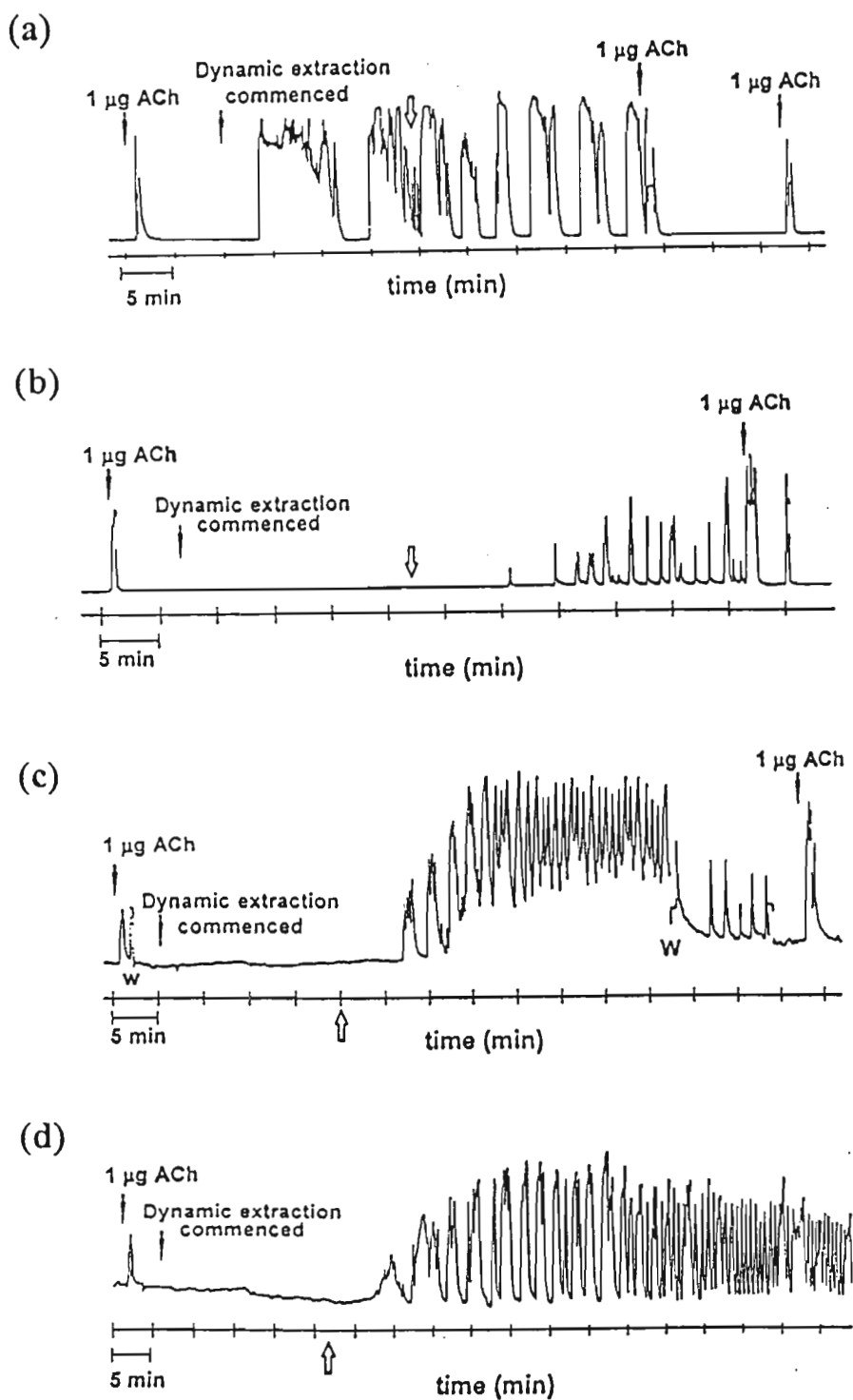


Figure 8.6 The effect of SFE extract of *C. miniata* on Guinea Pig uterine smooth muscle. a) total 400 atm extract, b) sequential extract at 200 atm, c) 300 atm d) 400 atm demonstrating that the 400 atm extract was most potent.

↑ point at which contents of the extract collection chamber was transferred to the muscle bath; W = muscle wash with Tyrodes solution.

8.3 Conclusions

The results presented herein show that the on-line assay is a rapid, safe and sensitive method for determining the uterotonic activity of medicinal plants. The selectivity of the extraction was successfully varied through pressure control thereby minimising the possibility of interfering compounds. The method could be adapted to screen plants with other therapeutic potential (eg. plants used in the treatment of diabetes mellitus and hypertension). On-line bioassay guided fractionation further enhanced the potential of this technique as it allowed expeditious identification of the most potent fractions which could then be subjected to further analysis.

References

1. M.W. Modey, D.A. Mulholland, H. Mohamed and M.W. Raynor, *J. Microcol. Sep.*, **8** (1996), 67.
2. Q.L. Xie, K.E. Markides and M.L. Lee, *J. Chromatogr. Sci.*, **27** (1989), 365.
3. J.B. Nair and J.W. Huber, *LC.GC, Mag. Chromatogr. Sci.*, **6** (1988), 1071.
4. E. Stahl and E. Willing, *Planta Med.*, **34** (1978), 258.
5. E. Stahl and W. Schilz, *Fresenius Z. Anal. Chem.*, **280** (1976), 99.
6. C. H. Kirschner and L.T. Taylor, *Proceedings of the 4th International Symposium on Supercritical Fluid Chromatography and Extraction*, Cincinnati, Ohio, USA (1992), p.173.
7. H.T. Kalinoski, H.R. Udseth, B.W. Wright and R.D. Smith, *Anal. Chem.*, **58** (1986), 2421.
8. M.F. Wolfe, J.N. Seiber and D.E. Hinton, *Proceedings of the 5th International Symposium on Supercritical Fluid Chromatography and Extraction*. Baltimore, USA (1994), 20.
9. P. Subra and P. Boissinot, *J. Chromatogr.* **543** (1991), 413.
10. B. Thomas, P. Wilhelm, T. Gerda, *J. Prakt. Chem.*, **334** (1992), 403.
11. G.K. Stearman, M.J.M. Wells, S.M. Adkisson and T.E. Ridgill, *Analyst*, **120**, (1995), 2617.
12. J.F. Morrison, S.N. Chesler and J.L. Reins, *J. Microcol. Sep.* **8** (1996), 37.

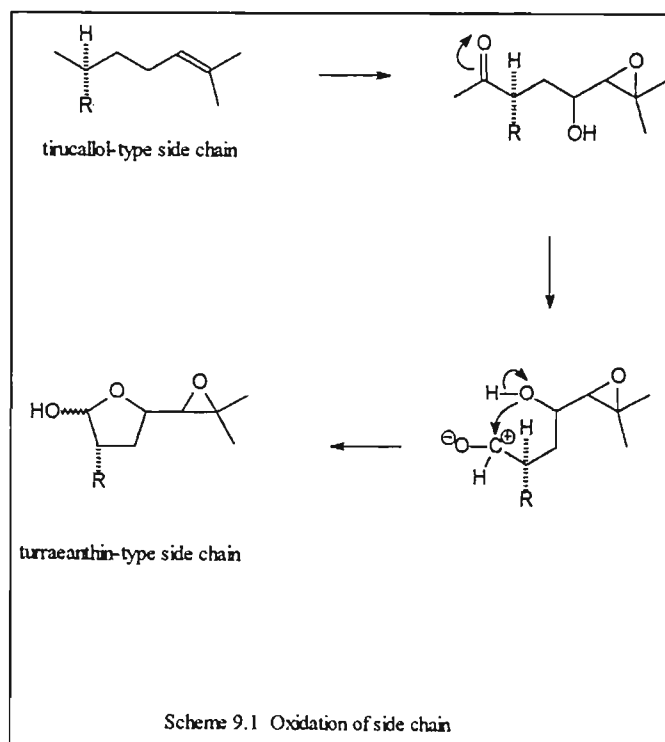
13. H. Engelhardt and A. Gross, *Trends in Anal. Chem.* **10** (1991), 64.
14. J.L. Janicot, M. Caude and R. Rosset, *J. Chromatogr.* **505** (1990), 247.
15. D.J.H. Veale, D.W. Oliver, N.S. Arangies and K.I. Furman, *J. Ethnopharm.* **27**, (1989), 341.
16. D.J. Crankshaw, In: *Uterine Contractility - Mechanisms of control*, R. E. Garfield (Ed.), Serano Symposia, USA (1990), p.85.
17. J. Baggott, in *Textbook of Biochemistry with Clinical correlations*, T.M. Delvin, (Ed.), John Wiley & Sons, New York, USA (1982), p.1088.
18. M. Roche E Silva, *Arch. Int. Pharmacodyn. Thér*, **128** (1960), 355.
19. M. Roche E Silva, in *Handbook of Experimental Pharmacology*, **18**, Springer Publishing Co., Inc., New York, USA (1966), p.225.
20. J. Kock-Weser, *Am. J. Physiol.*, **204**, 957-962 (1963).
21. J.M. Norton and R. Detar, *Am. J. Physiol.*, **222** (1972), 474.
22. R.S. Cole and C.H. Fry, *J. Physiol.*, **391** (1987), 49p.
23. V. Mrwa, I. Achtig and J.C. Ruegg, *Blood Vessels*, **2** (1974), 277.
24. V. Pieper, *J. Cardiovascular Pharm.* **6** (1984), 5328.
25. V. Pieper, M. Ehl, V. Johnson and R. Laven, *Pfluegers Arch.* **364** (1976), 135.
26. S. Wray, *Am. J. Physiol.*, **254** (1988), C213.
27. C.H. Fry and P.A. Poole-Wilson, *J. Physiol.* **313** (1981), 141.
28. R.D. Cohen and R.A. Iles, *Crit. Rev. Clin. Lab. Sci.* **6** (1975), 101.

CHAPTER 9

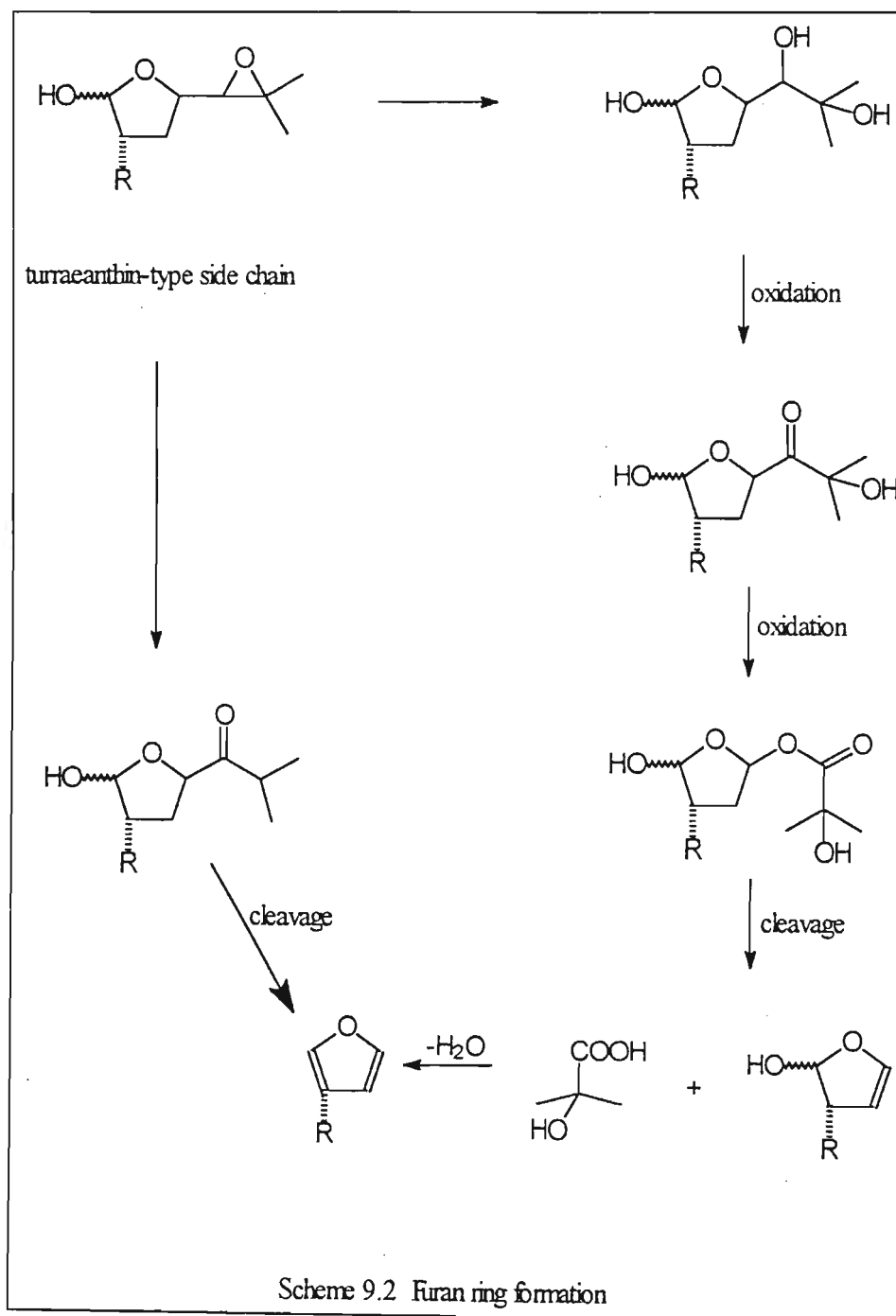
Extractives from Ekebergia capensis Sparrm.

9.1 The Genus *Ekebergia*

The genus *Ekebergia* belongs to the family Meliaceae. Previous investigations into the chemical constituents of this genus resulted in the isolation and identification of a group of tetranortriterpenoids known as limonoids. Structurally, the limonoids are derived from tetracyclic triterpenoids similar to euphol or tirucallol by a series of oxidative changes, brought about by peroxidase enzymes in the plant, interspersed with molecular rearrangements. A step wise oxidation has been proposed for this process during which four of the side chain carbon atoms are eliminated. According to the proposed mechanism (1), the tirucallol side chain is first oxidised to form a C-21 aldehyde group, a C-23 hydroxy group and a C-24,25 epoxide in place of the double bond to afford, after a subsequent cyclisation, a turraeanthin side chain (Scheme 9.1).



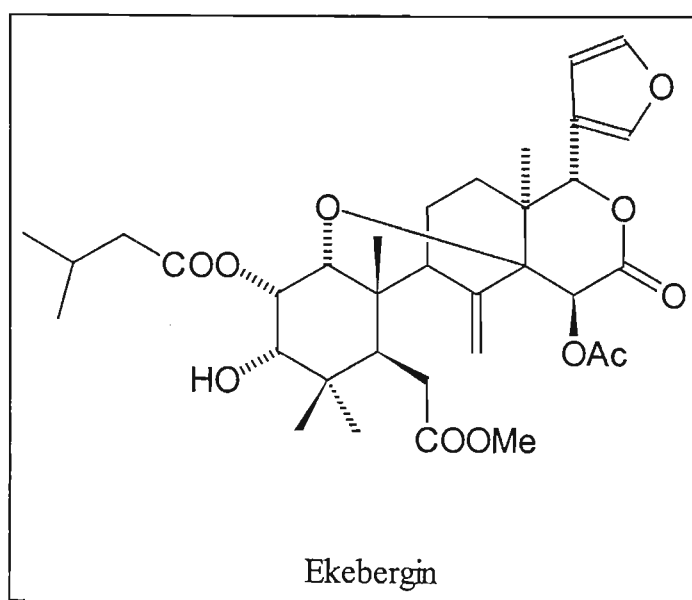
Further oxidation goes via the formation of a C-24 ketone, either directly by rearrangement of the epoxide, or by formation of the diol from the epoxide with further oxidation of the C-24 hydroxy group into a ketone followed by Baeyer-Villiger oxidative cleavage. This process affords a β -substituted furan ring at C-17 α (Scheme 9.2)



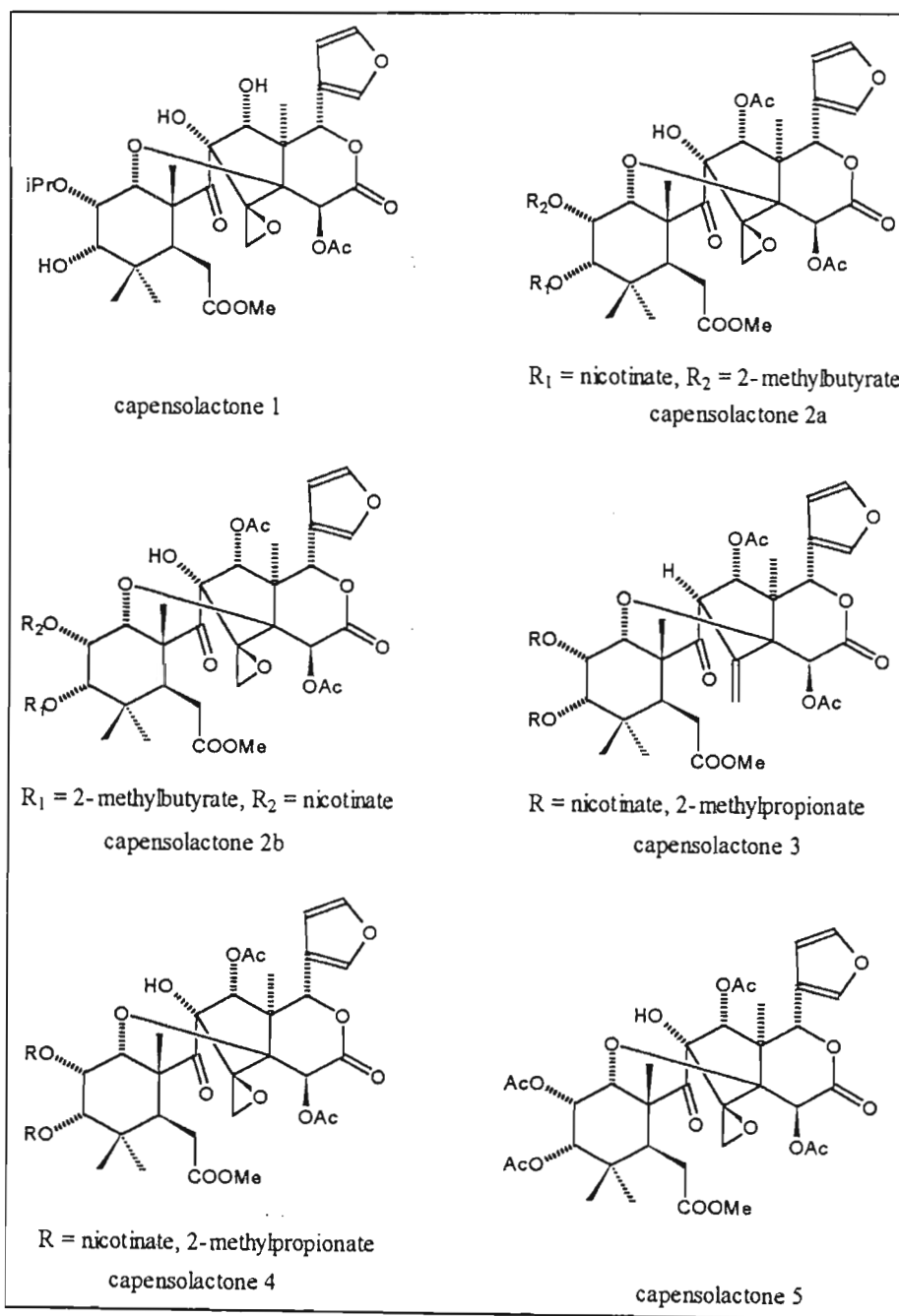
The validity of the proposed pathway was also supported by a number of synthetic studies where partial synthesis of the furan ring was carried out (2, 3). Limonoids are classified according to the modifications of their triterpenoid rings, which brings about twelve possible groups.

Ekebergia capensis is a fairly large tree, widespread in eastern Africa from Sudan to the Cape. The timber is not durable, but the tree is cultivated for shade and as an ornamental on account of its striking clusters of cherry-like but inedible red fruit. The tree is also known to be used for medicinal purposes. Decoctions made from the chopped bark are taken as emetics for heartburn and for respiratory chest complaints and coughs (4). Leaves are used in an infusion as a purgative parasiticide. The work reported in the previous chapters has shown this plant to contain uterotonic properties supporting its claim to induce or augment labour (5).

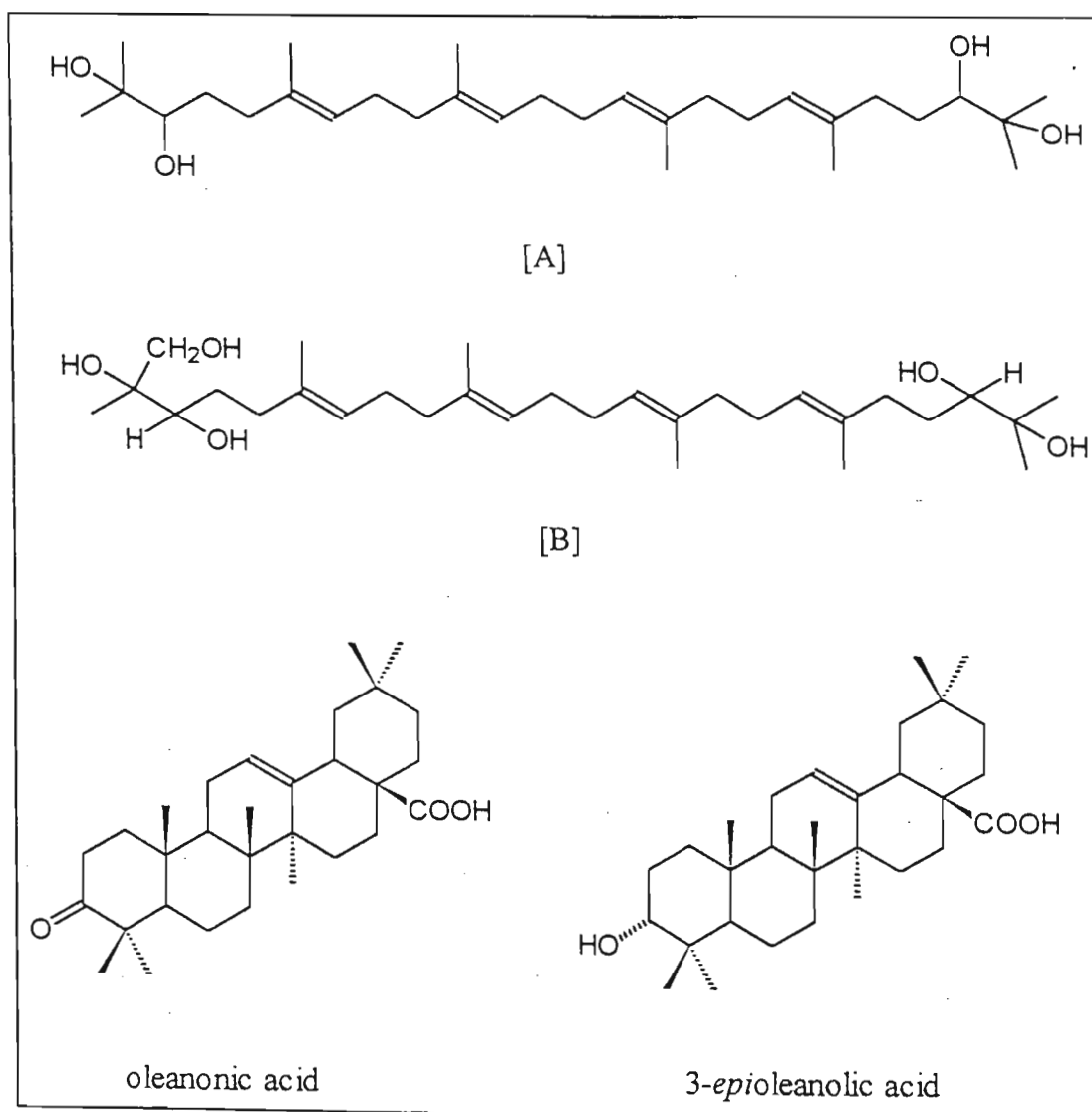
A previous investigation of the seed of *E. capensis* collected in the Eastern Cape yielded a crystalline limonoid to which the name ekebergin was given (6). This compound was identified as a diacylated methyl angolensate derivative.



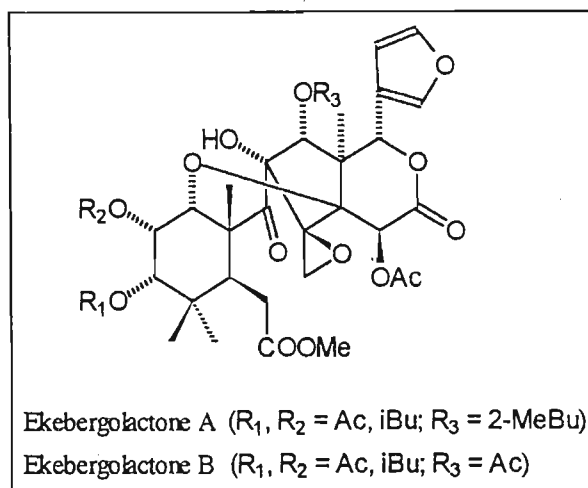
Continued investigations into the hexane extract of the seed of *Ekebergia capensis* yielded a number of different esters of the ekebergolactones as seen below (14).



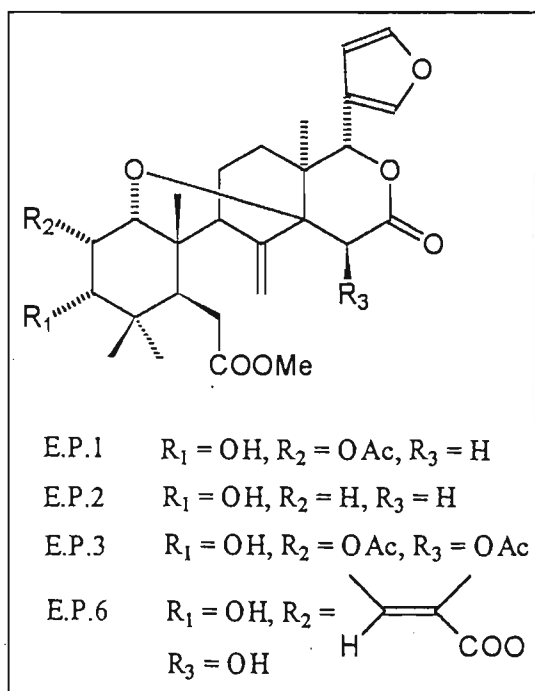
Further investigations into the chemical constituents of the bark of *E. benguelensis* resulted in the isolation of two acyclic triterpenoids [A] and [B] along with oleanonic acid and 3-*epi* oleanolic acid (7).



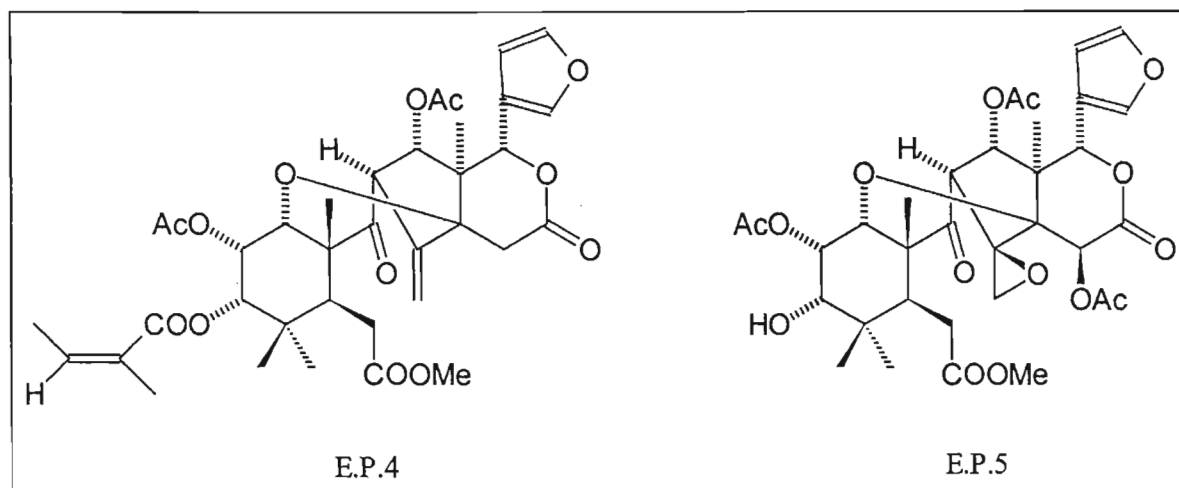
A previous investigation of the timber of *E. senegalensis* (collected in Nigeria), which is now considered conspecific with *E. capensis* (8), yielded the ekebergolactones A and B (9).



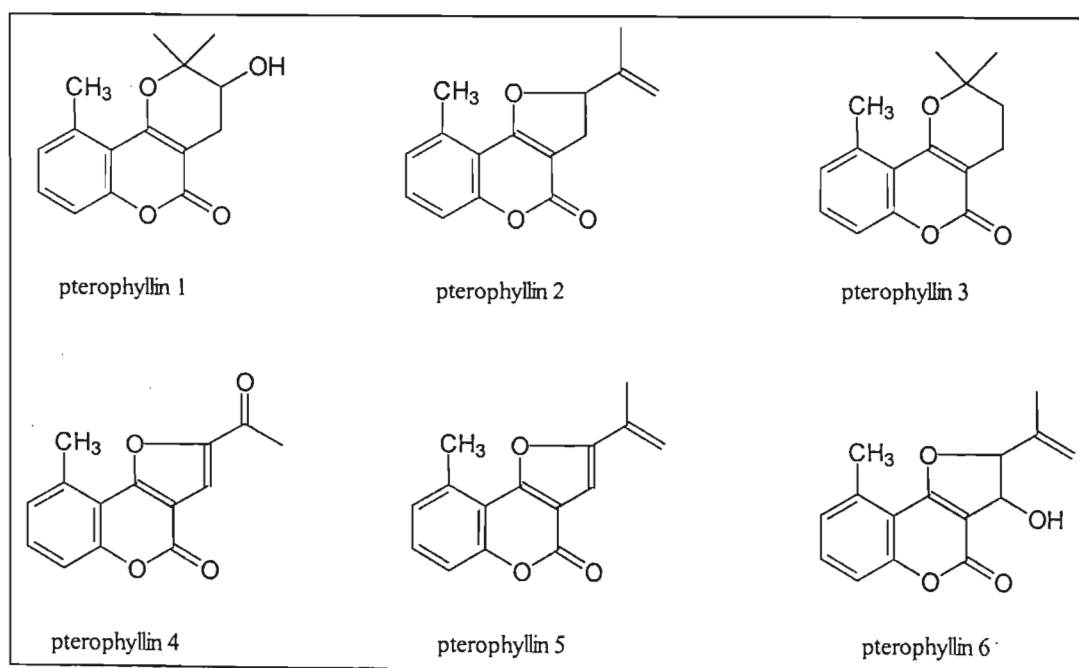
Investigations undertaken by Taylor *et al.* (10) on the seeds of *E. pterophylla* revealed the presence of ekebergin as well as compounds named E.P.1 (methyl 2 α -acetoxy-3 α -hydroxy-3-deoxoangolensate), E.P.2 (methyl 3 α -hydroxy-3-deoxoangolensate), and E.P.3 (methyl 2 α , 15 β -diacetoxy-3 α -hydroxy-3-deoxoangolensate).



Further studies on the seed of *E. pterophylla* by Kehrli *et al.* (11) led to the isolation of the above mentioned compounds including two other compounds named E.P.4 and E.P.5, whose structures were shown to be similar to those of the trijugins isolated from *Heynea trijuga* (12).



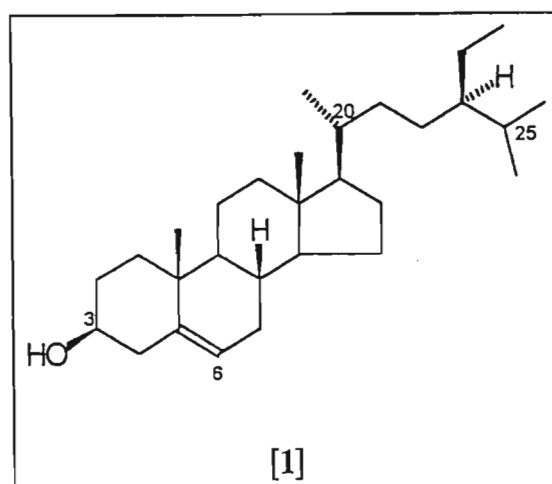
Although coumarins are not common in the Meliaceae family, in recent studies (14), the seed of *E. pterophylla* yielded six novel coumarins, the structures of which are given below.



In the current investigation of the supercritical fluid extract of *E. capensis* wood, extensive silica gel chromatography led to the isolation of five compounds. From spectral evidence and chemical transformation, the compounds were identified as β -sitosterol; oleanonic acid; 3-*epioleanolic* acid; 2,3,22,23-tetrahydroxy-2,6,10,15,19,23-hexamethyl-6,10,14,18-tetracosatetraene and 7-hydroxy-6-methoxycoumarin. The structure elucidation of these compounds is discussed.

9.2 Structure elucidation of compounds isolated

9.2.1 Compound 1



This compound was isolated as a white precipitate and displayed an R_f value of 0.67 with a mixture of ethyl acetate (10%), hexane (15%) and methylene chloride (75%). High resolution mass spectrometry indicated that the compound had a molar mass of 414.3848 $\text{g}\cdot\text{mol}^{-1}$ consistent with a molecular formula $\text{C}_{29}\text{H}_{50}\text{O}$ (calculated 414.3861) (spectrum 1a). The mass spectrum displayed a peak at m/z 396 $[\text{M} - \text{H}_2\text{O}]^+$, due to the ready dehydration of the compound, indicating the presence of one hydroxy group.

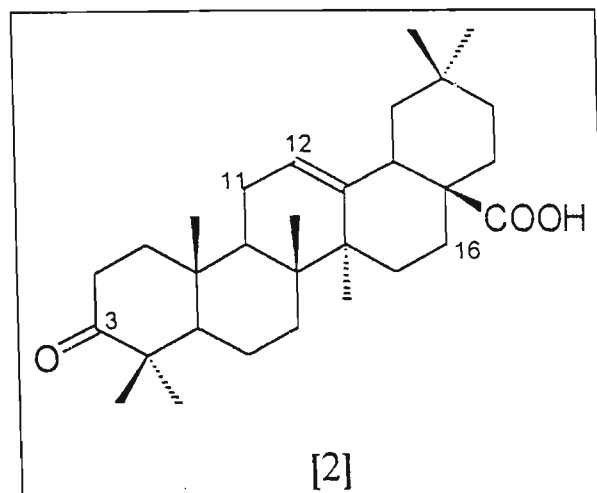
The infrared spectrum (spectrum 1b) displayed a strong band at 3430 cm^{-1} indicating the presence of a hydroxyl group. Differentiation between primary, secondary and tertiary alcohols is possible in many cases from the position of the C-O stretching bands. In this

spectrum, the strongest C-O stretching band at 1049 cm^{-1} suggested a secondary hydroxy group. The strong bands at 2936 cm^{-1} and 2867 cm^{-1} arose due to the presence of alkyl groups and the presence of methyl groups was shown by C-H deformation bands at 1460 cm^{-1} and 1378 cm^{-1} .

The ^1H NMR spectrum (spectrum 1c) was compared with library spectra which suggested the compound to be β -sitosterol. Characteristic resonances of this compound were the multiplet at $\delta 5.32$ assigned to the H-6 proton in the steroid skeleton. Another multiplet at $\delta 3.50$ ($W_{1/2} = 15\text{ Hz}$) was ascribed to the H-3 α proton, with a hydroxyl group attached at C-3 β .

The ^{13}C NMR spectrum (spectrum 1d) indicated a doublet occurring at $\delta 71.8$, a typical chemical shift for a carbon atom with an attached oxygen and was assigned to the C-3 carbon atom. The singlet at $\delta 141.0$ and doublet at $\delta 121.9$ indicated the presence of one trisubstituted double bond and were assigned to C-5 and C-6 respectively. Chemical shifts for the methyl group protons as well as the melting point and optical rotation correlated well with published data. This compound was hence undoubtedly confirmed to be β -sitosterol. This compound is frequently found in the plant kingdom.

9.2.2 Compound 2



This compound was isolated as colourless needles after recrystallisation from chloroform and displayed an R_f value of 0.50 with a mixture of ethyl acetate (10%), hexane (15%) and methylene chloride (75%). High resolution mass spectrometry of this compound showed that the M^+ peak occurred at m/z 454.3471 which correlated with the molecular formula $C_{30}H_{46}O_3$ (calculated 454.3447 $g \cdot mol^{-1}$) suggesting that compound 2 was a triterpenoid (spectrum 2a). The mass spectrum also displayed peaks at m/z 439 $[M - CH_3]^+$ and m/z 410 $[M - CO_2]^+$, the latter indicative of a carboxylic acid.

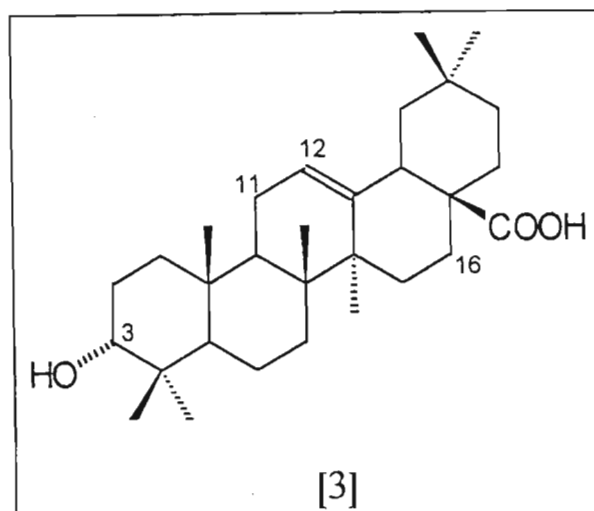
The infrared spectrum (spectrum 2b) displayed two prominent bands at 2922 cm^{-1} and 2850 cm^{-1} indicating the presence of alkyl groups and this was confirmed by the band at 1462 cm^{-1} while the band at 1377 cm^{-1} indicated that methyl groups were present. The bands at 1749 cm^{-1} and 1726 cm^{-1} were due to the carbonyl stretching vibrations of a ketone and a carboxylic acid group respectively while the band at 1271 cm^{-1} was due to C-O stretching vibrations. The medium band at 3421 cm^{-1} was due to the O-H stretching vibrations.

The ^{13}C NMR spectrum (spectrum 2d) displayed strong resonances for 30 carbons. Multiplicity assignments made from the DEPT spectrum indicated seven quartets, ten triplets and four doublets. The remaining nine carbon resonances were assigned as

singlets. The resonances at δ 122.3 (d) and δ 143.6 (s) confirmed the presence of a trisubstituted double bond, the chemical shifts of which are characteristic for oleanane triterpenoids with a Δ^{12} double bond (13). The two singlet resonances at δ 184.4 and δ 217.8 were ascribable to the carboxylic acid carbonyl carbon and the keto group carbon respectively.

The ^1H NMR spectrum (spectrum 2c) displayed a resonance at δ 5.24 (1H, bs) assigned to H-12. In the HETCOR spectrum (spectrum 2e), this was observed to correlate with the carbon resonance at δ 122.3 (d). A comparison of the data with that of a previously isolated compound indicated that this compound was oleanonic acid. The carbon and proton resonances were found to correspond with values reported in earlier studies (14). Furthermore, from the COSY spectrum (spectrum 2f), H-12 was seen to be coupled to a broad multiplet at δ 1.93 (2H, m) and this resonance was ascribed to 2H-11. The resonance assigned to 2H-11 was, in turn, coupled to a multiplet at δ 1.60 (1H, m) ascribed to H-9. The doublet of doublets at δ 2.80 (1H, dd) was assigned to the H-18 proton, which was seen to be coupled to H-19a (δ 1.56, m) and H-19b (δ 1.10, m). Hence on the basis of this information, compound 2 was confirmed as being oleanonic acid and has been isolated previously from this species.

9.2.3 Compound 3



This compound displayed an R_f value of 0.20 with a mixture of ethyl acetate (5%), hexane (15%) and methylene chloride (80%) and was isolated as colourless needles after recrystallization from methanol. High resolution mass spectrometry of this compound showed a molecular ion peak at m/z 456.3590, suggesting a molecular formula $C_{30}H_{48}O_3$ (required 456.3603 $g \cdot mol^{-1}$) (spectrum 3a).

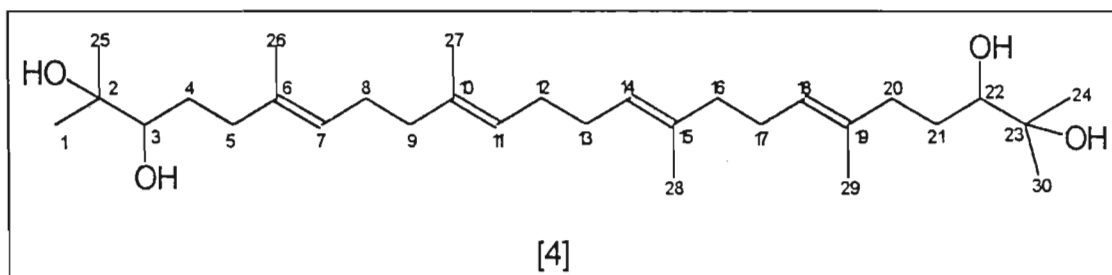
The infrared spectrum (spectrum 3b) displayed an intense band at 3404 cm^{-1} due to O-H stretching vibrations. The bands at 2947 cm^{-1} and 2879 cm^{-1} arose from alkyl groups while the presence of methyl groups were shown by the presence of a band at 1379 cm^{-1} . The strong sharp band at 1709 cm^{-1} was due to a carbonyl stretching vibration while the band at 1249 cm^{-1} was attributed to a C-O stretch. These bands suggested that a carboxylic acid group was present in the molecule. The band at 1444 cm^{-1} was due to the O-H in-plane bending vibration.

The ^{13}C NMR and 1H NMR spectra closely resembled the spectra of oleanonic acid with a few minor changes observed. The ^{13}C NMR spectrum (spectrum 3d) showed resonances for 30 carbon atoms. Multiplicity assignments indicated seven quartets, ten triplets and five doublets, while the remaining eight signals were assigned as singlets. The ^{13}C NMR

spectrum, unlike that of oleanonic acid, lacked the singlet ascribed to the C-3 keto group carbon at δ 217.8 however a doublet at δ 76.2 was now observed. The double bond carbon resonances occurred at δ 122.7 and δ 143.6 while the resonance at δ 183.1 ascribable to the carbonyl carbon of the carboxylic acid group, remained unchanged.

The ^1H NMR spectrum (spectrum 3c) showed the resonances for H-12 of the Δ^{12} double bond at δ 5.23 and the characteristic H-18 doublet of doublets at δ 2.79. The two H-2 proton multiplets at δ 2.20 and δ 2.50 in the spectrum of oleanonic acid, now occurred at δ 1.87 and δ 1.66 and a new broad singlet appeared at δ 3.39. This suggested that the keto group at C-3 had been replaced by a hydroxy group. Furthermore, a $W_{1/2}$ value of 7 Hz indicated that H-3 was β orientated leaving the hydroxy group in the α position. This compound was hence identified as being 3-*epioleanolic* acid. Though it has been demonstrated that the biosynthesis in plants leads to the 3 β -configuration, subsequent epimerisation could occur to produce the 3 α compounds (15). 3-*epioleanolic* acid is a known compound in the plant kingdom although not as widely spread as the 3 β -isomer.

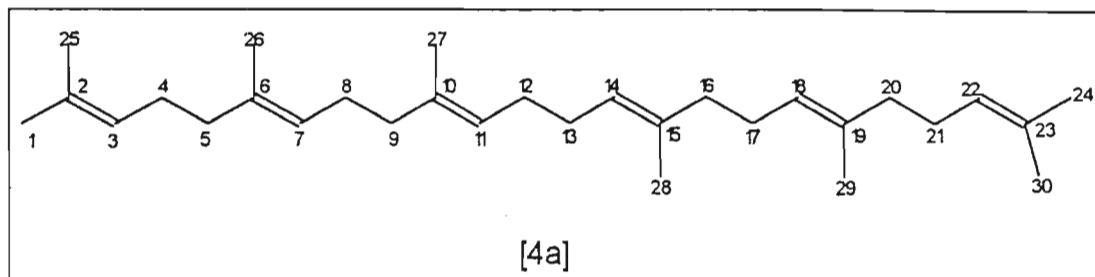
9.2.4 Compound 4



This compound was isolated as a colourless oil and displayed an R_f value of 0.17 with a mixture of ethyl acetate (50%) and methylene chloride (50%). The highest peak in the mass spectra occurred at m/z 348.2287, however the molecular formula obtained ($C_{21}H_{32}O_4$) for this analysis did not agree with other spectroscopic data, indicating that the compound may have decomposed or undergone a rearrangement reaction in the ion source or perhaps the molecular ion may have been too weak to be detected (spectrum 4a). The 1H NMR and the ^{13}C NMR spectra indicated that this compound closely resembled squalene.

The infrared spectrum (spectrum 4b) showed a strong band at 3437 cm^{-1} indicative of a hydroxy group. The bands between 3000 cm^{-1} and 2800 cm^{-1} are due to alkyl groups, and the presence of methyl groups is shown by bands at 1459 cm^{-1} and 1381 cm^{-1} . The band at 1638 cm^{-1} is due to $C=C$ stretching vibrations while the strong sharp band at 763 cm^{-1} arises due to the $C-H$ out of plane bending vibrations.

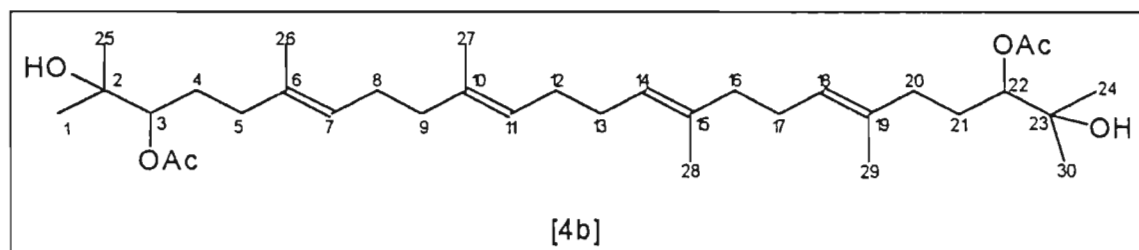
The structure of this compound was established on the basis of the 1H NMR and ^{13}C NMR data, all of which compared well with data for these compounds which were recently isolated from *Ekebergia benguelensis* from Tanzania. The ^{13}C NMR spectrum (spectrum 4d) showed resonances for fifteen carbons however the 1H NMR spectral features (spectrum 4c) indicated that this compound structurally resembled squalene [4a], an acyclic triterpenoid. Consequently, a symmetrical structure with thirty carbons was suggested.



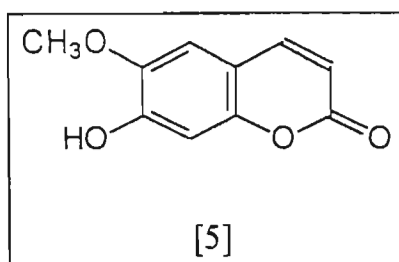
The ^{13}C NMR spectrum displayed strong resonances for fifteen carbons. Since squalene is formed from the alignment of two C_{15} units in a tail-to-tail fashion, it was quite evident that the ^{13}C NMR spectrum represented one of these units as it was a symmetrical molecule. Multiplicity assignments made from the DEPT spectrum indicated four quartets, five triplets and three doublets. The remaining three carbon resonances were assigned as singlets. The four resonances at $\delta 134.9$ (s), $\delta 134.8$ (s), $\delta 125.1$ (d) and $\delta 124.4$ (d) were due to olefinic carbons in the molecule while the signals at $\delta 78.3$ (d) and $\delta 73.0$ (s) indicated the presence of a secondary and tertiary carbinol group respectively. Since squalene is known to form the 2,3-epoxide, the two oxygen-bearing carbons were placed at positions 2 and 3 since this was the most biosynthetically probable position.

The ^1H NMR spectrum displayed resonances at $\delta 1.12$ (6H, s, $2 \times \text{CH}_3$) and $\delta 1.17$ (6H, s, $2 \times \text{CH}_3$) indicative of four methyl groups. In squalene, the four terminal methyl groups are attached to sp^2 carbons and hence resonate at $\delta 1.68$ and $\delta 1.60$. In contrast, the corresponding methyl groups of this compound suggested that these methyl groups were attached to sp^3 carbons as the signals appeared higher upfield. A further two signals occurring at $\delta 1.57$ (6H, s, $2 \times \text{CH}_3$) and $\delta 1.59$ (6H, s, $2 \times \text{CH}_3$) were indicative of four methyl groups attached to sp^2 carbons. The spectrum also showed a four proton multiplet at $\delta 5.14$ ascribable to H-7, H-11, H-14 and H-18. Two equivalent CH group protons were present as observed by the resonance at $\delta 3.32$ (2H, dd, $J_1 = 2.1$ Hz, $J_2 = 10.3$ Hz, H-3, H-22).

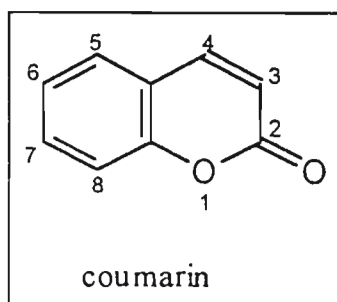
To confirm whether the molecule contained an epoxide or hydroxy groups, acetylation of [4] with acetic anhydride/pyridine at room temperature was carried out. A diacetate [4b] was formed. This product was isolated as a colourless oil. The ^1H NMR of [4b] showed a signal at $\delta 2.08$ (6H, s) due to two acetate group methyl protons (spectrum 4e). The double doublet that initially resonated at $\delta 3.32$ was shifted downfield to $\delta 4.35$ due to deshielding induced by the acetate carbonyl groups. Because both C-3 and C-22 hydroxyl groups were acetylated, [4b] was a symmetrical compound. The tertiary hydroxy groups at C-2 and C-23 did not acetylate as special conditions are required for the acetylation of tertiary hydroxy groups. Hence, based on these results, structure [4] was concluded to be the acyclic triterpenoid 2,3,22,23-tetrahydroxy-2,6,10,15,19,23-hexamethyl-6,10,14,18-tetracosatetrene. This suggested that [4] was a derivative of squalene in which two hydroxyl groups were added to each of the terminal double bonds. The rest of the signals closely matched literature values.



9.2.5 Compound 5



This compound was found to be a coumarin known as scopoletin and was isolated as colourless needles after recrystallisation from methanol. This compound did not show up on a TLC plate after using the anisaldehyde spray reagent. Instead, it fluoresced with a bright blue spot under UV light at 365 nm having an R_f value of 0.25 with a mixture of ethyl acetate (10%), methylene chloride (80%) and hexane (10%). The most obvious physical property of most natural coumarins is the fluorescence they display under UV light at 365 nm and this feature has been employed widely for their detection on paper (16, 17). It is often possible to make tentative assignments of the structural class of a coumarin from the colour it displays (18). 7-Alkoxy coumarins generally have a purple fluorescence whereas 7-hydroxy coumarins and 5,7-dioxygenated coumarins tend to fluoresce blue. The structure given below outlines the numbering system of a basic coumarin. The vast majority of natural coumarins carry an oxygen substituent at C-7.



High resolution mass spectrometry indicated that [5] had a molar mass of 192.0418 g.mol⁻¹ consistent with a molecular formula C₁₀H₈O₄ (calculated 192.0422 g.mol⁻¹) (spectrum 5a). Characteristic peaks were displayed at *m/z* 177 [M - CH₃]⁺; *m/z* 149 [M - CH₃ - CO]⁺ and *m/z* 121 [M - CH₃ - 2CO]⁺.

The infrared spectrum (spectrum 5b) showed an intense band at 3335 cm⁻¹ due to the O-H stretching vibration. The medium band at 2850 cm⁻¹ was due to the symmetrical stretch of a methoxy group with the symmetric bend at 1450 cm⁻¹. The strong sharp band at 1706 cm⁻¹ is due to the carbonyl stretching vibrations of an α,β unsaturated lactone. The sharp bands at 1565 cm⁻¹ and 1509 cm⁻¹ indicated that this was an aromatic compound. The sharp bands at 922 cm⁻¹ and 860 cm⁻¹ were due to the C-H out-of-plane bending vibrations of the aromatic ring while the C-H in-plane bending vibrations occurred at 1020 cm⁻¹. The strong band at 1292 cm⁻¹ was due to C-H in-plane bending of olefinic carbons.

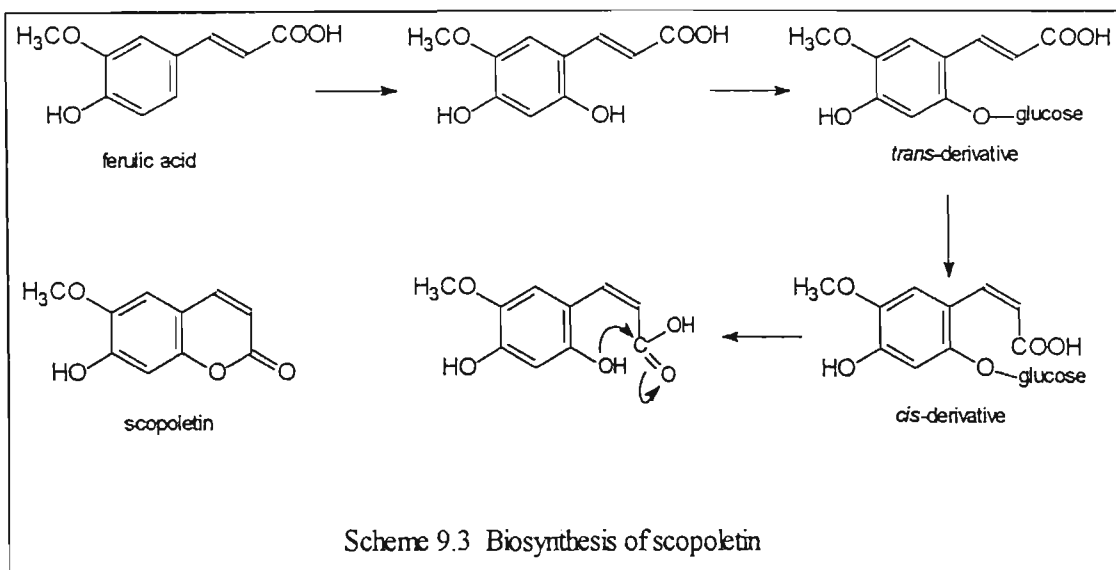
The ¹H-NMR spectrum (spectrum 5c) showed a resonance at δ 3.94 (3H, s) arising due to methoxy group protons. A pair of doublets at δ 7.58 (1H, *J*_{3,4} = 9.5 Hz) and δ 6.24 (1H, *J*_{3,4} = 9.5 Hz) were characteristic of the H-4 and H-3 signals respectively. The H-4 resonance is found in the region of δ 7.5-7.9 in coumarins lacking a C-5 oxygen function (19) as an oxygen or alkyl substituent at C-5 will characteristically shift the resonance of H-4 downfield by ~0.3 ppm (the peri effect) with H-4 being found at δ 7.9-8.2 (20, 21). The signal at δ 6.10 (1H, s) was due to a hydroxy proton while the H-5 (1H,s) and H-8 (1H, s) resonances were observed at δ 6.83 and δ 6.90 respectively.

Nuclear Overhauser Effect (NOE) experiments were carried out to establish the position of the methoxy and hydroxy groups. This experiment is useful for studying molecular conformation and depends on the dipolar relaxation of one proton by another. The effect is proportional to the inverse sixth power of the internuclear distance and is thus sensitive to conformational changes. Irradiation of the signal at δ 7.58 (H-4) led to the observation of difference peaks at δ 6.83 (s) and δ 6.24 (d) hence verifying the close proximity of these

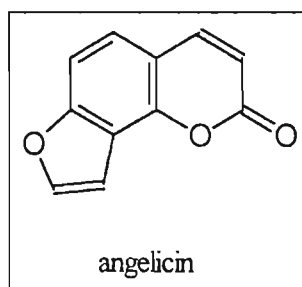
protons to H-4 (spectrum 5d). The doublet at $\delta 6.24$ has already been assigned to H-3, hence the resonance at $\delta 6.83$ was assigned to H-5. Upon saturation of the H-5 signal, the intensities of the resonances at $\delta 7.58$ (H-4, d) and $\delta 3.94$ (OCH₃) were increased (spectrum 5e). From this it was concluded that the methoxy group was in close proximity to H-5 and hence must be located at C-6. Subsequent irradiation of the methoxy signal only increased the intensity of the H-5 signal (spectrum 5f). This indicated that the substituent at C-7 was the hydroxy group. The resonance at $\delta 6.90$ (H-8) was irradiated but there was no NOE observed between H-8 and the other protons confirming the position of the hydroxy group at C-7.

The ¹³C NMR spectrum (spectrum 5g) however only showed resonances for five carbons as the sample was extremely weak. The signals at $\delta 143.3$ (d), $\delta 113.4$ (d), $\delta 107.5$ (d) and $\delta 103.2$ (d) were due to methine carbons while the signal at $\delta 56.4$ (q) was due to the methoxy group at C-6. The singlet carbons were not observed. Based on the data obtained, compound 5 was assigned structure [5] and identified as 7-hydroxy-6-methoxycoumarin, the common name of which is scopoletin.

Scopoletin [5] is possibly biosynthetically derived from ferulic acid following the scheme outlined below. Normally the *ortho* - hydroxy group undergoes glucosylation (which results in isomerisation of *trans* ferulic acid derivatives to the *cis* form). The subsequent hydrolysis of the sugar moiety leads to closure of the ring leading to scopoletin (22).



This compound occurs widely in the plant world and could possibly be used as a spasmolytic agent. Patnaik *et al.* isolated angelicin from the aerial parts of *Heracleum thomsoni* (Apiaceae) and found this compound to exhibit nonspecific spasmolytic activity in a variety of *in vivo* and *in vitro* test models (23). This compound had a relaxant effect on a wide variety of smooth muscle preparations from various species.



Various other coumarins have been isolated and all have displayed spasmolytic activity (24-27).

References

1. C.W.L. Bevan, D.E.U. Ekong, T.G. Halsall and P. Toft, *J. Chem. Soc. (C)*, (1967), 820.
2. J.G.St.C. Buchanan and T.G. Halsall, *Chem. Comm.*, (1969), 48.
3. J.G.St.C. Buchanan and T.G. Halsall, *Chem. Comm.*, (1969), 242.
4. A. Hutchings, A.H. Scott, G. Lewis and A. Cunningham, *Zulu Medicinal Plants*, University of Natal Press, South Africa (1996), p.157.
5. V. Sewram, M.W. Raynor, D.A. Mulholland, D.M. Raidoo, *Journal of Pharmaceutical and Biomedical Analysis*, in press.
6. D.A.H. Taylor, *Phytochemistry*, **20** (1981), 2263.
7. S.A. Jonker, M.H.H. Nkunya, L. Mwantobe, J. Geenevasen and G-J, Koomen, *Nat. Prod. Lett.*, **10** (1997), 245.
8. T.D. Pennington, and B.T. Styles, *Blumea*, **22** (1975), 476.
9. J.D. Connolly, *Chemical Society Symposium on Natural Products*, (1976), Nottingham.
10. A.R.H. Taylor and D.A.H. Taylor, *Phytochemistry*, **23** (1984), 2676.
11. A.R.H. Kehrl, D.A.H. Taylor and M. Niven, *Phytochemistry*, **29** (1990), 153.
12. K.K. Purushothaman, M. Venkatanarasimhan, A. Sarada, J.D. Connolly and D.S. Rycroft, *Can. J. Chem.*, **65** (1987), 35.
13. P.K. Agrawal and D.C. Jain, *Progress in NMR Spectroscopy*, **24** (1992), 1.
14. S. E. Iourine, *Extractives from the Celastraceae and Meliaceae*, PhD thesis, University of Natal (1996).
15. P. Crews and E. Kho-Wiseman, *Tetrahedron Lett.*, 1978, 2487.
16. T. Beyrich, *J. Chromatogr.*, **13** (1964), 181.
17. D.J. Crosby and R.V. Berthold, *Anal. Biochem.*, **4** (1962), 349.
18. R.D.H. Murray, J. Méndez, S.A. Brown, *The Natural Coumarins*, J. Wiley & Sons, New York, USA (1982), p.22.
19. W. Steck and M. Mazurek, *Lloydia*, **35** (1972), 418.
20. J. F. Fisher and H.E. Nordby, *J. Food Sci.*, **30** (1965), 869.

21. J. F. Fisher and H.E. Nordby, *Tetrahedron*, **22** (1966), 1489.
22. Reference 14, p.62.
23. G.K. Patnaik, K.K. Banaudha, K. A. Khan, A. Shoeb and B.N. Dhawan, *Planta Med.*, (1987), 517.
24. G.K. Patnaik, A. Shoeb, M.D. Manandhar, R.S. Kapil, S.P. Popli and B.N. Dhawan, *Indian J. Pharmacol.*, **10** (1978), 82.
25. A. Shoeb, M.D. Manandhar, R.S. Kapil and S.P. Popli, *J. Chem. Soc. Chem. Commun.*, (1979), 281.
26. S.H. Rizvi, A. Shoeb, R.S. Kapil, S.P. Popli, *Indian J. Pharm. Sci.*, **41** (1979), 205.
27. G.K. Patnaik and B.N. Dhawan, *J. Ethnopharmacol.*, **6** (1982), 127.

CHAPTER 10.

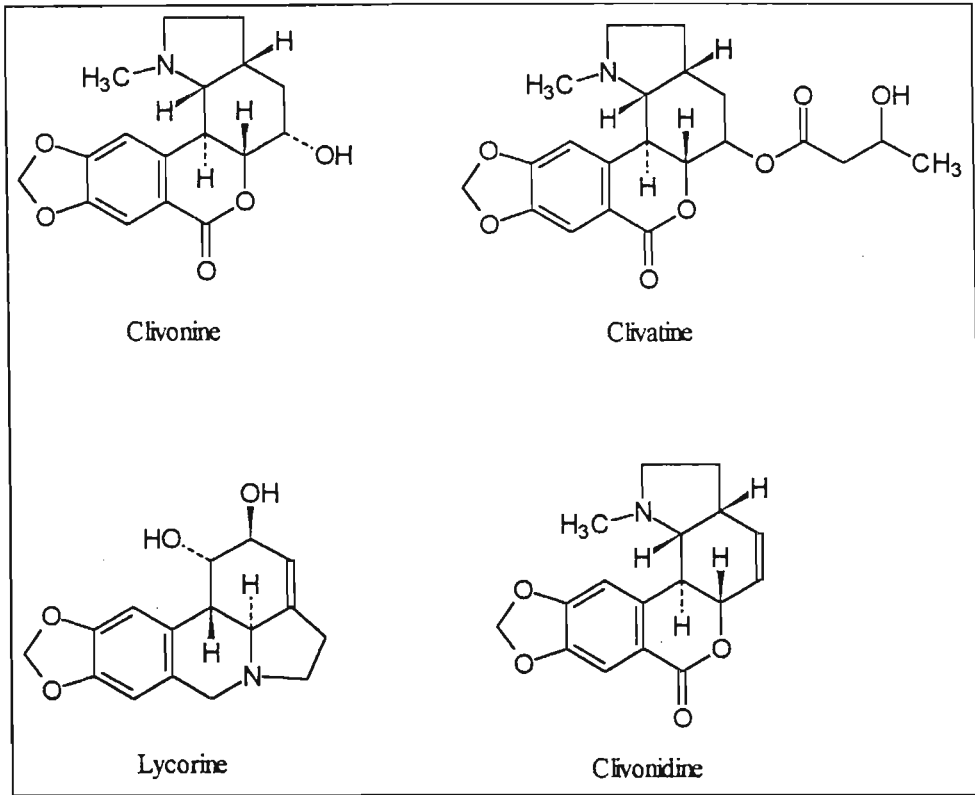
Extractives from Clivia miniata (Lindl.) Regel.

10.1 The genus *Clivia*

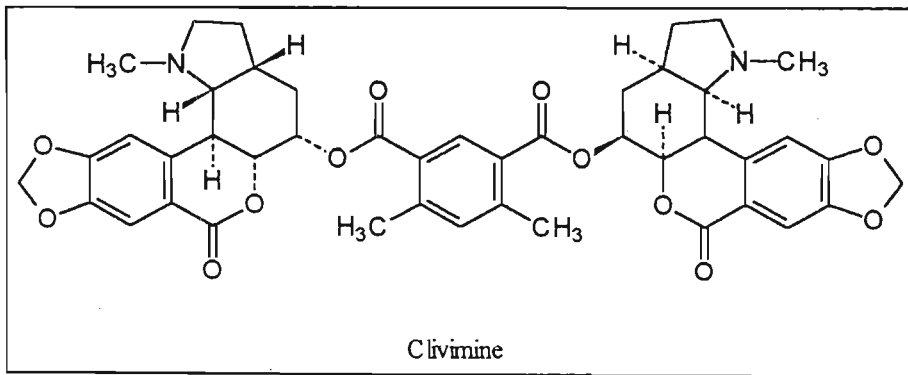
Clivia miniata belongs to the Amaryllidaceae family which is extremely widespread. This family contains a large number of species that are indigenous to nearly every part of the world except the tropics where only few species have been found (1). The Amaryllidaceae alkaloids have aroused interest in a wide range of biological fields. They are known to exhibit different pharmacological and microbiological effects such as antiviral, antitumoral and anticholinergic (2). Some of them have been used in the treatment of myasthenia gravis, myopathy, and diseases of the nervous system.

Clivia miniata is indigenous to KwaZulu-Natal and is used for a number of medical purposes. The root is used as a snake-bite remedy by the Zulu and by the Xhosa in the Transkei (3). The Zulu also use the root in treating febrile conditions and the herb to facilitate delivery at childbirth or to initiate parturition when its onset is retarded (4). The bulb decoctions are also used by the Xhosa for infertility and urinary complaints (3).

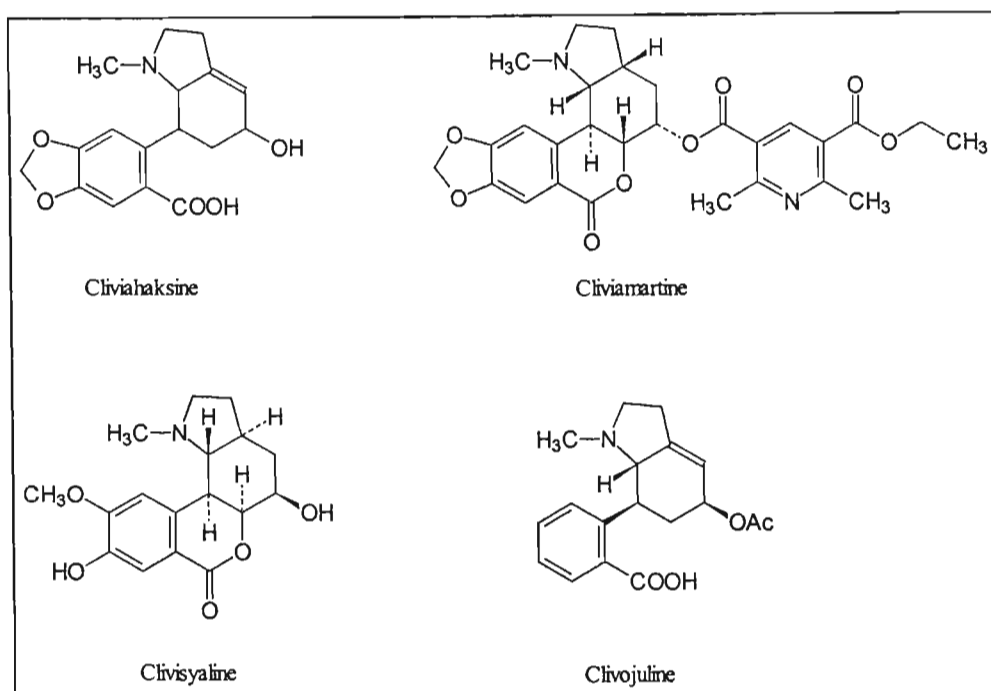
Previous investigations into the chemical constituents of this plant has resulted in the isolation of several alkaloids. The alkaloids clivonine, clivatine, lycorine and clivonidine were isolated from the total plant cultivated in Egypt (5).



Small amounts of clivimine and lycorine have also been isolated from the leaves by Jaspersen-Schib (6).



Other alkaloids isolated from the plant include cliviahaksine, cliviamartine, clivojuline and clivisyaline (8-11)

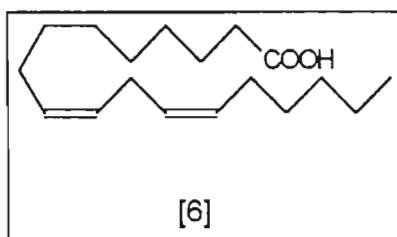


Lycorine is the most widespread of the Amaryllidaceae alkaloids and is responsible for the antiviral activity this plant is said to exhibit (12). Poliomyelitis virus inhibition occurred at lycorine concentrations as low as $1\mu\text{g/ml}$, while concentrations exceeding $25\mu\text{g/ml}$ were cytotoxic. Clivimine, clivonine and cliviamartine showed no antiviral properties.

In this study the supercritical fluid extract of the roots of *C. miniata* were analysed in an attempt to identify the uterotonic principle present. While the literature review of this plant indicated that alkaloids were the main group of compounds present, there were no alkaloids found in the SFE extract of this plant suggesting that the extraction conditions employed were not favorable for the extraction of these compounds.

10.2 Structural elucidation of compounds isolated from *Clivia miniata*

10.2.1 Compound 6



Compound 6 was identified as linoleic acid [6] and it was the major component contained in the fatty acid mixture. This mixture was insoluble in methanol and it appeared as a white precipitate as the SFE extract was passed into methanol during extraction. However, upon removing this precipitate from methanol, it turned into a colourless oil. The ^1H NMR spectrum of this compound (spectrum 6a) revealed that it was a fatty acid. Since fatty acids generally occur as mixtures and are difficult to separate by gravity column chromatography, GC-MS analysis was carried out on this mixture. The experimental conditions for analysis are outlined in section 5.15. Free fatty acids are highly polar and often have great difficulty in eluting from a GC column. Hence, the methyl esters of these fatty acids were formed so that analysis could be made possible. The fatty acid fraction was esterified following the method described in section 5.16.

Figure 10.1 shows the total ion chromatogram of the esterified fraction with the major component having a retention time of 34.74 minutes. The mass spectrum of this compound compared well with the mass spectrum of methyl linoleate (Figure 10.2), hence the major component in the esterified fraction was identified as linoleic acid.

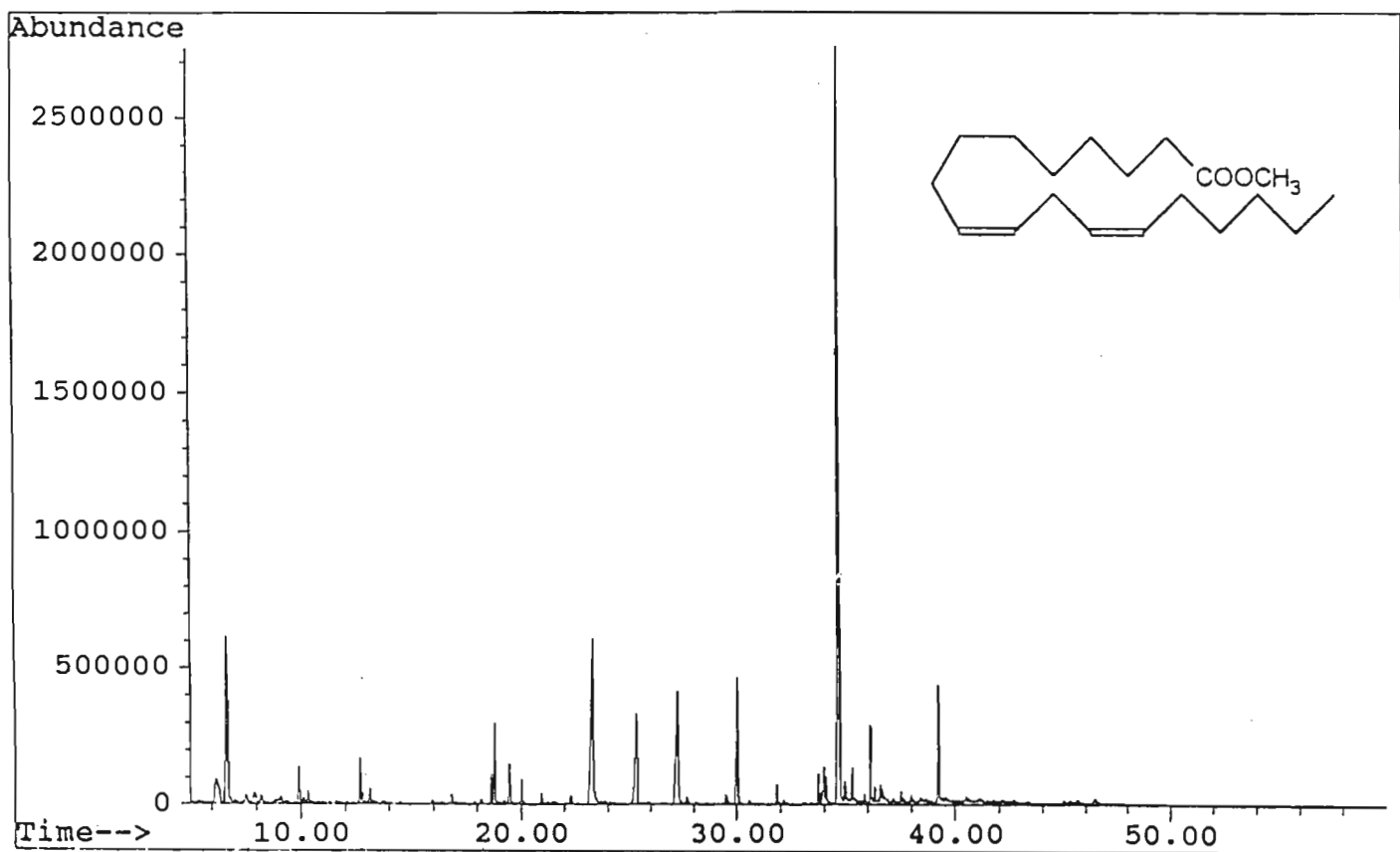


Figure 10.1 GC-MS total ion chromatogram of esterified fatty acid mixture showing methyl linoleate as the major component.

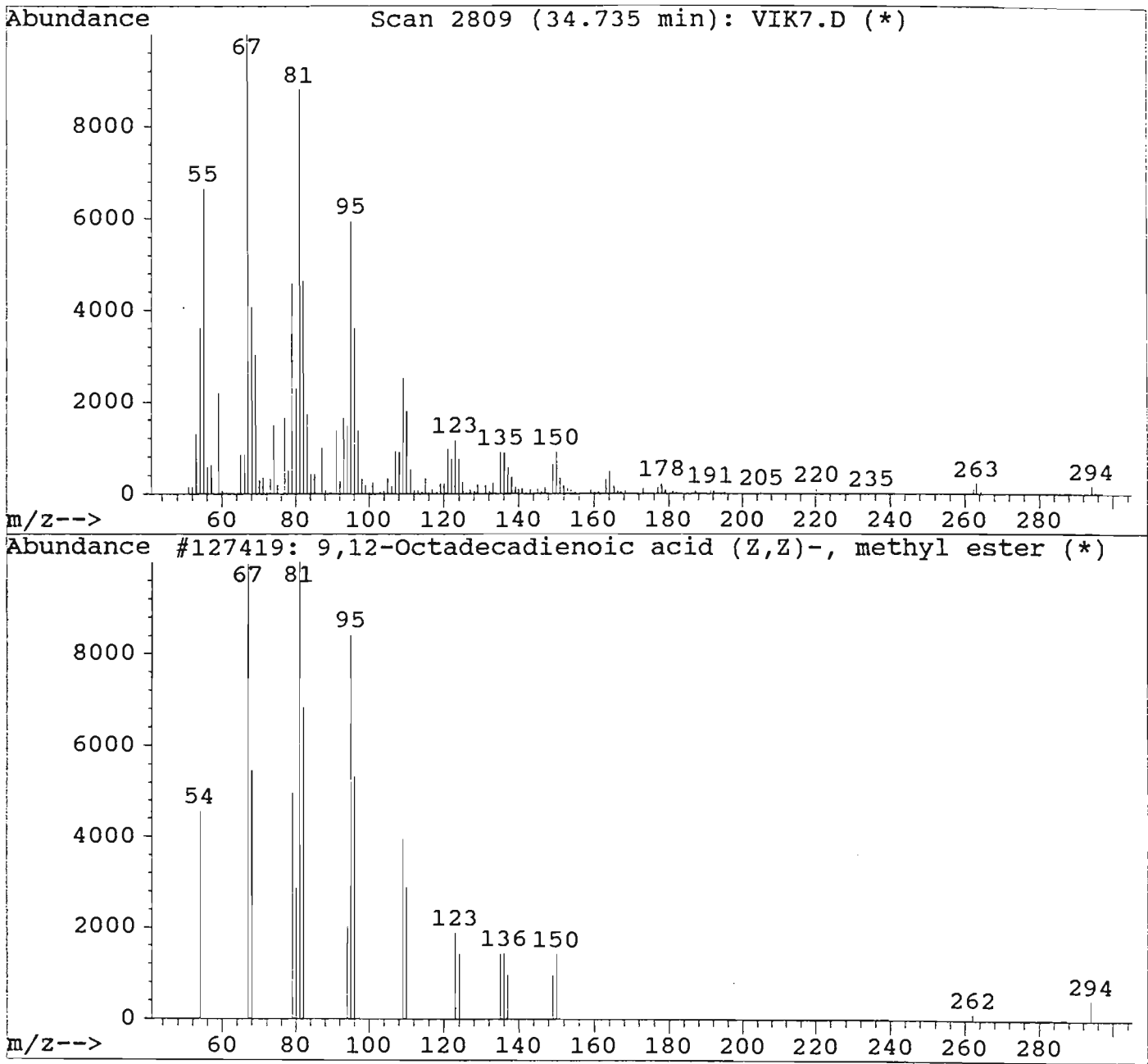
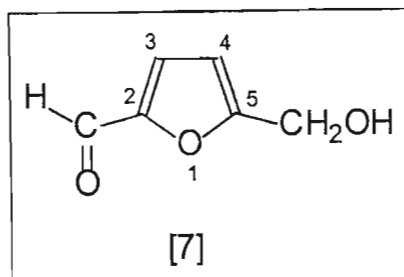


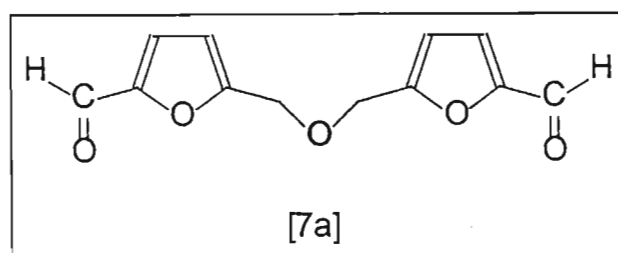
Figure 10.2 EI mass spectrum for methyl linoleate with the matching spectrum from the Wiley library confirming the identity of linoleic acid.

Linoleic acid is of great significance in this plant as it may attribute to the uterotonic effects of this extract and hence support the ethnomedical claims of its use in initiating labour. It is a precursor of the eicosanoids (20-carbon fatty acids) which include leukotrienes, prostaglandins, thromboxanes and related compounds. Linoleic acid is esterified to form phospholipids (primarily phosphatidylethanolamine or phosphatidylcholine) in cell membranes activating phospholipase A₂ which, in turn, hydrolyses membrane phospholipids resulting in the release of arachidonic acid. The arachidonic acid is then acted on by the enzyme arachidonic acid cyclooxygenase (prostaglandin endoperoxide synthetase) to produce prostaglandins (13). Prostaglandins F₂α and E₂α have direct stimulatory effects on uterine contractility and are synthesised in large quantities during initiation of labour. In support of the proposition that the release of arachidonic acid is crucial to the onset and maintenance of labour, it was found that the concentration of nonesterified arachidonic acid in amniotic fluid obtained after the onset of labour increased six-fold compared with that in amniotic fluid obtained at term before the onset of labor (14).

10.2.2 Compound 7



High resolution mass spectrometry indicated that the compound had a molar mass of $126.0307 \text{ g}\cdot\text{mol}^{-1}$ correct for the formula $\text{C}_6\text{H}_6\text{O}_3$ (calculated 126.0317) (spectrum 7a). Characteristic fragments occurred at m/z 109 $[\text{M} - \text{OH}]^+$ and at m/z 97 $[\text{M} - \text{CHO}]^+$. The small signal at m/z 234 may have resulted due to dimer formation resulting in [7a] below.



This may have occurred in the GC-MS due to dehydration of the molecule.

The infrared spectrum (spectrum 7b) showed a strong band at 3423 cm^{-1} indicative of a hydroxy group. The intense sharp band at 1670 cm^{-1} together with the signals at 2924 cm^{-1} and 2855 cm^{-1} confirmed the presence of an α,β unsaturated aldehyde. The small, sharp band at 1190 cm^{-1} suggested that an ether linkage was present as this band arose from the C-O-C symmetric stretching vibrations. The band at 1521 cm^{-1} indicated unsaturation in the molecule.

indicated that the aldehyde group was attached to a quaternary carbon. Two resonances occurring at $\delta 7.42$ (1H, d, $J_{3,4} = 3.6\text{Hz}$) and $\delta 6.61$ (1H, d, $J_{3,4} = 3.6\text{ Hz}$) were due to vicinal protons in an unsaturated heterocyclic system and were assigned to H-3 and H-4 respectively. The signal at $\delta 3.39$ was due to a hydroxy group proton while the $-\text{CH}_2\text{O}$ group protons resonated at $\delta 4.65$ (2H).

The ^{13}C NMR spectrum displayed resonances for six carbons (spectrum 7d). Multiplicity assignments from the DEPT spectrum indicated three doublets and one triplet. The remaining two signals were assigned as singlets. The doublet at $\delta 177.7$ was due to the aldehyde carbon while the resonances at $\delta 122.7$ (d) and $\delta 110.0$ (d) were due to C-3 and C-4 respectively. The signal at $\delta 57.6$ (t) was due to a $-\text{OCH}_2$ group carbon and this was supported by the resonance in the ^1H NMR spectrum at $\delta 4.65$ (2H). The two singlets at $\delta 160.5$ and $\delta 152.4$ were due to quaternary carbons and were assigned to C-5 and C-2 respectively. This compound was established as a 2,5-disubstituted furan. The carbon resonances compared well with published data (15).

An NOE experiment was carried out by irradiating the aldehyde proton signal at $\delta 9.57$. This led to an increase in the intensity of the signal at $\delta 7.42$ revealing the close proximity of H-3 (spectrum 7e). Based on the spectral data, this compound was identified as 5-hydroxymethyl-2-furancarboxaldehyde. This compound is obtainable from various carbohydrates and is a constituent of numerous plants. Recently, it was found to be present in a Chinese crude drug (15) where it was found to possess aldose reductase (AR) inhibitory activity.

References

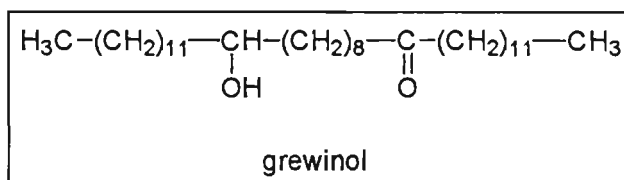
1. O. Queckenberg, A.W. Frahm, D. Müller-Doblies and U-Müller-Doblies, *Planta Med*, **58** (1992), A699.
2. M.A. Abd El Hafiz, M.A. Ramadan, M.L. Jung, J.P. Beck and R. Anton, *Planta Med.*, **57** (1991), 437.
3. J.M. Watt and M.G. Breyer-Brandwijk, *The Medicinal and Poisonous Plants of Southern and Eastern Africa*, E&S Livingstone Ltd, London, UK (1962), p.28.
4. D.J.H. Veale, K.I. Furman and D.W. Oliver, *J. Ethnopharm.*, **36** (1992), 185.
5. A.A. Ali, S.A. Ross, A.M. El-Moghazy and S.A. El-Moghazy, *J. Nat. Prod.*, **46** (1979), 350.
6. R. Von Jaspersen-Schib, *Pharm. Acta. Helv.*, **45** (1970), 424.
7. S. Kobayashi, H. Ishiawa, E. Sasakawa, M. Kihara, T. Shingu and A. Kato, *Chem. Pharm. Bull.*, **28** (1980), 1827.
8. W. Döpke and S.A. Roshan, *Z. Chem*, **22** (1982), 310.
9. W. Döpke and S.A. Roshan, *Z. Chem*, **20** (1980), 374.
10. W. Döpke and S.A. Roshan, *Z. Chem*, **21** (1981), 223.
11. W. Döpke and S.A. Roshan, *Heterocycles*, **16** (1981), 529.
12. M. Ieven, A.J. Vlietinck, D.A. Van Den Berghe, J. Totte, R. Dommissee, E. Esmans and F. Alderweireldt, *J. Nat. Prod.*, **45** (1982), 564.
13. Ronald F. Borne, In: *Principles of Medicinal Chemistry*, W.O. Foye, T.L. Lemke and D.A. Williams (Eds.), Williams & Wilkins, Baltimore, USA (1995), p.538.
14. J. Seitchik and N. Chattkof, *Obstet. Gynecol.*, **48** (1976), 436.
15. M. T. W. Hearn, *Aust. J. Chem.*, **29** (1976), 107.
16. M. Shimizu, Y. Zenko, R. Tanaka, T. Matsuzawa and N. Morita, *Chem. Pharm. Bull.*, **41** (1993), 1469.

CHAPTER 11

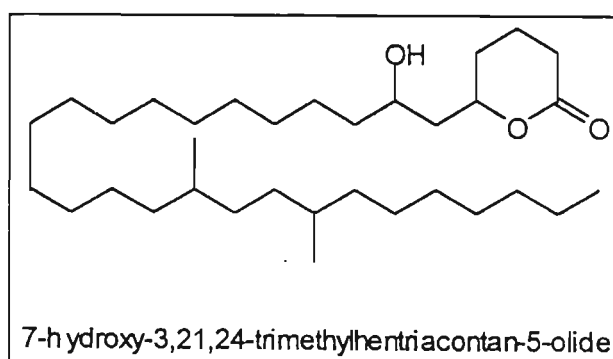
Extractives from Grewia occidentalis

11.1 The genus *Grewia*

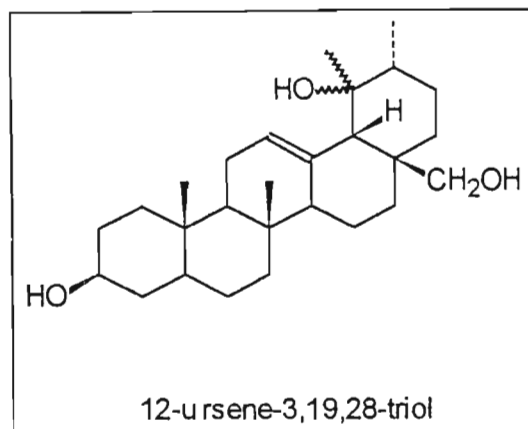
The genus *Grewia* belongs to the Tiliaceae family which is a fairly large family found throughout the world but especially abundant in the tropical and subtropical regions (1). *Grewia* is a large genus of more than 400 species widely distributed in Africa, Asia and Australia.. Extracts from *Grewia asiatica* Linn. produces significant hypoglycaemic effects in diabetic rats (2). Lakshmi and Chauhan (3) isolated grewinol, a long chain keto-alcohol from the flowers of this plant



Further investigations into this species resulted in the isolation of a new δ -lactone 7-hydroxy-3,21,24-trimethylhentriacontan-5-olide (1).



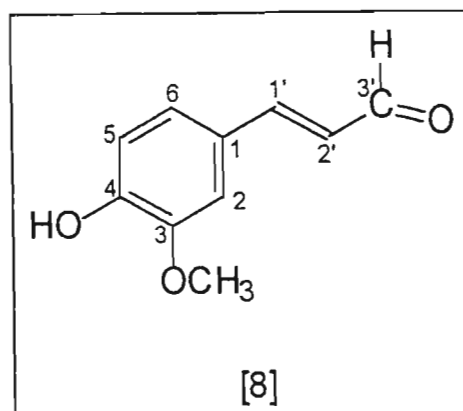
Bashir *et al.* (4) carried out chemical investigations on the roots of *Grewia villosa* and isolated 12-ursene-3,19,28-triol.



There have been no reports on the analysis of extracts from *Grewia occidentalis*. This plant is much used by the Zulu as a medicine. The root and wood are used to facilitate or procure delivery while the bark is used for bladder ailments (5). There have been no reports cited in the literature of chemical investigations being carried out on this plant. Hence the SFE extracts of the wood of this plant were analysed in order to determine the active principle responsible for its uterotonic effects.

11.2 Structural elucidation of compounds isolated from *Grewia occidentalis*

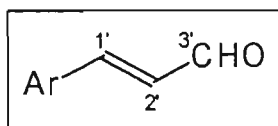
11.2.1 Compound 8



This compound was isolated as a light yellow amorphous material displaying an R_f value of 0.33 with a mixture of hexane (50%), methylene chloride (40%) and methanol (10%). High resolution mass spectrometric analysis (spectrum 8a) of this compound showed that the M^+ peak occurred at m/z 178.0625, correct for the formula $C_{10}H_{10}O_3$ (calculated 178.0630). The fragmentation pattern was consistent with a monomethoxy monohydroxy cinnamaldehyde (6). Characteristic peaks occurred at m/z 177 $[M - H]^+$, m/z 163 $[M - CH_3]^+$ and m/z 149 $[M - CHO]^+$.

The infrared spectrum (spectrum 8b) displayed a strong band at 3424 cm^{-1} indicating the presence of a hydroxy group. The sharp band at 1664 cm^{-1} was due to the presence of an α,β -unsaturated carbonyl group while the two bands between 2700 cm^{-1} and 2850 cm^{-1} strongly suggested that the compound possessed an aldehyde group. Strong sharp bands at 1587 cm^{-1} and 1514 cm^{-1} indicated that the compound was of an aromatic nature while the bands at 1286 cm^{-1} and 1130 cm^{-1} suggested that the aromatic nucleus was 1,3,4-trisubstituted. The band at 971 cm^{-1} was due to the C-H out-of-plane bending of a *trans* methine group.

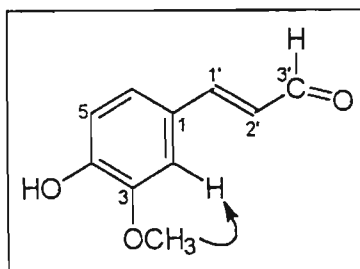
The ^1H NMR spectrum (spectrum 8c) displayed resonances at $\delta 9.63$ (1H, d, $J_{2,3'} = 7.65$ Hz), $\delta 7.38$ (1H, d, $J_{1,2'} = 15.9$ Hz) and a double doublet at $\delta 6.57$ (1H, dd, $J_{1,2'} = 15.9$ Hz, $J_{2,3'} = 7.65$ Hz) indicating the presence of a *trans* CH=CH-CHO moiety as shown below.



From the above diagram it can be seen that both H-3' and H-1' are split into doublets as a result of H-2' while H-2', in turn, is split by H-1' into a doublet and further by H-3' resulting in a double doublet. The coupling of H-2' to both H-1' and H-3' was confirmed by the COSY spectrum (spectrum 8d)

The ^1H NMR spectrum also showed resonances at $\delta 3.93$ (1H, s, OCH_3) and $\delta 5.95$ (1H, OH) due to methoxy and hydroxy group protons respectively. The hydroxy group proton signal was confirmed by its disappearance after addition of D_2O to the sample (spectrum 8e). The resonances in the region $\delta 6.88$ to $\delta 7.20$ were due to the protons on the aromatic nucleus. The resonance at $\delta 6.94$ (1H, d, $J_{5,6} = 8.2$ Hz) was due to H-5 and was *ortho* coupled to H-6. The resonance at $\delta 7.10$ (1H, dd, $J_{5,6} = 8.2$ Hz, $J_{2,6} = 1.8$ Hz) was attributed to H-6 as it was observed to be *ortho* coupled to H-5 resulting in a doublet followed by further splitting into a double doublet as a result of *meta* coupling to H-2, the signal of which was observed at $\delta 7.05$ (1H, d, $J_{2,6} = 1.8$ Hz). While at this point it was known that the aromatic ring was 1,3,4-trisubstituted, the position of the methoxy and hydroxy groups was uncertain.

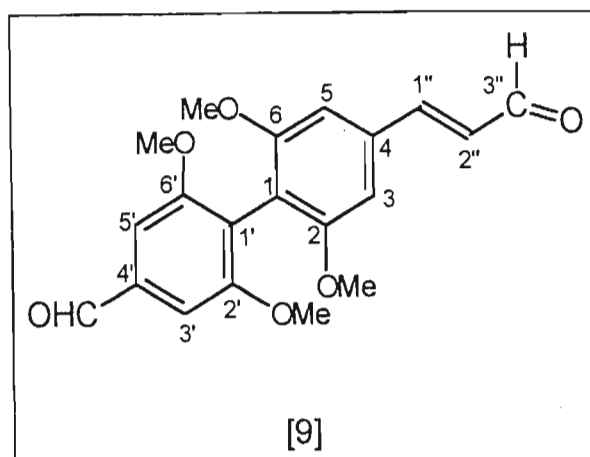
NOE experiments were carried out by irradiating the methoxy group proton signal at $\delta 3.93$. This resulted in an enhancement of the H-2 signal at $\delta 7.05$ as shown below (spectrum 8f). As there were no more NOE signals observed, it was clear that the hydroxy group was attached to the neighbouring carbon.



Irradiation of the H-2 signal at $\delta 7.05$ resulted in the enhancement of the resonances at $\delta 3.93$, $\delta 6.57$ (H-2') and $\delta 7.38$ (H-1') indicating that this proton was in close proximity to the propanoid side chain (spectrum 8g). There is free rotation about the C-1, C-1' bond, thus one would expect to get positive signals for both these protons when H-2' is irradiated.

This compound was hence deduced as 3-(4-hydroxy-3-methoxyphenyl)-2-propenal, the common name of which is coniferaldehyde. This compound compared well to published data and has also been reported to occur in the roots of *Tamarix nilotica* (Tamaricaceae) (6).

11.2.2 Compound 9

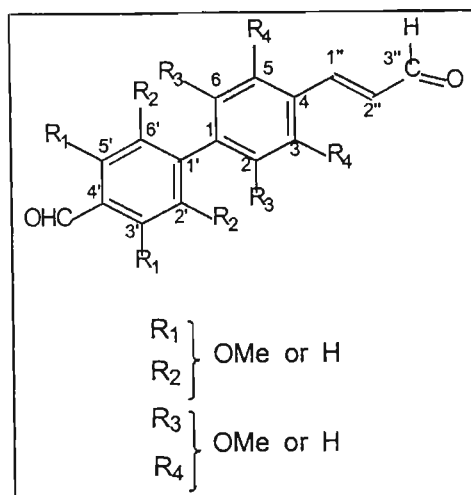


This compound was isolated as a brown amorphous substance displaying an R_f value of 0.25 with a mixture of hexane (50%), methylene chloride (20%) and ethyl acetate (30%). High resolution mass spectrometric analysis indicated a molar mass of 208.0700 $\text{g}\cdot\text{mol}^{-1}$ correct for the molecular formula $\text{C}_{11}\text{H}_{12}\text{O}_4$ (calculated 208.0735) (spectrum 9a) but subsequent elucidation of the structure using NMR techniques indicated that this was not the molecular ion. Hence, the mass spectrum results were inconclusive as the molecular ion peak may have been too weak to be detected or the molecule may have fragmented prior to detection of the molecular ion.

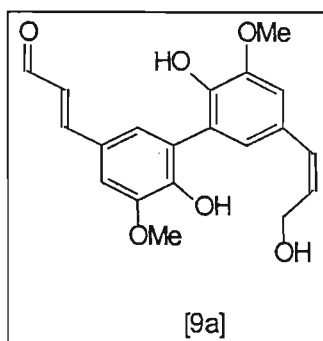
The infrared spectrum (spectrum 9b) displayed a resonance at 3418 cm^{-1} due to OH stretching vibrations. This band was later attributed to traces of water contained in the sample as the final structure did not possess a hydroxy group. The strong, sharp band at 1677 cm^{-1} was due to the presence of a carbonyl group while the bands at 2939 cm^{-1} and 2847 cm^{-1} suggested that the compound contained an aldehyde group. The strong band at 1588 cm^{-1} indicated unsaturation in the molecule while the bands in the region 1513 cm^{-1} to 1330 cm^{-1} indicated that the compound was of an aromatic nature.

The ^1H NMR spectrum of this compound (spectrum 9c) showed certain similarities to that of the previous compound. The resonances at $\delta 9.64$ (1H, d, $J_{2',3'} = 7.65$ Hz), $\delta 7.36$ (1H, d, $J_{1',2'} = 15.9$ Hz) and a double doublet at $\delta 6.59$ (1H, dd, $J_{1',2'} = 15.9$ Hz, $J_{2',3'} = 7.65$ Hz) once again indicated the presence of a *trans* CH=CH-CHO group. A second aldehyde proton resonance at $\delta 9.80$ (1H, s) indicated that this group was attached to a quaternary carbon atom as no splitting of the signal was observed. The resonances at $\delta 7.13$ (2H, s) and $\delta 6.79$ (2H, s) were each due to two chemically equivalent aromatic protons as observed from the integration signal. The resonances at $\delta 3.92$ (6H, s) and $\delta 3.95$ (6H, s) were each due to the protons of two chemically equivalent methoxy groups.

The ^{13}C NMR spectrum (spectrum 9d) displayed twelve resonances. Multiplicity assignments revealed six doublets and one quartet. The remaining five signals were assigned as singlets. The signals at $\delta 153.1$ (d) $\delta 126.8$ (d) correlated with proton resonances at $\delta 7.36$ (H-1") and $\delta 6.59$ (H-2") respectively in the HETCOR spectrum (spectrum 9e), while the signals at $\delta 106.7$ (d) and $\delta 105.6$ (d) correlated with proton resonances at $\delta 7.13$ (2H) and $\delta 6.79$ (2H) respectively. The latter observation indicated that the carbon signals were each due to two equivalent carbon atoms. The carbon resonance at $\delta 56.4$ (q) was found to correlate with the four methoxy group proton signals at $\delta 3.92$ (6H) and $\delta 3.95$ (6H). The signal at $\delta 147.3$ (s) was attributed to the four chemically equivalent fully substituted carbons bearing the methoxy groups while the resonances at $\delta 125.3$ (s), $\delta 128.4$ (s), $\delta 138.0$ (s) and $\delta 140.9$ (s) were attributed to the quaternary aromatic carbons. It was evident that the compound possessed twenty carbons and the spectral information gathered thus far indicated two symmetrical benzene rings each with two equivalent methoxy groups and two equivalent protons, hence the following biphenyl derivative was proposed:



NOE experiments were carried out to establish the position of the methoxy groups and aromatic protons. Irradiation of the signal at $\delta 7.36$ (H-1'') led to the enhancement of the signals at $\delta 9.64$ (H-3'') and $\delta 6.79$ (2H, s) (spectrum 9f). This led to the conclusion that the two equivalent aromatic protons were in close proximity to the propanoid skeleton and were placed at carbons 3 and 5 indicating two methoxy groups to be placed at C-2 and C-6. Irradiation of the other aromatic proton signal at $\delta 7.13$ (2H) led to the enhancement of the signals at $\delta 9.80$ (1H, s, CHO) and $\delta 3.92$ (6H, s, $2 \times \text{OCH}_3$) confirming the position of H-3' and H-5' as well as showing that these protons occurred adjacent to the aldehyde and methoxy groups (spectrum 9g). Hence this compound was identified as 2,2',6,6'-tetramethoxy-4'-al-4-(ω -oxo-*E*-propenyl)-biphenyl. This compound has not been isolated previously although biphenyl derivatives such as zeyherol [9a] which was isolated from the wood of *Zeyhera digitalis* (Bignoniaceae) (7) are known.



11.2.3 Compound 10

This compound was identified as oleanonic acid [2] on the basis of its $^1\text{H-NMR}$ spectrum and was also isolated from the SFE extract of the wood of *Ekebergia capensis*. The structure elucidation of this compound is discussed in section 9.2.2.

References

1. V. Lakshmi, S.K. Agarwal and J.S. Chauhan, *Phytochemistry*, **15** (1976), 1397.
2. I.A. Dogar, M. Ali and M. Yaqub, *J. Pak. Med.Ass.*, **38** (1988), 289.
3. V. Lahshmi and J.S. Chauhan, *J. Nat. Prod.*, **39** (1976), 372.
4. A.K. Bashir, M.S.F. Ross and T.D. Turner, *Fitoterapia*, **53** (1982), 71.
5. J.M. Watt and M.G. Breyer-Brandwijk, *The Medicinal and Poisonous Plants of Southern and Eastern Africa*, E&S Livingstone Ltd, London, UK (1962), p.28.
6. H.H. Barakat, M.A.M. Nawwar, J. Buddrus and M. Linscheid, *Phytochemistry*, **26** (1987), 1837.
7. J. C. Da Silveira, O.R. Gottlieb and G. G. De Oliveira, *Phytochemistry*, **14** (1975), 1829.

CHAPTER 12

In vitro screens and functional assays of isolated compounds

12.1 Introduction

In the drug discovery process, compounds that demonstrate therapeutic potential must have limited, or preferably be free, of undesirable side effects. Compounds that interact with more than one target, such as membrane and cytoplasmic proteins and receptors, have the potential to elicit side effects, in comparison to those compounds that are selective for a single target. One predictive measure of whether a compound demonstrates specificity is to profile a compound's activity through a series of receptor binding assays in what is termed a safety screen. For example, activity in an α - or β -adrenergic receptor assay may be indicative of potential cardiovascular side effects. If a compound shows activity in an opiate receptor assay, then further studies to determine analgesic activity or addictive liability need to be considered. This chapter discusses the muscle activity induced by some of the pure compounds isolated from the three plant extracts followed by a further study on receptor pharmacology.

12.2 Receptors and biological response

The interaction of a drug with a receptor is analogous to a lock and a key. Thus, certain compounds would fit into the receptor and activate it, leading to a high degree of specificity. Although such a situation might be considered ideal for drug therapy, in actuality, few drugs interact only with their intended receptors. A receptor site may bind only one of many conformations of a flexible drug molecule (1). This pharmacophoric conformation has the correct spatial arrangement of all the binding groups of the drug molecule for alignment with the corresponding binding sites on the receptor, as shown in Figure 12.1. Molecules that can adopt the conformation required for binding may act as agonists or antagonists to the action of the receptor. An antagonist molecule may be bound to a receptor site and therefore not trigger the pharmacologic response because of

the absence of some key functional groups in the molecule. Alternatively, in the bound state, the molecule may be conformationally constrained in such a way that the functional group that effects the response cannot interact with the receptor to elicit the reaction.

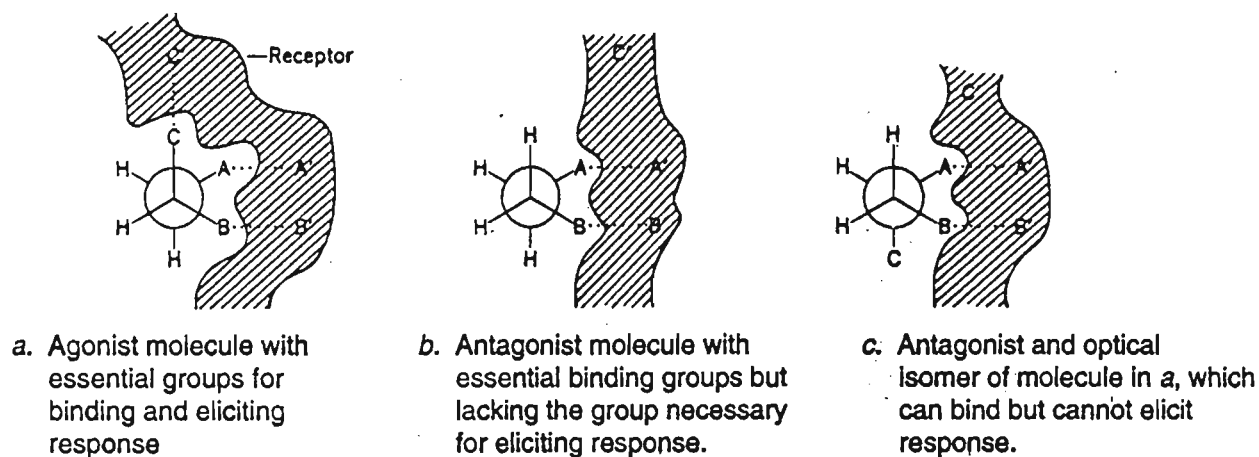


Figure 12.1 Illustration of the different conformations of drug molecules and their ability to bind to the receptor surface (7).

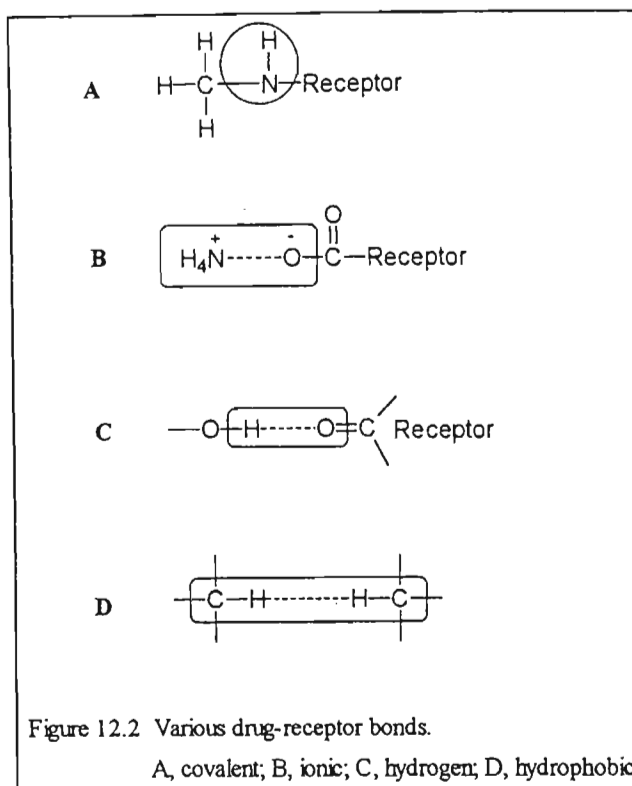
For example, in Figure 12.1a, groups A and B are essential for binding, and group C triggers the response. A molecule possessing groups A and B and not possessing group C (Figure 12.1b) will probably bind to the receptor surface but the receptor will not elicit a response because of the absence of group C's effect on it. In Figure 12.1c, the optical isomer of the original molecule (Figure 12.1a) would possibly be an antagonist, because it can adopt a conformation that permits binding to the receptor but cannot adopt the conformation that permits both binding and correct alignment of group C, which elicits the response.

The activation of receptors by drugs in isolated tissues can be divided into three processes: [1] the delivery of the drug from the organ bath solution to the receptor compartment, [2]

compartment, [2] the interaction of the drug with the receptor, and [3] in the case of agonists, the transduction of receptor stimulus into tissue response (2). These latter two processes are termed the “pharmacodynamic” phase of drug action (3,4). The first step is the delivery of the drug to the drug receptor, a bulk diffusion phenomenon that can be affected by chemical, physical, and biochemical processes.

12.3 The role of chemical bonding

When a drug interacts with a receptor, several chemical attractive forces are responsible for the initial interaction. Assuming a compound has been distributed properly to the general area of the receptor in the body, a function simply of its physical characteristics, the ability of that compound to diffuse in close enough proximity to the receptor to interact with it depends initially on the types of chemical bonds that can be established between the drug and the receptor. The overall strengths of these bonds vary (Figure 12.2) and determine the degree of affinity between the drug and the receptor (5). Most therapeutically useful drugs bind only transiently to their intended receptor. The combination of a variety of bonds including ionic, hydrogen and van der Waal’s attractive forces can contribute to the initial binding of a drug to the receptor. Once the drug has bound, a biological response may result (if an agonist). Following binding of the receptor, a conformational change in the receptor may occur that initiates the activation of the biological response and also changes the attractive environment between the drug and the receptor, thereby allowing for the dissociation of the drug-receptor complex. Specific three-dimensional requirements must be satisfied for a compound to act effectively as an agonist.



In this study, all the compounds isolated from the three plants were subjected to further uterotonic bioassays to identify those responsible for uterine muscle contraction. Compounds 1, 4, 5 and 9 did not induce muscle contractions at the doses administered hence, these compounds were not discussed any further in this chapter. The solubility of the compounds in certain cases posed a problem because of limited solubility in 0.9% saline solution. Tan *et al.* (6) reported on the use of a 1% DMSO solution to overcome the solubility problem. In this study, the muscle did not show any adverse effects to 1% DMSO and was hence used to solubilise the sparingly soluble compounds prior to the bioassay. After having identified the active compounds, these compounds were subjected to further functional assays to assess their receptor pharmacology in order to gain an understanding of their mode of action. The activity induced by the active compounds are discussed.

12.4 Analysis of compounds from *Ekebergia capensis*

12.4.1 Compound 2

Oleanonic acid [2] was dissolved in a 1% DMSO solution at a concentration of 1.83 $\mu\text{g}/\mu\text{l}$. Following an agonistic response to 5 μg ACh, the muscle was observed to develop spontaneous contractions that were monitored over a 15 minute period (Figure 12.3). Oleanonic acid was found to elicit a muscle response after five cumulative additions of 366 μg quantities of this compound to the organ bath. Subsequent addition of ACh produced a larger response than initially observed. This trend with the increase in ACh response has been consistent throughout the screening process of *Ekebergia* extracts. The contractile activity induced by oleanonic acid was of varied amplitude, with each contractile pulse lasting approximately 40 seconds.

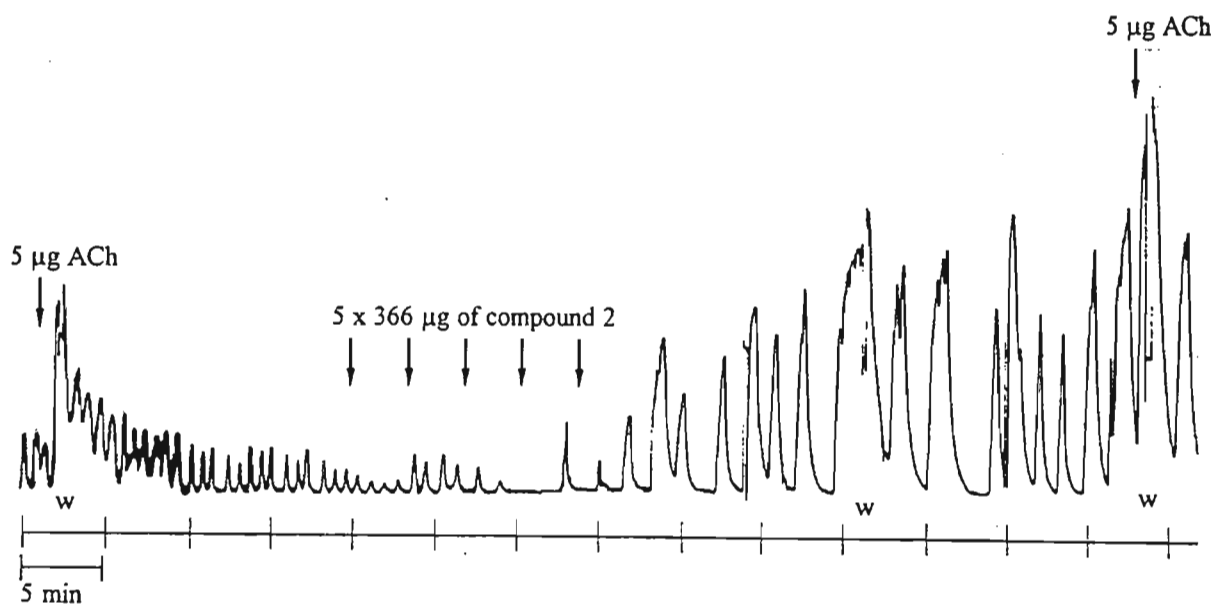


Figure 12.3 Electrical recording of contractions induced by compound 2 of *Ekebergia capensis* on a non-pregnant uterus. w = muscle wash

12.4.2 Compound 3

3-*epioleanolic acid* [3] was dissolved in a 1% DMSO solution at a concentration of 1.77 $\mu\text{g}/\mu\text{l}$. 10 μg ACh was administered to produce a muscle response followed by the addition of 354 μg quantities of 3-*epioleanolic acid* to the organ bath (Figure 12.4). Apart from the spontaneous contractions of the muscle, a cumulative dose of 708 μg was observed to increase the amplitude of the contractions in the spontaneously contracting uterus. Further additions of 354 μg quantities of this compound was found to further increase the amplitude of the contractions in a concentration-dependent manner. The muscle was thereafter washed and a subsequent addition of 10 μg ACh showed an increased ACh response once again.

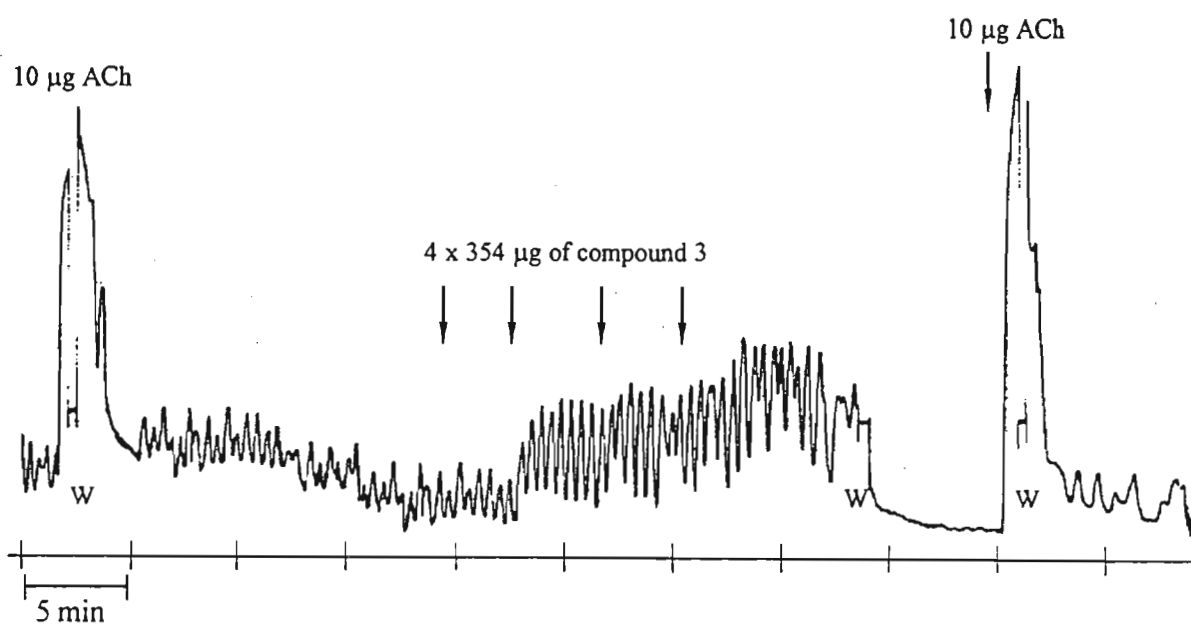


Figure 12.4 Electrical recording of contractions induced by compound 3 of *Ekebergia capensis* on a non-pregnant uterus. w = muscle wash

Unlike oleanonic acid, this compound displayed efficacy at much lower doses. An increase in both the tonicity and frequency of contractions was also observed. The only difference between these two compounds was the presence of a keto group at carbon 3 for oleanonic acid and the α -hydroxy group for 3-*epioleanolic* acid. These minor changes in the molecule can affect its intrinsic activity on the muscle (7). 3-*epioleanolic* acid was found to induce muscle contraction at much lower doses and within a shorter time period than oleanonic acid. This may have resulted from the ability of the 3-*epi* compound to reach the active site of the receptor or to be metabolised more readily than oleanonic acid. The longer time period necessary for oleanonic acid to induce activity may have resulted due to a longer diffusion period required for the compound to enter the receptor compartment.

The dissolution of a drug from the point of injection into a well mixed organ bath occurs relatively rapidly, however the diffusion coefficient of drugs in tissues is slower than in free solution (8). This is due to the longer path that a drug must take through a tissue to accommodate the numerous obstructions in the morphological organization of the muscle. One factor thought to be responsible for the difference in diffusion rates is tissue thickness. The diffusion time is related to tissue thickness (L) by the following equation (9):

$$t = \frac{L^2}{2D} \quad (12.1)$$

Considering the morphological architecture of the tissues to be reflected by the tortuosity factor (λ), this equation can be modified to:

$$t = \frac{L^2 \lambda^2}{2D} \quad (12.2)$$

where D is the diffusion coefficient of the drug in free solution. Factors which affect L will correspondingly alter the diffusion time.

Physicochemical properties, such as electronegativity, polarizability, bond angles, van der Waal's radii, number of substituents and charge of the atom can greatly influence the physicochemical characteristics of the molecule. Drug molecules in turn exert their effect by influencing receptor sites through their physicochemical properties. It follows therefore, that alteration of a group in a molecule will change the physicochemical properties of the molecule and thereby the biological response to it. The other compounds that were isolated from this plant were also subjected to bioassays however these were found to be inactive as there was no indication of uterine muscle stimulation.

12.5 Analysis of compounds from *Clivia miniata*

12.5.1 Compound 6

Compound 6 was identified as linoleic acid [6] and has a limited solubility in aqueous media and even a 1% DMSO solution failed to adequately dissolve this compound. 3 ml of 1% DMSO solution was added to 37.8 mg of this compound and the vial shaken to adequately disperse the compound in solution. Thereafter a cumulative volume of 150 μ l ($3 \times 50 \mu$ l) was added before a maximum contractile response was observed (Figure 12.5). The dose was repeated however this time the muscle was set into a series of irreversible, irregular contractions. Further washing failed to stop the contractile process. Linoleic acid is able to penetrate cellular membranes rapidly to exert its effect, as it is extremely fat soluble. Washing with tyrodes solution failed to wash away the compound due to its hydrophobic nature. The significance of linoleic acid is important as it serves as a precursor to arachidonic acid which, in turn, leads to the production of the eicosinoids, two of which are the prostaglandins E_2 and $F_{2\alpha}$. During pregnancy, the uterus produces large quantities of these prostaglandins which increase myometrial tone hence it is not surprising that this compound induced uterine muscle contractions.

One must always be aware that when performing *in vitro* assays, disparity between the concentration of the drug in the organ bath and the active drug at the receptor site can arise if the drug promotes release of an endogenous substance in the tissue. It would be

expected that the magnitude of the response would be increased if the endogenous substance produced the same qualitative response.

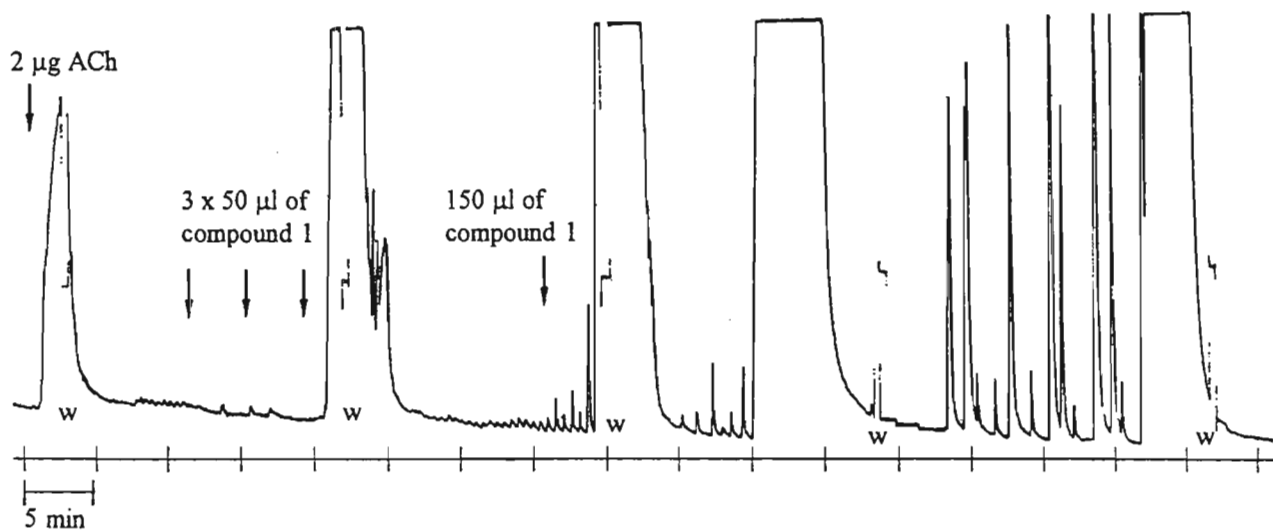


Figure 12.5 Electrical recording of pregnant guinea pig uterine smooth muscle contraction induced by compound 6 of *Clivia miniata* (Lindl.) Regel. w = muscle wash

12.5.2 Compound 7

Compound 7 was identified as 5-hydroxymethyl-2-furancarboxaldehyde [7] and was dissolved in 0.9 % saline at a concentration 1.27 $\mu\text{g}/\mu\text{l}$. This compound (190 μg) was dispensed into the muscle bath and a contractile response was observed (Figure 12.6). Subsequent washing of the muscle decreased the muscle tension that initially developed however the contractions failed to stop. The compound set the muscle into a series of contraction-relaxation cycles with the contractile responses being of an irregular nature. The contractions were observed over a 35 minute period before removal of the muscle from the bath. Although previous investigations have shown this plant to contain alkaloids, alkaloids were not detected, however, in the SFE extracts.

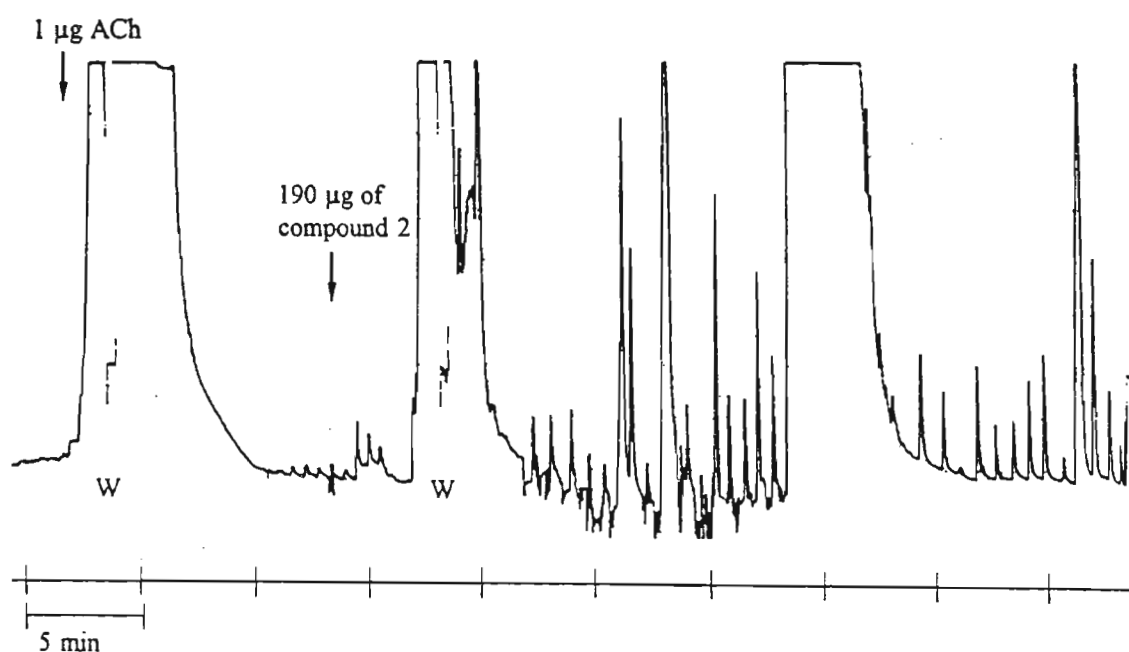


Figure 12.6 Electrical recording of pregnant guinea pig uterine smooth muscle contraction induced by compound 7 of *Clivia miniata* (Lindl.) Regel.
w = muscle wash

12.6 Analysis of compounds from *Grewia occidentalis*

12.6.1 Compound 8

Compound 8 was identified as coniferaldehyde [8] and was dissolved in 0.9% saline at a concentration of $1.67 \mu\text{g}/\mu\text{l}$. The muscle was found to respond adequately to $1 \mu\text{g}$ ACh after which the addition of this compound in known doses were carried out. A cumulative dose of $250 \mu\text{g}$ was observed to bring about a maximum contractile response (Figure 12.7a). This was followed by a muscle wash and a subsequent addition of $175 \mu\text{g}$ of the compound elicited a contraction in a dose-response manner. The addition of a cumulative dose of $500 \mu\text{g}$ ($2 \times 250 \mu\text{g}$ quantities) produced muscle contractions of irregular amplitude but of almost equal time intervals (Figure 12.7b).

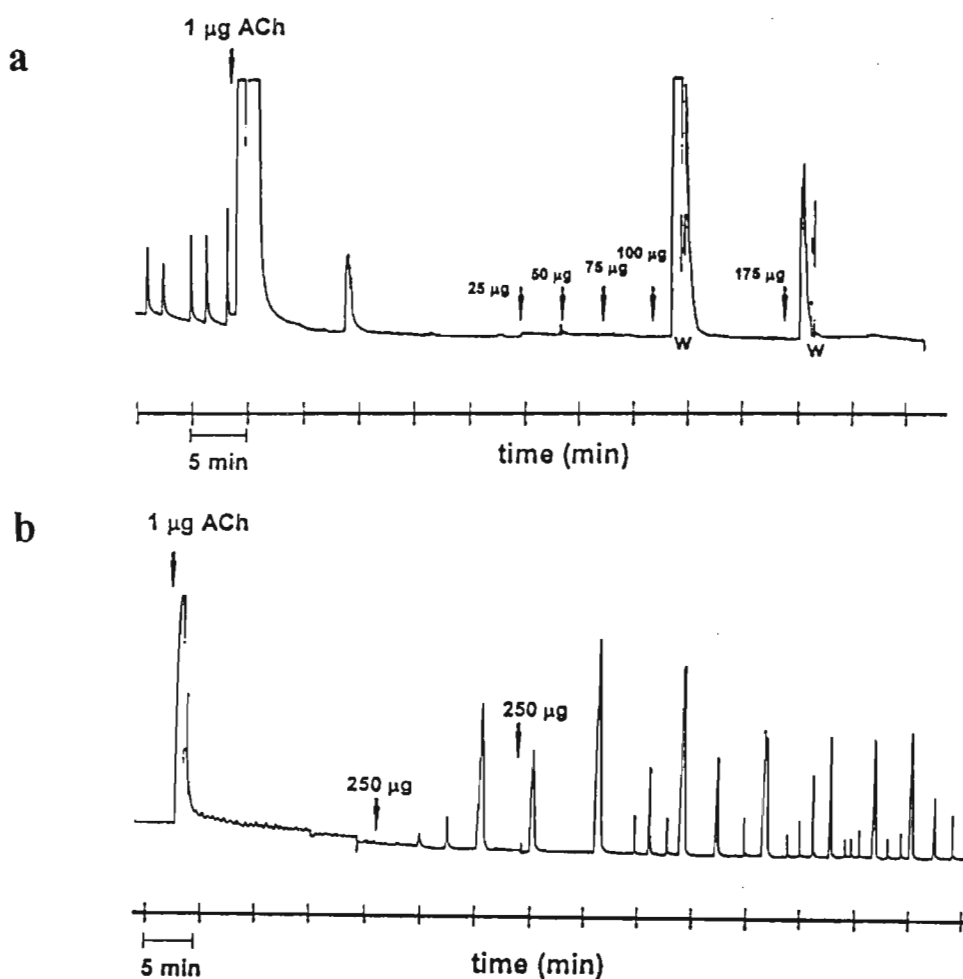


Figure 12.7 Electrical recording of pregnant guinea pig uterine smooth muscle contraction induced by compound 8 of *Grewia occidentalis* L. after a cumulative dose of (a) $250 \mu\text{g}$ and (b) $500 \mu\text{g}$. w = muscle wash

12.7. Assessment of mode of action through receptor binding assays

In order to determine the receptor/s through which these compounds mediated their effects, use was made of two receptor agonists and antagonists. Two receptors that can be involved in smooth muscle contraction are the bradykinin B₂ receptor and the muscarinic cholinergic receptor. Bradykinin was used as the standard B₂ receptor agonist while acetylcholine was used as the cholinergic receptor agonist. It is well accepted that bradykinin can contract or dilate vascular smooth muscle (10) depending on (a) the type of kinin receptor, (b) the type and potency of kininases present on endothelial cells and (c) the ability to generate nitric oxide (NO) also known as endothelium derived relaxing factor (EDRF) (11). The cholinergic receptors are also responsible for stimulating contractions of smooth muscles. The biological activity of the compounds were assessed both before and after addition of the receptor blockers. HOE 140 (a peptide antagonist) (Sigma Chemicals, St. Louis, MO, USA) was used as the B₂ receptor blocker while atropine (Sigma Chemicals, St. Louis, MO, USA) was used as the cholinergic blocking agent as it blocks postganglionic receptors by binding to them and preventing access of acetylcholine.

12.7.1 Compound 3 from *Ekebergia capensis*

Bradykinin (15 ng) was administered to the uterine muscle to elicit a maximum response (Figure 12.8). Thereafter 500 µg of HOE 140 was added to the muscle bath to block the B₂ receptors. Bradykinin was added once again to establish whether the B₂ receptors were blocked. Failure of a muscle contraction indicated that B₂ receptors were blocked as bradykinin did not produce a muscle response. Compound 3 was thereafter added to the muscle bath. A dose of 354 µg induced a maximum response indicating that this compound did not mediate its response through the B₂ receptors as the muscle still contracted even after blocking off the bradykinin receptors.

A subsequent addition of 1 µg ACh elicited a response and this showed the specificity of the B₂ receptor blocker in that, although it blocked the B₂ receptor, it did not block the cholinergic receptor since acetylcholine acts via the cholinergic receptors. 30 µg atropine was thereafter dispensed into the organ bath to block off the cholinergic receptors. To

confirm this, a ten fold increase of ACh was added to the bath and this failed to produce an agonistic response. Subsequent addition of two 354 μg doses of compound 3 did not initiate a muscle response indicating that the compound mediated its effect through the cholinergic receptor since blocking the receptor failed to produce a muscle response.

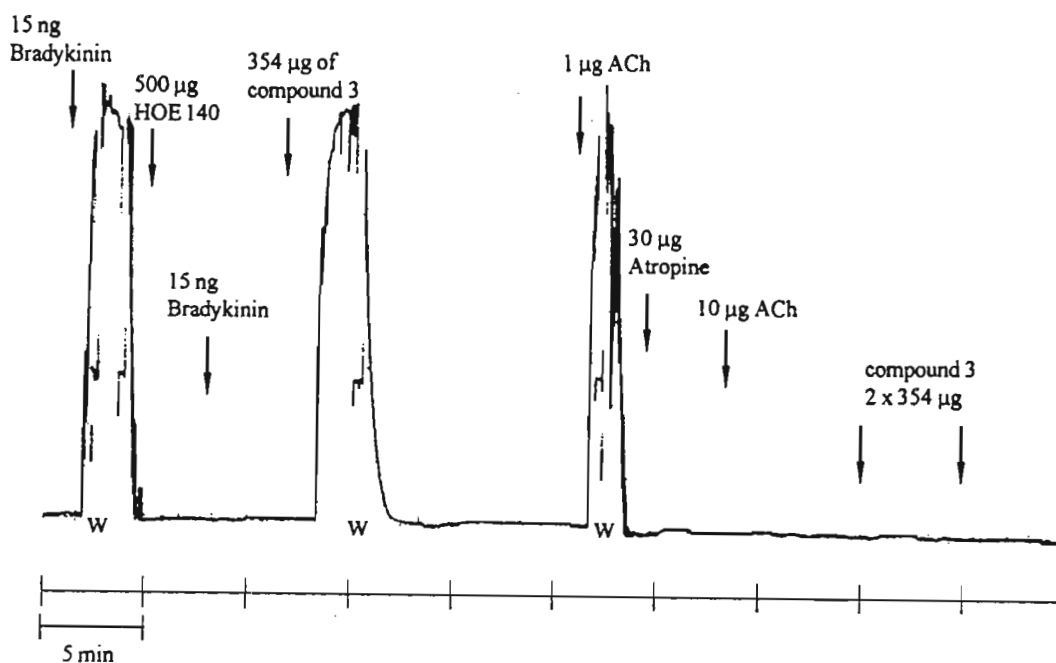


Figure 12.8 Receptor binding assays of compound 3 from *E. capensis*.
w = muscle wash

12.7.2 Compound 7 from *Clivia miniata*

Compound 7 also produced a muscle response at a dose of 190 μg even after blocking off the B_2 receptors with HOE 140 (Figure 12.9). The cholinergic receptors were blocked with 30 μg atropine and the addition of 190 μg of the compound failed to elicit a response. A further dose of 190 μg however produced an increase in tone followed by a spasmodic type of activity. This could be explained by the fact that at high concentrations the compound has the ability to competitively displace the cholinergic receptor blocker and bind to the receptor thereby bringing about a biological response. These results indicate that this compound is a competitive or surmountable agonist hence bringing about responses at high concentrations in the presence of the receptor blocker.

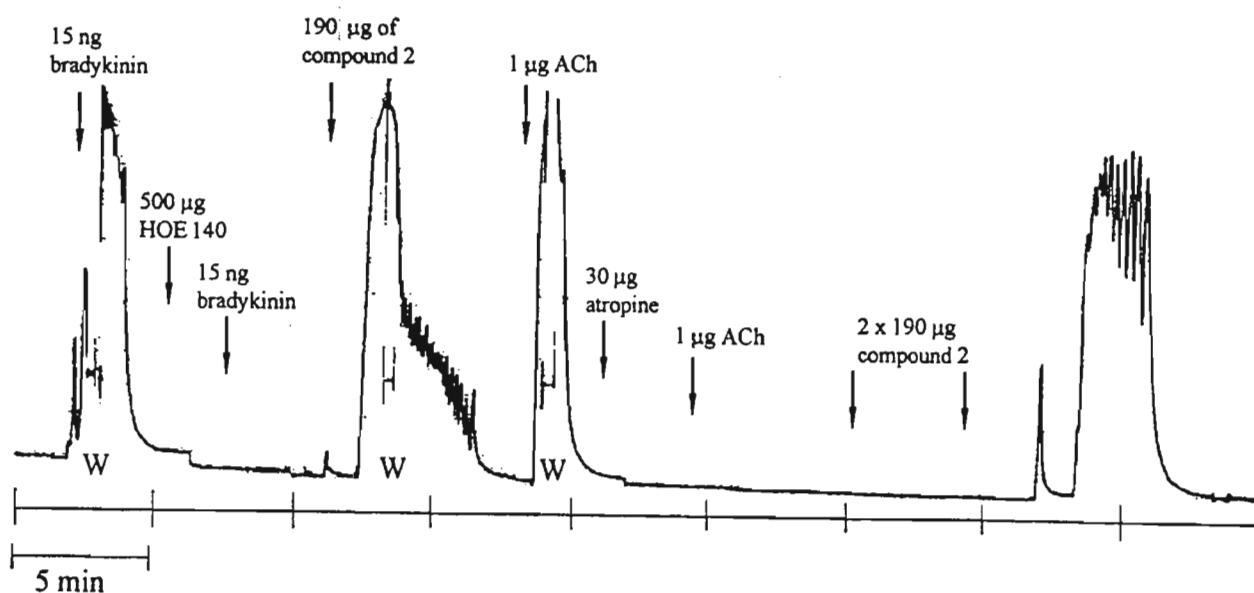


Figure 12.9 Receptor binding assays of compound 7 from *C. miniata*.
w = muscle wash

12.8 Conclusion

These studies have indicated that the compounds analysed mediated their effects through the cholinergic receptors. This indicates that apart from uterine muscle contractions, such compounds may also have the potential to cause vasodilation or decrease the cardiac rate. The compounds may have also brought about muscle contraction by increasing the permeability of the cell membranes to calcium ions, however, there were no studies performed using ionic channel blockers to confirm such a mechanism. Receptor pharmacology can play an important role in the area of general pharmacology, including the identification of new lead compounds and the evaluation of these compounds for potential side effects in a safety screen.

References

1. B. Belleau, *J. Med. Chem.*, **7** (1964), 776.
2. E.J. Ariëns, J.M. van Rossum and P.C. Koopman, *Arch. Int. Pharmacodyn. Ther.*, **127** (1960), 459.
3. E.J. Ariëns, *Clin. Pharmacol. Ther.*, **16** (1974), 155.
4. E.J. Ariëns and A.M. Simonis, In: *Beta-Adrenoceptor Blocking Agents*, P.R. Saxena and R.P. Forsyth (Eds.), North-Holland Publishing Company, Amsterdam (1976), p.3.
5. T.J. Maher, *Receptor and Drug Action*, In: *Principles of Medicinal Chemistry*, W.O. Foye, T.L. Lemke and D.A. Williams (Eds.), Williams and Wilkins, Baltimore, USA (1995), p.75.
6. G.T. Tan, J.M. Pezzuto, A.D. Kinghorn and S.H. Hughes, *J. Nat. Prod.*, **54** (1991), 143.
7. I. W. Mathison, W.E. Solomons and R.R. Tidwell, *Structural Features and Pharmacologic Activity*, In: *Principles of Medicinal Chemistry*, W.O. Foye, T.L. Lemke and D.A. Williams (Eds.), Williams and Wilkins, Baltimore, USA (1995), p.25.
8. N. Brookes and D. Mackay, *Br. J. Pharmacol.*, **41** (1971), 367.

9. R.B. Setlow and E.C. Pollard, *Molecular Biophysics*, Addison-Wesley Inc., MA, London (1962), p.42.
10. D.M. Raidoo, K.D. Bhoola, *Immunopharmacology*, **36** (1997), 153.
11. D. Regoli, J. Barabé, *Pharmacol. Rev.*, **32** (1980), 1.

CHAPTER 13

Chromatographic and electrophoretic analysis of the plant extracts

13.1 Introduction

The quality control of plant products is a general requirement and is necessary if plant products are to fill the need for cheap and reliable medicines, or if natural products are to be used as templates for new drug molecules. Plants biosynthesize a large variety of compounds and the variation of the active principles from batch to batch needs to be monitored so that dosage forms can be altered to maintain consistency in pharmacological activity. In the previous chapter, the active principles were identified, hence it is the aims of this chapter to characterise the plant extracts and identify the active components within the plant matrix using different chromatographic techniques.

13.2 Reverse-phase HPLC

Reverse-phase HPLC is a widely accepted, well established and reliable analytical method, and numerous applications in the field of natural products have been developed (1-4)

13.2.1 Analysis of extracts from *Ekebergia capensis*

The total extract of the wood of *E. capensis* obtained at 400 atm was dissolved in 2 ml methanol and 25 μ l aliquots injected onto the column. Figure 13.1 shows the HPLC separation of the *Ekebergia* components by gradient elution using the conditions described in section 5. The components were eluted within 30 minutes and the identity of the peaks were confirmed by injecting the pure compounds that were isolated and further confirmation was obtained by comparison of the UV spectrum on the photodiode array detector. Scopoletin, being more polar eluted first from the column while oleanonic acid and 3-epioleanolic acid eluted at higher methanol concentrations.

Figure 13.2 shows the chromatograms of the sequentially extracted fractions. It is quite evident that the extraction yield of the isolated compounds increased at higher extraction pressures. Other subtle differences in chemical composition was also observed. The column efficiency (N) was calculated for each of the isolated compounds using equation 4.6 and was found to be 7862, 9409, and 18010 for scopoletin, oleanonic acid and 3-*epioleanolic acid* respectively. The mild uterotonic effects of the 200 atm extract can be explained due to the lower concentration of the active components than at 400 atm. Although SFF was initially performed to fractionate the extracts and differentiate active from inactive fractions, one must realise that in complex matrices, fractionation by SFE is frequently difficult unless appreciable differences exist in molecular sizes, polarities or volatilities of the mixture components. However it was observed that by increasing the pressure of the extraction fluid, enrichment of the solute fractions occurred, however this result is countered by a time-based fractionation effect.

Upon comparison of Figure 13.3 with Figure 13.1, one can see appreciable differences in the two batches of *Ekebergia capensis*. It is quite evident that the first batch, obtained in autumn, possesses a much lower concentration of the active components than the second batch, obtained in spring. Seasonal changes are known to affect the chemical composition of plants (5) and the magnitude of this effect has been observed in this study. In the first batch, the 300 atm sequentially fractionated extract was observed to be toxic to uterine muscle while the 300 atm sequentially fractionated extract of the second batch indicated uterotonic activity with an increased agonistic response to ACh.

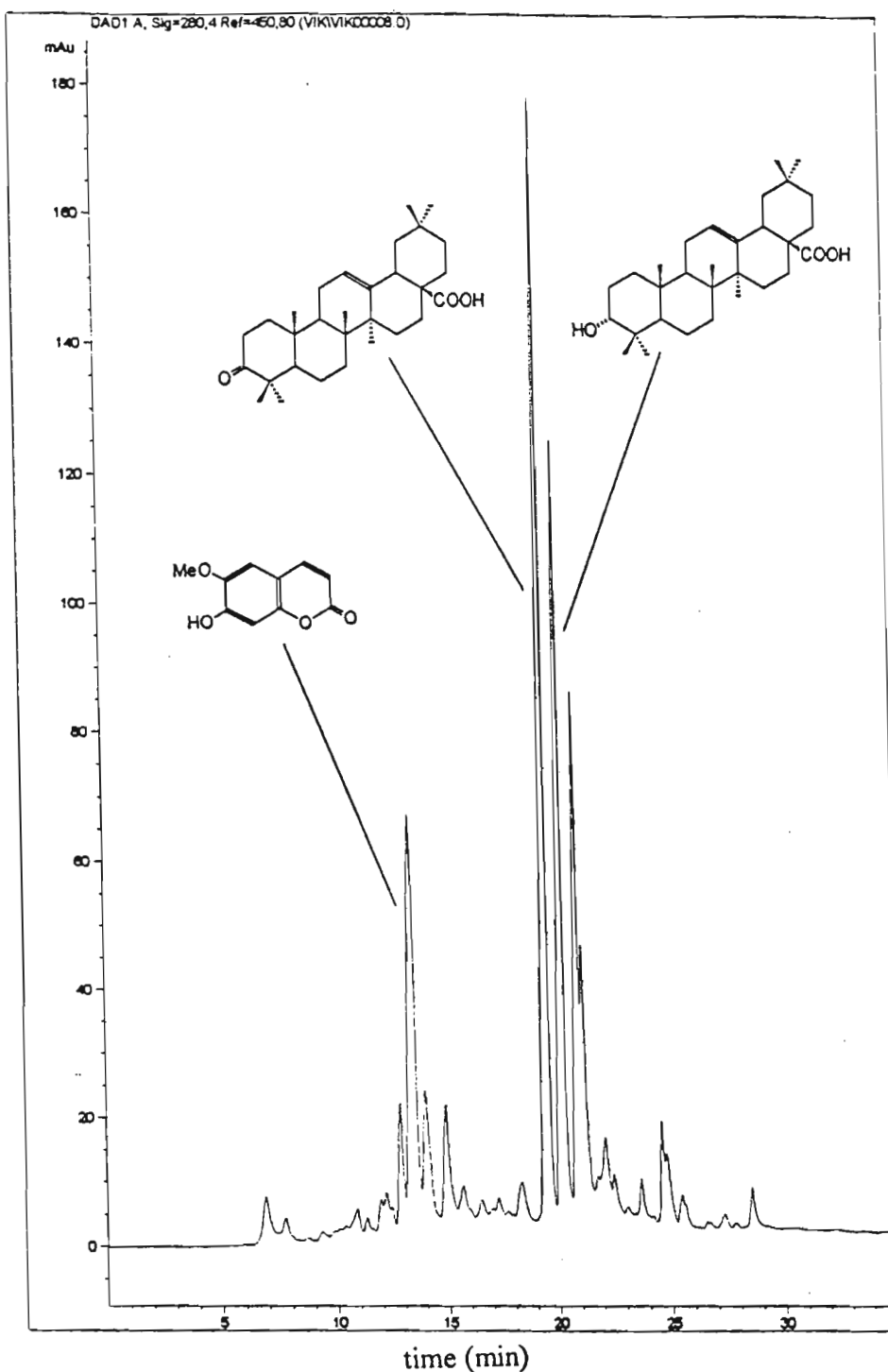


Figure 13.1 Reverse-phase HPLC chromatogram of total SFE extract of *E. capensis* wood obtained at 400 atm and 80 °C. Conditions: Bondclone-10 C18 reverse phase column; gradient elution (methanol/water); column temperature 40 °C; UV detection at 280 nm.

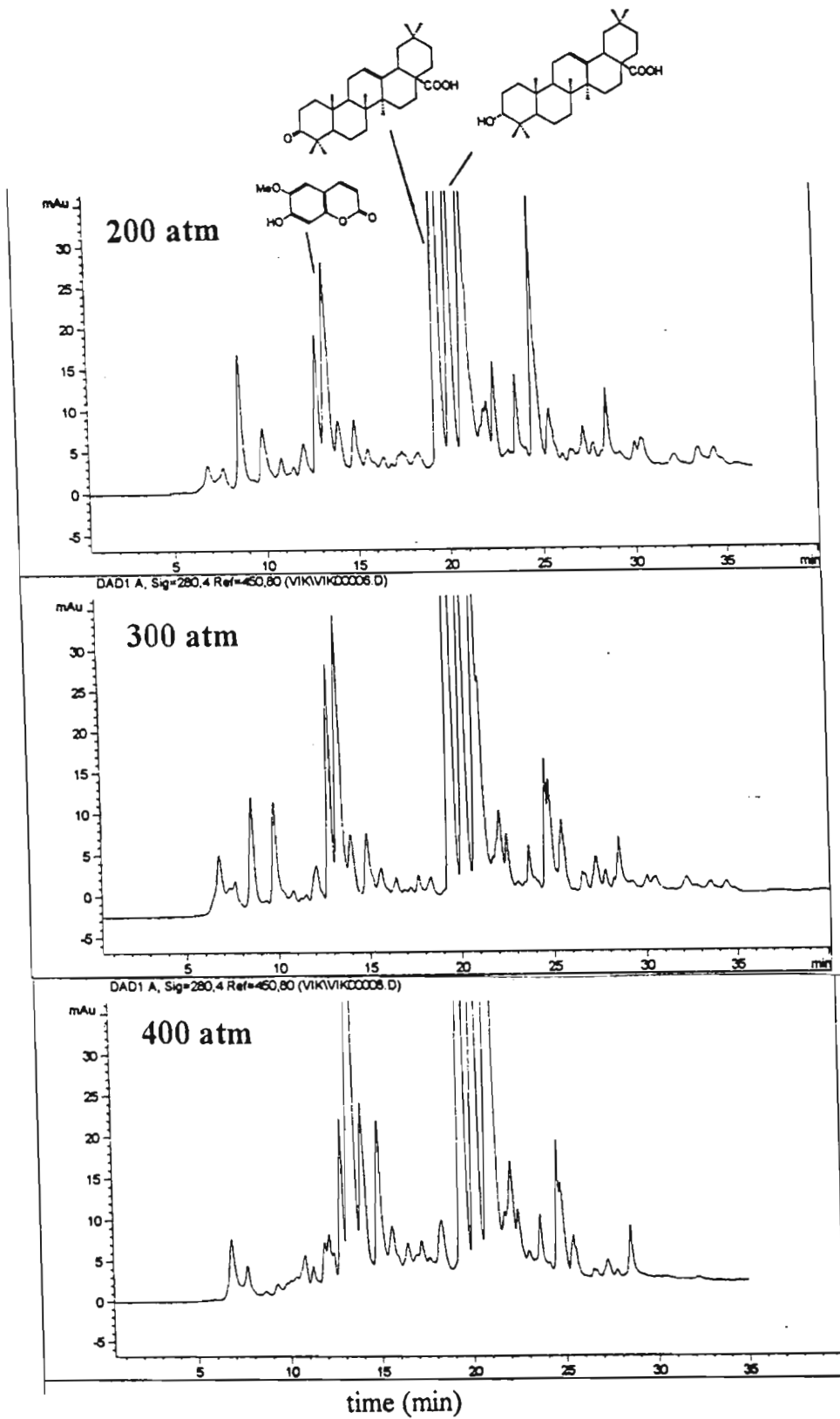


Figure 13.2 Reverse-phase HPLC chromatogram of sequentially extracted SFE fractions of *E. capensis* wood. Conditions: Bondclone-10 C18 reverse phase column; gradient elution (methanol/water); column temperature 40 °C; UV detection at 280 nm.

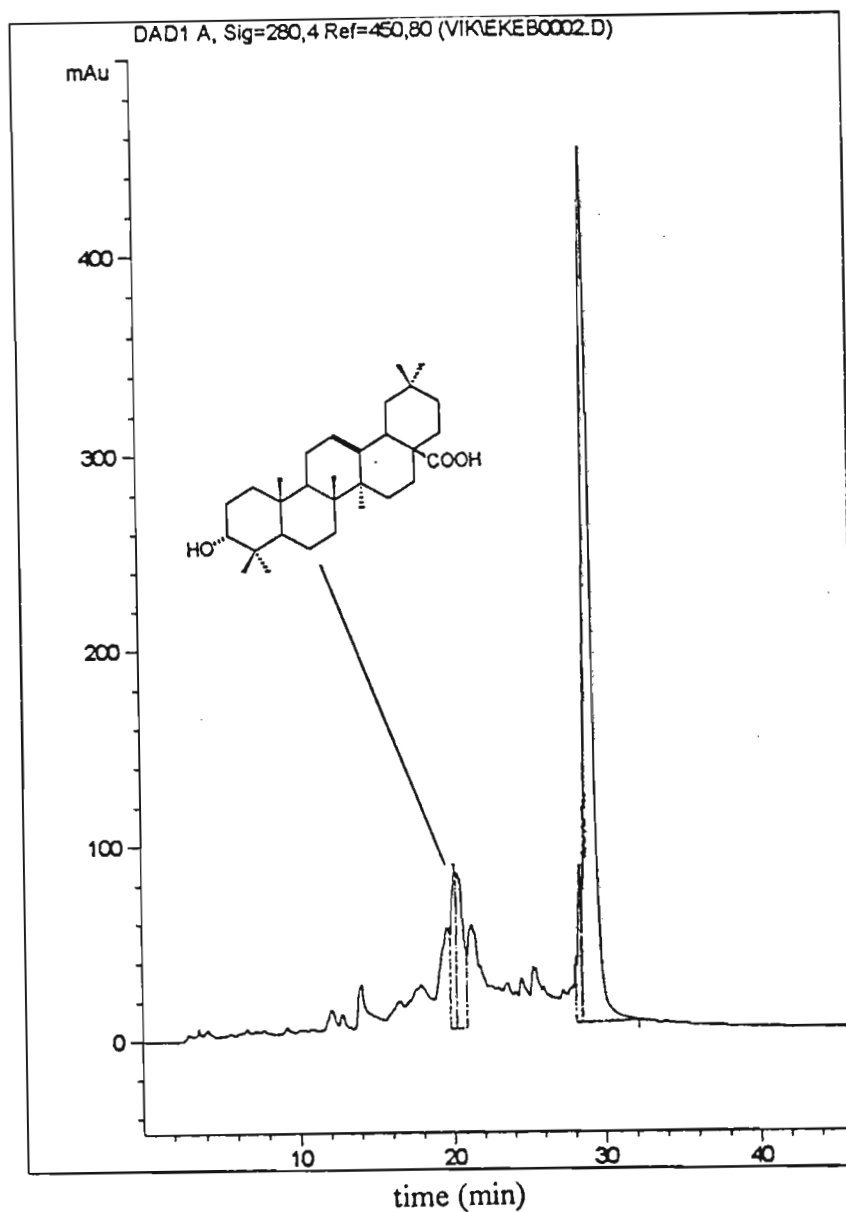


Figure 13.3 Reverse-phase HPLC chromatogram of first batch of SFE extract of *E. capensis* wood showing the variation of chemical composition with seasonal changes.

Conditions: Bondclone-10 C18 reverse phase column; gradient elution (methanol/water); column temperature 40 °C; UV detection at 280 nm.

13.2.2 Analysis of extracts from *Clivia miniata*

The total 400 atm extract was chromatographed under similar conditions as for *Ekebergia capensis*. Two major peaks were observed at 7.71 and 23.09 min (Figure 13.4). This extract showed a positive response when tested for uterotonic activity. Bioassay-guided fractionation indicated that the sequential extract at 400 atm was most potent. Further chromatography on the sequentially extracted fractions showed the influence of extraction pressure on selectivity of the components. Upon increasing the extraction pressure, the extraction yield of peak 1, identified as 5-hydroxymethyl-2-furancarboxaldehyde, was found to increase (Figure 13.5). Peak 2 however decreased suggesting that this was unlikely to be the active component. Peak 1 was subsequently identified as the active component. Attempts to isolate peak 2 and identify the compound failed as this compound decomposed. Figure 13.6 shows the effect of seasonal changes on the chemical constituents of this plant. In spring, the concentration of the active principle was observed to be high as judged from the peak intensities of this compound in both the batches.

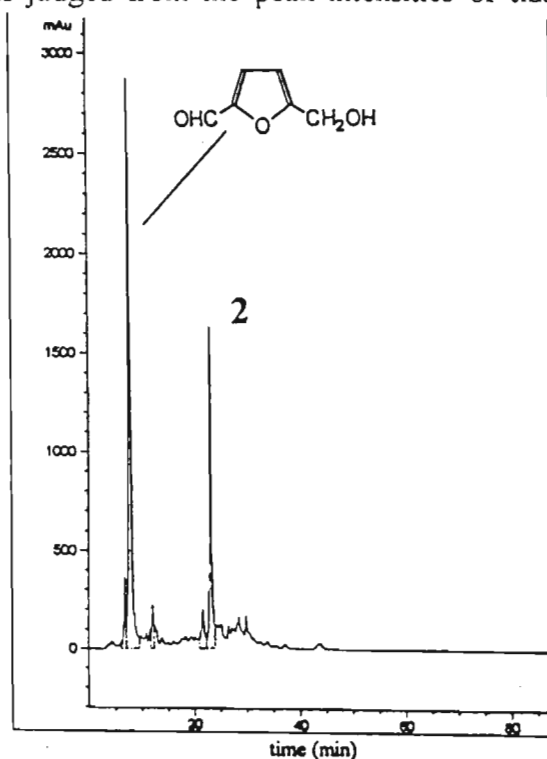


Figure 13.4 Reverse-phase HPLC chromatogram of total SFE extract of *C. miniata* root obtained at 400 atm and 80 °C. Conditions: Bondclone-10 C18 reverse phase column; gradient elution (methanol/water); column temperature 40 °C; UV detection at 280 nm.

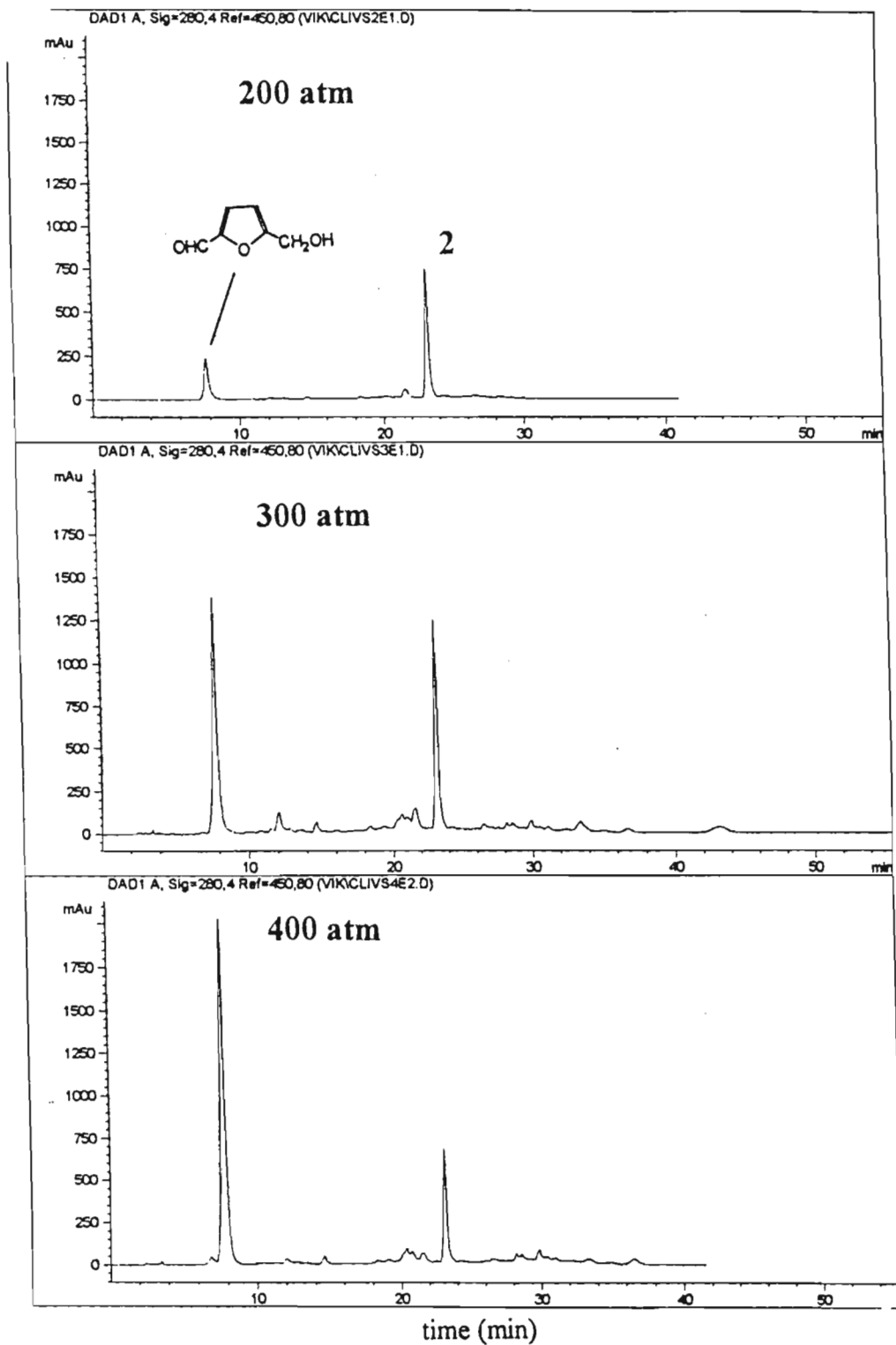


Figure 13.5 Reverse-phase HPLC chromatogram of sequentially extracted SFE fractions of *C. miniata* root. Conditions: Bondclone-10 C18 reverse phase column; gradient elution (methanol/water); column temperature 40 °C; UV detection at 280 nm.

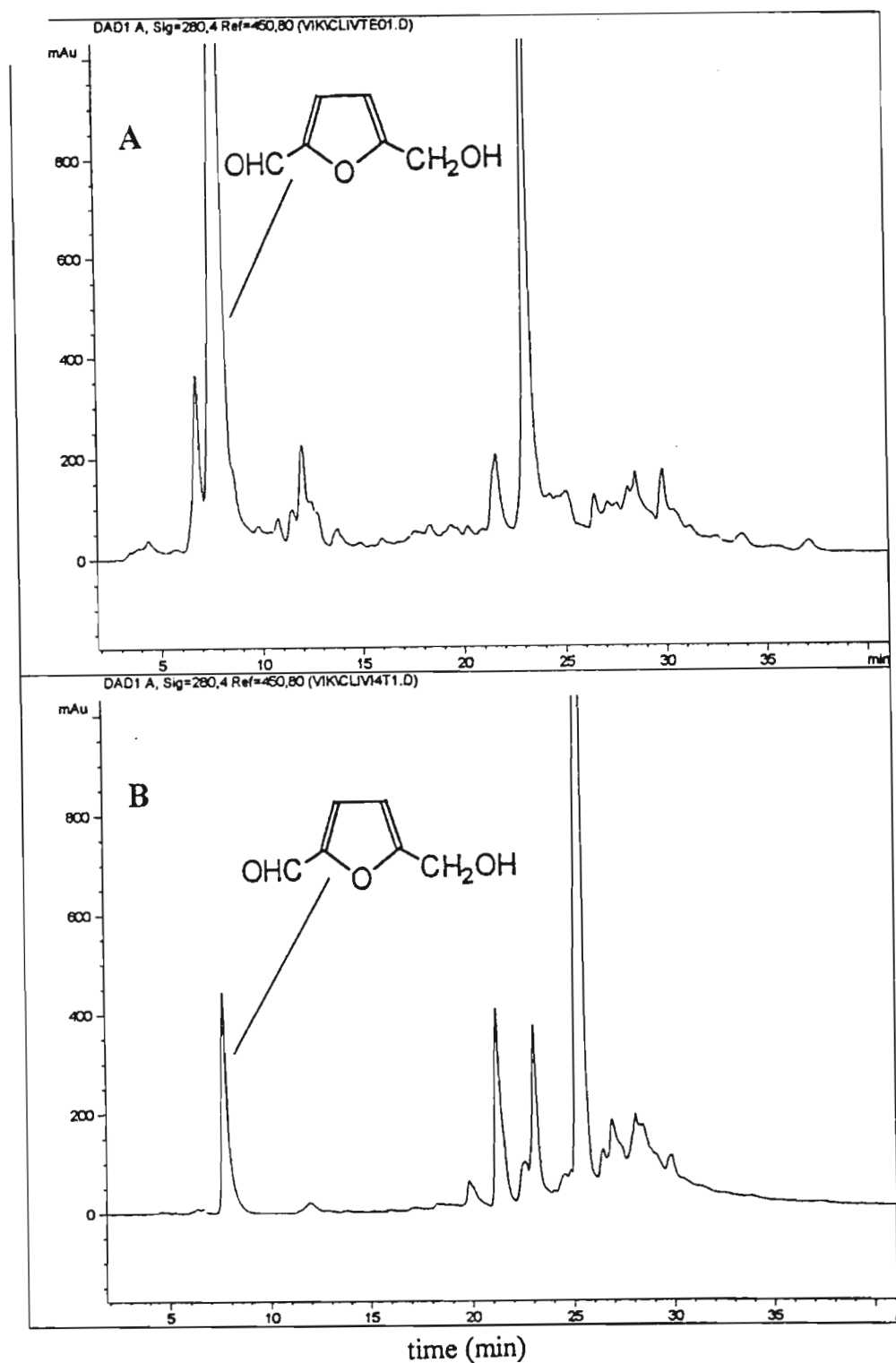


Figure 13.6 Reverse-phase HPLC chromatogram of total 400 atm SFE extracts of *C. minata* root showing the variation of chemical composition with seasonal changes. (A) second batch of plant material obtained during Spring
 (B) first batch of plant material obtained during Autumn
 Conditions: Bondclone-10 C18 reverse phase column; gradient elution (methanol/water); column temperature 40 °C; UV detection at 280 nm.

13.2.3 Analysis of extracts from *Grewia occidentalis*

The total 400 atm extract showed the presence of two major components although other minor chemical constituents were observed to co-elute (Figure 13.7). The results obtained following bioassay-guided fractionation indicated that the sequentially fractionated extract at 300 atm was most potent. Hence the sequential extracts were chromatographed in order to observe the differences in the complexity of the matrix as a result of pressure changes (Figure 13.8). The 200 atm extract showed three minor peaks however the 300 atm extract displayed two major peaks at 12.78 and 14.83 min respectively, as observed for the total 400 atm extract. The extract at 400 atm displayed an increase in the second peak height indicating an increase in the concentration of this compound (Figure 13.8, $n = 4089$). Peak 1 was found to be the active component and the difference in uterotonic activity between the 300 atm and 400 atm extracts can be attributed to the possible antagonistic effects of peak 2 hence limiting the agonistic ability of peak 1 to induce uterine muscle contractions.

Upon comparison of this batch of extract with the first batch, it is quite apparent from the chromatographic results that seasonal changes influence the complexity of the extracts (Figure 13.9). The extract obtained from the first batch showed positive uterotonic effects although trace levels of the active component was present. There were also trace levels of interfering compounds, unlike in the second batch, where both high levels of the active and interfering compounds were present. In such cases, SFF does prove to be a valuable method for fractionating extracts as observed in Figure 8.5.

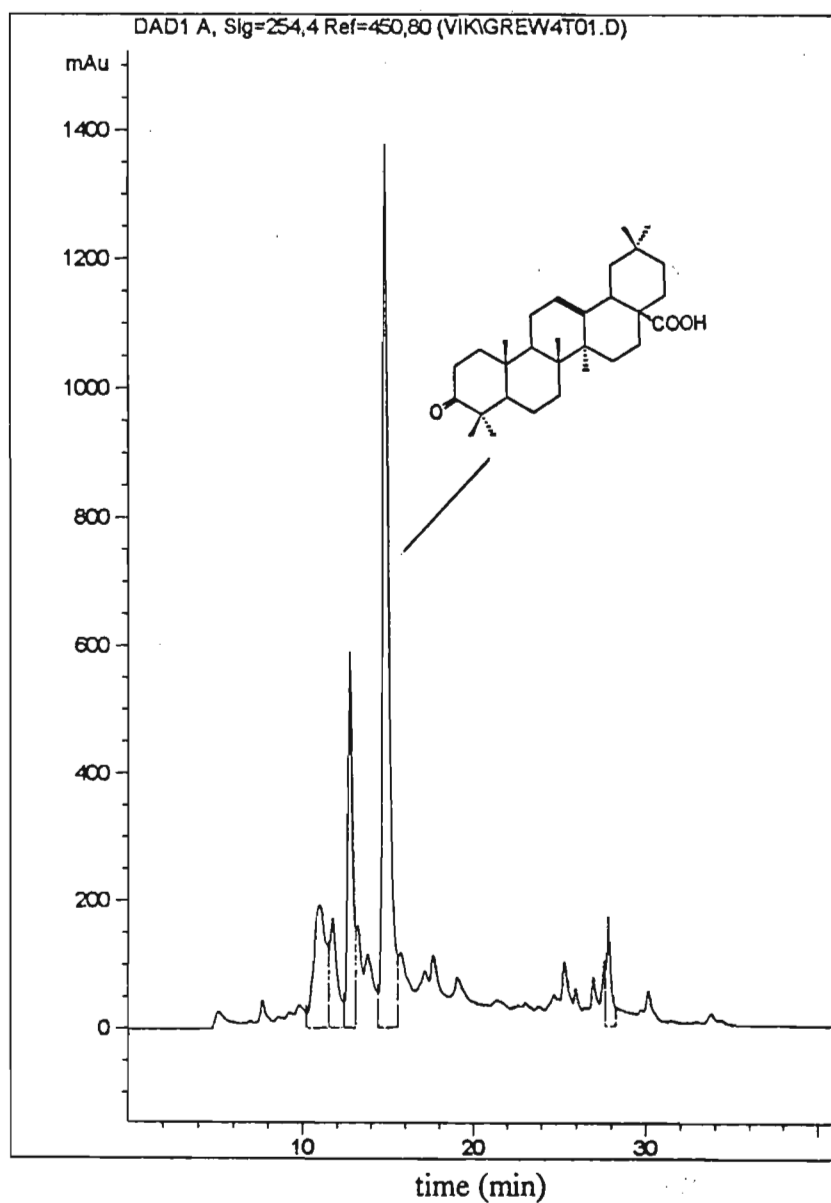


Figure 13.7 Reverse-phase HPLC chromatogram of total SFE extract of *G. occidentalis* wood obtained at 400 atm and 80 °C. Conditions: Bondclone-10 C18 reverse phase column; gradient elution (methanol/water); column temperature 40 °C; UV detection at 254 nm.

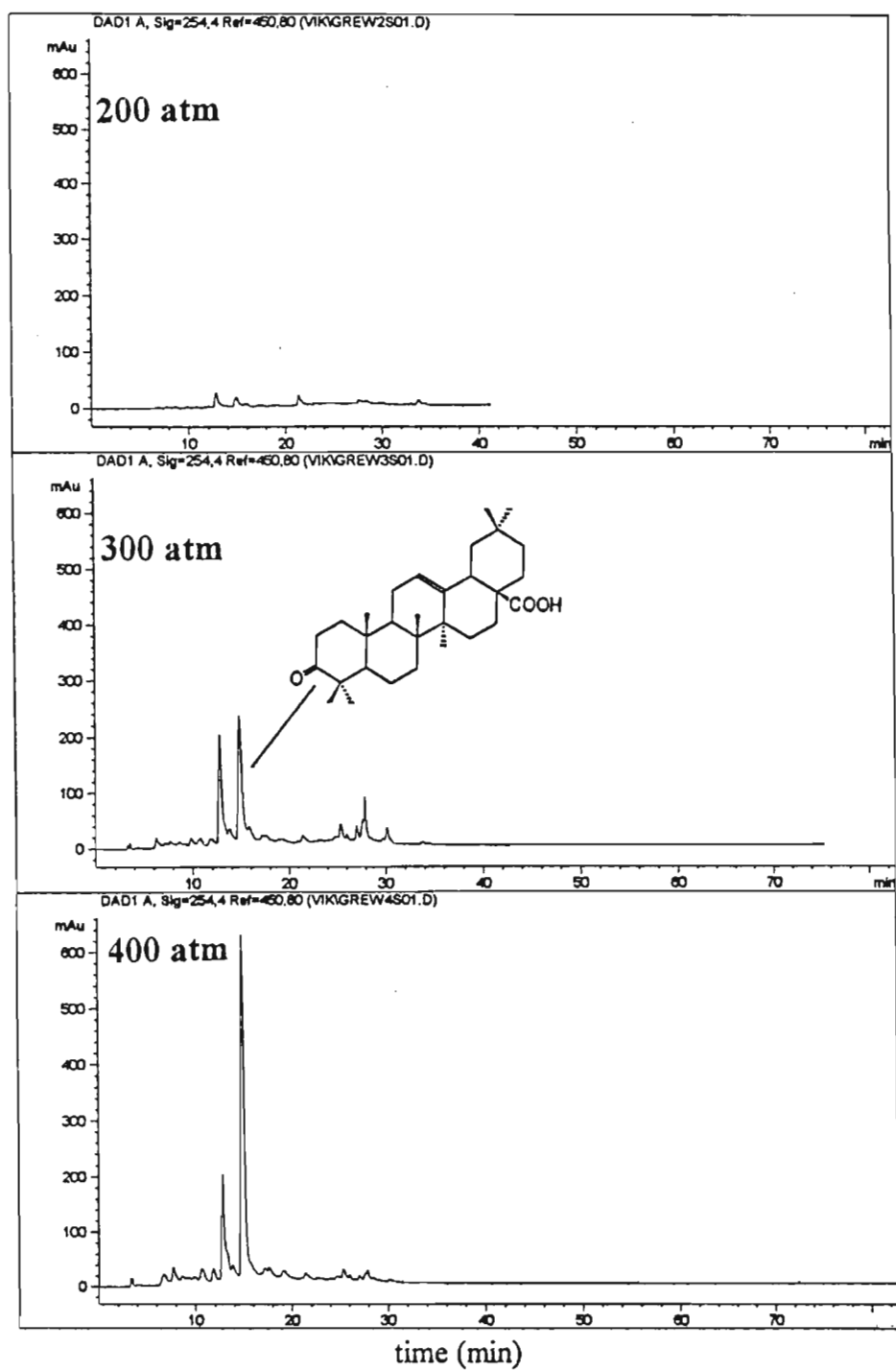


Figure 13.8 Reverse-phase HPLC chromatogram of sequentially extracted SFE fractions of *G. occidentalis* root. Conditions: Bondclone-10 C18 reverse phase column; gradient elution (methanol/water); column temperature 40 °C; UV detection at 254 nm.

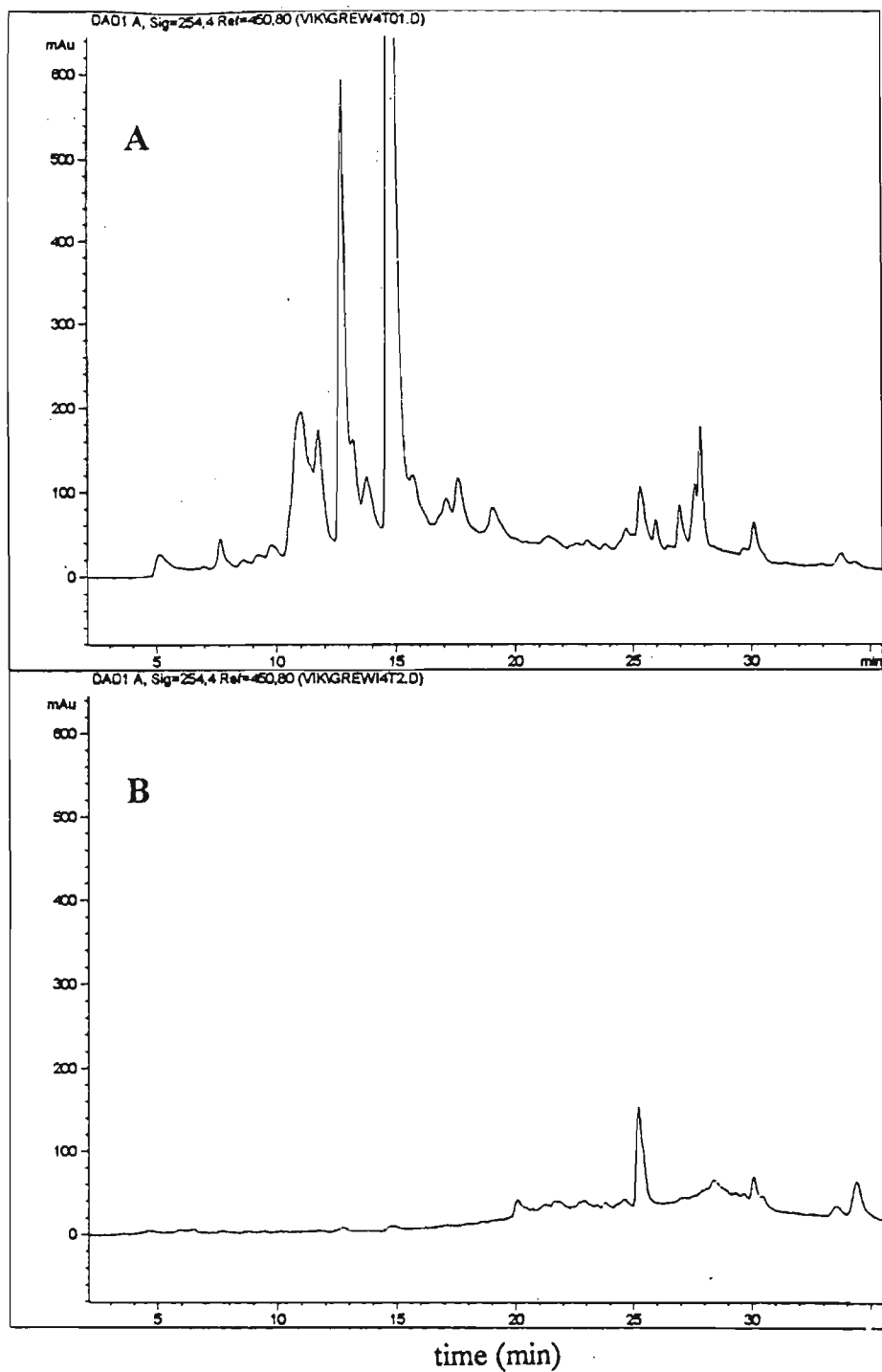


Figure 13.9 Reverse-phase HPLC chromatogram of total 400 atm SFE extracts of *G. occidentalis* wood showing the variation of chemical composition with seasonal changes.

(A) second batch of plant material obtained during Spring

(B) first batch of plant material obtained during Autumn

Conditions: Bondclone-10 C18 reverse phase column; gradient elution (methanol/water); column temperature 40 °C; UV detection at 254 nm.

13.3 Capillary electrophoresis

CE has attracted considerable attention and the main reason for this is the possibility of generating very high efficiencies due to its characteristic flat flow profile as discussed in section 4.3.5. The fundamental difference in flow profile is the main reason for the extremely high efficiencies achievable in CE, where narrower peaks and potentially better resolution can be readily obtained. Furthermore, peak capacity in CE is much higher than that in HPLC. Column efficiencies in CE of several hundred thousand to millions of theoretical plates have been reported (6-11), allowing the resolution of closely eluting peaks and the separation of a large number of components in a mixture.

This technique has received wide acclaim and has thus been used widely in natural product analyses. Shue and Lu (12) used this technique for the determination of six bioactive ingredients in a Chinese herbal formula. A carrier composed of aqueous buffer solution (50 mM sodium cholate, 15 mM sodium dihydrogen phosphate, and 4.25 mM sodium borate) - acetonitrile (3:2) was found to be the most suitable electrolyte for the separation.

Gil *et al.* (13) used MECC with sodium borate buffer and SDS micelles to analyse herbs and spices for thirty four methylated flavone aglycones. The effect of the structures on their electrophoretic mobilities were also studied. A MECC method was also developed by Li and Sheu (14) for the simultaneous assay of six scute flavanoids and four coptis alkaloids in the scute-coptis herb couple. The effect of pH value, surfactant concentration and acetonitrile concentration of the carrier on the migration and separation of the solutes were studied. The electrolyte comprising of 5 mM sodium borate, 15 mM sodium dihydrogen phosphate and 50 mM sodium cholate together with acetonitrile (3:2) was found to be most suitable. MECC methods were also developed for the separation of coumarins from *Chrysanthemum segetum* L. (15) and in a crude drug of *Angelicae Tuhou* Radix. (16).

In this study MECC was investigated to separate the components and evaluate the complexity of the extracts in an attempt to identify the active principles as performed by

HPLC. Comparisons were made with respect to analysis time, resolution and efficiency. Both SDS and sodium cholate were added to the buffers to influence selectivity.

13.3.1 Analysis of extracts from *Ekebergia capensis*

The components contained in this extract were successfully separated in a single run under suitable conditions. The separation was achieved through selection of an appropriate buffer and surfactant and further optimization of the concentration of surfactant, pH of the buffer and applied voltage.

13.3.1.1. Buffer selection

Buffer selection is important in CE as the sensitivity of EOF to pH changes requires the use of buffers that maintain a constant pH. The effect of pH drift in CE was studied by Zhu *et al.* (17) and they found that if a buffer solution with high buffering capacity was chosen as the background electrolyte, then the pH of this electrolyte during CE separations will remain constant for a relatively long period. Di-sodium tetraborate (20 mM) was chosen as the background electrolyte as it had a useful pH range of 8.24 - 10.24 which ensured ionization of the solutes of interest.

13.3.1.2 Optimization of surfactant concentration

Preliminary experiments were first carried out using 20 mM di-sodium tetraborate with SDS in the electrophoretic medium. With SDS, the components in the mixture are separated on the basis of their relative affinities for the micellar environment against the bulk aqueous phase. In order to study the effect of SDS concentration on the separability, two electrolyte systems containing 30 mM and 60 mM SDS were used. The migration time of all the compounds increased with increasing SDS concentration. At 30 mM three peaks were observed at migration times of 24.99, 26.27 and 28.17 minutes respectively. At higher SDS concentrations, the peaks began to resolve however this was countered by a tremendous increase in migration time. At this point, SDS did not seem to be an appropriate surfactant to influence the separability. The results obtained are shown in Figure 13.10.

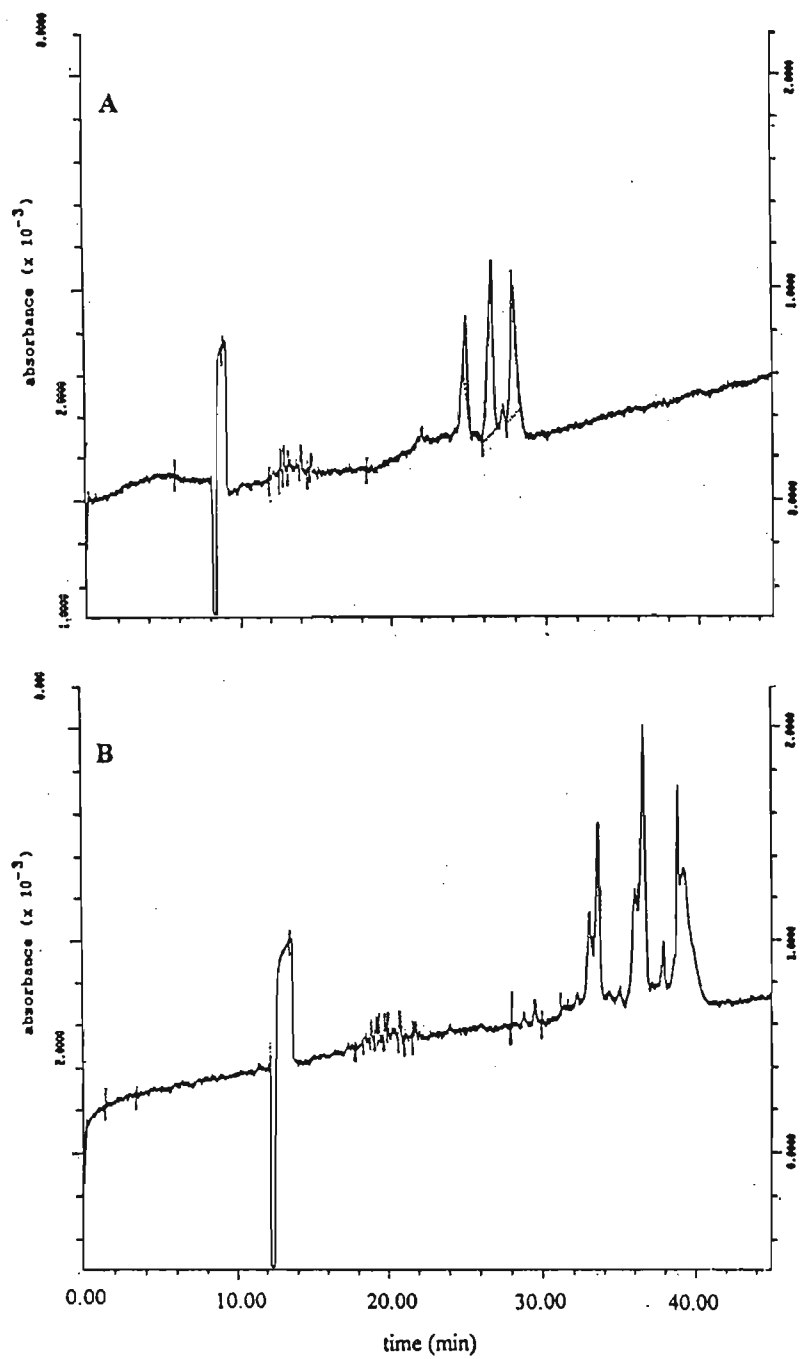


Figure 13.10 Electrochromatogram of total 400 atm extract of *E. capensis* wood obtained with 20 mM $\text{Na}_2\text{B}_4\text{O}_7 \cdot 10\text{H}_2\text{O}$ and (A) 30 mM SDS and (B) 60 mM SDS, pressure injection for 1 sec, UV detection at 280 nm.

MECC with sodium cholate was thereafter investigated with 20 mM di-sodium tetraborate. Four electrolyte systems containing 50, 100, 120 and 150 mM sodium cholate were used to study the effects of sodium cholate concentration on separability. The results obtained are shown in Figure 13.11, where the migration times of the components are plotted against sodium cholate concentrations. There was an increase in the migration times of the components when the sodium cholate concentration in the electrophoretic solution increased. This increase can be explained by the fact that at higher sodium cholate concentration, the phase ratio of the micelle to the aqueous phase would be larger. Hence the probability of solubilization of the components by the micelles would be higher, resulting in an increase in the migration times for these compounds.

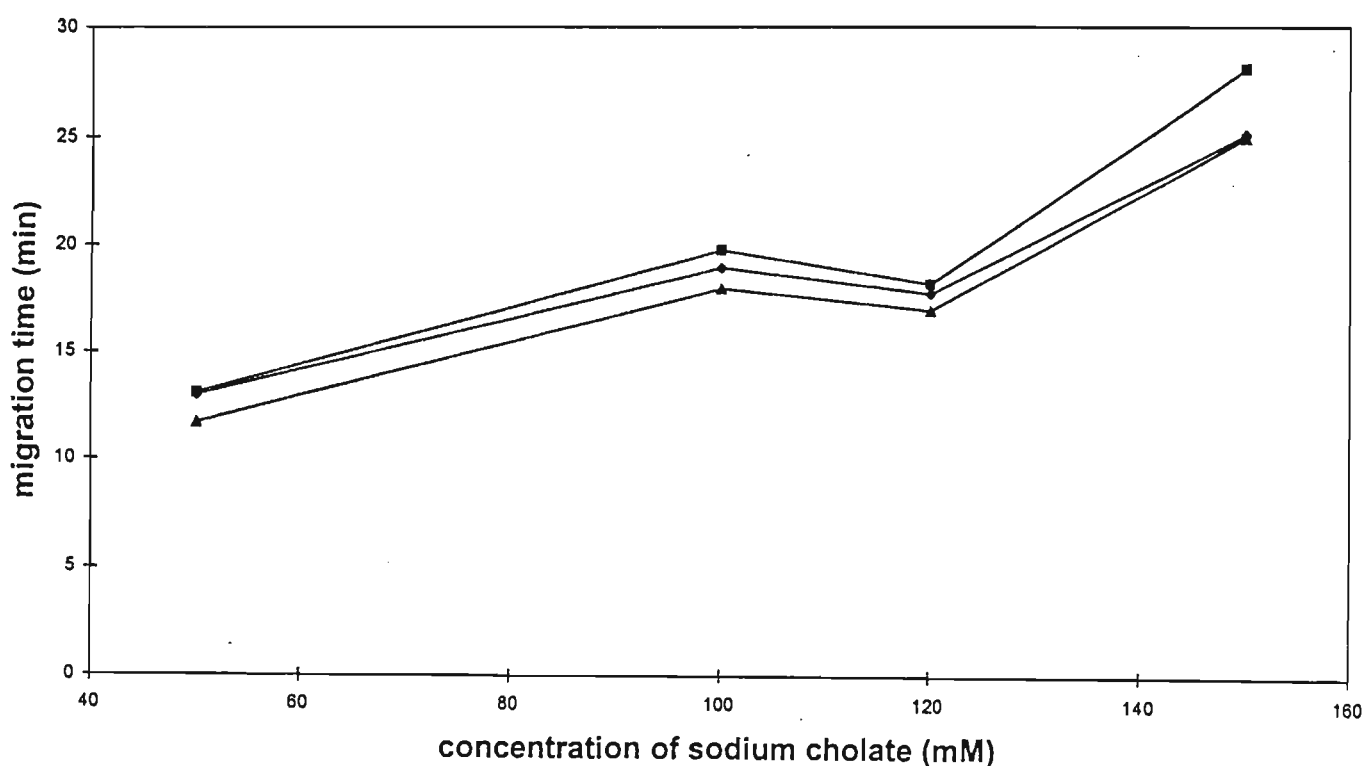
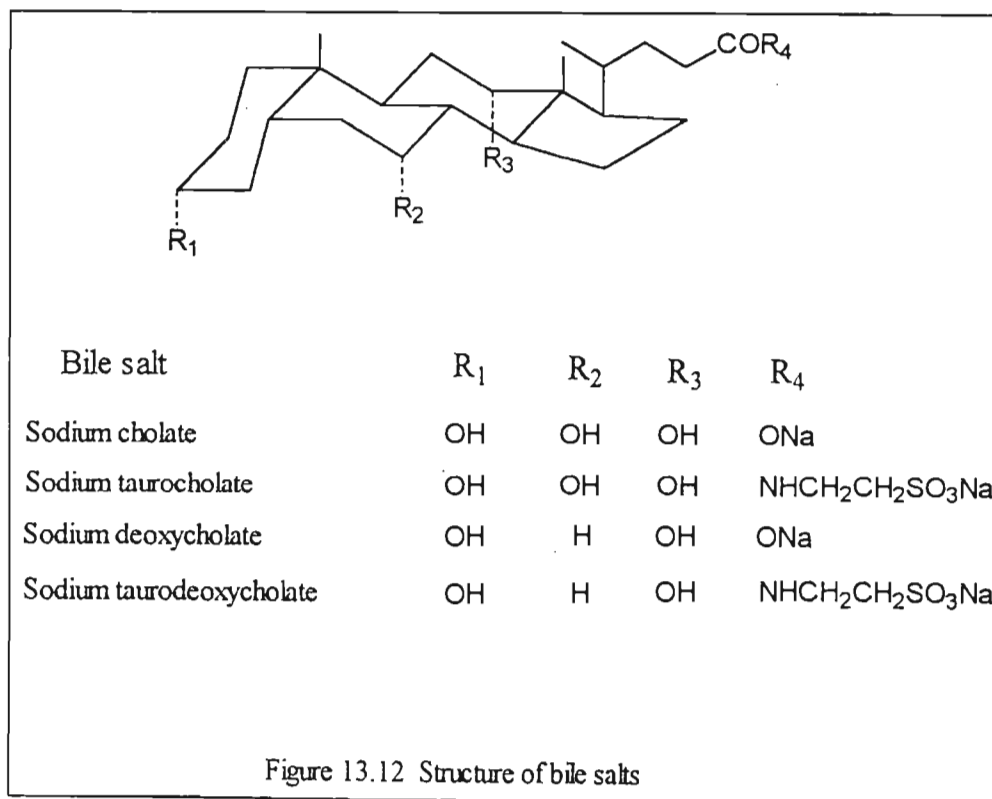


Figure 13.11 Variation of migration time as a function of sodium cholate concentration. (▲ oleanonic acid, ◆ scopoletin, ■ 3-epioleanolic acid)

Bile salts differ significantly in molecular structure from the long chain alkyl surfactants such as SDS. They consist of a relatively flat-shaped steroid portion, in which the A ring is *cis* with respect to the B ring, and a side chain having either a carboxyl or amino group (18). All hydroxyl groups at the 3 α -, 7 α - and 12 α - positions in the 5 β - cholane structure are orientated in the same direction, nearly perpendicular to the steroidal frame. Therefore, the bile salts have both a hydrophilic and a hydrophobic face and tend to combine together at the hydrophobic face in an aqueous phase. Hence bile salts are considered to form a primary micelle with up to ten monomers. The structures of bile salts are shown in Figure 13.12. The fact that the bile salt monomer is more polar than SDS leads to a general reduction in k' in MECC (19). This is particularly advantageous in dealing with hydrophobic compounds, as separations which prove difficult with conventional SDS systems are more easily attained with bile salts. In addition, the unique inverted bile salt micelle appears to tolerate high concentrations of solvents such as methanol without drastic loss of efficiency or dramatic increase in analysis time.



SDS displayed poor selectivity when compared to sodium cholate. Since the SDS micelle has a strong solubilization affect, these solutes possibly migrate with almost the same migration time as that of the micelle. Sodium cholate, on the other hand, exhibits several useful chromatographic properties such as the ability to recognise specific enantiomeric conformations and an increased micelle polarity. Unique selectivity is achieved by the highly ordered nature of the micelle. In this study, sodium cholate appeared to have a lower solubilization affect relative to SDS for the extracted components and clearly exhibited enhanced selectivity over SDS surfactant. The optimum concentration of sodium cholate was found to be 120 mM.

13.3.1.3 pH optimization

The pH of the buffer is a critical parameter for the separation of ionizable analytes (20). In separations with closely spaced peaks, it is often essential to find the optimum pH. The magnitude of the EOF can be expressed in terms of velocity or mobility by:

$$v_e = (\epsilon\zeta / \eta)E \quad (13.1)$$

or
$$u_e = (\epsilon\zeta / \eta) \quad (13.2)$$

where ϵ is the dielectric constant of the solvent; ζ , the zeta potential at the capillary wall; η , the bulk solution viscosity.

The zeta potential is essentially determined by the surface charge on the capillary wall. Since this charge is strongly pH dependent, the magnitude of the EOF varies with pH (21). At high pH, where the silanol groups are predominantly deprotonated, the EOF is significantly greater than at low pH where they become protonated. While the EOF is usually beneficial, it often needs to be controlled. At high pH, for example, the EOF may be too rapid resulting in elution of solute before separation has occurred. Conversely, at low or moderate pH, the negatively charged wall can cause adsorption of cationic solutes through coulombic interactions.

The pH dependence of migration times was examined with a buffer comprising of 20 mM borate with 120 mM sodium cholate in the pH range 9.37 to 10.10 and the results shown

in Figure 13.13. The pH of the run buffer was adjusted with 0.1 M NaOH. The migration times of the components decreased negligibly with increasing pH, although the electroosmotic velocity remained almost constant, as judged from the migration time of methanol which can be detected from the ultraviolet absorption due to the slight change in the refractive index (22). These results can be attributed to the fact that the surface silanol groups on the fused silica capillary are almost fully ionised resulting in the production of a constant EOF. In addition to this, another contributing factor is that the electrophoretic mobility of the solutes in this pH region is constant, indicating that no further ionisation of the compounds occurred. At low pH it would be expected that the oleanane triterpenoids isolated would exist in un-ionised forms and would be strongly retained resulting in higher k' values. The optimum pH was observed to be 9.7 and Figure 13.14 shows the electrophoretic separation of the compounds from *Ekebergia capensis* at this pH.

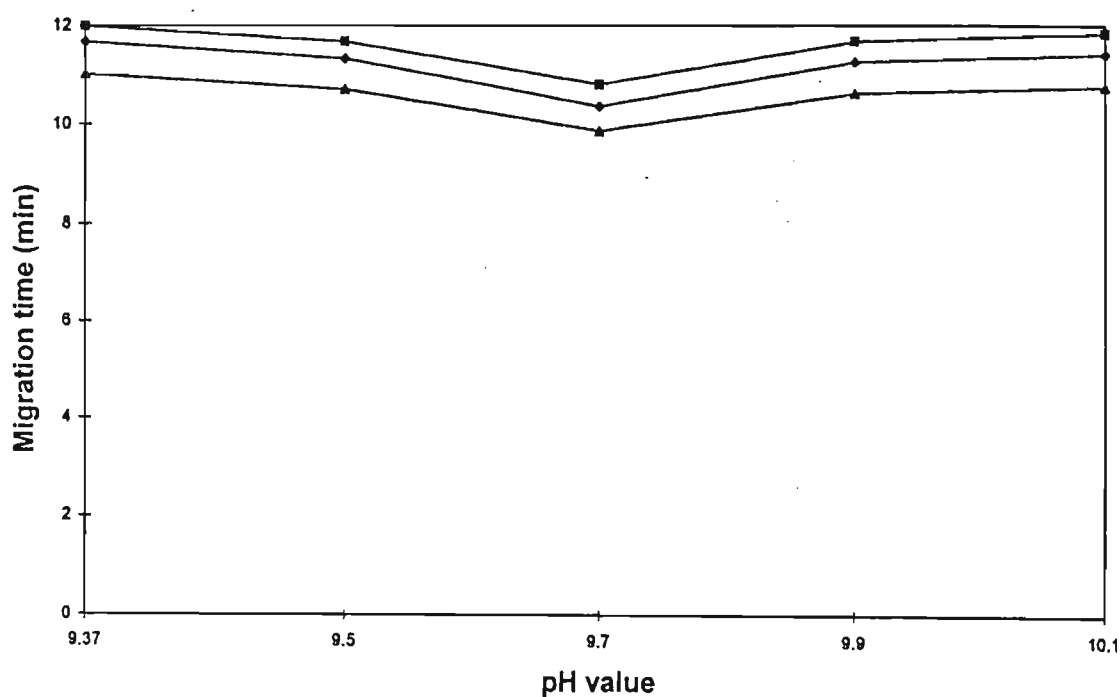


Figure 13.13 Variation of migration time of the *Ekebergia* components as a function of buffer pH. Run buffer: 20 mM $\text{Na}_2\text{B}_4\text{O}_7 \cdot 10\text{H}_2\text{O}$ with 120 mM sodium cholate. (▲ oleanonic acid, ◆ scopoletin, ■ 3-epioleanolic acid)

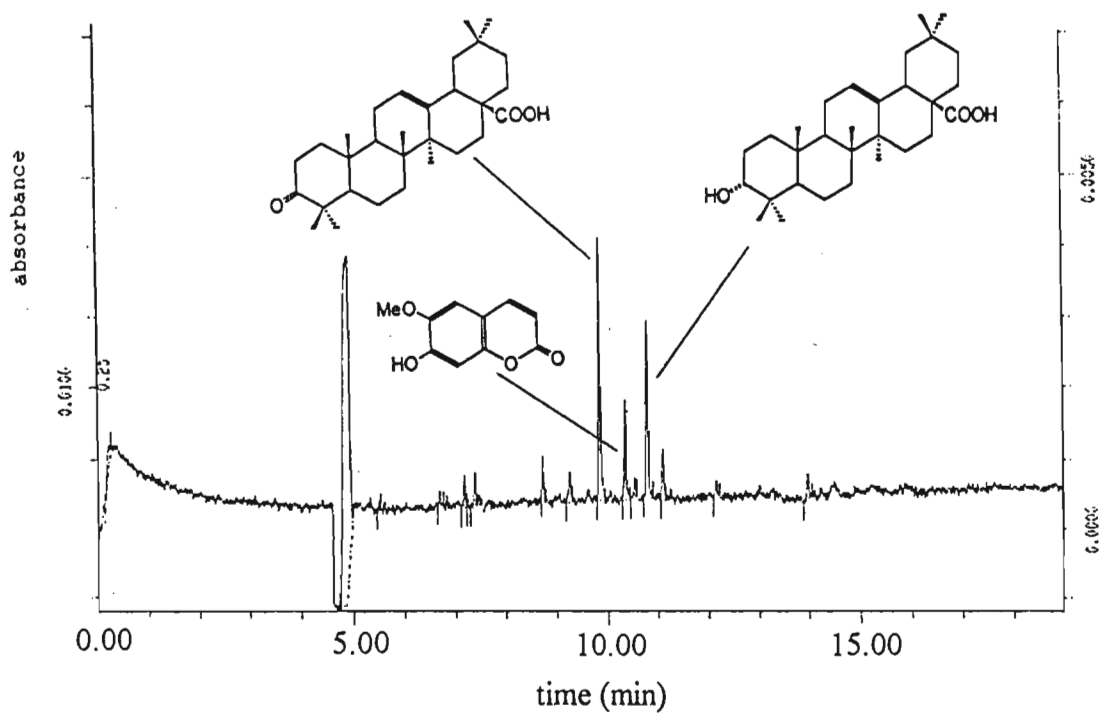


Figure 13.14 Electropherogram of total 400 atm extract of *E. capensis* wood obtained at pH 9.70.

13.3.1.4 Variation of applied voltage

Variation of the voltage and changing the electric field can have several effects (e.g. variation in the migration time of samples, EOF, analysis time, resolution, peak sharpness, and Joule heating) (23). The Joule heating that results from an increase in voltage might lead to changes in EOF, ion mobility, analyte diffusion and band broadening (24). Figure 13.15 shows the electropherogram of the extract running in 20 mM borate buffer with 120 mM sodium cholate at different applied voltages. The migration times decreased with increasing voltages. At 25 kV, the migration times of the components were halved in comparison to the migration time at 15 kV. The elution time was shortened due to the increased velocity of the analytes and EOF. This is to be expected as equation 13.1 predicts an increase in electroosmotic flow velocity as the field strength increases. The peak shapes were also greatly improved, however there was a slight compromise on resolution. High concentration (ionic strength) buffers also produce good peak efficiency and symmetry because there is effective suppression of electrophoretic dispersion. EOF can also be affected by adjusting the concentration and ionic strength of the buffer. High buffer concentrations limit coulombic interactions of solutes with the capillary walls by decreasing the effective charge at the wall. The zeta potential is also dependent on the ionic strength of the buffer, as described by the double-layer theory. Increased ionic strength results in double layer compression, decreased zeta potential, and reduced EOF. The disadvantages however, include high conductivities, high temperatures, Joule heating, and viscosity changes that results in poor migration time reproducibility (25).

13.3.1.5 Separation of components under optimized conditions

Figure 13.16 shows the electropherogram of the total extract obtained at 400 atm using the optimised separation conditions. Analysis was complete within 15 minutes unlike the 30 minute analysis time required for HPLC. Furthermore, high efficiency separations were achieved. The number of theoretical plates (N) for oleanonic acid, scopoletin and 3-*epioleanonic acid* was calculated to be 7.676×10^6 , 9.752×10^6 and 10.815×10^6 respectively. The high N values obtained is the primary driving force for the better separations that are possible through capillary electrophoretic techniques.

MECC was also performed on the sequentially fractionated extracts and similar conclusions, as drawn from the HPLC analysis, were made (Figure 13.17). There were no distinct differences in the electropherograms although the active components did increase with increasing extraction pressures.

During the injection of samples into the capillary, short injection times were used. Large injection times would have resulted in sample overload with the end result being a compromise on the high efficiency of this technique. The injection volume can affect efficiency by two distinct mechanisms (26). One mechanism relates to the volume of the sample injected (q_{inj}) relative to the total volume of the capillary (q_c). From equation 13.3 below, it can be seen that the maximum number of theoretical plates (N_{max}) of the overall system is constrained to a value proportional to the square root of the ratio of the volume of the injected sample to the volume of the column.

$$N_{max} = 12 (q_c / q_{inj})^2 \quad (13.3)$$

The second mechanism imposes a limit on the concentration of the sample injected and is related to the difference in electrical conductivity of the sample and the electrophoretic medium. At high sample concentration, system efficiency can be degraded due to perturbation in the potential field gradient by the sample within the column. Severely distorted peaks may result. A pressure injection time of 1 second was found to provide adequate solute signals without any loss in efficiency or the appearance of distorted peaks.

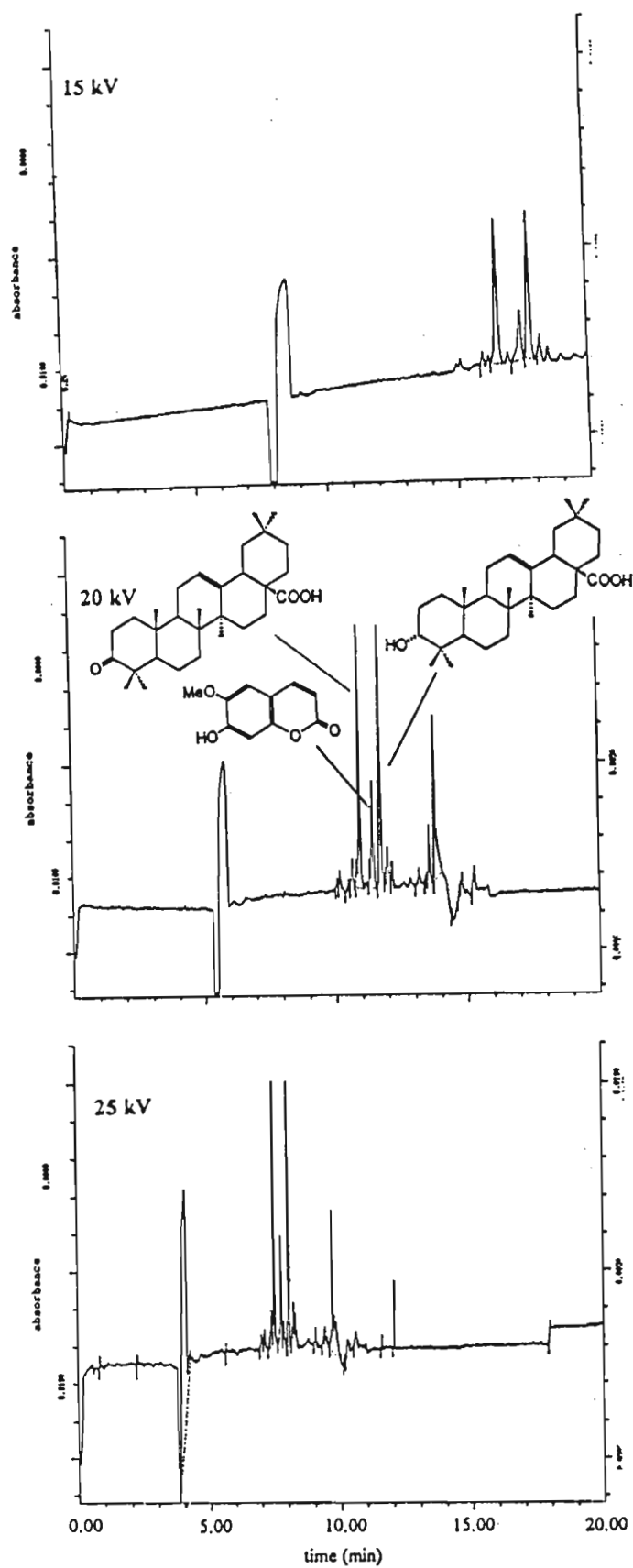


Figure 13.15 Variation of migration time of *Ekebergia* components as a function of applied voltage.

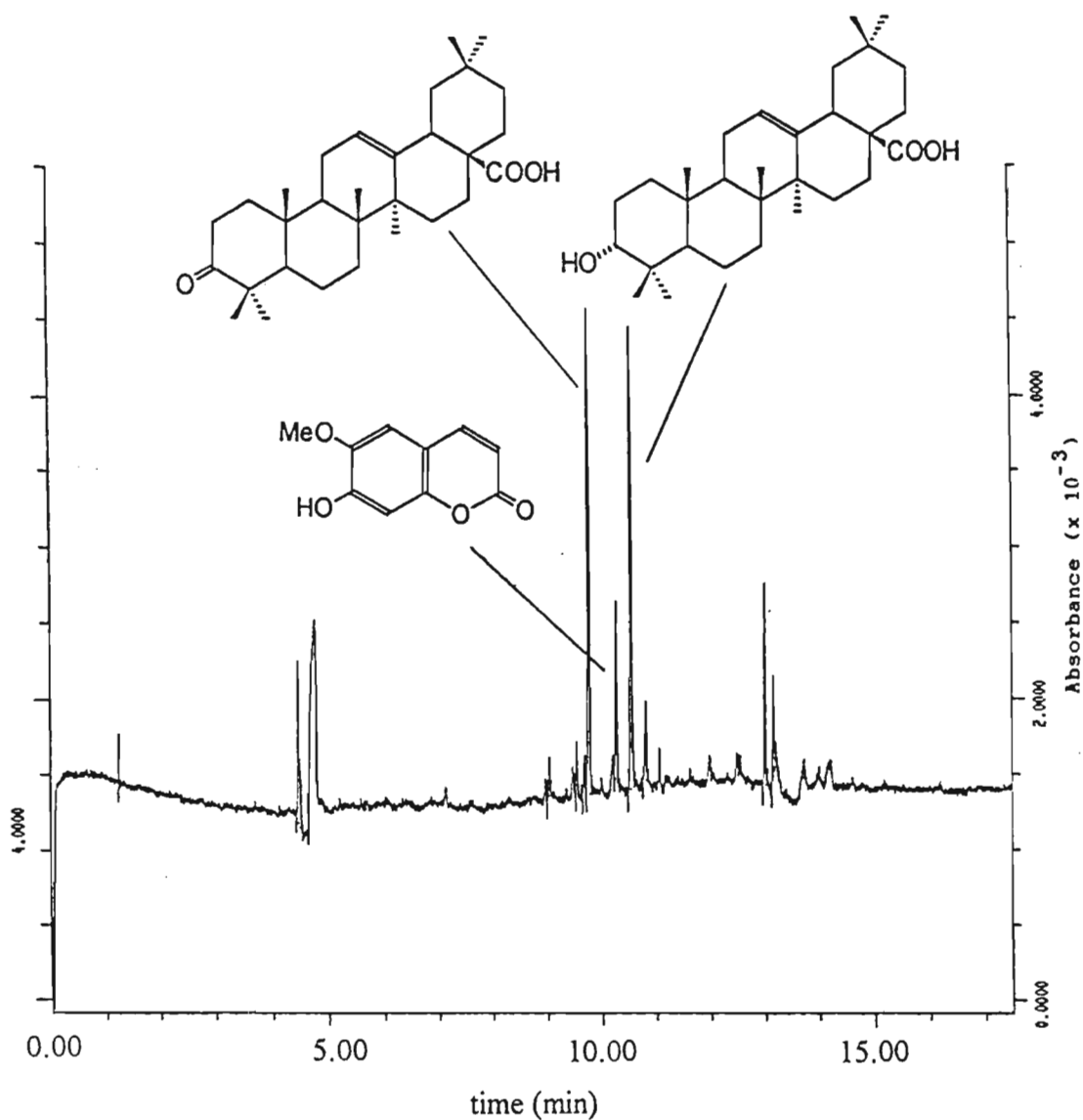


Figure 13.16 Electropherogram of total 400 atm extract of *E. capensis* wood obtained under optimised pH conditions
 Conditions: 20 mM $\text{Na}_2\text{B}_4\text{O}_7 \cdot 10\text{H}_2\text{O}$ with 120 mM sodium cholate at pH 9.70, pressure injection for 1 sec, UV detection at 280 nm.

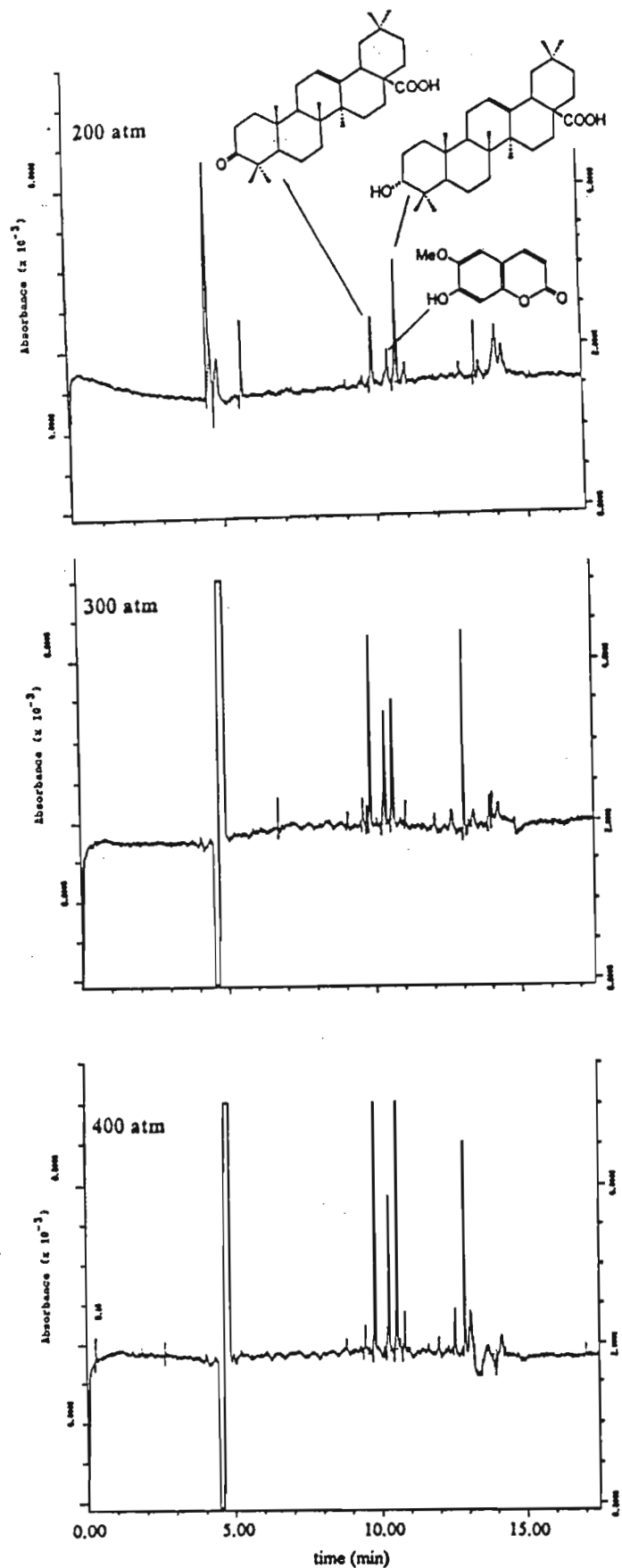


Figure 13.17 Electropherograms of sequentially extracted fractions of *E. capensis* wood obtained under optimised pH conditions
 Conditions: 20 mM $\text{Na}_2\text{B}_4\text{O}_7 \cdot 10\text{H}_2\text{O}$ with 120 mM sodium cholate at pH 9.70, pressure injection for 1 sec, UV detection at 280 nm.

13.3.2 Analysis of extracts from *Clivia miniata*

The extracts of *Clivia miniata* were separated using a phosphate buffer (pH range 6.21-8.21) comprising of 30 mM Na₂HPO₄, 30 mM NaH₂PO₄ and 120 mM sodium cholate. Separation was performed at 20 kV at pH 6.95. Figure 13.18 shows the electropherograms of the sequentially fractionated extracts. The results obtained are similar to those obtained by HPLC analysis however, the analysis time was reduced by 7 minutes. 5-Hydroxymethyl-2-furancarboxaldehyde had a migration time of 6.18 minutes as opposed to a retention time of 7.7 minutes. Although, the migration time of this compound did not vary considerably from the retention time, a comparison of the efficiencies clearly indicated the superiority of this technique. The number of theoretical plates was calculated to be 1.350×10^6 . There was no need to carry out further optimisation of conditions as the matrix did not reveal any complexity.

When 5-hydroxymethyl-2-furancarboxaldehyde was isolated, it was thought to be an artefact of the extraction process as this compound can result from sucrose under acidic conditions and high pressure (27). Since water modified CO₂ was used as the extracting fluid, it was likely to be an artefact due to carbonic acid formation in the extraction vessel. However, such thoughts were dismissed upon comparison of the electropherograms of the pure compound with that of the aqueous extract of this plant (Figure 13.19). It was quite evident that this active compound was present in large quantities in the aqueous extract and that water modified CO₂ possessed the solvating ability to extract this water soluble compound.

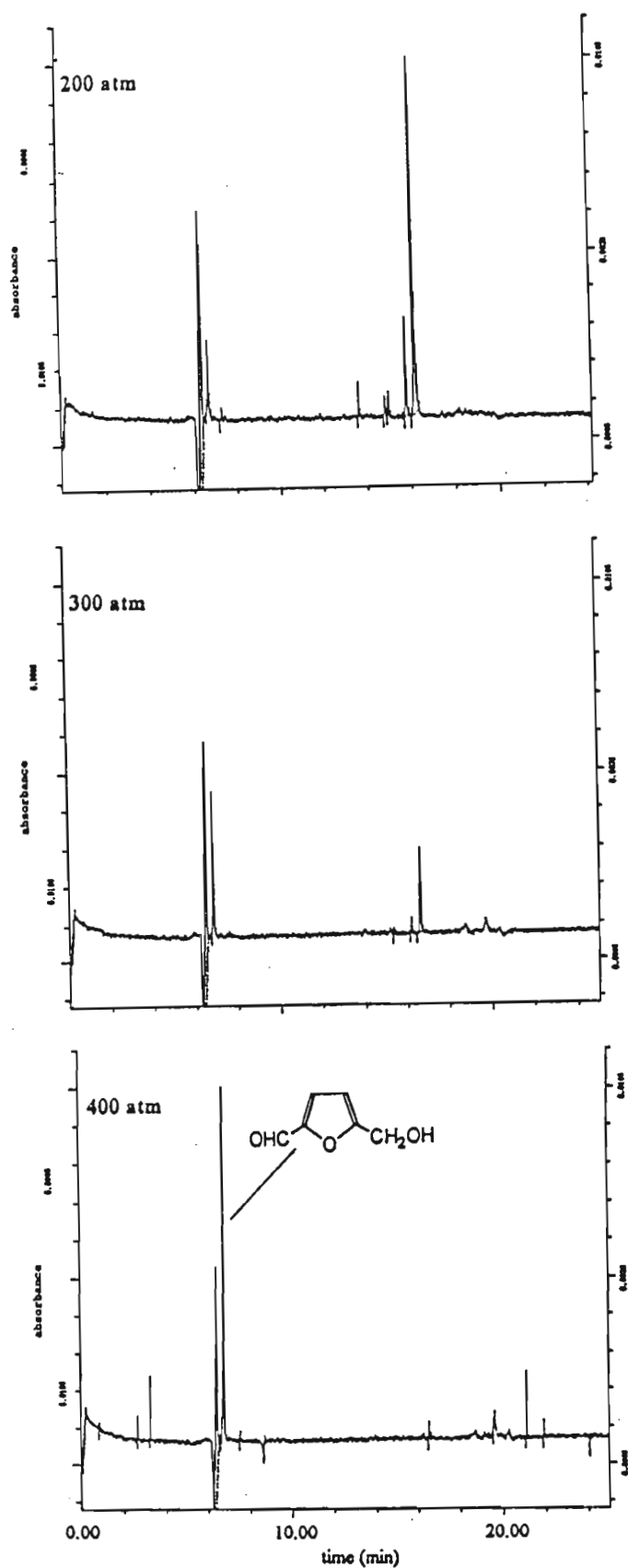


Figure 13.18 Electropherograms of sequentially extracted fractions of *C. miniata* root. Conditions: 30 mM Na₂HPO₄, 30 mM NaH₂PO₄, 120 mM sodium cholate, pH 6.95, applied voltage of 20 kV, pressure injection for 1 sec, UV detection at 280 nm.

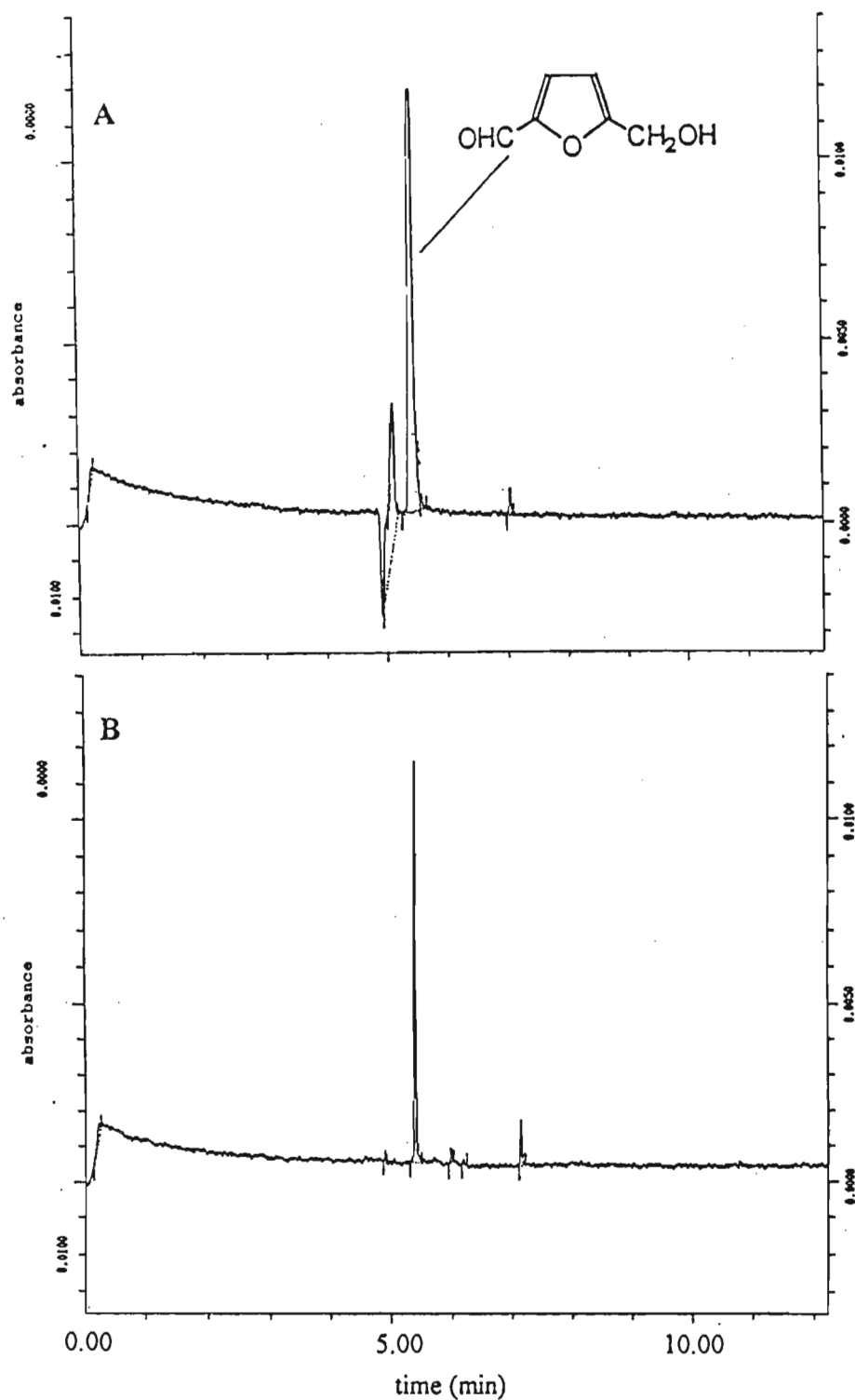


Figure 13.19 Electropherograms of (A) SFE and (B) aqueous extracts of *C. miniata* root showing the presence of 5-hydroxymethyl-2-furancarboxaldehyde in both extracts.

Conditions: 30 mM Na₂HPO₄, 30 mM NaH₂PO₄, 120 mM sodium cholate, pH 6.95, applied voltage of 20 kV, pressure injection for 1 sec, UV detection at 280 nm.

13.3.3 Analysis of extracts from *Grewia occidentalis*

The components in this extract were separated using 20 mM borate buffer with 100 mM sodium cholate at 20 kV. The effect of pH on migration time was studied in the pH range 8.10 to 10.30 and the results shown in Figure 13.20. The EOF was almost constant however the migration times of the components increased with increasing pH.

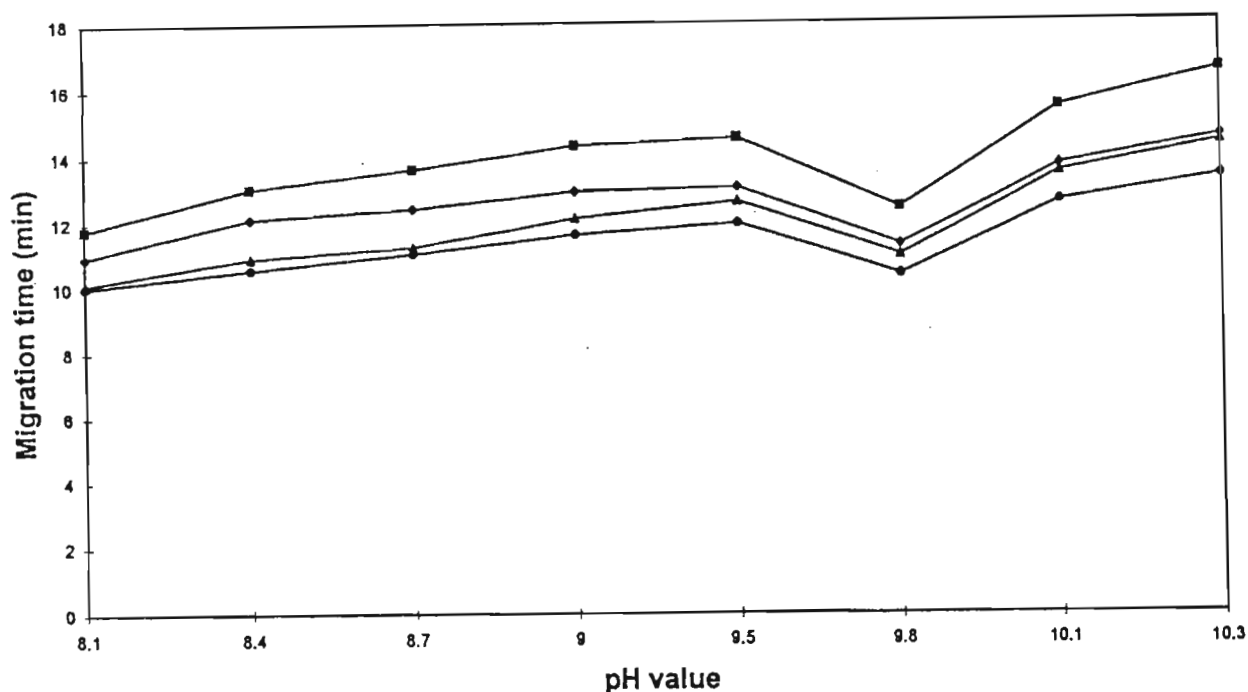


Figure 13.20 Variation of migration time as a function of pH for the components of *G. occidentalis* obtained at 400 atm. (■ oleanonic acid, ◆ coniferaldehyde, ▲ 2,2',6,6'-tetramethoxy-4'-al-4-(ω -oxo-*E*-propenyl)-biphenyl)

The constant EOF can be attributed to the fact that the surface silanol groups on the fused silica capillary are almost fully ionised. The increase in migration times may have resulted due to electric effects since this is an electrodriven separation. The compounds contained in this extract contain hydroxy and methoxy groups which are susceptible of ionisation at high pH and will have a negative charge and therefore an electrophoretic migration to the

anode (injection end) and will show higher migration times. Increasing the pH increases the number of negative charges on the molecules and hence the electrophoretic migration towards the anode. Nevertheless, all the components are finally carried by the EOF towards the cathode. The optimum pH for the separation of these compounds was 9.80. Figure 13.21 shows the electrophoretic separation obtained under optimised conditions. The analysis time was similar to HPLC, however, while it was envisaged that only two compounds were present in the extract following HPLC analysis, MECC was able to provide a true reflection of the complexity of the extract. Four peaks were observed with only three of the compounds being identified. Coniferaldehyde and oleanonic acid are active principles and are well separated using this technique. This application clearly demonstrates the high resolving power of CE.

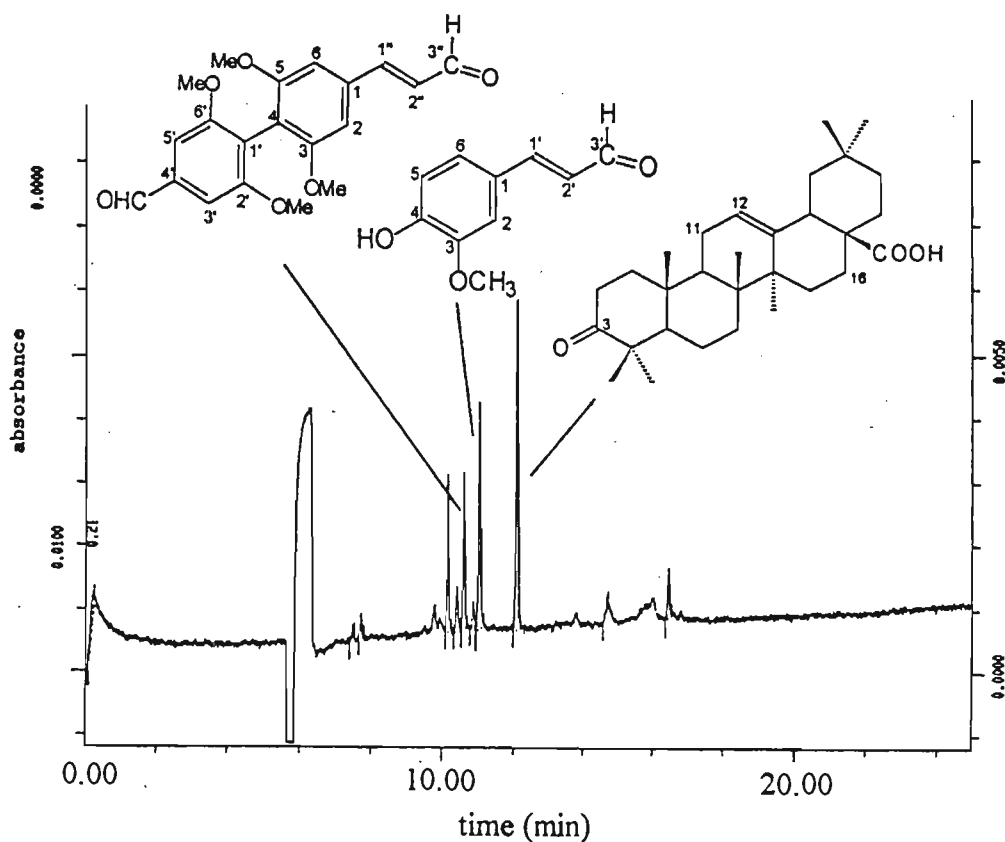


Figure 13.21 Electropherogram of total 400 atm extract of *G. occidentalis* wood obtained under optimised conditions
 Conditions: 20 mM $\text{Na}_2\text{B}_4\text{O}_7 \cdot 10\text{H}_2\text{O}$ with 100 mM sodium cholate at pH 9.80, pressure injection for 1 sec, UV detection at 254 nm.

MECC of the sequentially fractionated extracts revealed the sensitivity of the compounds to the extraction pressures (Figure 13.22). At 200 atm, a negligible concentration of oleanonic acid was extracted while at 300 atm and 400 atm, the compounds becomes extremely soluble in the extraction fluid. Oleanonic acid was also extracted from *Ekebergia capensis* at 200 atm, however in larger concentrations, and one may argue how such phenomenon is possible. The limited solubility of oleanonic acid at 200 atm in this case could be attributed to matrix effects. In certain cases, chemical compounds can be very strongly bound to the matrix they are contained in hence the sample matrix can have a profound effect on the results that are obtained, as discussed in chapter 2.

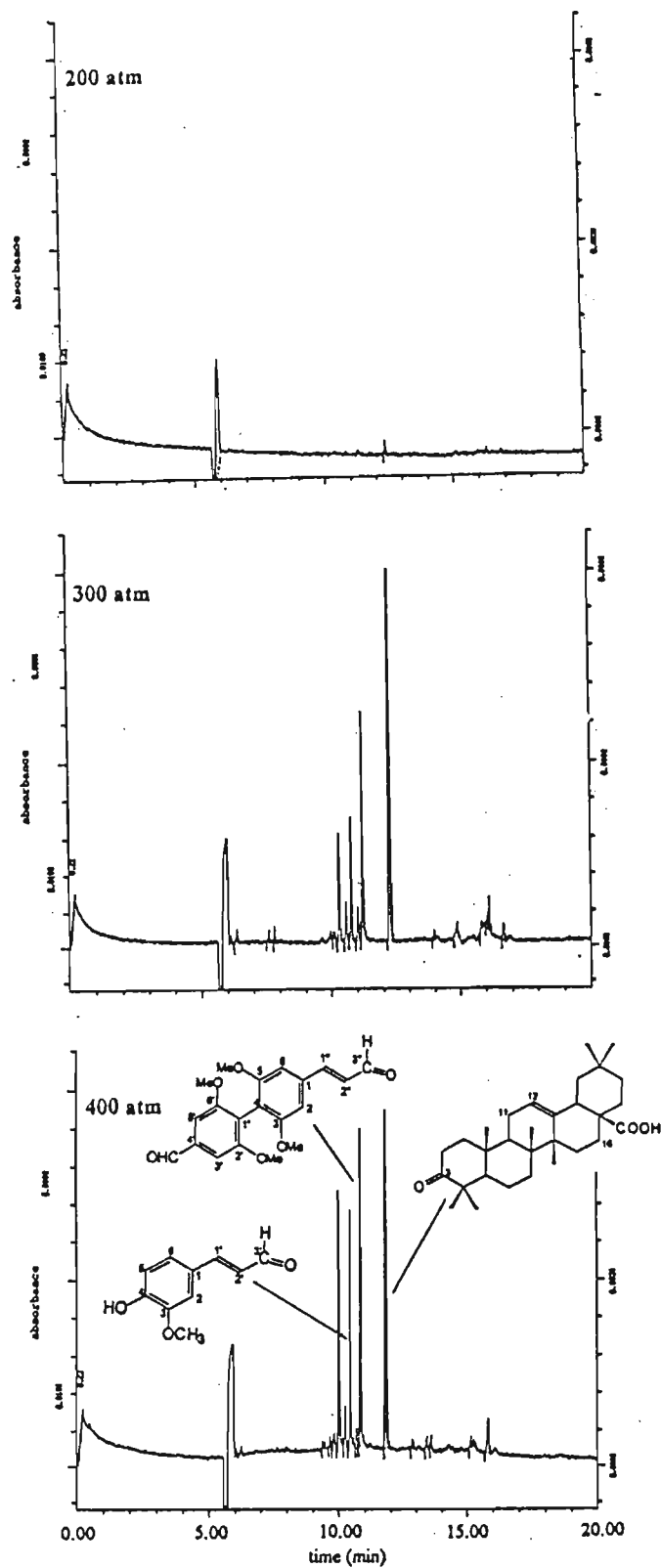


Figure 13.22 Electropherograms of sequentially extracted fractions of *G. occidentalis* wood.
 Conditions: 30 mM Na_2HPO_4 , 30 mM NaH_2PO_4 , 120 mM sodium cholate, pH 6.95, applied voltage of 20 kV, pressure injection for 1 sec, UV detection at 254 nm.

13.4 Packed capillary column SFC

Open tubular SFC has received considerable attention and has been used widely in separating a wide variety of natural products (28-35). However, in this study an attempt was made in using packed column SFC as a possible separation technique for characterising the components contained in the fractionated 400 atm extract of *Ekebergia capensis*. Both pure CO₂ and a hydrofluorocarbon were evaluated as mobile phases.

Slurry packing methods are commonly employed and can be successful in the preparation of both packed conventional and packed capillary columns. Recently, dry and supercritical CO₂ packing techniques have been developed to prepare packed capillary columns (36, 37). The physical properties of CO₂, such as low viscosity and low surface tension, favour efficient packing which leads to the formation of a dense and uniform packed bed. These columns can advantageously combine many of the valuable properties of both low flow rates (38), moderate sample capacities and loadabilities (39), high analysis speeds (40) and the possibility of using a wide variety of commercially available stationary phases. The results of a number of SFC separations using packed capillary columns are reported (41).

In this study a 30 cm length of fused silica capillary was packed with Spherisorb ODS2 using the method outlined in chapter 5. The stability of the packed bed is very important in SFC because pressurisation and depressurisation are repeated quite often. From a practical point of view, a loose packing will cause instability and result in voids at the top of the column, which markedly decreases the column efficiency due to extensive rearrangement of the packing material. However, under the experimental conditions studied, no such voids were observed.

13.4.1 SFC with CO₂

Prior to injection of the sample, naphthalene was injected as a test sample using a timed-split injection of 100 msec and excellent peak symmetry was obtained under the conditions used (Figure 13.23). However there were no positive results for the extract of *Ekebergia*

capensis. The pressure was initially ramped to increase the solvating power of the mobile phase followed by an increase in the temperature in order to reduce the solutes' cohesive energy density, but all attempts failed. This may be due to interaction of the compounds with the residual active sites on the packing material.

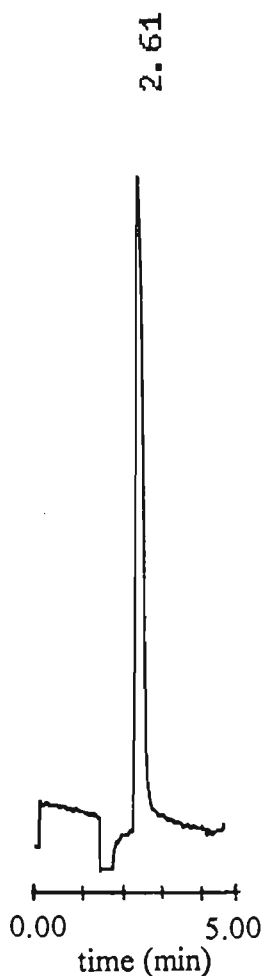
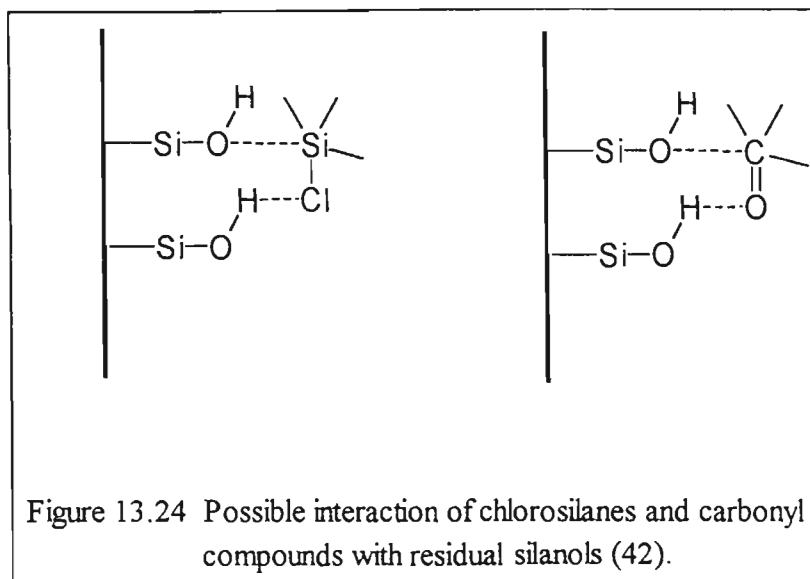
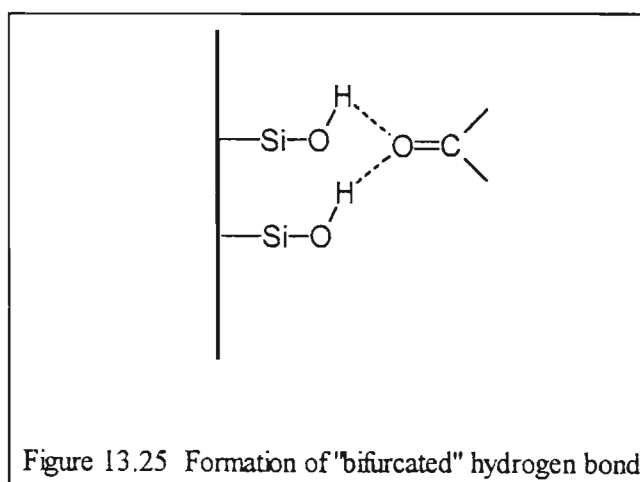


Figure 13.23 Packed capillary SFC of 5 mg/ml naphthalene standard
Conditions: 300 atm, 50 °C, 30 cm × 100 μm i.d. column
packed with ODS2, UV detection at 254 nm

Anthony *et al.* (42) studied the interaction of aldehydes and ketones on silanol groups and reasoned that these compounds behaved similarly to chlorosilanes. With the bonded silanols, a concerted effect may have been possible in which the proton of one silanol interacted with the electronegative oxygen atom, while the oxygen of the other hydroxyl would interact at the electropositive silicon atom as shown in Figure 13.24.



Carbonyl compounds can also interact preferentially at bonded silanols through the formation of a “bifurcated” hydrogen bond as seen in Figure 13.25.



Finally, it was concluded that pure CO_2 was not a suitable mobile phase for these compounds. Other alternatives would have been to use a modified fluid or a more polar mobile phase such as a hydrofluorocarbon.

13.4.2 SFC with hydrofluorocarbon

1,1,1,2-Tetrafluoroethane (HFC-134a) was thereafter investigated as a mobile phase as earlier studies with packed columns indicated that hydrofluorocarbons are comparable in eluotropic strength to CO₂ for polar compounds (43, 44). It has also been stated that hydrofluorocarbons are more polarizable than CO₂ and compounds capable of interacting with this mobile phase *via* hydrogen bonding interactions should also be more strongly solvated and eluted. Attempts to elute the compounds of *Ekebergia capensis* from the column failed, possibly due to the strong hydrogen bonds between the silanol and the carbonyl compounds. At this point the prospect of using SFC for the current studies did not seem viable and further analysis of the extracts was terminated.

13.5 Conclusion

From this study, it was concluded that both HPLC and CE can be successfully used to separate the components contained in the extracts of *Ekebergia capensis* and *Clivia miniata*. The principles of separation in HPLC are entirely different to MECC and, therefore, a good agreement between the two techniques strongly supports the integrity of the data. The differences in selectivity between HPLC and MECC, as observed for the extracts of *Grewia occidentalis*, resulted in discrepancies in results with HPLC showing an underestimation of the complexity of the extract. This occurrence signifies that further method optimization is required for HPLC. MECC has clearly demonstrated superiority by its high resolving capabilities and high efficiencies as judged from the theoretical plate numbers. Although packed capillary column SFC has many advantages, the use of this technique with both CO₂ and 1,1,1,2-tetrafluoroethane as mobile phases did not prove successful in the analysis of the extracts from *Ekebergia capensis*. This indicated that modifiers were necessary to overcome possible interactions between solutes and residual silanol groups in order to elute the compounds. The CE methods can be successfully used to monitor the occurrence of these compounds at various periods during the year in order to obtain a concentration profile of the active components in these plants. In this way total quality assurance of the plant products can be established.

References

1. A. Hasler, O. Sticher and B. Meier, *J. Chromatogr.*, **508** (1990), 236.
2. A.A. Elujoba, A.F. Fell and P.A. Linley, *J. Pharm. Biomed. Anal.*, **9** (1991), 711.
3. P. Pietta and C. Gardana, *J. High Resolut. Chromatogr.*, **15** (1992), 136.
4. S. L. Richheimer, D.M. Tinnermeier and D.W. Timmons, *Anal. Chem.*, **64** (1992), 2323.
5. T. Uno, *Chem. Abstr.*, **77** (1972), 98769.
6. J.W. Jorgenson and K.D. Lukacs, *Anal. Chem.*, **53** (1981), 1298.
7. J.W. Jorgenson and K.D. Lukacs, *J. Chromatogr.*, **218** (1981), 209.
8. J.W. Jorgenson and K.D. Lukacs, *J. High Resolut. Chromatogr. & Chromatogr. Comm.*, **4** (1981), 230.
9. J.W. Jorgenson and K.D. Lukacs, *Clin. Chem.*, **27** (1981), 1551.
10. A.S. Cohen and B.L. Karger, *J. Chromatogr.*, **397** (1987), 409.
11. A.S. Cohen, A. Paulus and B.L. Karger, *Chromatographia*, **24** (1987), 14.
12. S-J, Sheu and C-F Lu, *J. High Resolut. Chromatogr.*, **19** (1996), 409.
13. M.I. Gil, F. Ferreres and F.A. Tomás-Barberán, *J. Liq. Chromatogr.*, **18** (1995), 3007.
14. K-L Li and S-J Sheu, *Anal. Chim. Acta.*, **313** (1995), 113.
15. R.J. Ochocka, D. Rajzer, P. Kowalski and H. Lamparczyk, *J. Chromatogr. A*, **709** (1995), 197.
16. C-T Chen and S-J. Sheu, *J. Chromatogr. A*, **710** (1995), 323.
17. T. Zhu, Y. Sun, C. Zhang, D. Ling and Z. Sun, *J. High Resolut. Chromatogr.*, **17** (1994), 563.
18. S. Terabe, M. Shibata and Y. Miyashita, *J. Chromatogr.*, **480** (1989), 403.
19. R.O. Cole, M. J. Sepaniak, W. L. Hinze, J. Gorse and K. Oldiges, *J. Chromatogr.*, **557** (1991), 113.
20. S. Fugiwara, S. Iwase and S. Honda, *J. Chromatogr.*, **447** (1988), 133.
21. R.M. McCormik, *Anal. Chem.*, **60** (1988), 2322.
22. S. Terabe, K. Otsuka and T. Ando, *Anal. Chem.*, **57** (1985), 834.
23. J.H. Knox, *Chromatographia*, **26** (1988), 329.

24. S. Hjertén, *Electrophoresis*, **11** (1990), 665.
25. T. Tsuda, K. Nomura and G. Nakagawa, *J. Chromatogr.*, **264** (1983), 385.
26. H. Lauer and D. McManigill, *Trends Anal. Chem.*, **5** (1986), 11.
27. W.N. Haworth and W.G.M. Jones, *J. Chem. Soc.*, (1944), 667.
28. P. Morin, H. Pichard, M. Caude, H. Richard and R. Gosset, In: *Progress in Terpene Chemistry*, D. Joulain, (Ed.), Frontiers, Gif/Yvette, (1986), p.343.
29. M. W. Raynor, R. Moulder, I.L. Davies, J.P. Kithinji, J.E. Hall, A.A. Clifford and K.D. Bartle, In: *Proc. Tenth Int. Symp. Cap. Chromatogr.*, P. Sandra and G. Redant, (Eds.), Huethig, Heidelberg, (1989), p.1366.
30. J. Balsevich, L.R. Hogge, A.J. Berry, D.E. Games and I.C. Mylchreest, *J. Nat. Prod.*, **51** (1988), 1173.
31. G. Holzer, L.H. Zalkow and C.F. Asibal, *J. Chromatogr.*, **400** (1987), 317.
32. J.L. Janicot, M. Caude and R. Rosset, *J. Chromatogr.*, **437** (1988), 351.
33. P. Morin, H. Pichard, H. Richard, M. Caude and R. Rosset, *J. Chromatogr.*, **464** (1989), 125.
34. P. Morin, M. Caude and R. Rosset, *Analisis*, **15** (1987), 117.
35. V. Sewram, J.J. Nair, D.A. Mulholland and M.W. Raynor, *J. High Resolut. Chromatogr.*, **18** (1995), 363.
36. G. Crescentini and A.R. Mastrogiacomo, *J. Microcol. Sep.*, **3** (1991), 539.
37. A. Malik, W. Li and M.L. Lee, *J. Microcol. Sep.*, **5** (1993), 361.
38. M. Novotny, *Anal. Chem.*, **53** (1981), 1294A.
39. Y. Hirata, F. Nakata and M. Horihata, *J. High Resolut. Chromatogr. Chromatogr. Commun.*, **11** (1988), 81.
40. T. Saito and M. Takeuchi, *JEOL News*, **25A** (1989), 14
41. W. Li, A. Malik and M.L. Lee, *J. Microcol. Sep.*, **6** (1994), 557.
42. L.J. Anthony, R.A. Holland and S.A. Heffner, *J. High Resolut. Chromatogr. Chromatogr. Commun.*, **11** (1988), 167.
43. J.W. Jordan and L.T. Taylor, *J. Chromatogr. Sci.*, **24** (1986), 82.
44. T.A. Berger and J. F. Deye, *J. Chromatogr. Sci.*, **29** (1991), 390.

CHAPTER 14

Overview of this study and concluding remarks

This study successfully validated the uterotonic properties of the three selected medicinal plants through a multidisciplinary approach. Water modified supercritical CO₂ demonstrated a high solvating ability by producing plant extracts that displayed distinctive results when screened for uterotonic activity. The activities were comparable to those induced by the aqueous plant extracts. The application of a dynamic extraction model to optimize extraction conditions was successful although little was known about the solutes' molecular structures at the time. During the extraction of all three plants, the model indicated that solubility was the controlling factor in achieving an interactive extraction.

In vitro biological assays using guinea pig uterine smooth muscle were found to be a simple and sensitive method for detecting uterotonic compounds. Furthermore, the success of coupling SFE directly on-line to the bioassay made this approach more attractive due to the shorter analysis times and elimination of sample handling prior to the bioassay hence eliminating the possibility of sample contamination. On-line bioassay guided fractionation further enhanced the potential of this technique as it increased its specificity by identifying the most potent fractions which were subjected to further analysis.

Repetitive gravity column chromatography of the plant extracts using various mobile phases yielded pure compounds whose structures were elucidated through various spectroscopic and chromatographic techniques. Two compounds from *Ekebergia capensis*, two from *Clivia miniata* and one from *Grewia occidentalis* were found to induce uterine muscle contractions. A further evaluation on the physiological mode of action indicated that these compounds mediated their effects through the cholinergic

receptors. It still remains speculative that these compounds may also have increased the permeability of the cell membranes to calcium ions, however there were no ionic channel blockers used to confirm such a mechanism.

CE and HPLC displayed good resolving capabilities for the evaluation of the complexity of these extracts. However, from a practical viewpoint, the small sample, buffer, and waste volumes required and generated by CE were less than those generated by HPLC making this technique an attractive one. The optimized analytical conditions were used to observe the effect of seasonal changes on the composition of the extracts. As the composition of the plant components varied with seasonal changes, it becomes important to monitor the magnitude of these changes so that the doses of the extract can be regulated to maintain consistency in activity. A further evaluation on the toxicity of these compounds is required and can be done using cells in culture.

APPENDIX 1

¹³C NMR data for compounds isolated

Table A1: ¹³C NMR data for compounds 1, 2, 3 and 4 (75MHz, CDCl₃, TMS as internal standard). All chemical shift values are expressed in ppm (δ) and multiplicities are included in brackets.

Carbon number	Compound 1	Compound 2	Compound 3	Compound 4
1	37.3 (t)	39.3 (t)	32.5 (t)	23.3 (q)
2	31.7 (t)	34.1 (t)	27.6 (t)	73.0 (s)
3	71.8 (d)	217.8 (s)	76.2 (d)	78.3 (d)
4	42.3 (t)	45.8 (s)	37.2 (s)	29.7 (t)
5	140.8 (s)	55.3 (d)	48.9 (d)	36.8 (t)
6	121.7 (d)	19.6 (t)	18.2 (t)	134.8 (s)
7	31.9 (t)	32.2 (t)	32.8 (t)	125.1 (d)
8	31.9 (s)	39.1 (s)	39.4 (s)	26.5 (t)
9	50.1 (d)	47.4 (d)	47.4 (d)	39.6 (t)
10	36.5 (s)	36.8 (s)	37.3 (s)	134.8 (s)
11	21.1 (t)	23.4 (t)	23.3 (t)	124.4 (d)
12	39.8 (t)	122.3 (d)	122.2 (d)	28.2 (t)
13	42.3 (s)	143.6 (s)	143.5 (s)	28.2 (t)
14	56.8 (d)	41.1 (s)	41.7 (s)	124.4 (d)
15	24.3 (t)	27.7 (t)	25.2 (t)	134.9 (s)
16	28.2 (t)	23.0 (t)	22.9 (t)	39.6 (t)
17	56.1 (d)	46.9 (s)	46.5 (s)	26.50 (t)
18	11.9 (q)	41.8 (d)	40.9 (d)	125.1 (d)
19	19.4 (q)	46.5 (t)	45.9 (t)	134.9 (s)
20	36.1 (d)	30.7 (s)	30.7 (s)	36.8 (t)
21	18.8 (q)	33.8 (t)	33.8 (t)	29.7 (t)
22	33.9 (t)	32.4 (t)	32.5 (t)	78.3 (d)
23	26.1 (t)	26.4 (q)	28.3 (q)	73.0 (s)
24	45.8 (d)	21.4 (q)	22.2 (q)	23.3 (q)
25	29.1 (d)	15.0 (q)	15.1 (q)	26.4 (q)
26	19.1 (q)	16.9 (q)	17.2 (q)	16.0 (q)
27	19.0 (q)	25.8 (q)	26.1 (q)	15.9(q)
28	23.1 (t)	184.4 (s)	183.9 (s)	15.9 (q)
29	11.9 (q)	33.0 (q)	33.1 (q)	16.0 (q)
30		23.6 (q)	23.6 (q)	26.4 (q)

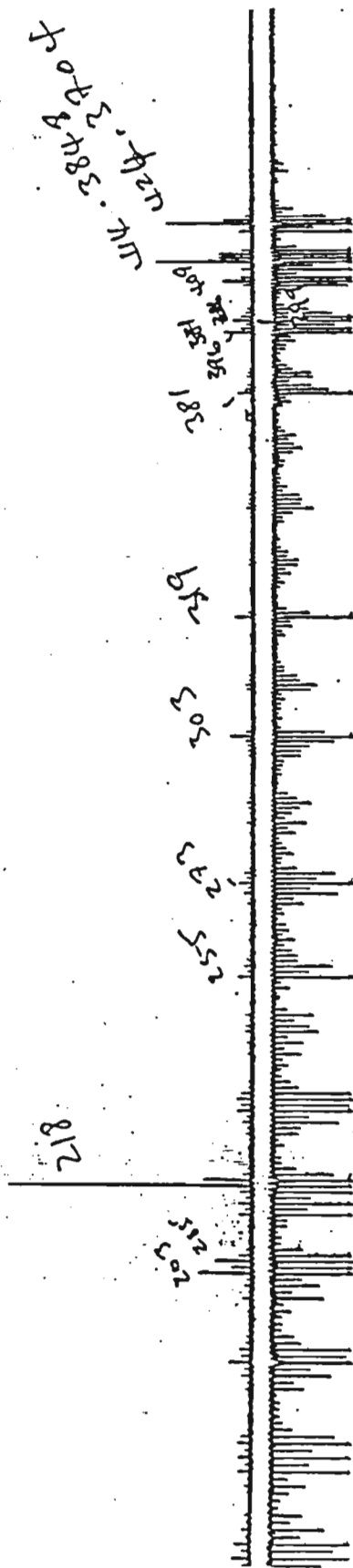
Table A1: ^{13}C NMR data for compounds 7 and 9 (75MHz, CDCl_3 , TMS as internal standard). All chemical shift values are expressed in ppm (δ) and multiplicities are included in brackets.

Carbon number	Compound 7	Compound 9
1		128.4 (s)
2	152.4 (s)	147.3 (s)
3	122.8 (d)	105.6 (d)
4	110.0 (d)	125.3 (s)
5	160.5 (s)	105.6 (d)
6		147.3 (s)
1'		138.0 (s)
2'		147.3 (s)
3'		106.7 (d)
4'		140.9 (s)
5'		106.7 (d)
6'		147.3 (s)
1''		153.1 (d)
2''		126.8 (d)
3''		193.5 (d)
CHO	177.7 (d)	191.0 (d)
4 \times OCH_3		56.4 (q)
OCH_2	57.6 (t)	

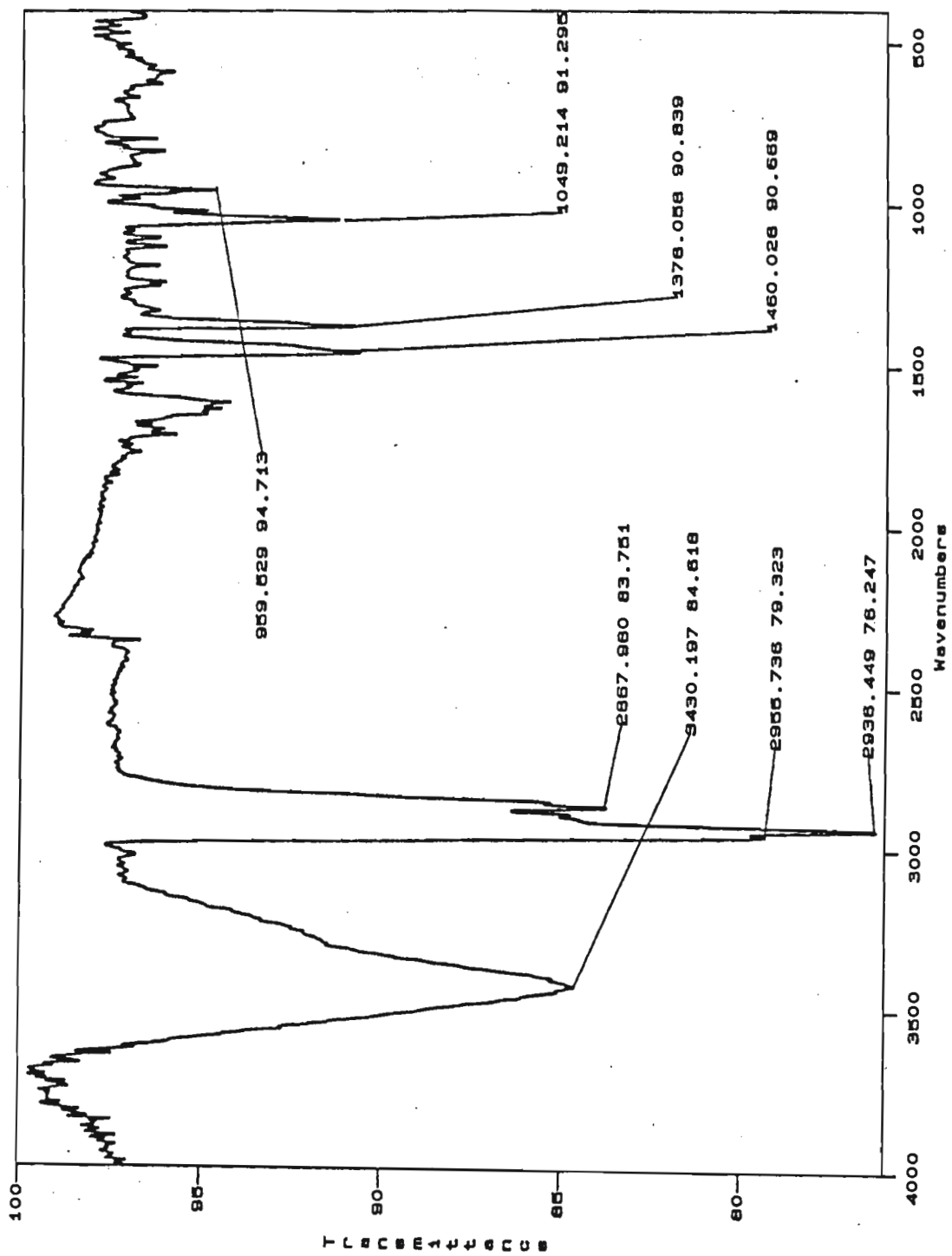
APPENDIX 2

List of Spectra		Page
Spectrum 1a	Mass spectrum of [1]	267
1b	Infrared spectrum of [1]	268
1c	¹ H NMR spectrum of [1]	269
1d	¹³ C NMR spectrum of [1]	270
Spectrum 2a	Mass spectrum of [2]	271
2b	Infrared spectrum of [2]	272
2c	¹ H NMR spectrum of [2]	273
2d	¹³ C NMR spectrum of [2]	274
2e	HETCOR spectrum of [2]	275
2f	COSY spectrum of [2]	276
Spectrum 3a	Mass spectrum of [3]	277
3b	Infrared spectrum of [3]	278
3c	¹ H NMR spectrum of [3]	279
3d	¹³ C NMR spectrum of [3]	280
Spectrum 4a	Mass spectrum of [4]	281
4b	Infrared spectrum of [4]	282
4c	¹ H NMR spectrum of [4]	283
4d	¹³ C NMR spectrum of [4]	284
4e	¹ H NMR spectrum of [4b]	285
Spectrum 5a	Mass spectrum of [5]	286
5b	Infrared spectrum of [5]	287
5c	¹ H NMR spectrum of [5]	288
5d	NOE spectrum of [5] showing irradiation of H-4	289
5e	NOE spectrum of [5] showing irradiation of H-5	290
5f	NOE spectrum of [5] showing irradiation of methoxy protons	291
5g	¹³ C NMR spectrum of [5]	292
Spectrum 6a	¹ H NMR spectrum [6]	293
Spectrum 7a	Mass spectrum of [7]	294
7b	Infrared spectrum of [7]	295
7c	¹ H NMR spectrum of [7]	296
7d	¹³ C NMR spectrum of [7]	297
7e	NOE spectrum of [7]	298

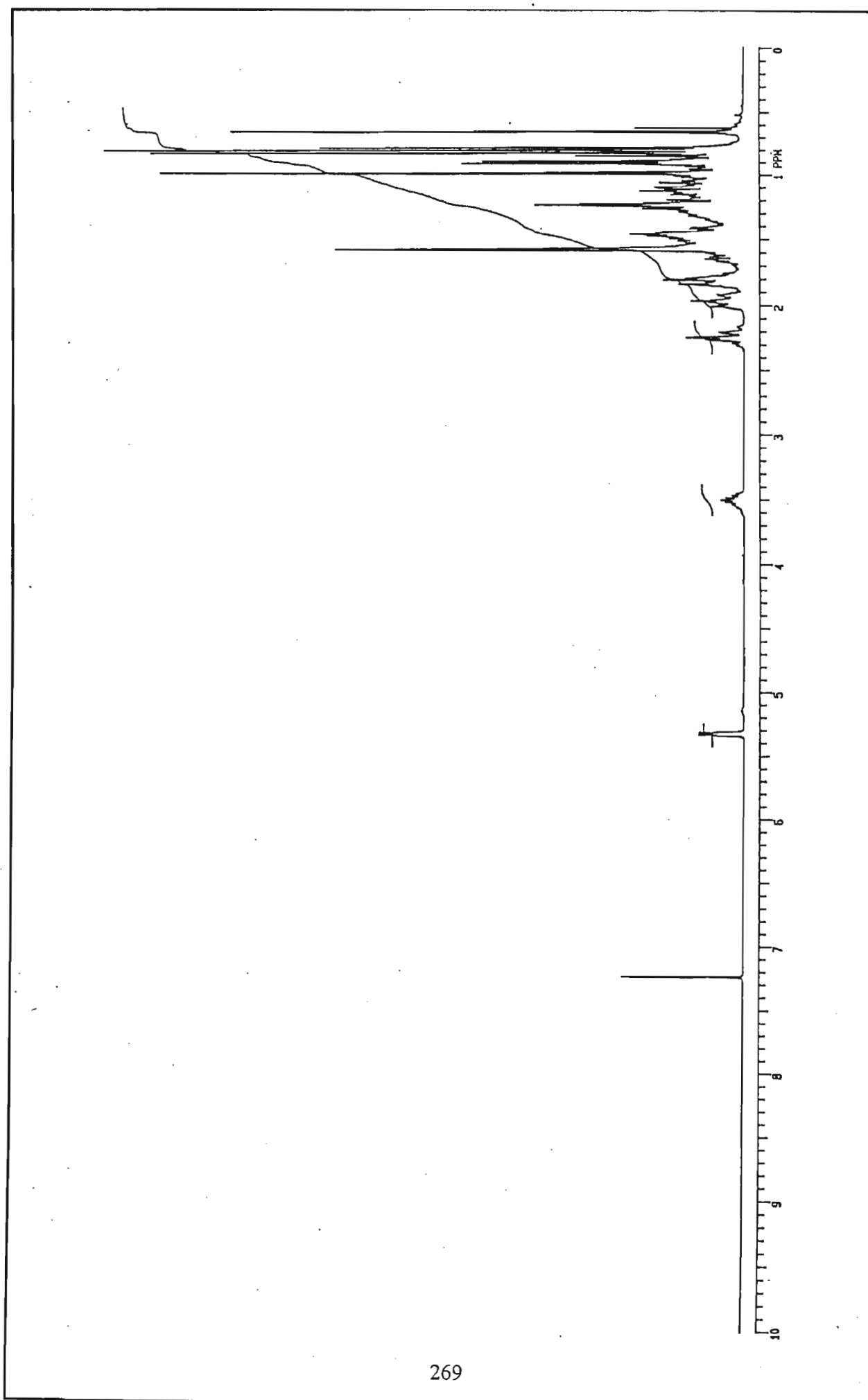
Spectrum 8a	Mass spectrum of [8]	299
8b	Infrared spectrum of [8]	300
8c	¹ H NMR spectrum of [8]	301
8d	COSY spectrum of [8]	302
8e	¹ H NMR spectrum of [8] with D ₂ O	303
8f	NOE spectrum of [8] showing irradiation of methoxy protons	304
8g	NOE spectrum of [8] showing irradiation of H-2	305
Spectrum 9a	Mass spectrum of [9]	306
9b	Infrared spectrum of [9]	307
9c	¹ H NMR spectrum of [9]	308
9d	¹³ C NMR spectrum of [9]	309
9e	HETCOR spectrum of [9]	310
9f	NOE spectrum of [9] showing irradiation of H-1''	311
9g	NOE spectrum of [9] showing irradiation of chemically equivalent H-3' and H-5'	312



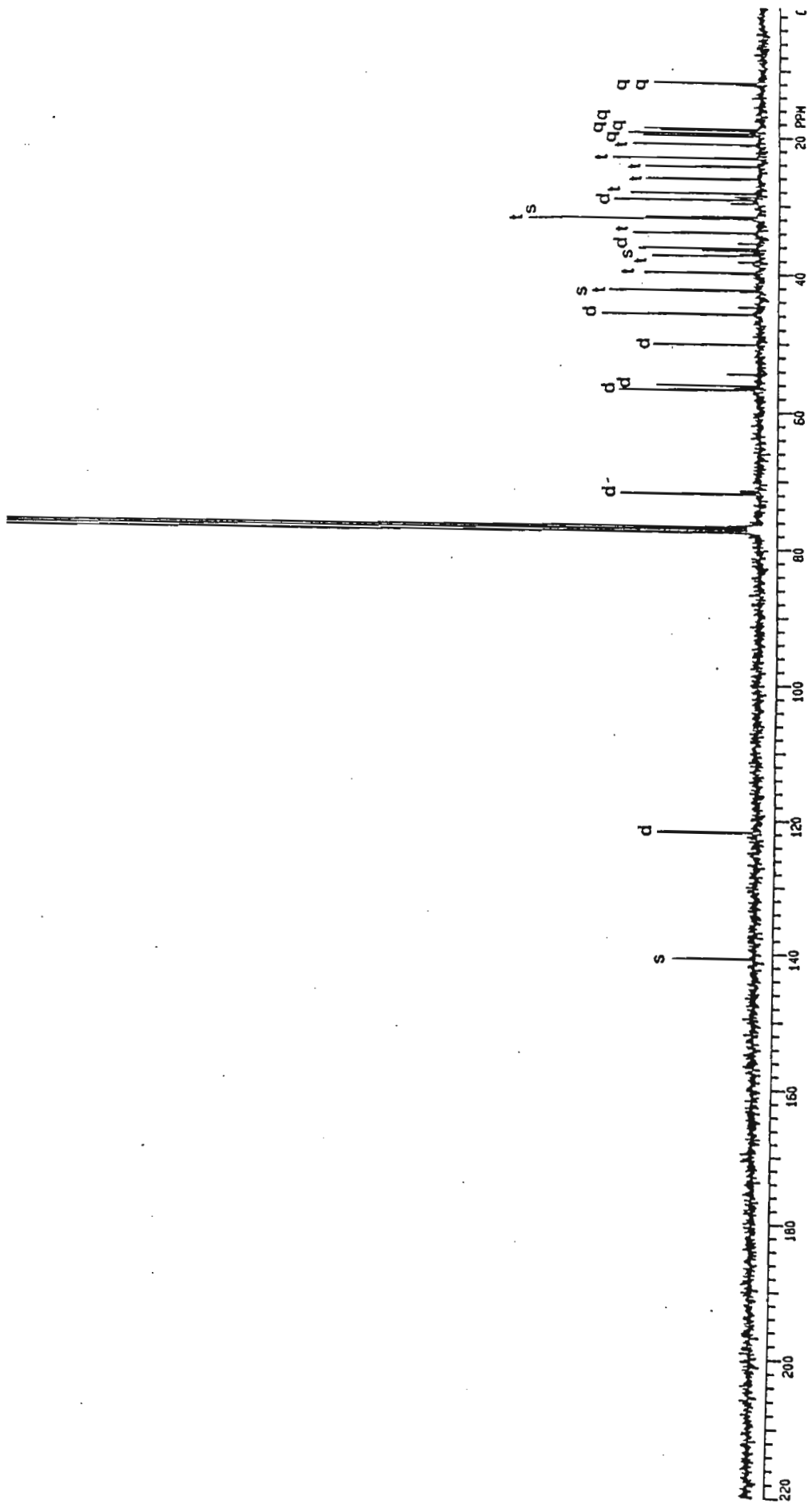
Spectrum 1a: Mass spectrum of [1]

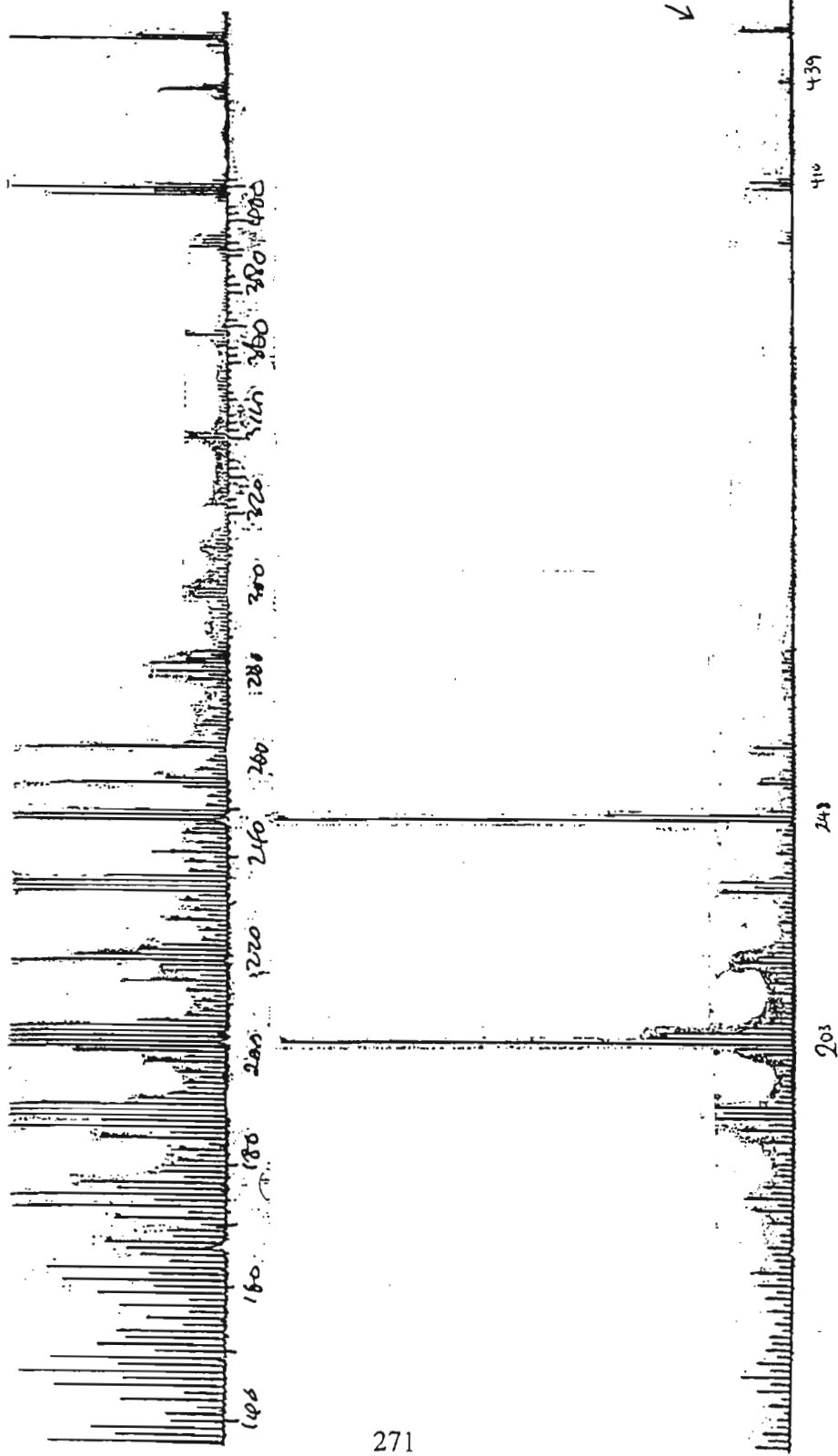


Spectrum 1b: Infrared spectrum of [1]

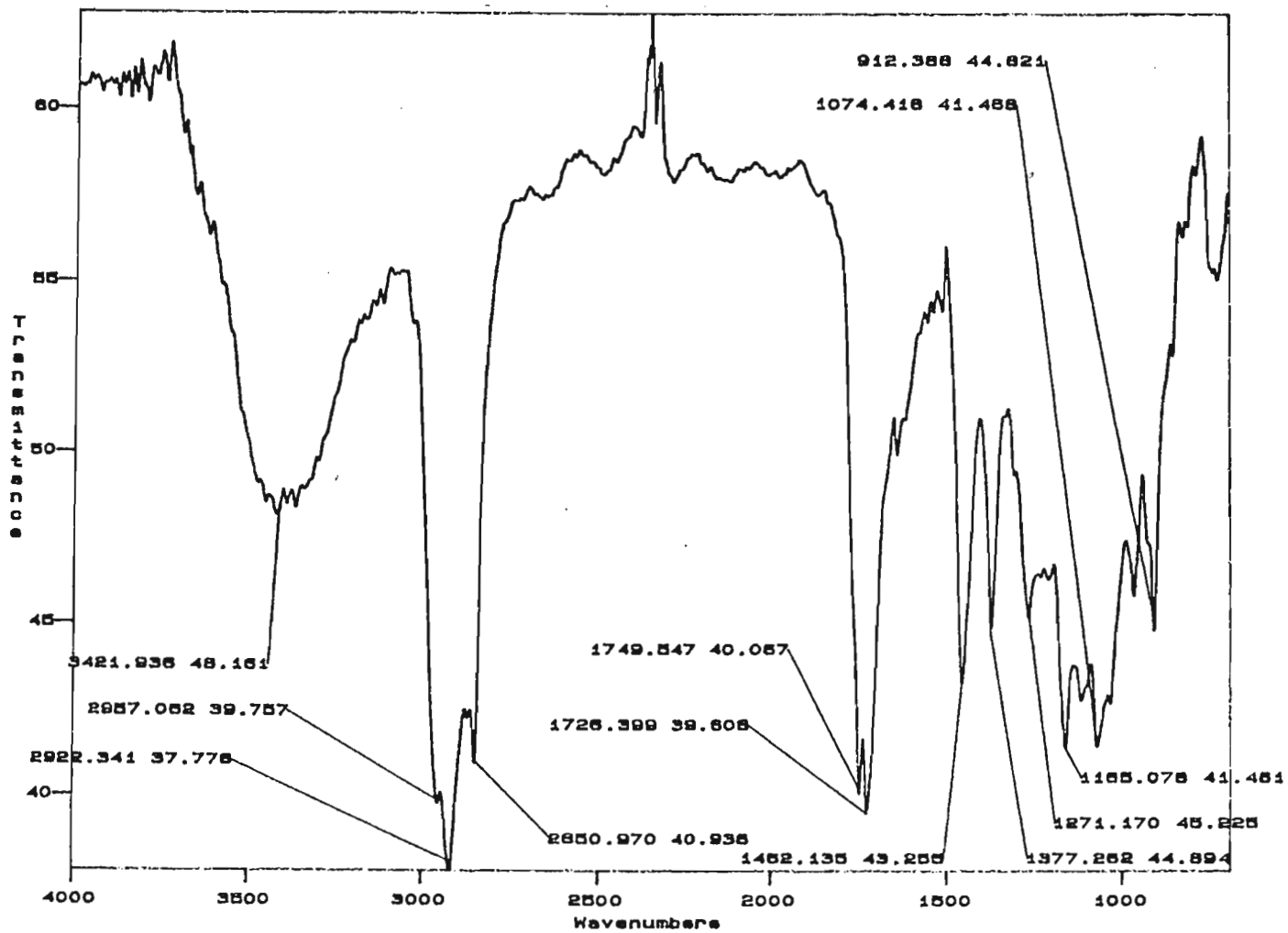


Spectrum 1c: ¹H NMR spectrum of [1]

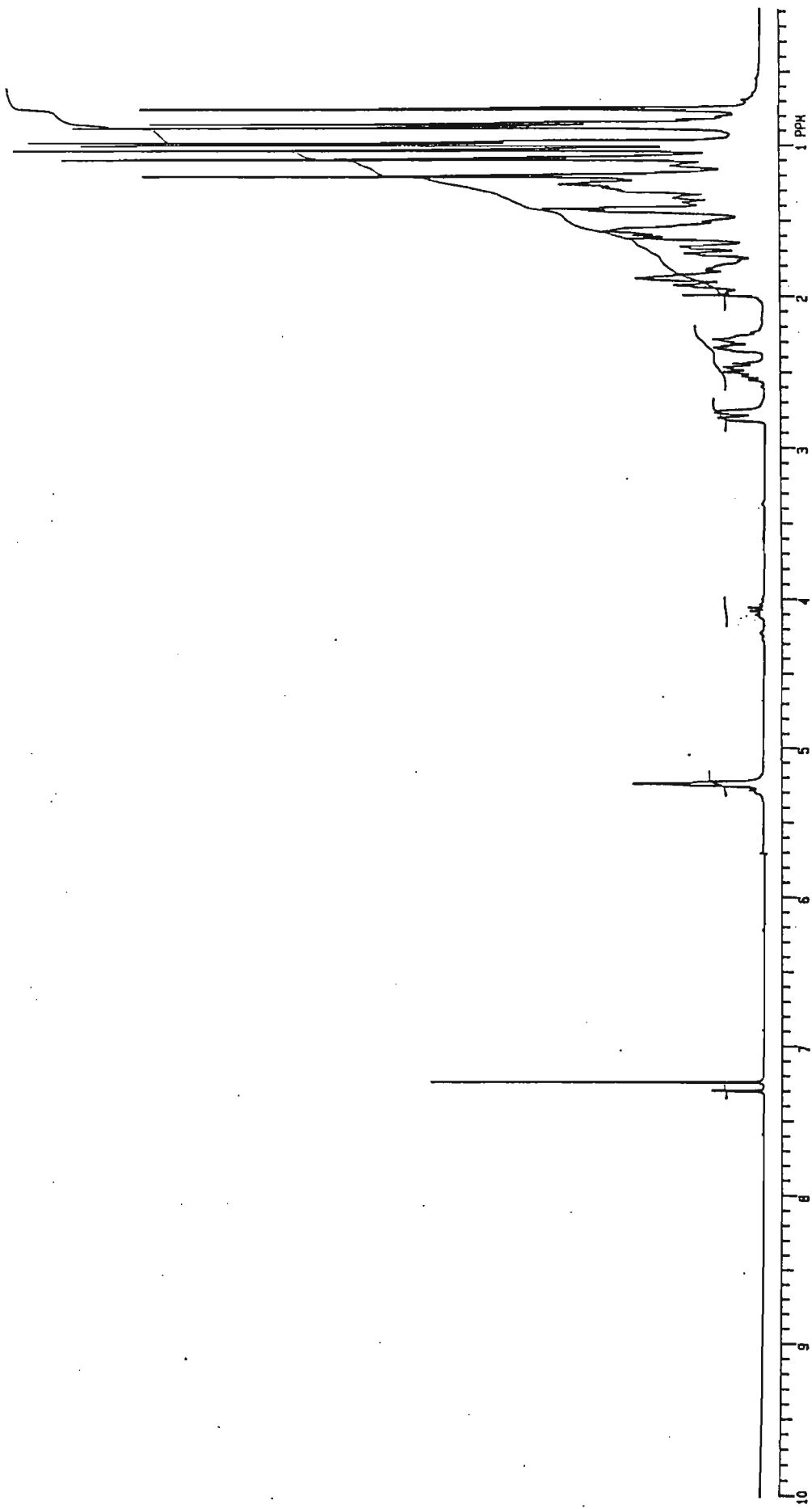




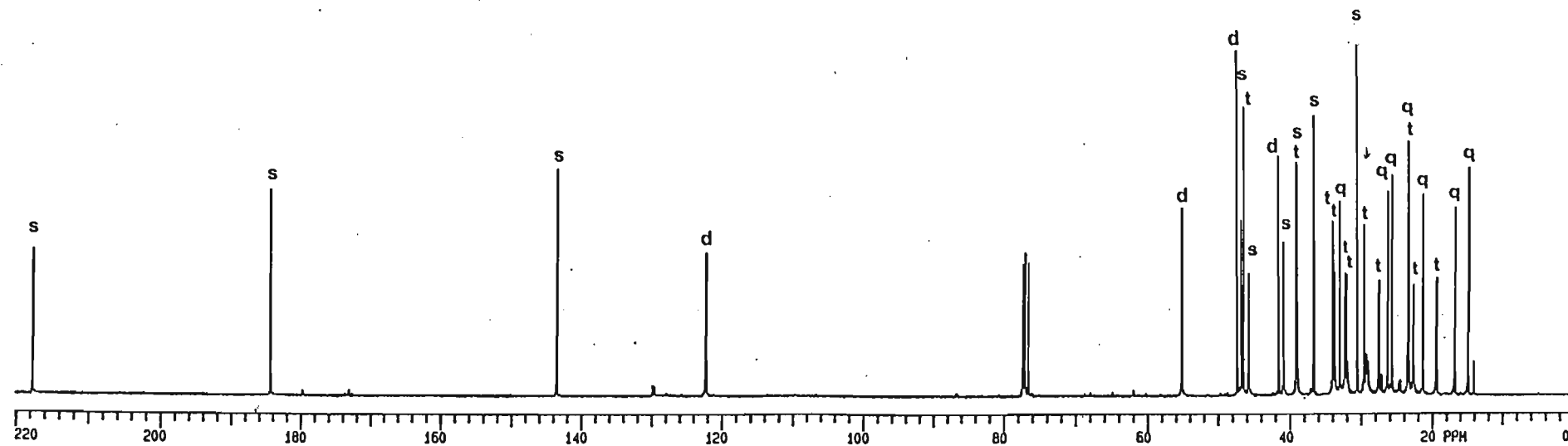
454.3471
 ↓ 454.3447
 ≡ C₃₀H₄₆O₃



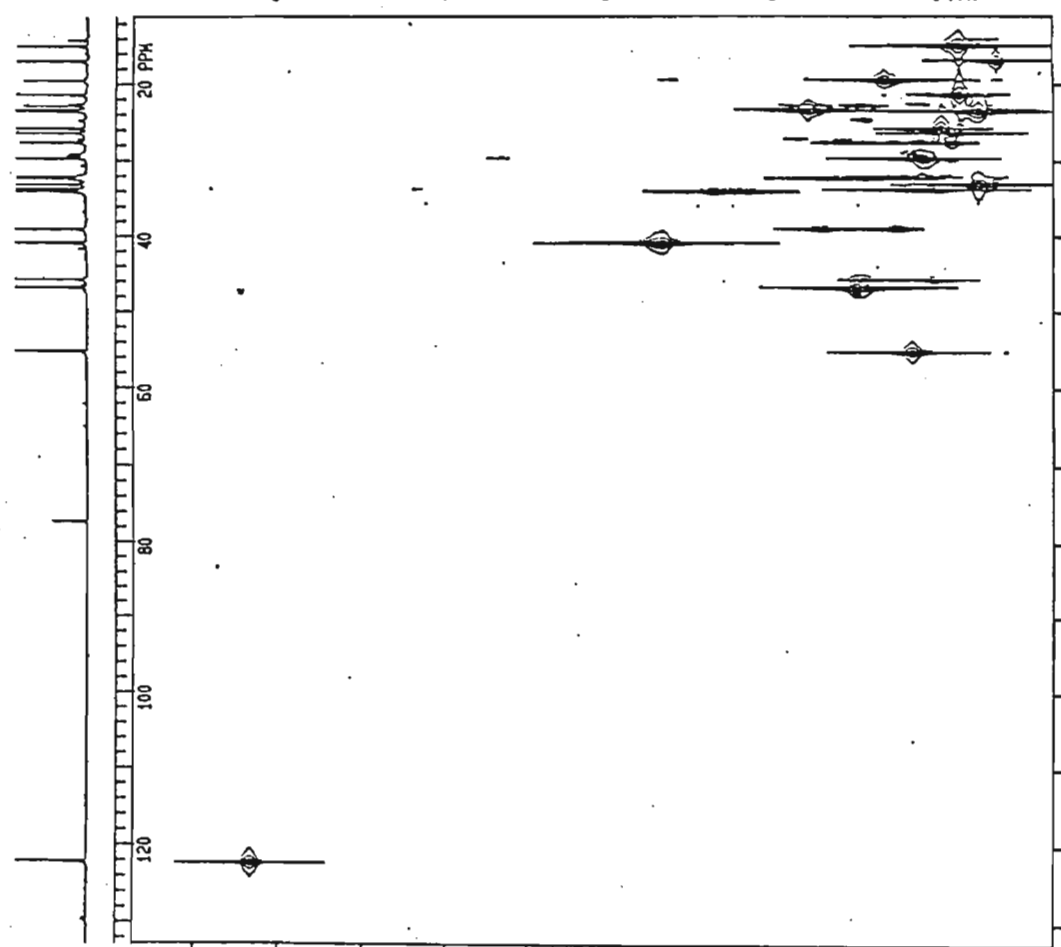
Spectrum 2b: Infrared spectrum of [2]

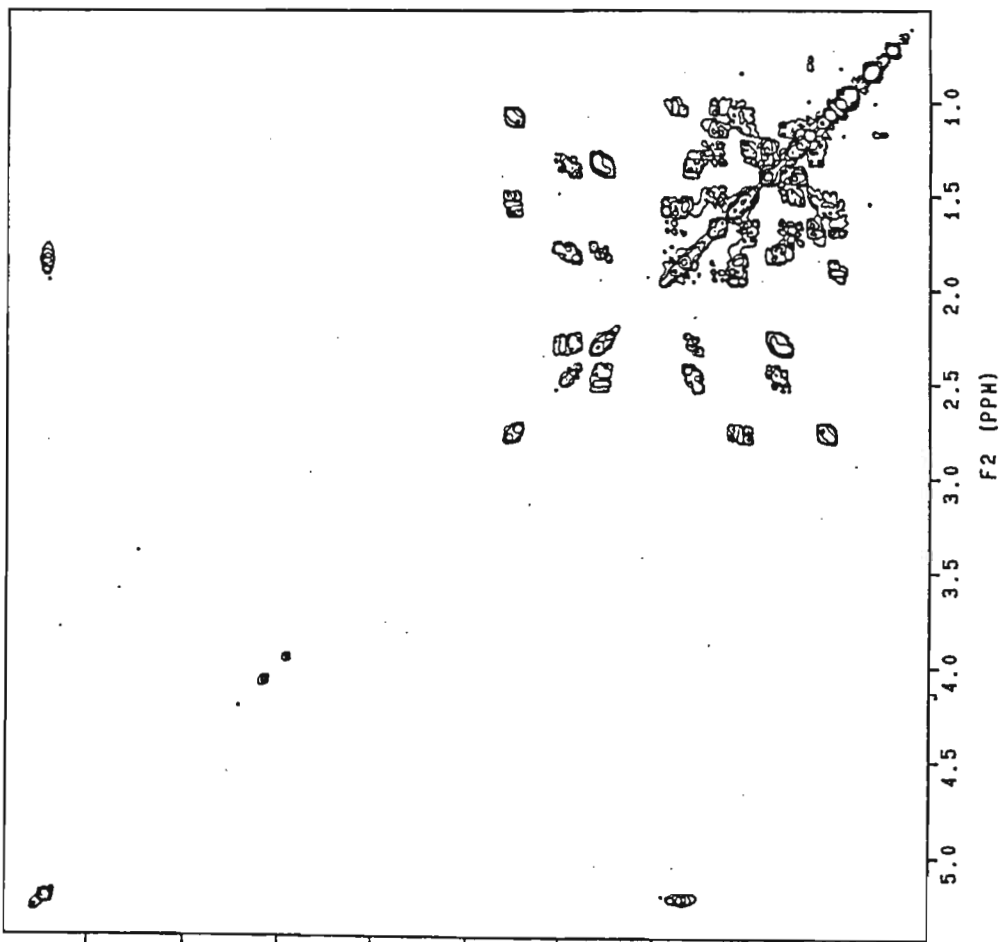
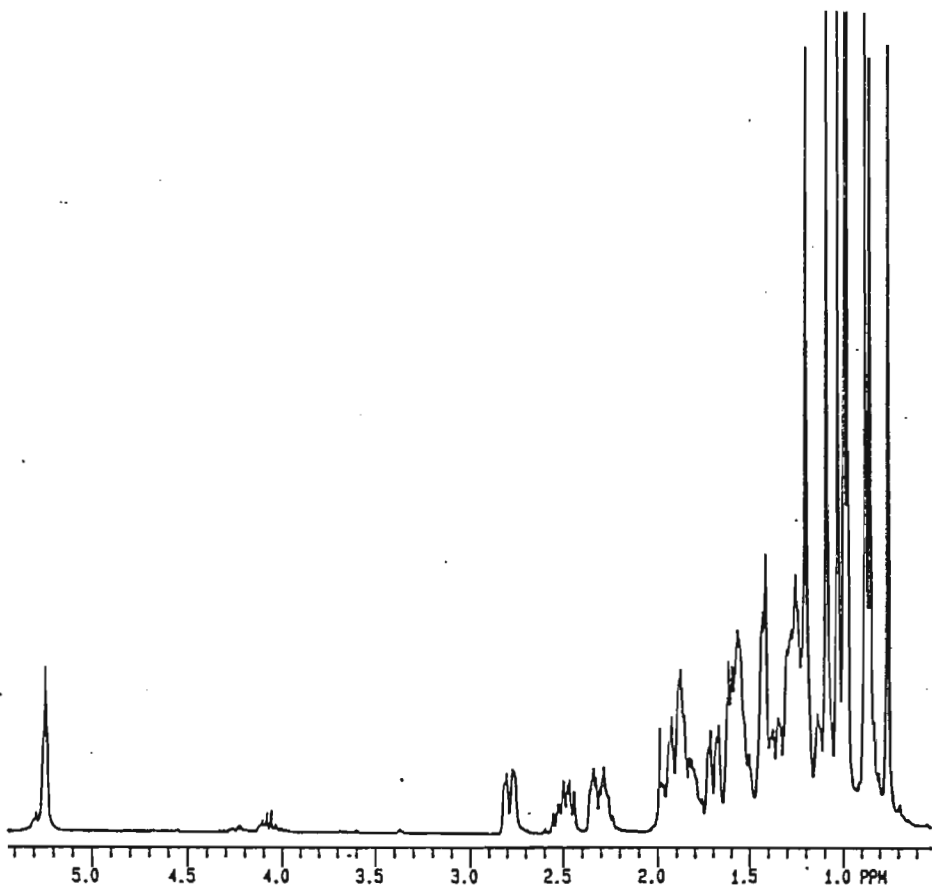


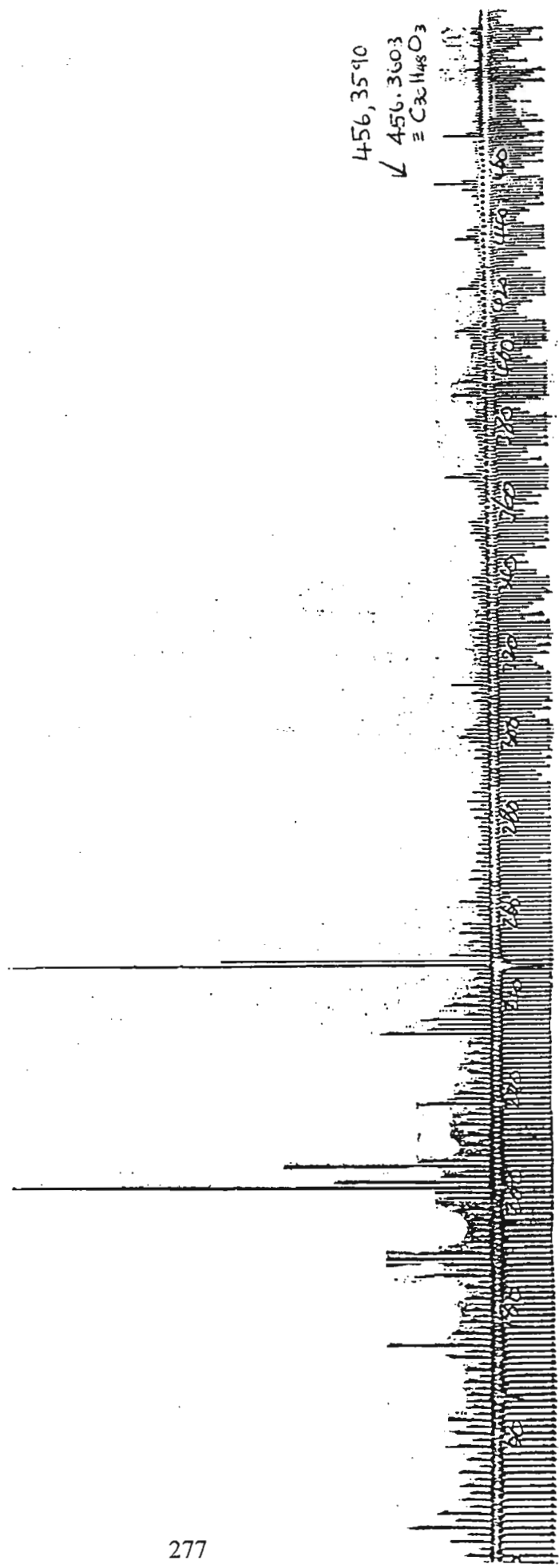
274



Spectrum 2d: ^{13}C NMR spectrum of [2]



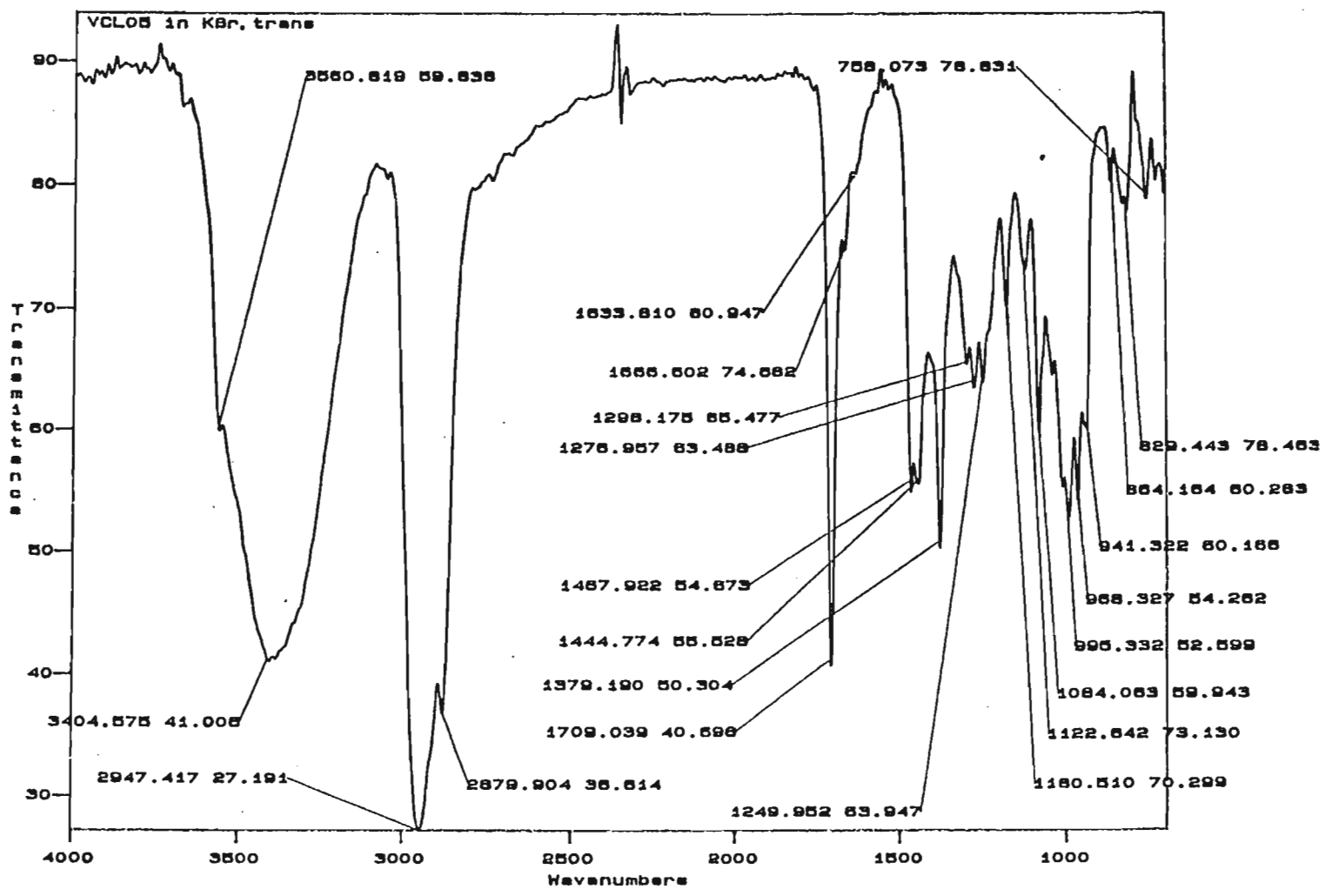




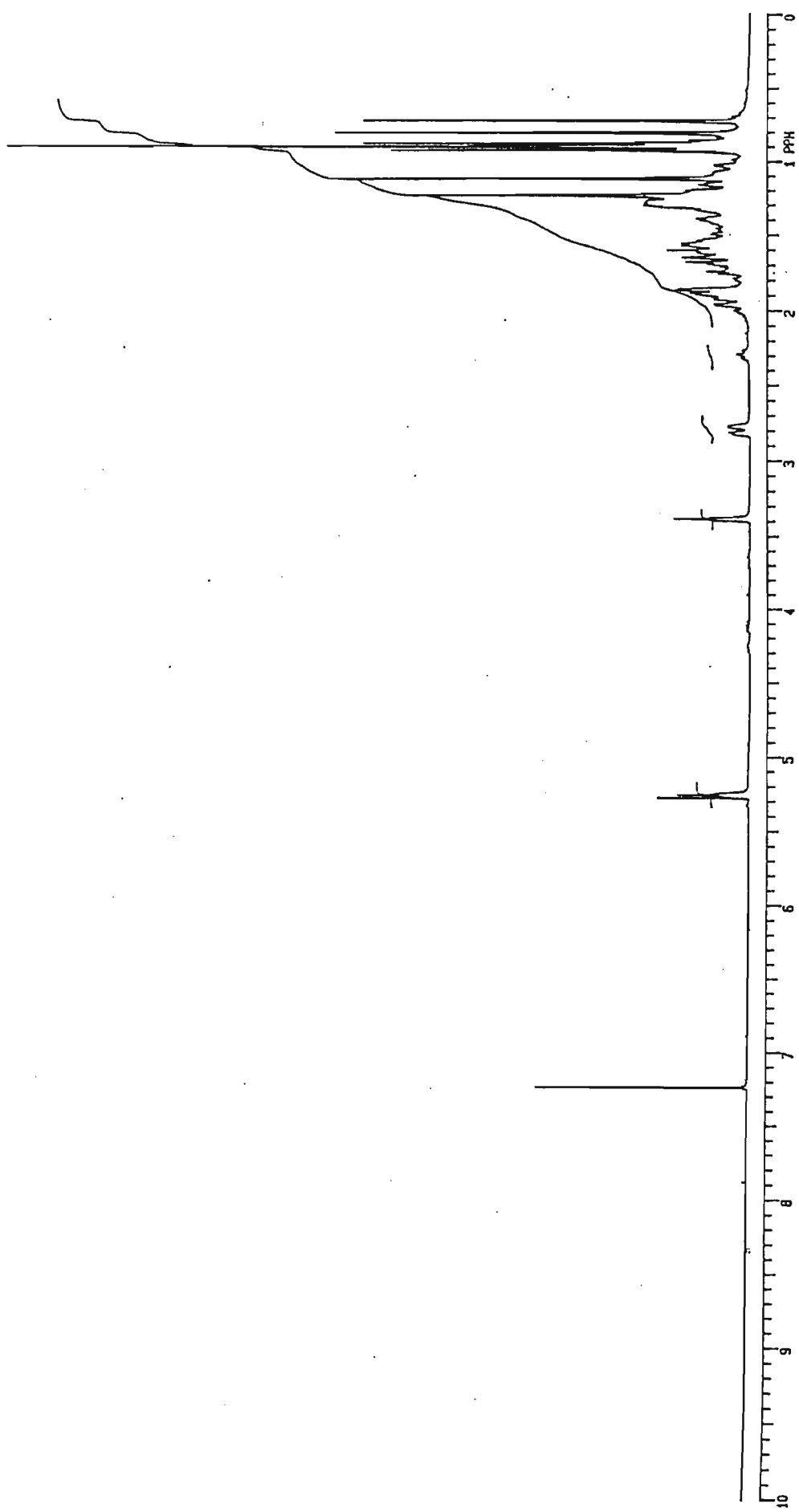
456, 3590
✓ 456, 3603
≡ C₃₅H₄₈O₃

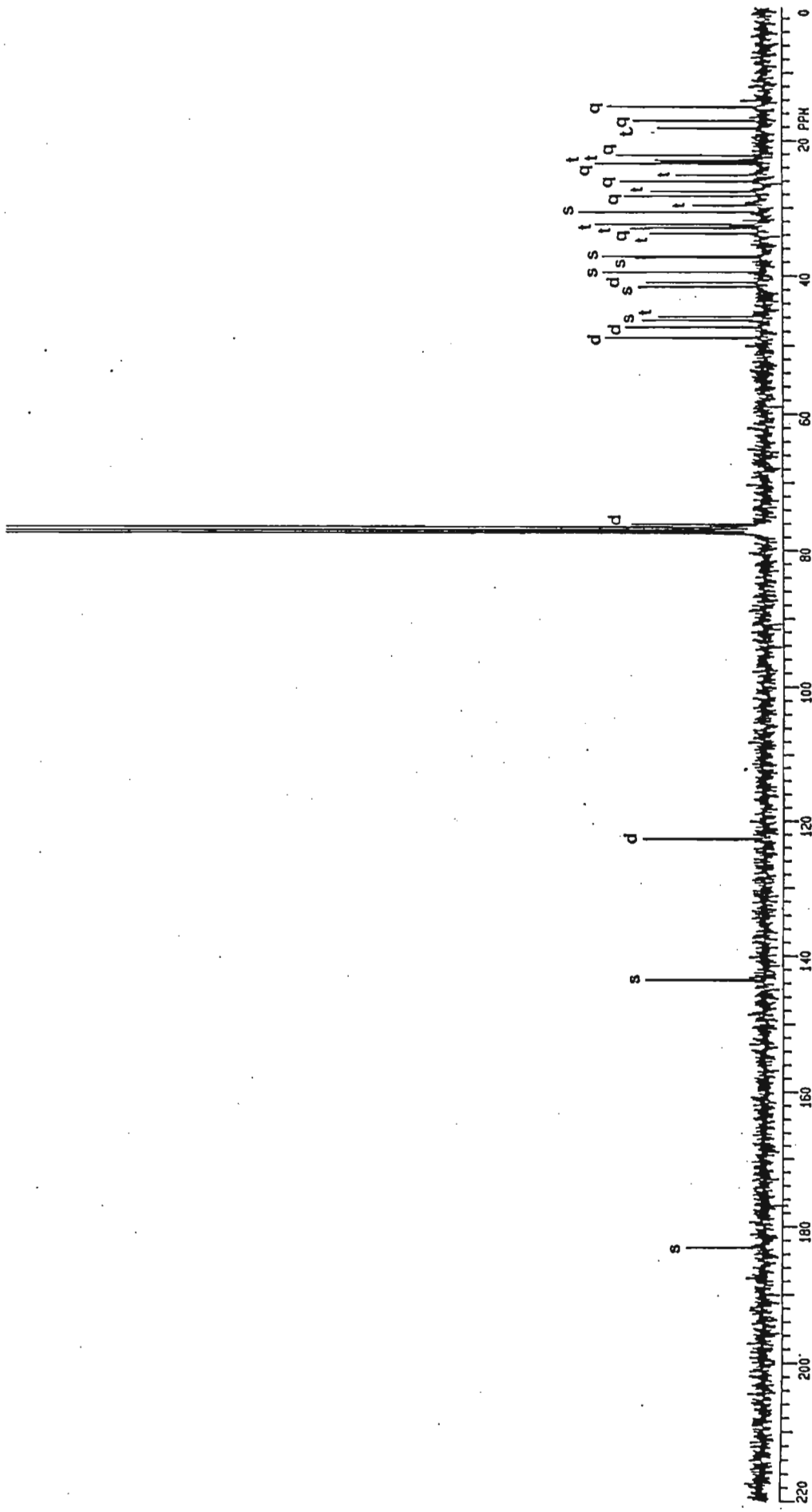
Spectrum 3a: Mass spectrum of [3]

278

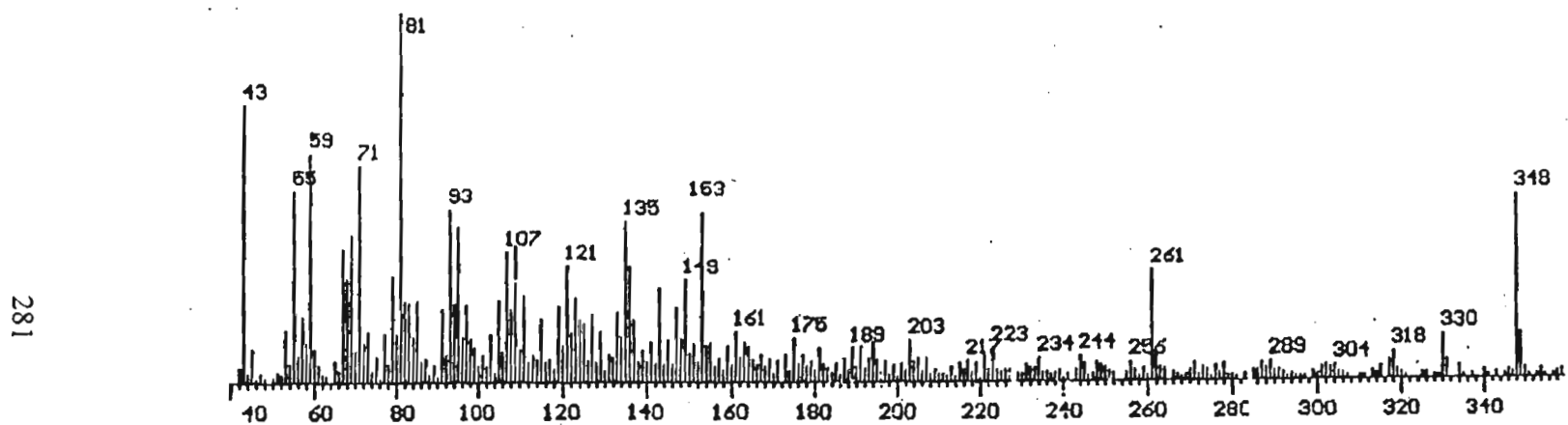


Spectrum 3b: Infrared spectrum of [3]

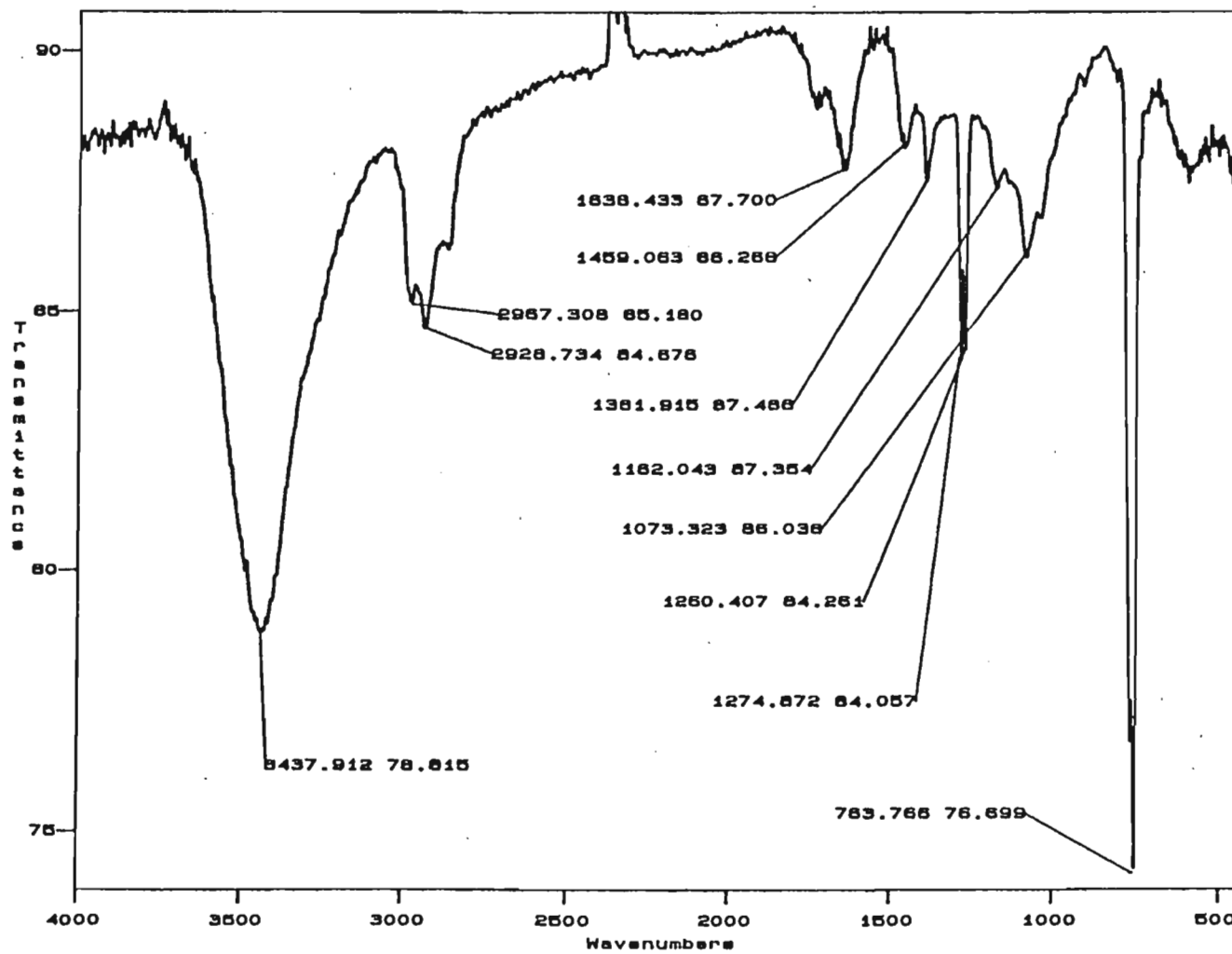




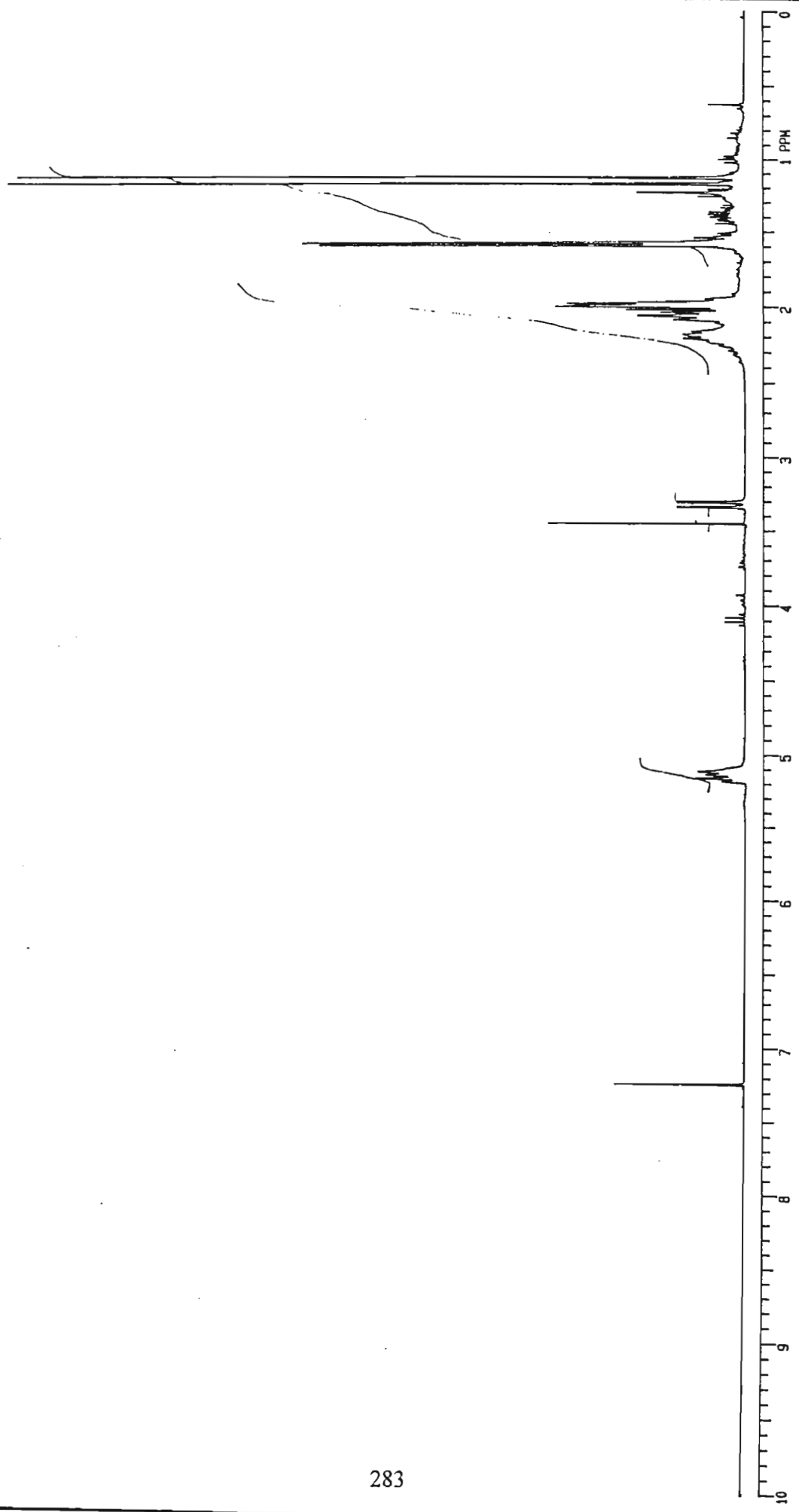
Spectrum 3d: ¹³C NMR spectrum of [3]

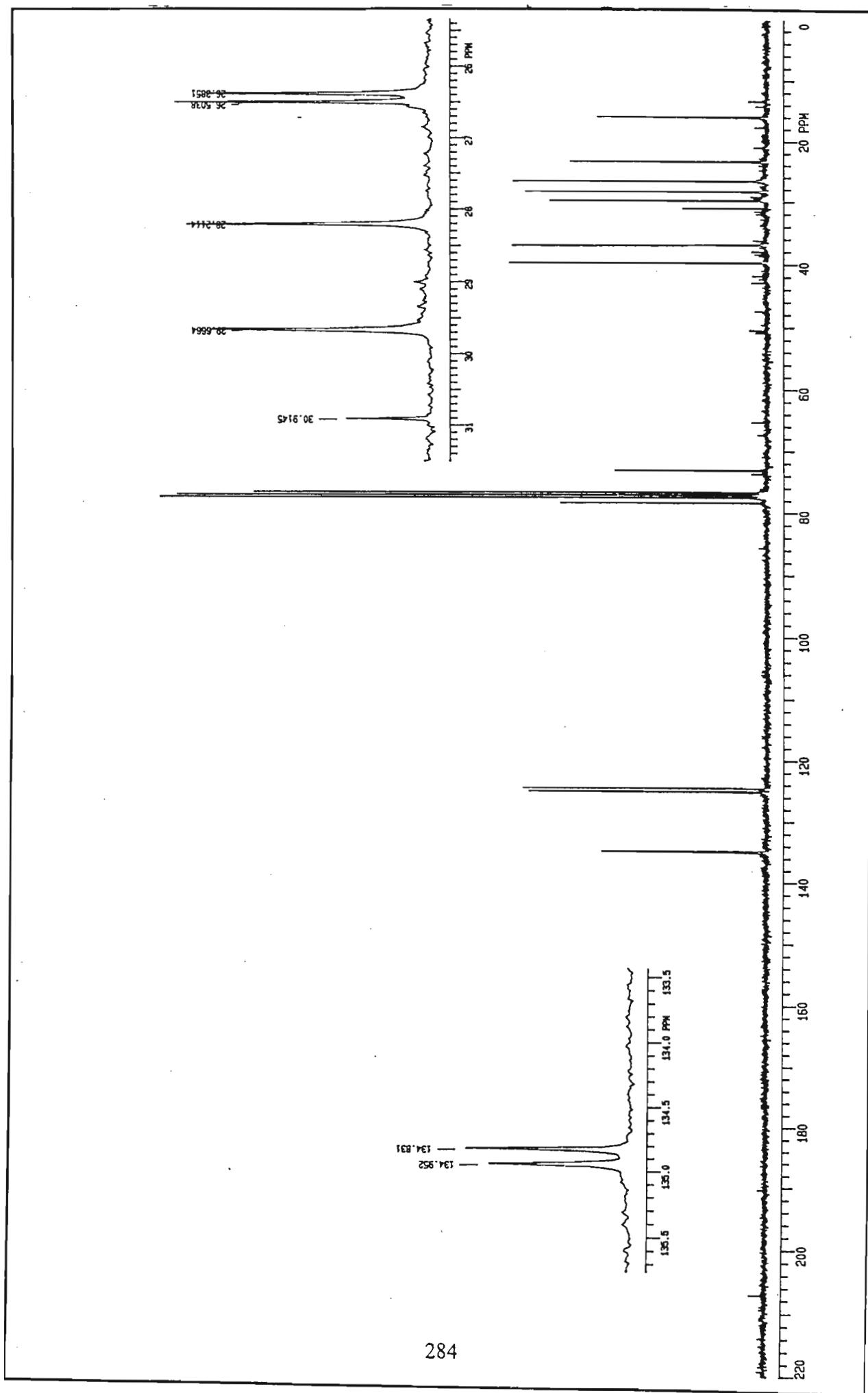


Spectrum 4a: Mass spectrum of [4]



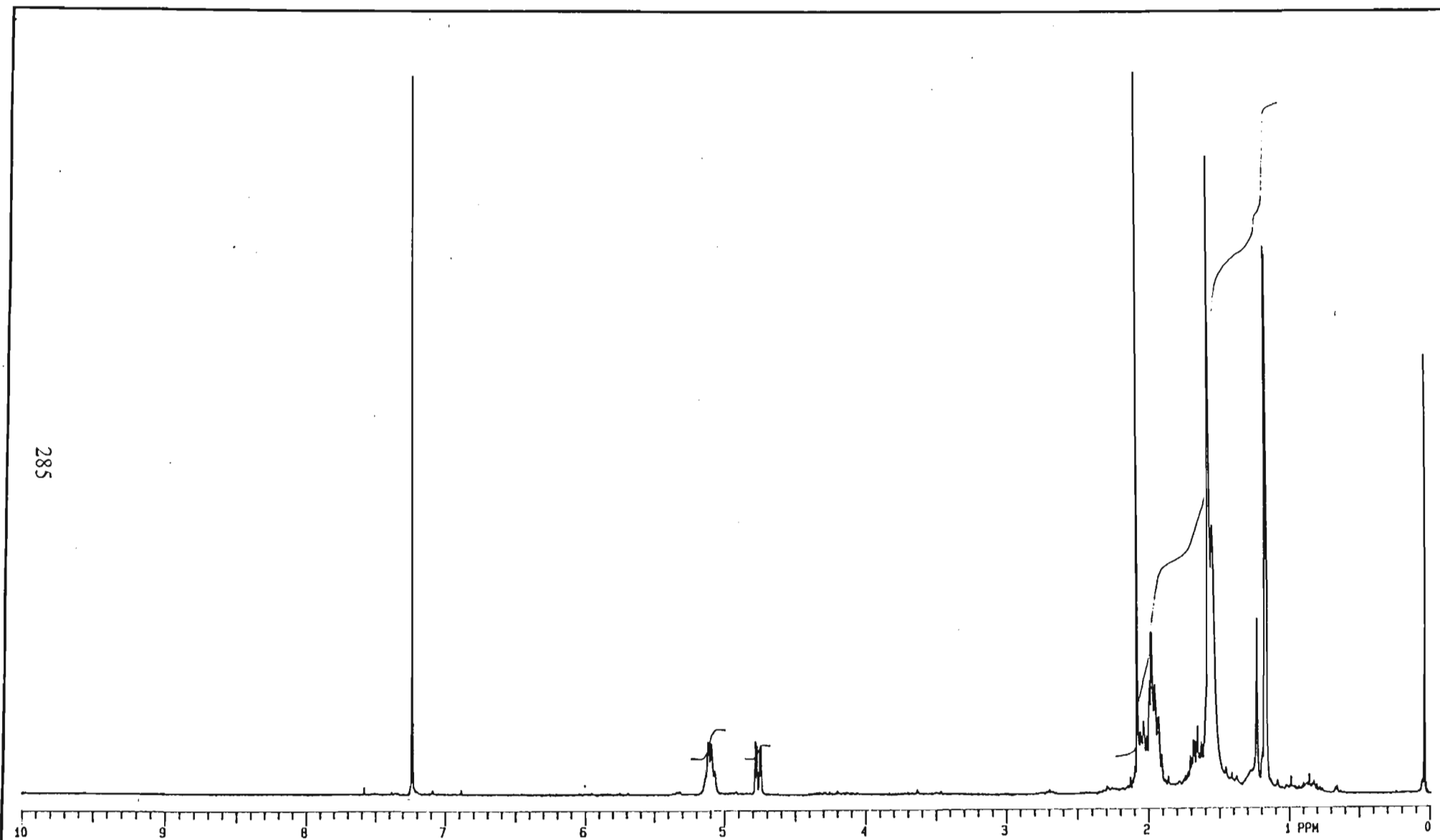
Spectrum 4b: Infrared spectrum of [4]





284

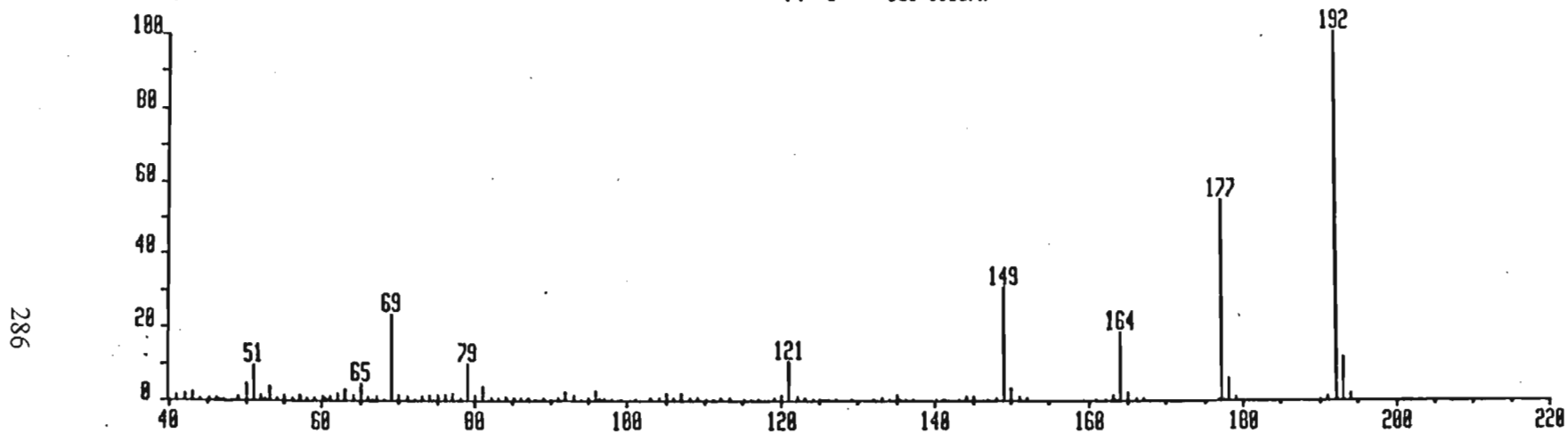
Spectrum 4d: ^{13}C NMR spectrum of [4]



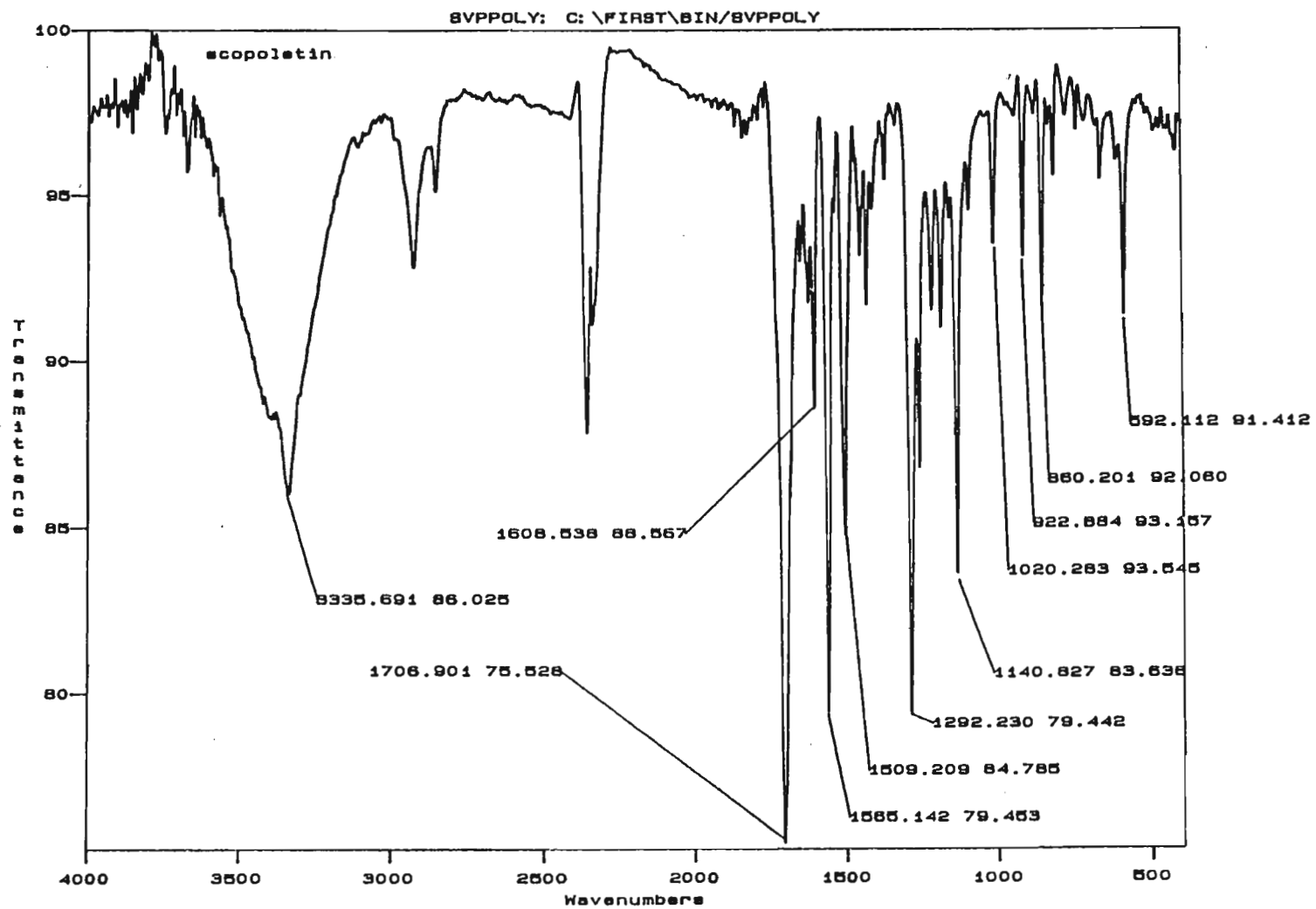
Spectrum 4e: ^1H NMR spectrum of **4b**

VFR179P114 x1 Bgd=1 12-OCT-97 14:04+0:02:07 70-250SEQ EI+
BpM=0 I=4.9v Hm=0 TIC=116699000 Acnt: Sys:SYSTEMDEF
2 PT= 0° Cal:11097A

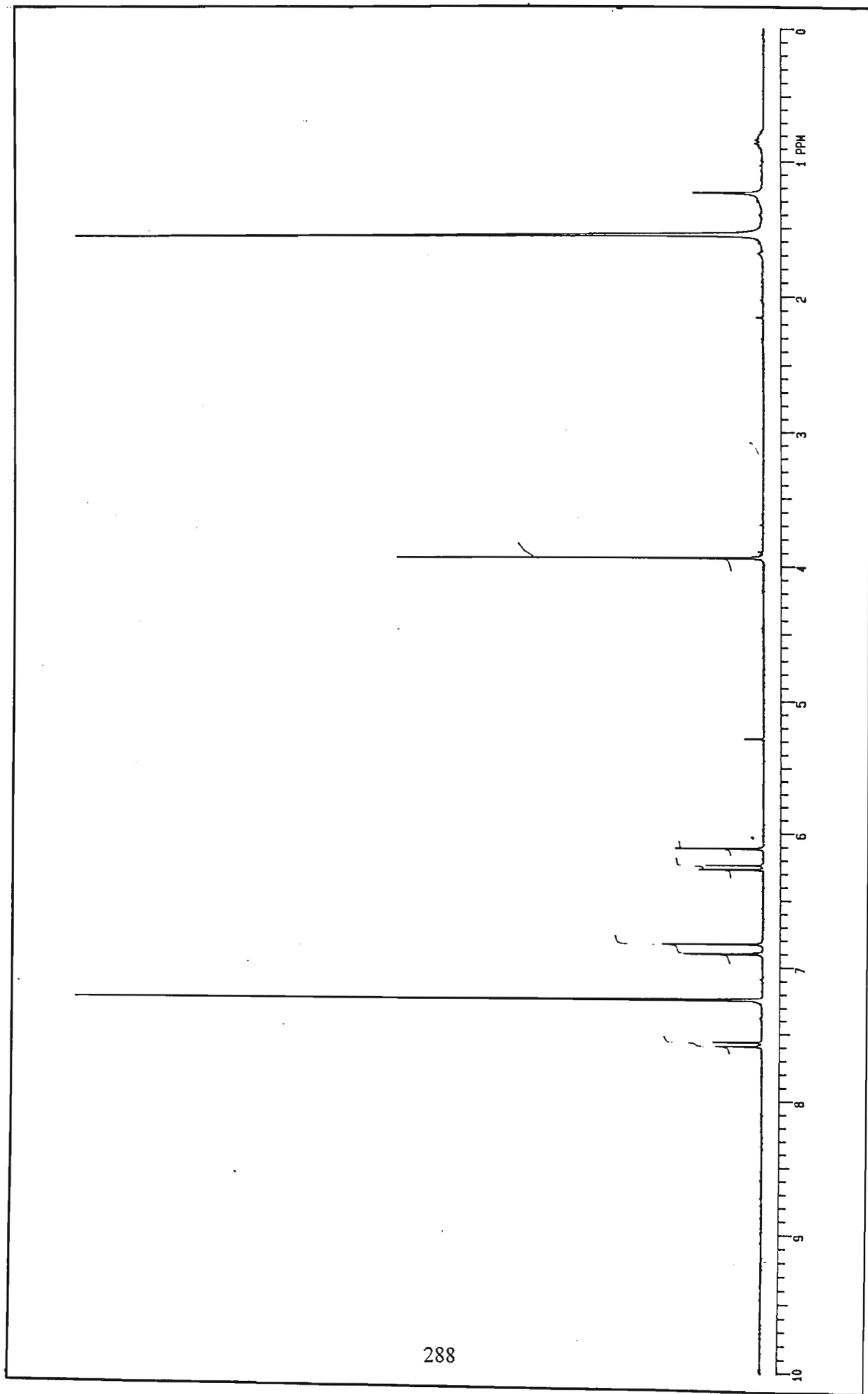
HMR: 32303000
MASS: 192



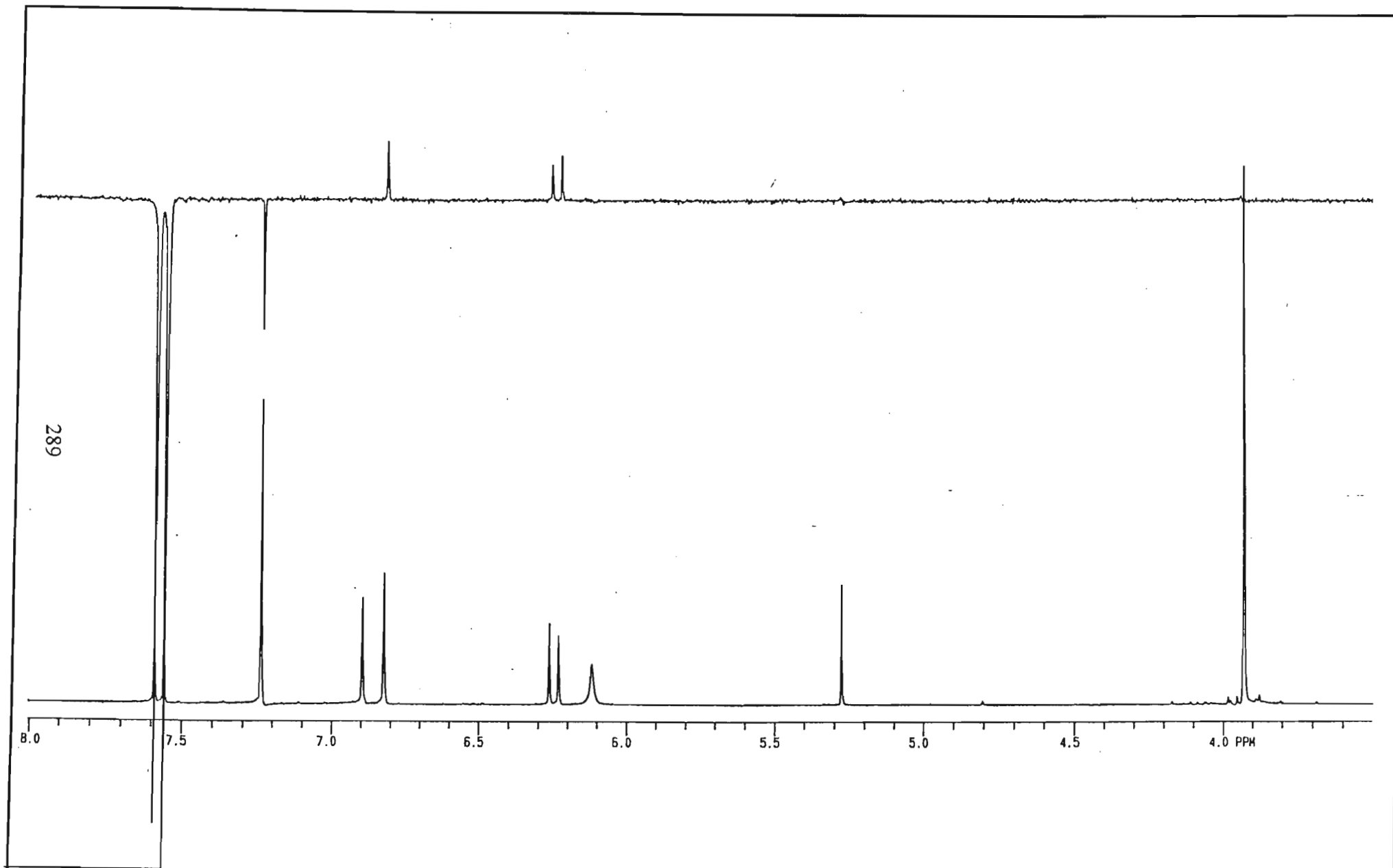
Spectrum 5a: Mass spectrum of [5]



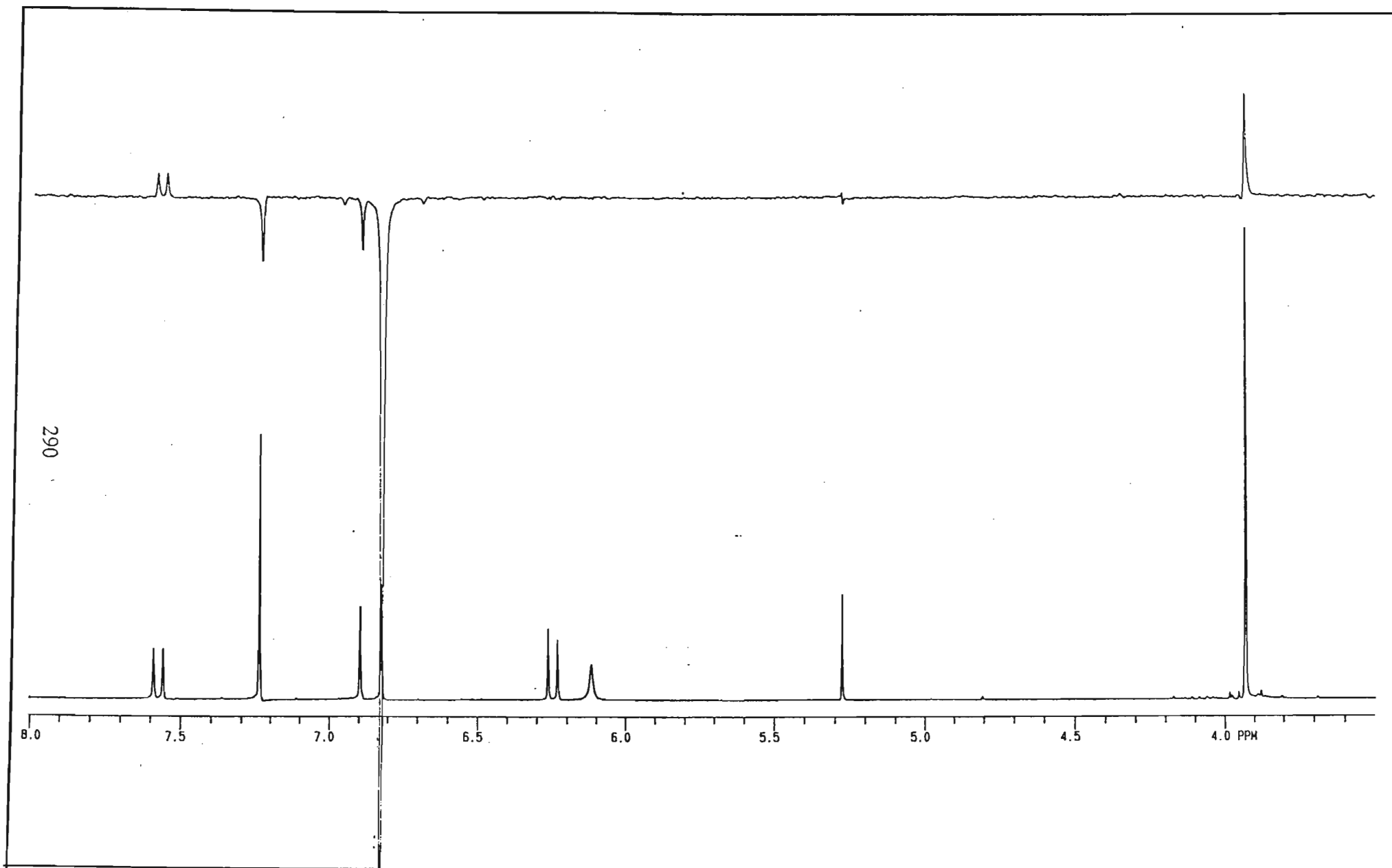
Spectrum 5b: Infrared spectrum of [5]



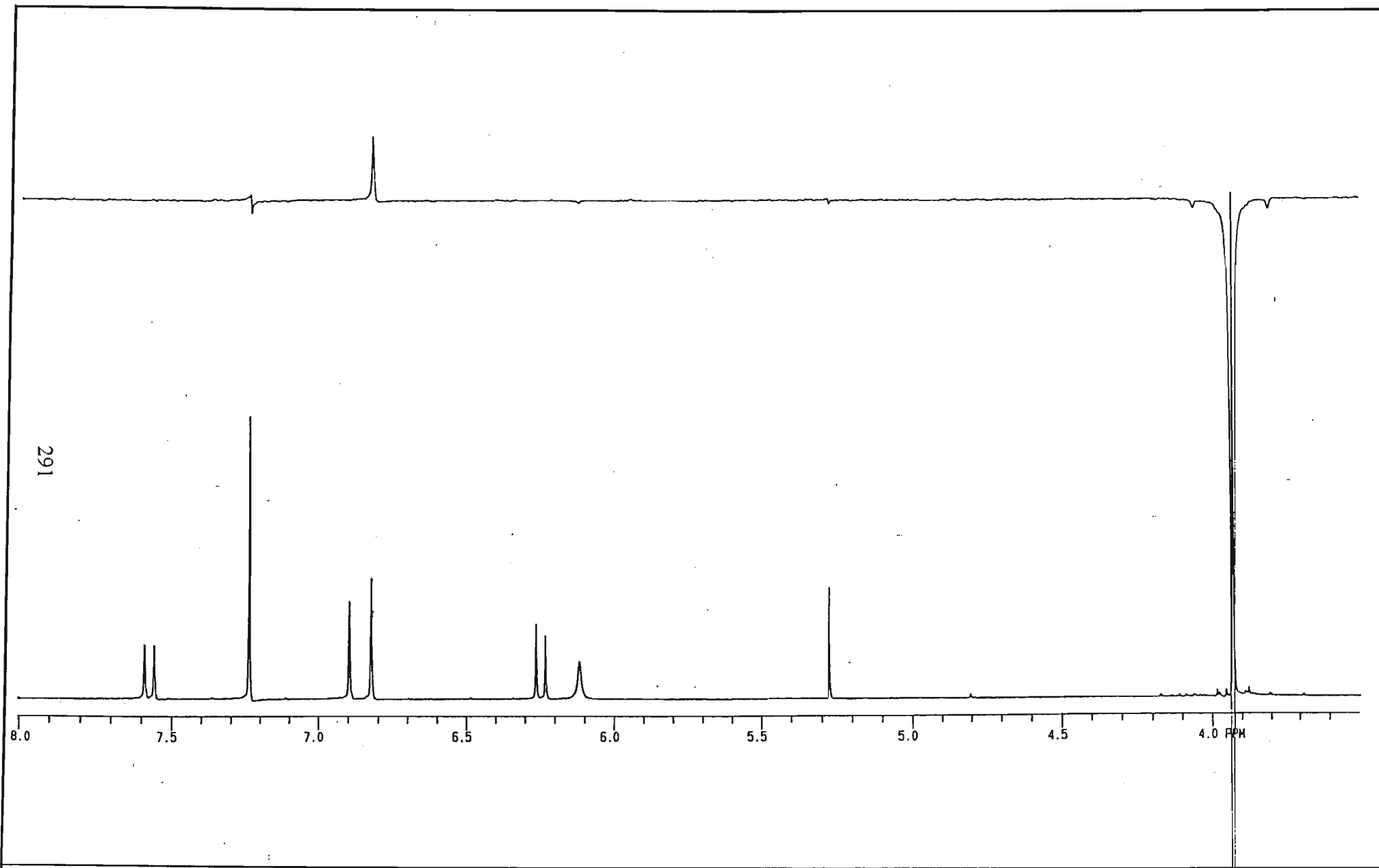
Spectrum 5c: ^1H NMR spectrum of [5]



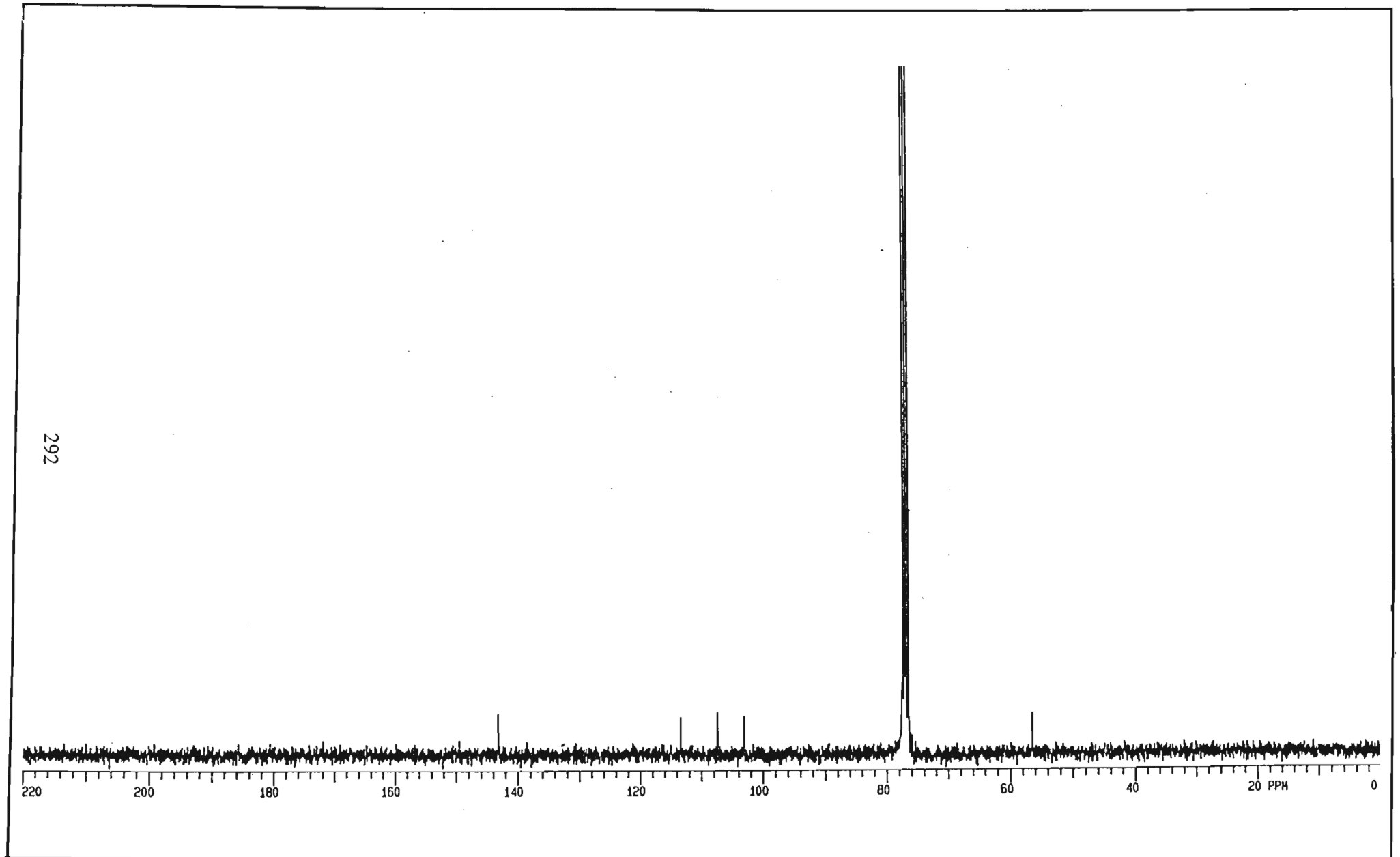
Spectrum 5d: NOE spectrum of [5] showing irradiation of H-4



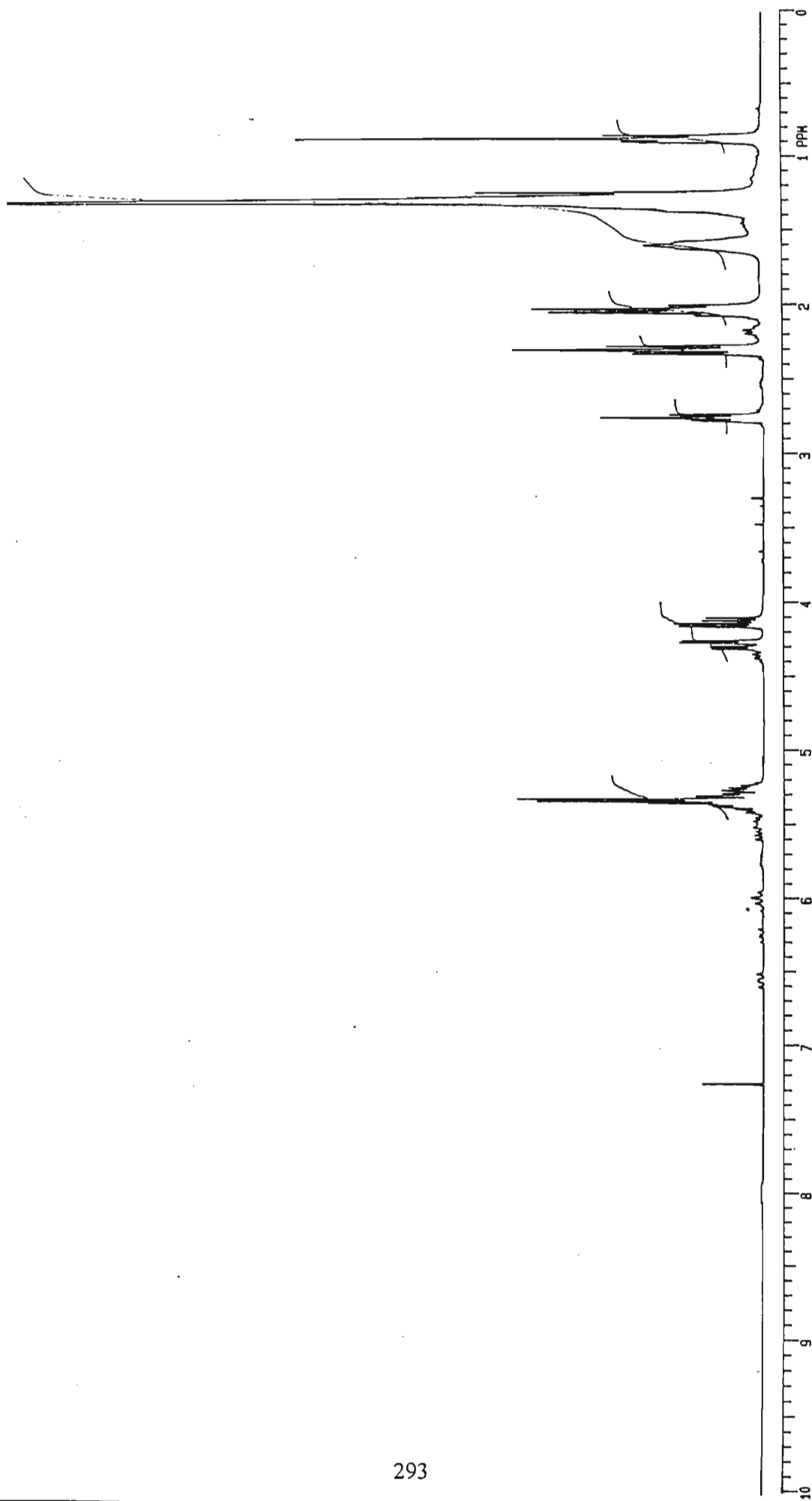
Spectrum 5e: NOE spectrum of [5] showing irradiation of H-5



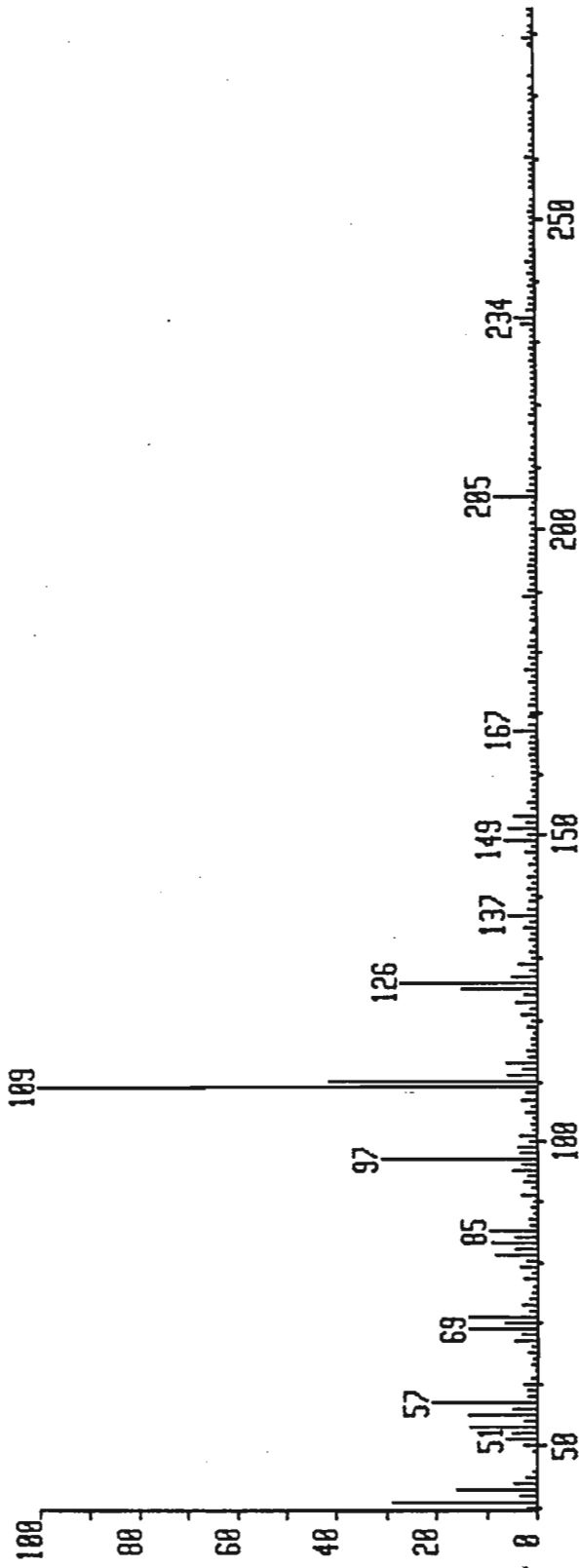
Spectrum 5f: NOE spectrum of [5] showing irradiation of methoxy group protons



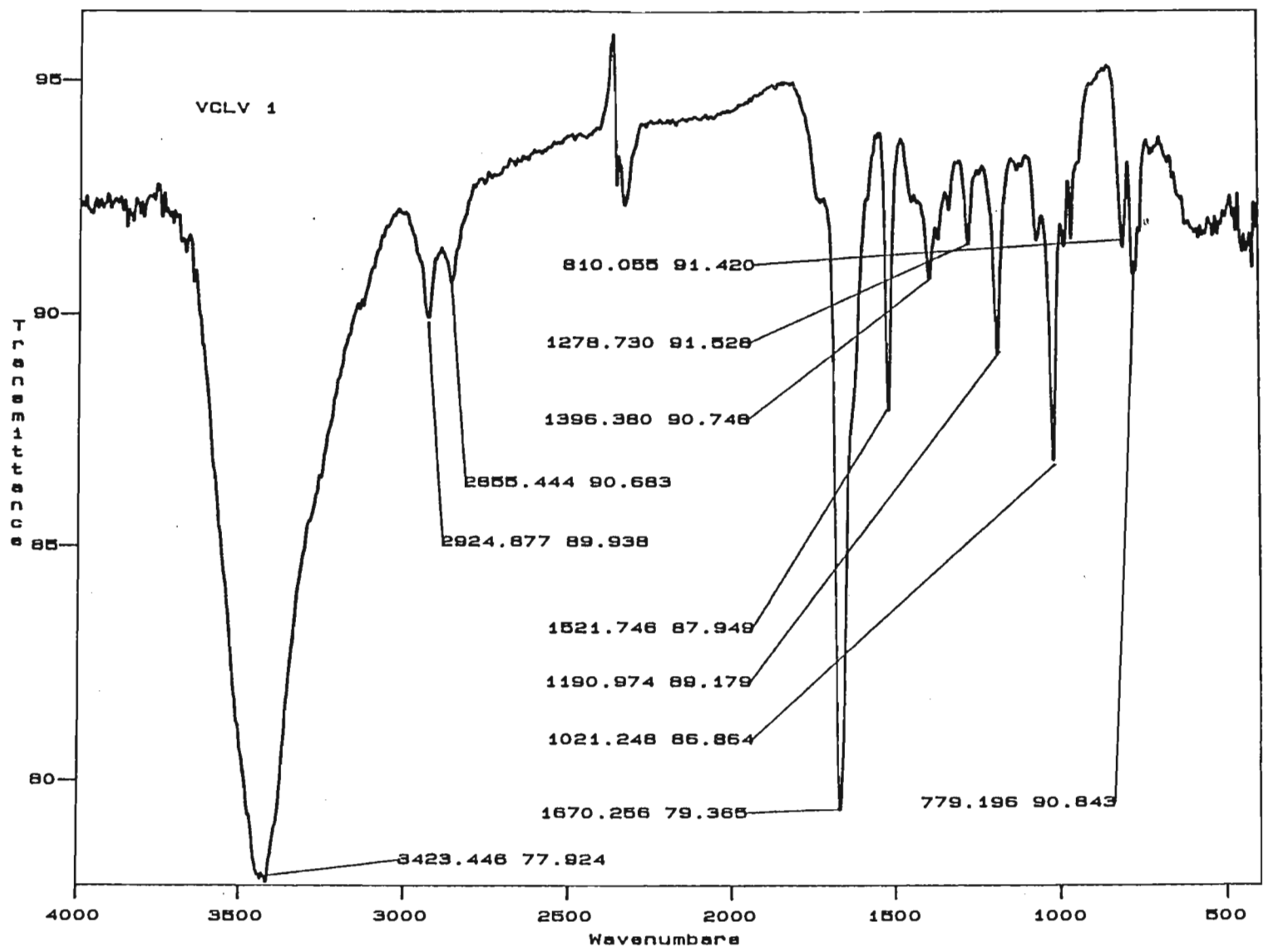
Spectrum 5g: ^{13}C NMR spectrum of [5]



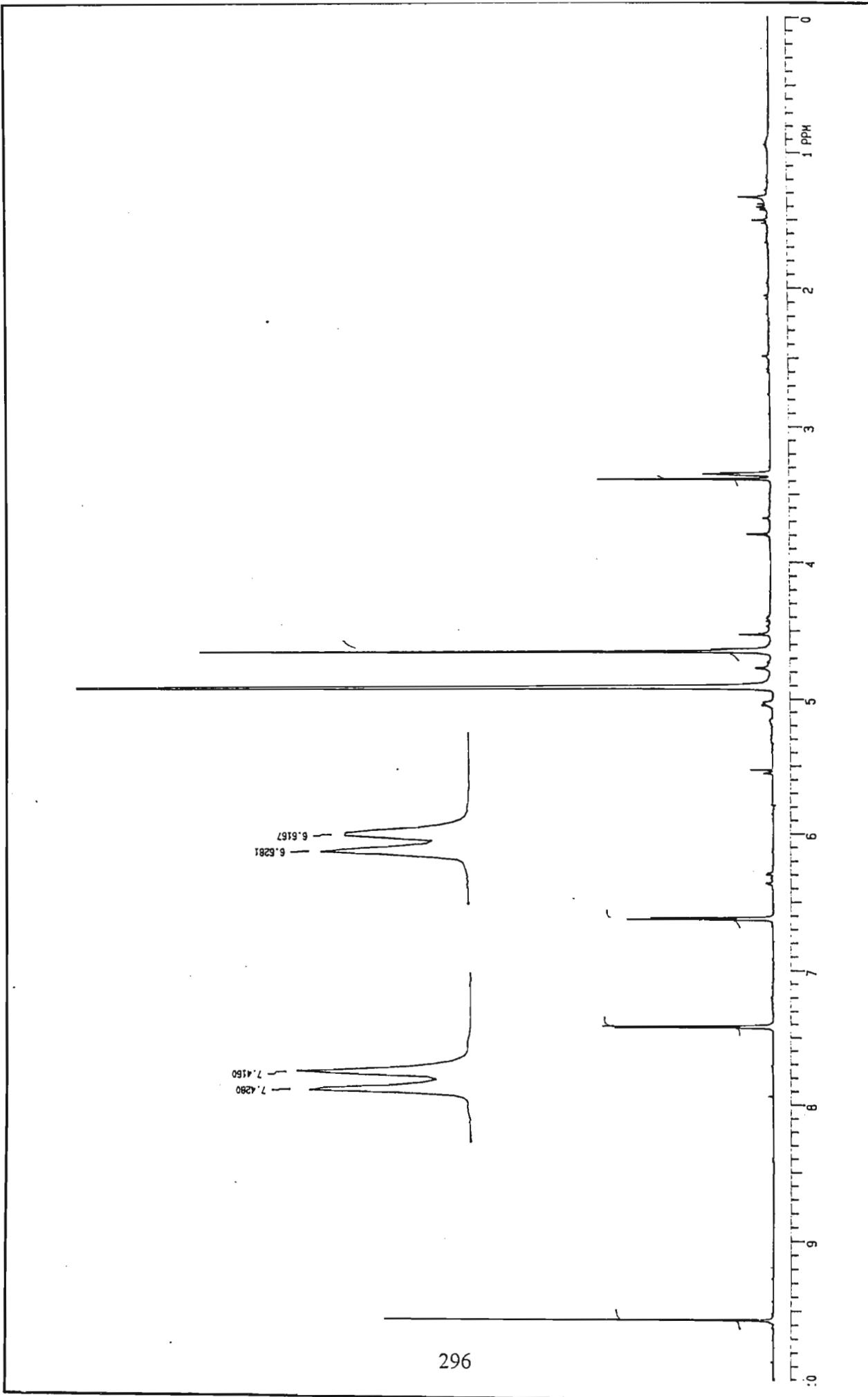
00H2#44 x1 Bgd=37 12-OCT-97 16:45:06:05 70-250SEQ EI+
BpM=0 I=1.4v Hm=8 TIC=63406888 Acnt: Sys:SYSTEMDEF
2 PT= 0° Cal: 11097A



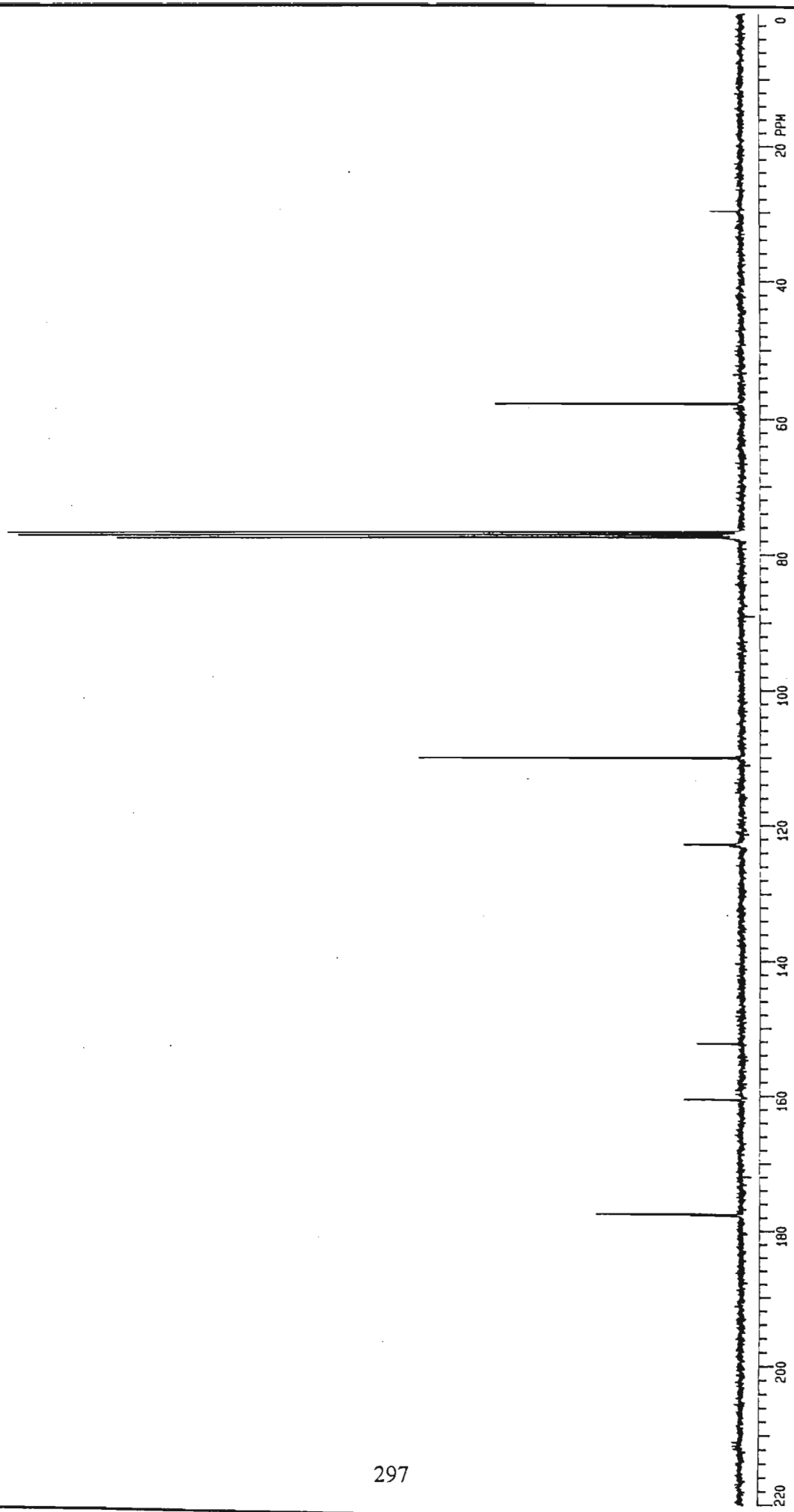
295



Spectrum 7b: Infrared spectrum of [7]

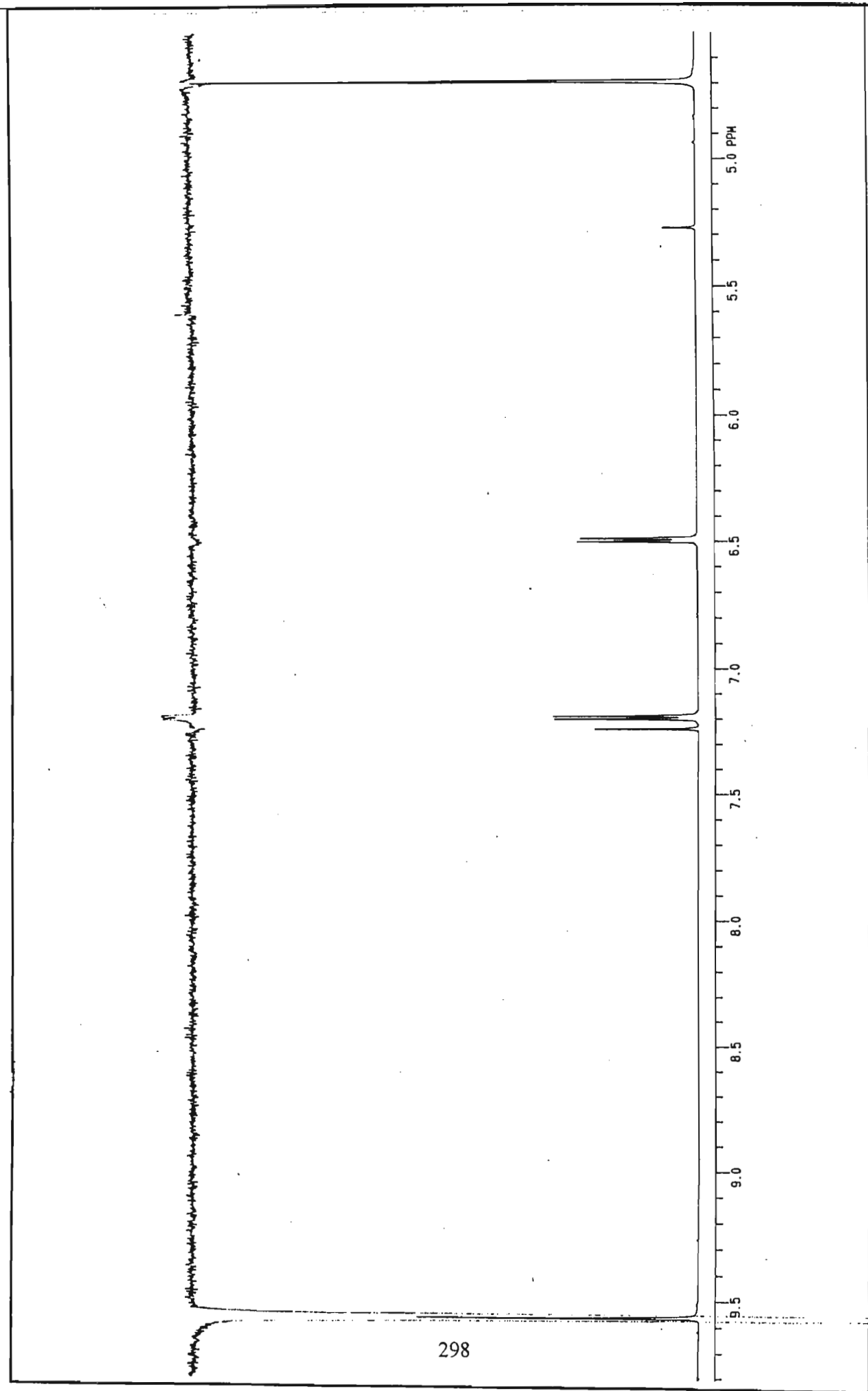


Spectrum 7c: ^1H NMR spectrum of [7]



297

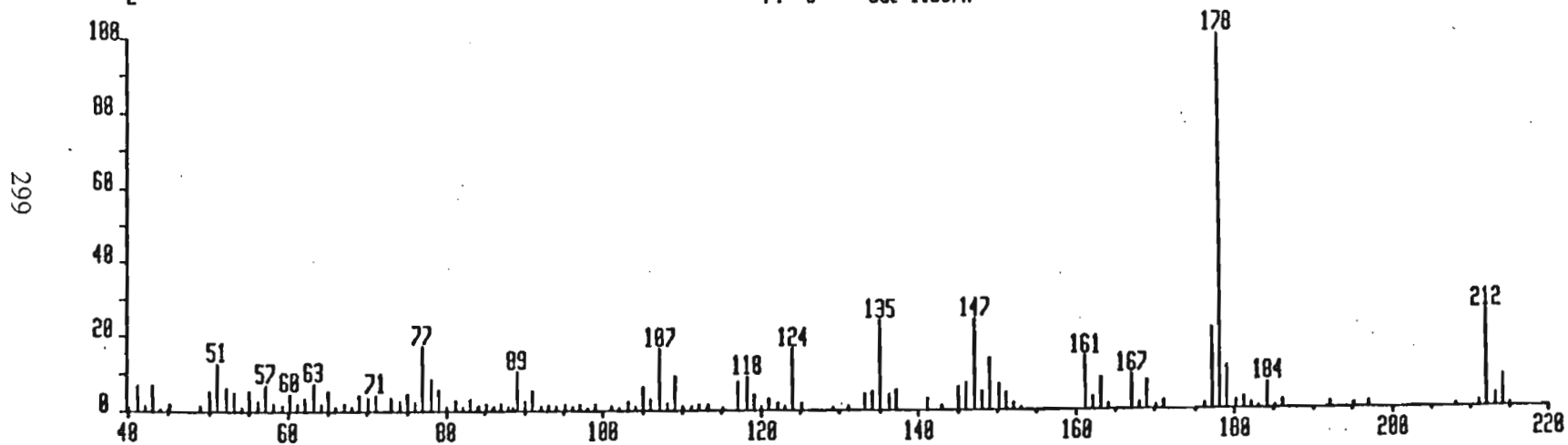
Spectrum 7d: ^{13}C NMR spectrum of [7]



Spectrum 7e: NOE spectrum of [7]

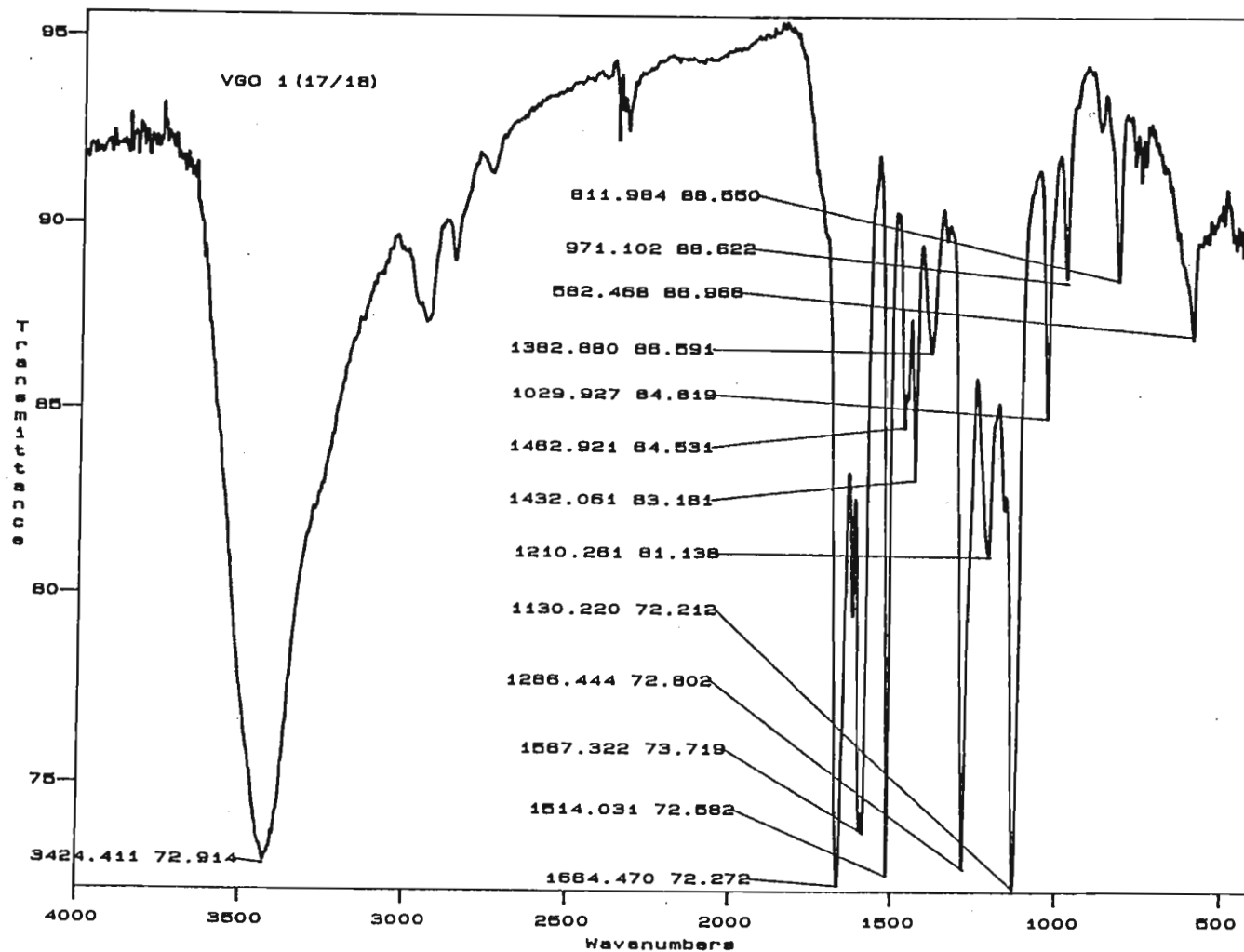
VG01011 x1 Bgd=1 12-OCT-97 14:49:08:01:44 70-250SEQ EI+
BpM=0 I=680nV Hn=0 TIC=28594000 Acnt: Sys:SYSTEMDEF
2 PT= 0° Cal:11097R

HMR: 4457800
MASS: 178

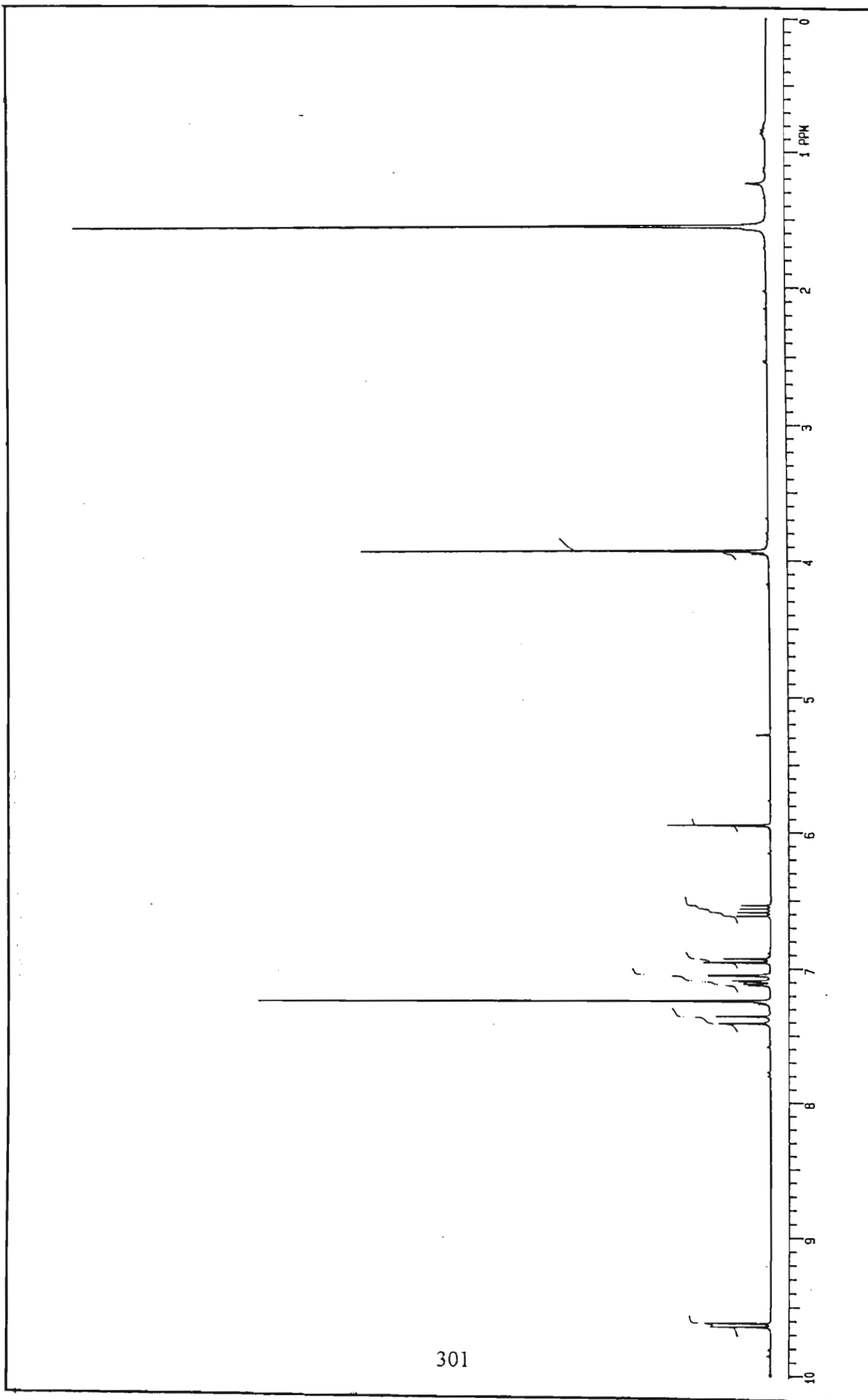


Spectrum 8a: Mass spectrum of [8]

300

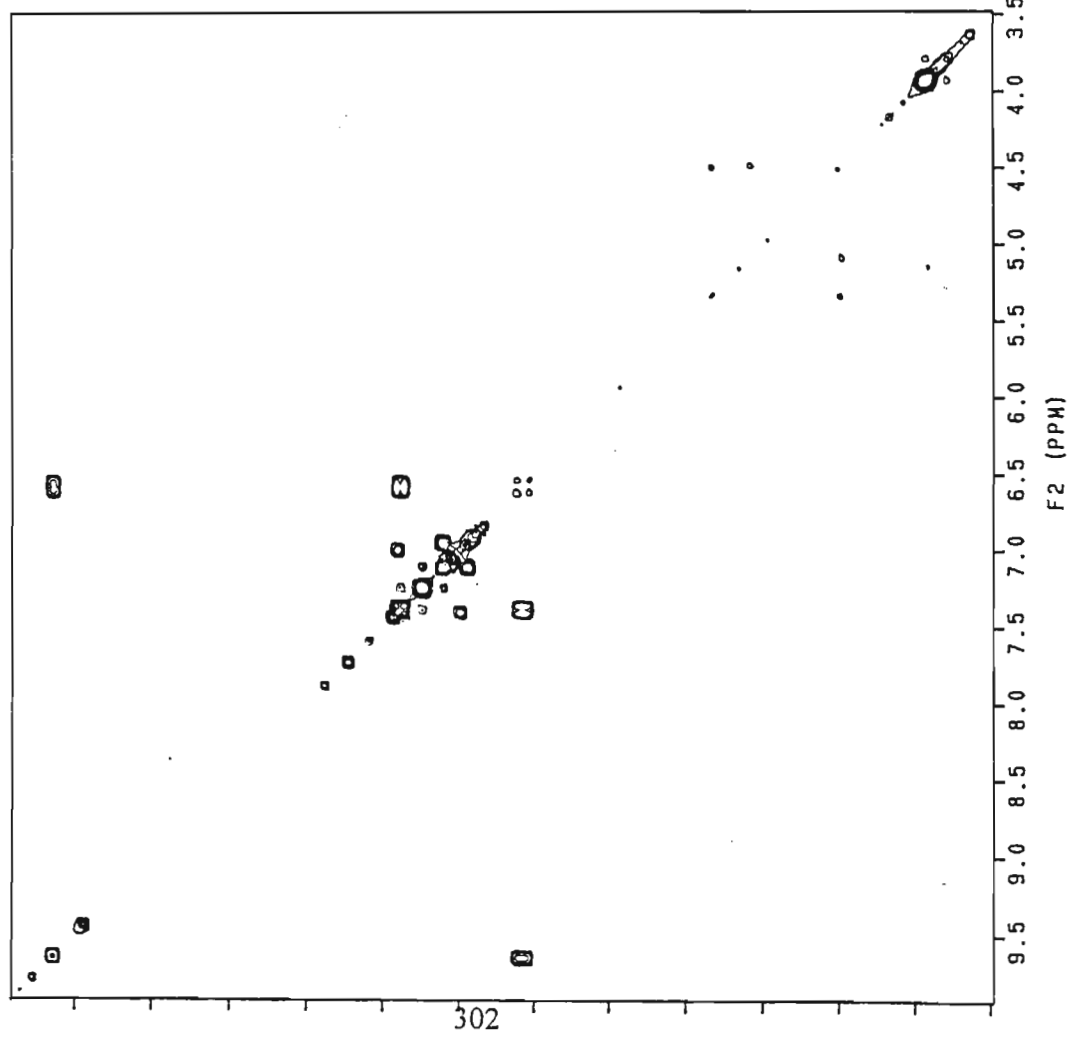
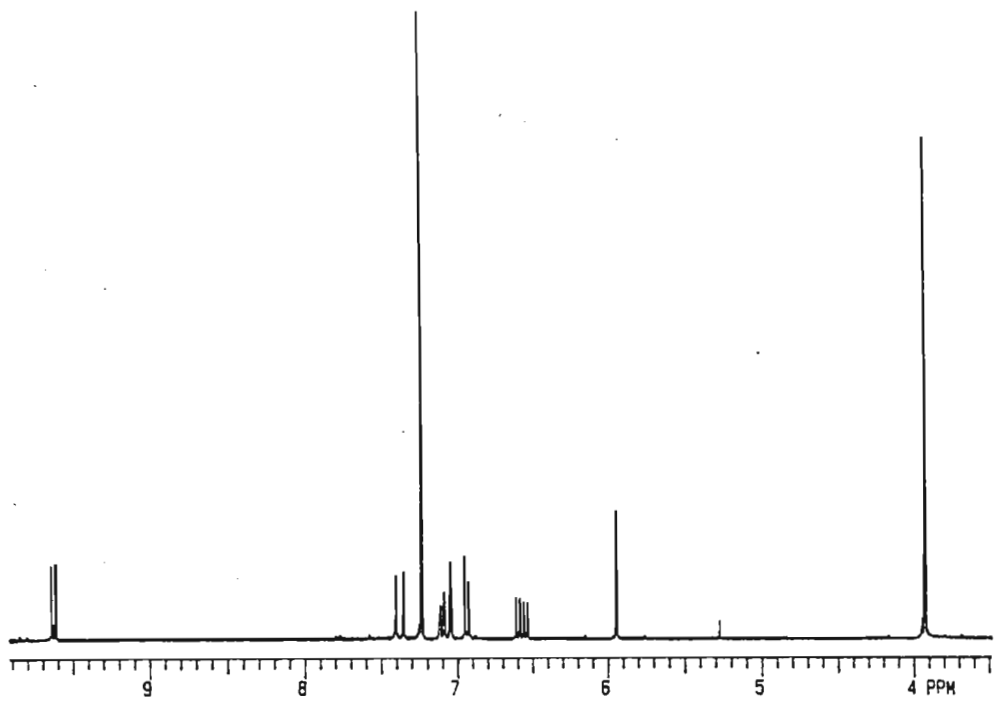


Spectrum 8b: Infrared spectrum of [8]

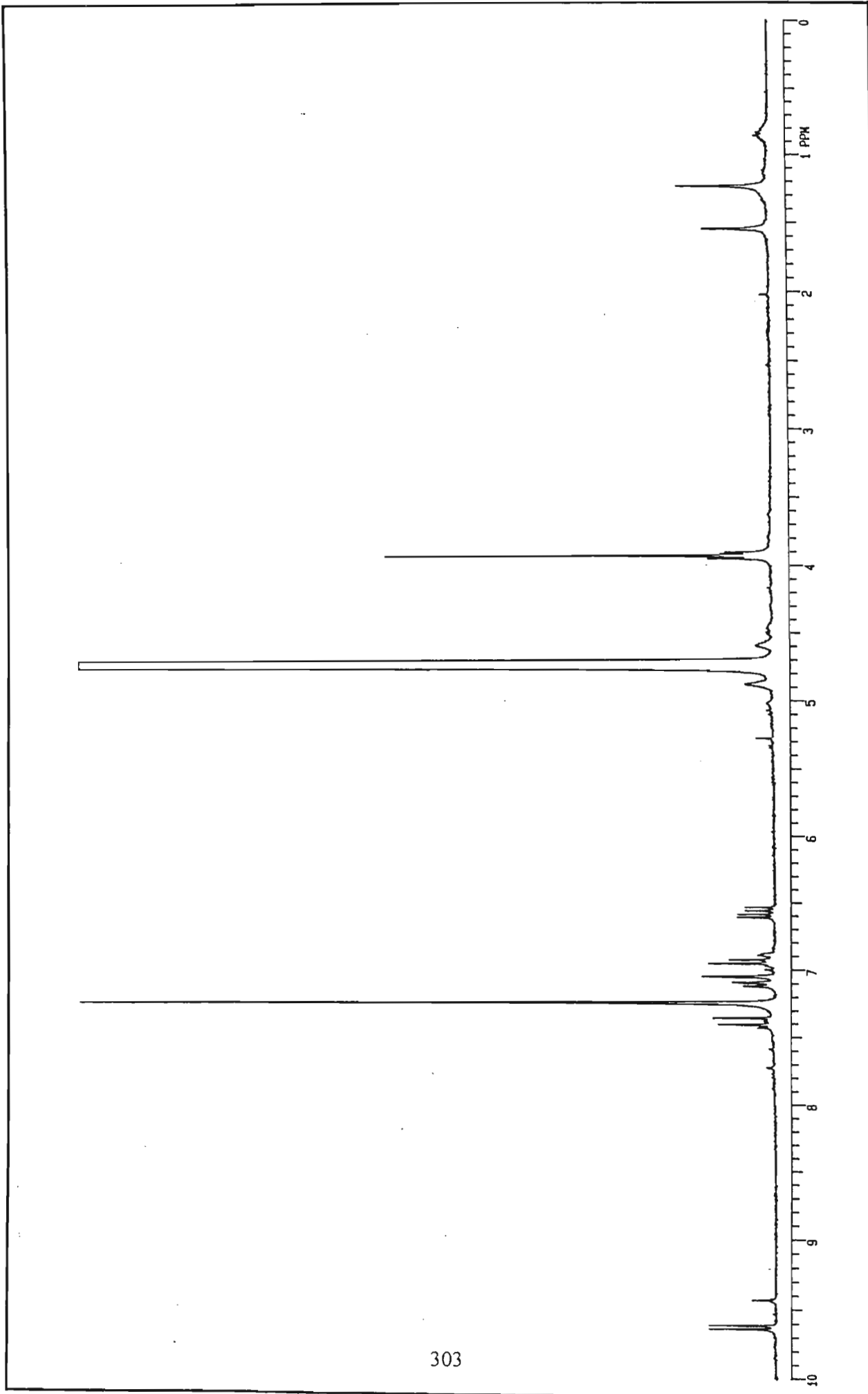


301

Spectrum 8c: ^1H NMR spectrum of [8]

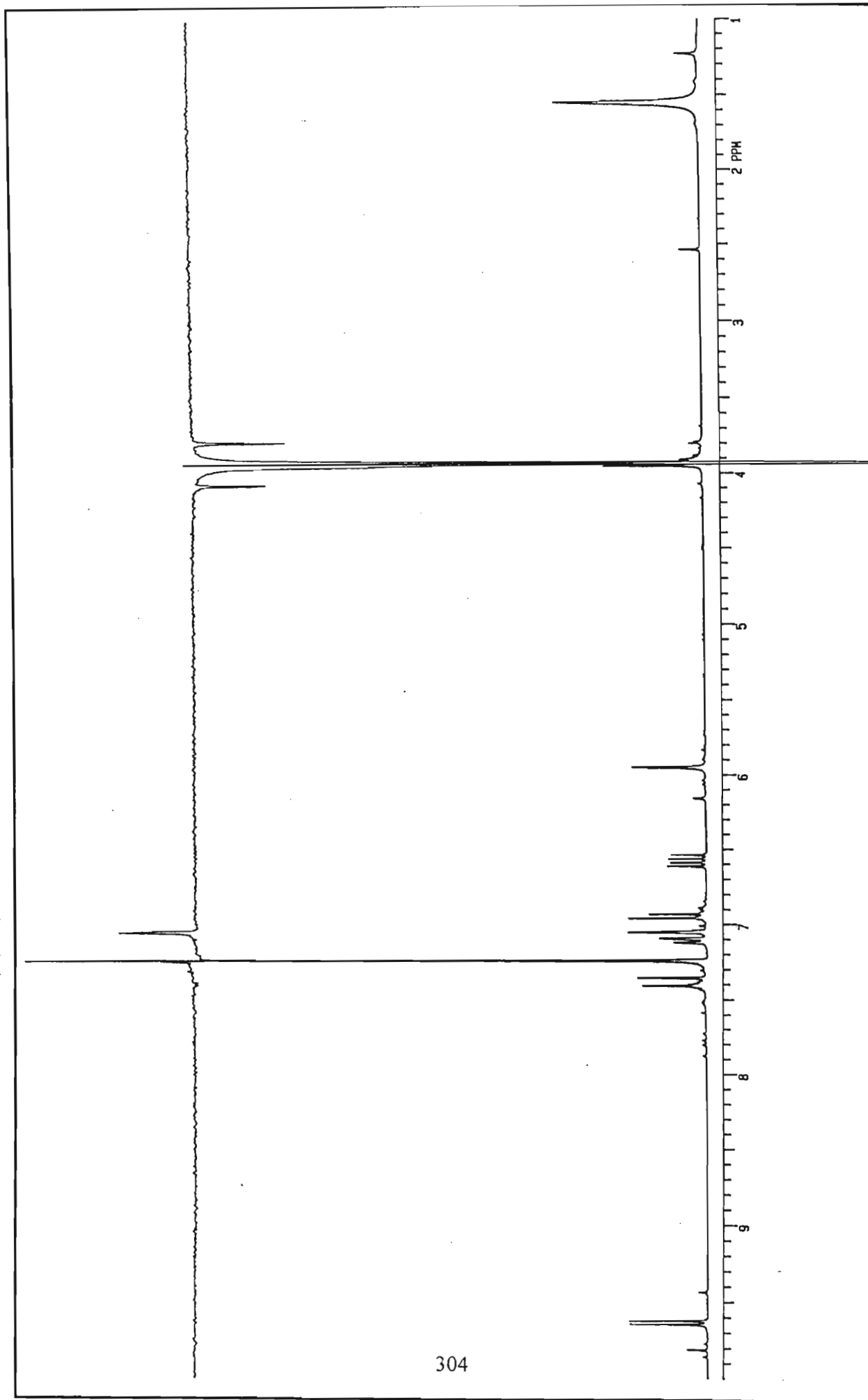


Spectrum 8d: COSY spectrum of [8]

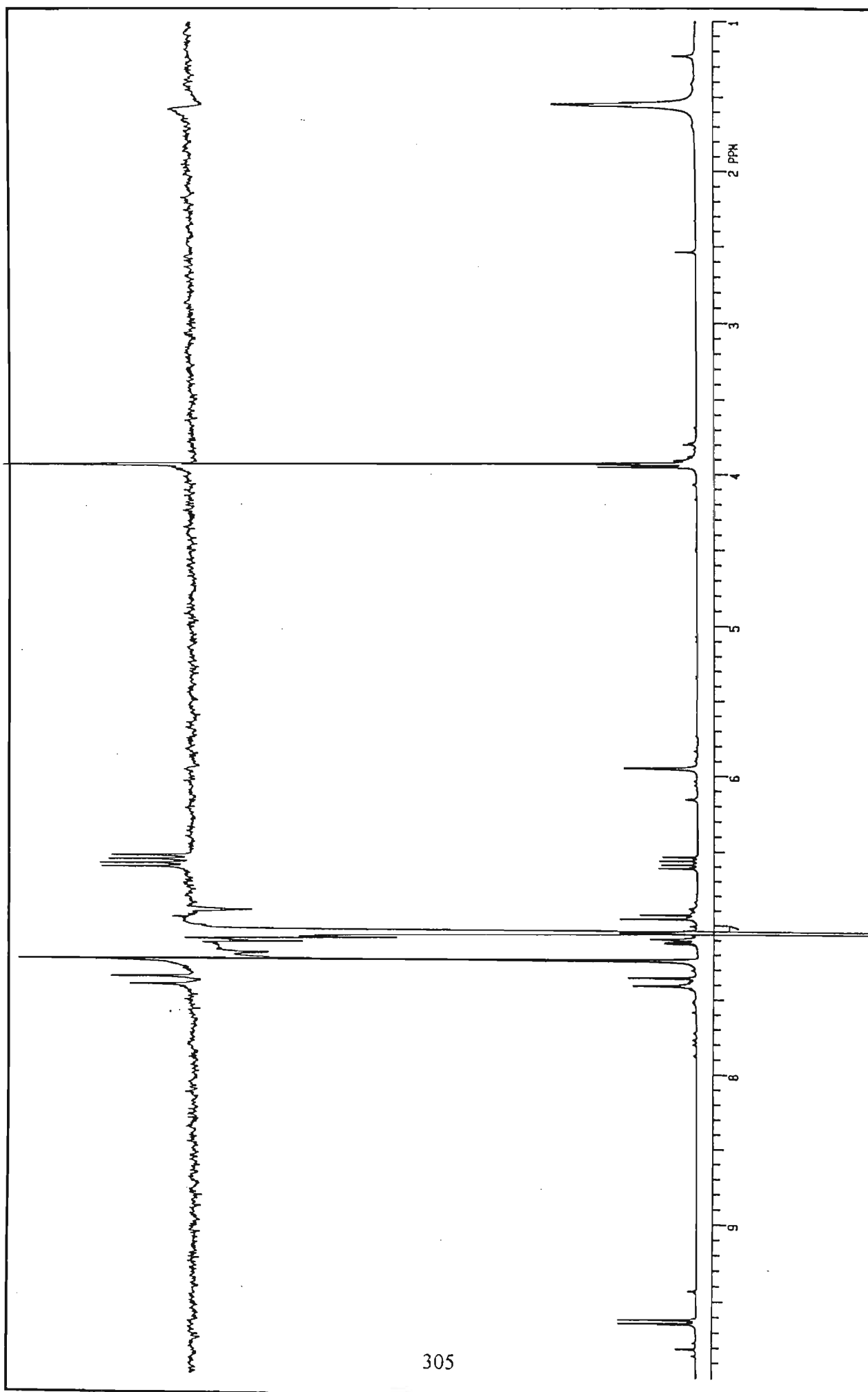


303

Spectrum 8e: ^1H NMR spectrum of [8] with D_2O



Spectrum 8f: NOE spectrum of [8] showing irradiation of methoxy protons



305

Spectrum 8g: NOE spectrum of [8] showing irradiation of H-2

VG020918#15 x1 Bpd=1 12-OCT-97 14:32:08.02:16 70-250SEQ EI+

BpM=0 I=392uv Ha=0 TIC=13130000

Acnt: Sys:SYSTEMDEF

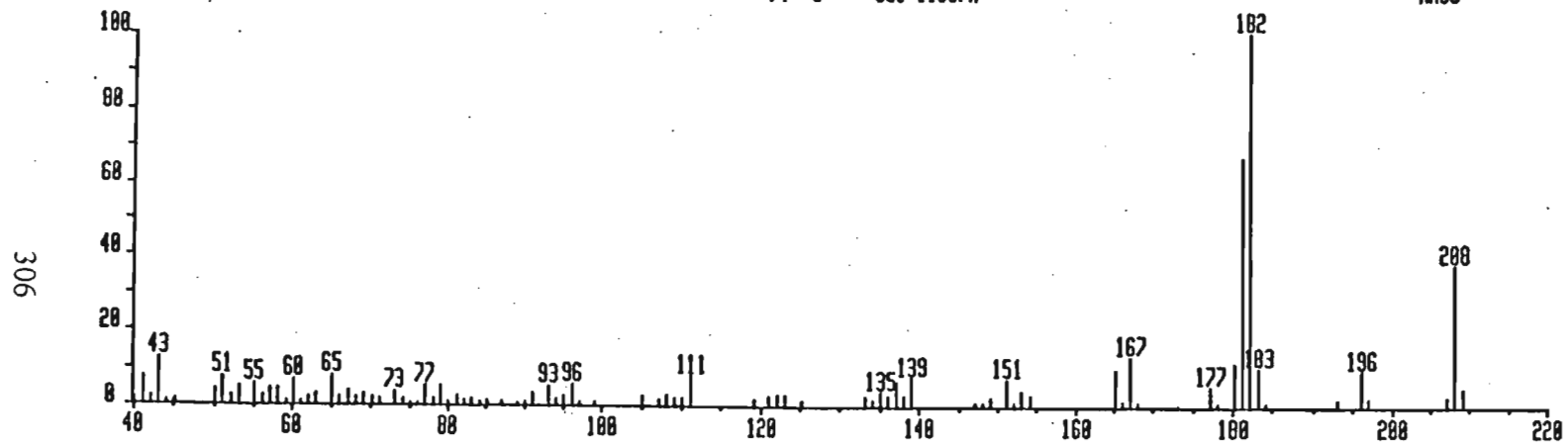
HMR: 2569000

2

PT= 0°

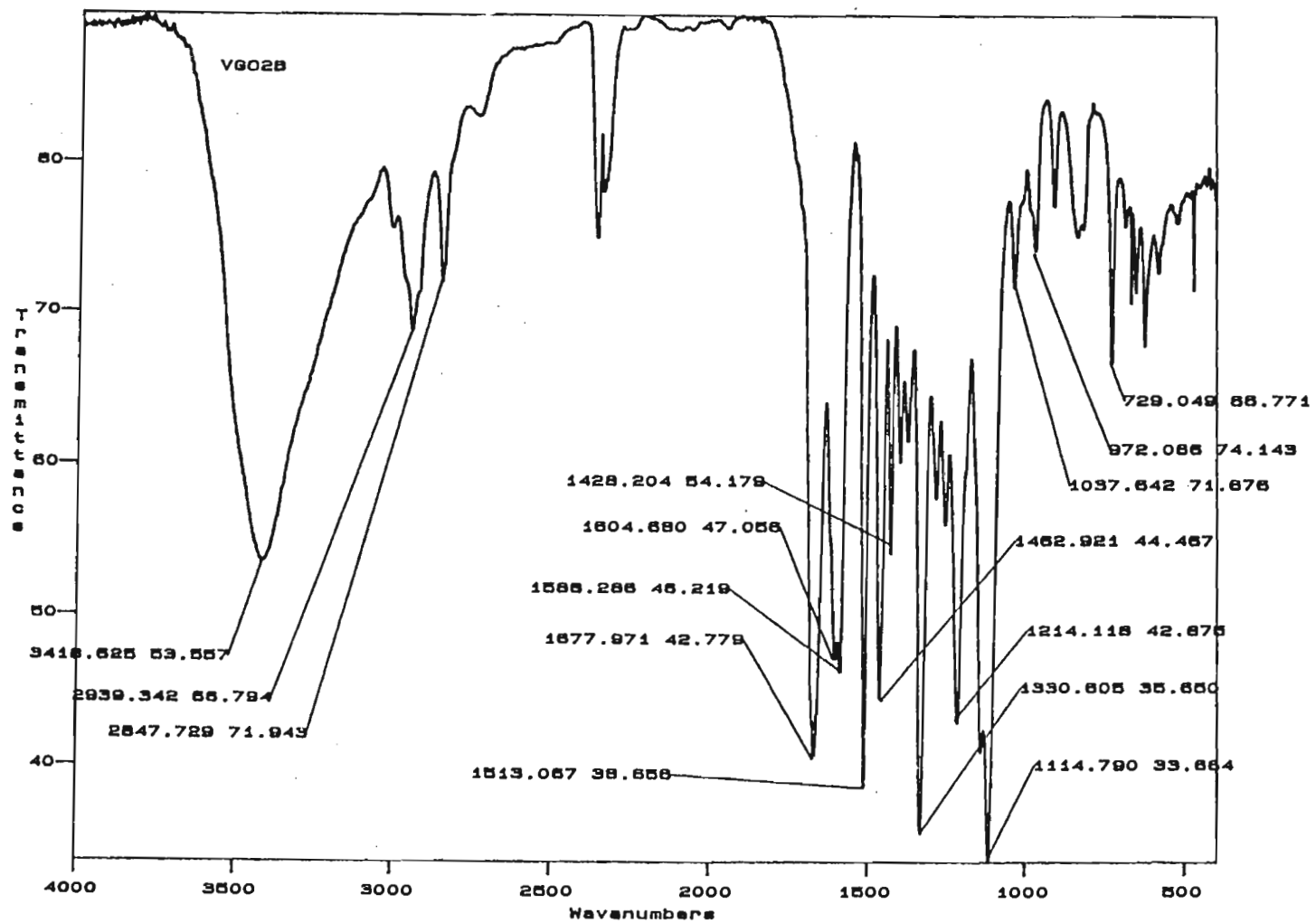
Cal:11097R

MASS: 182

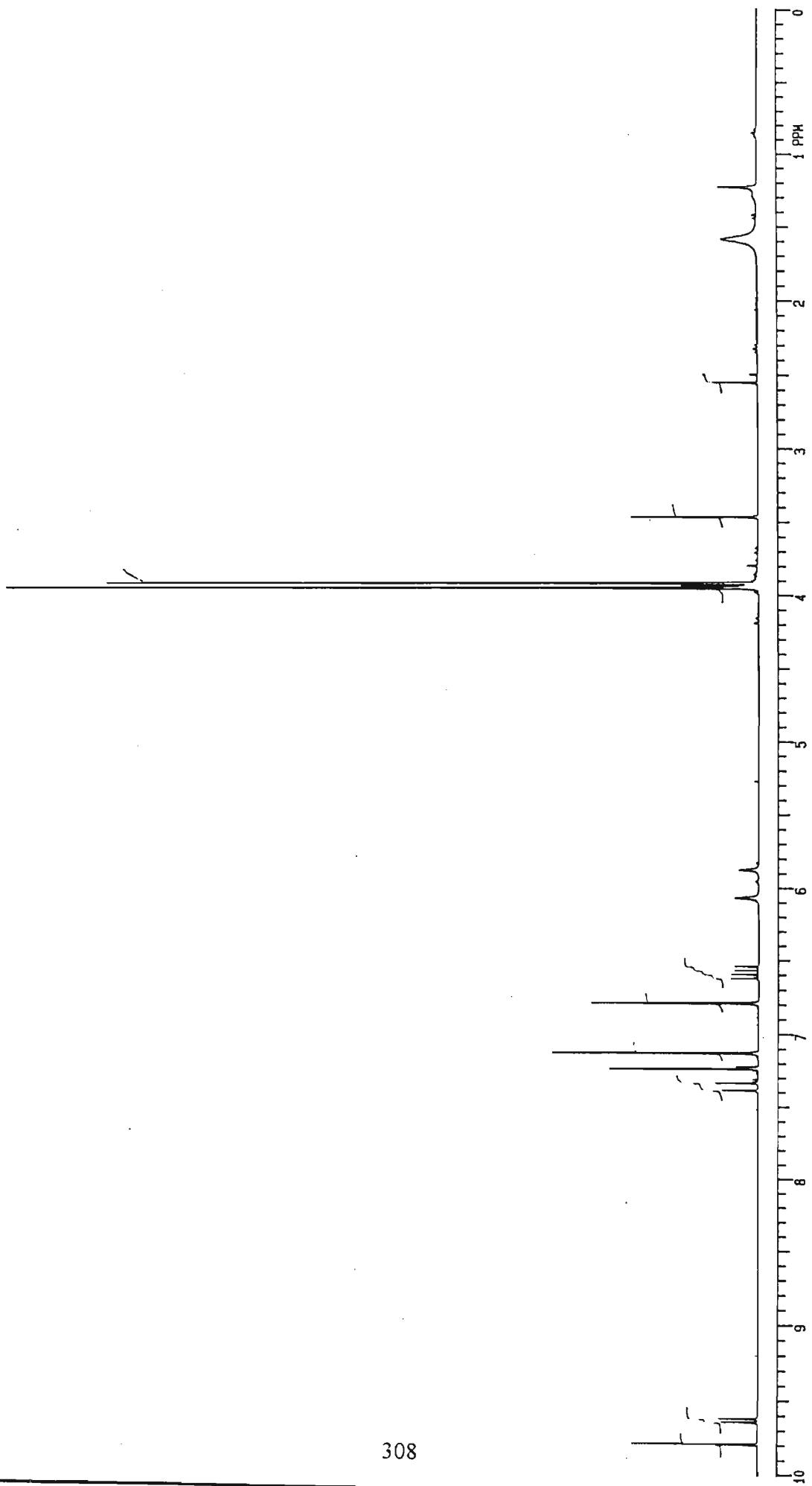


Spectrum 9a: Mass spectrum of [9]

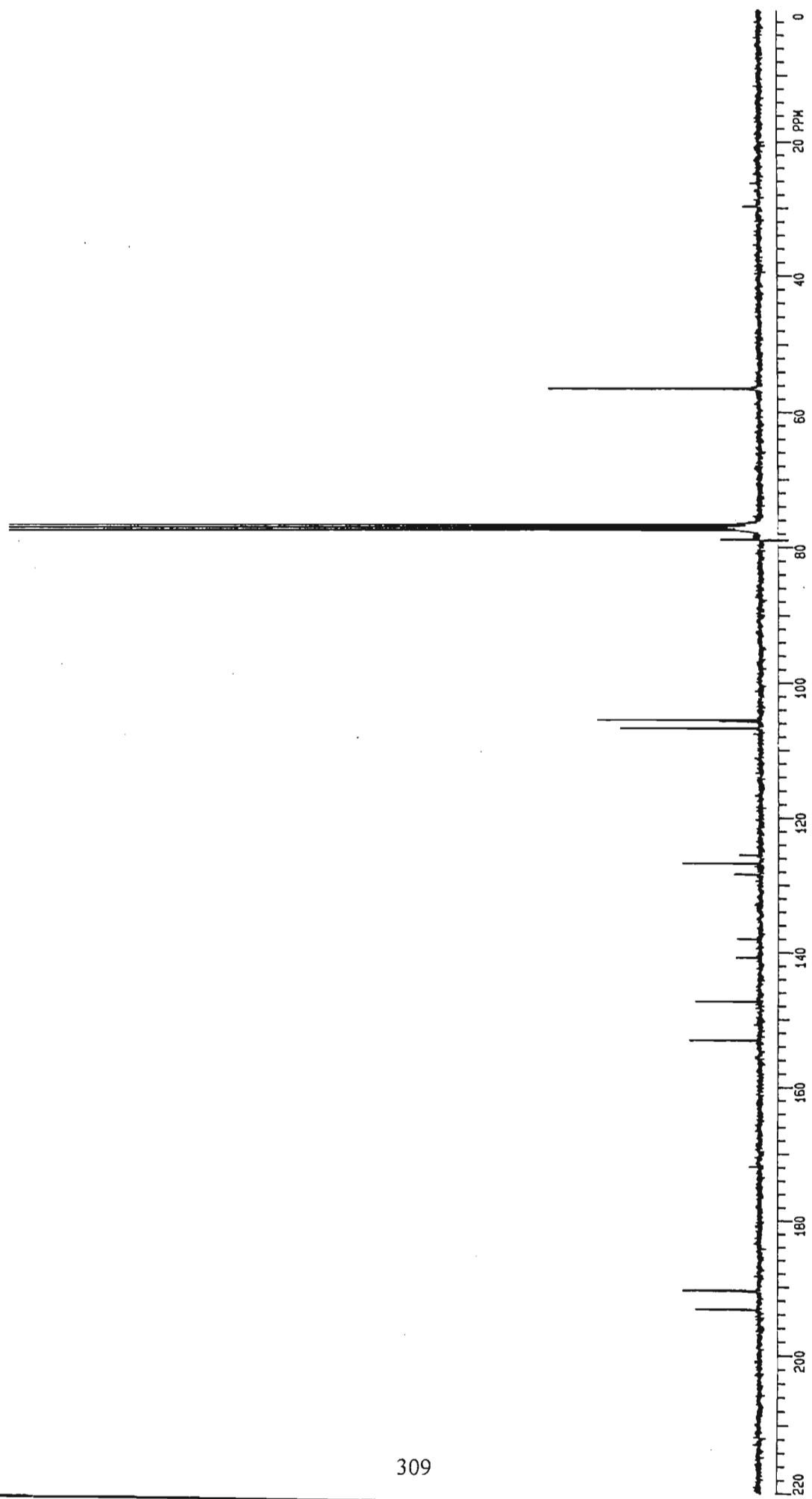
307

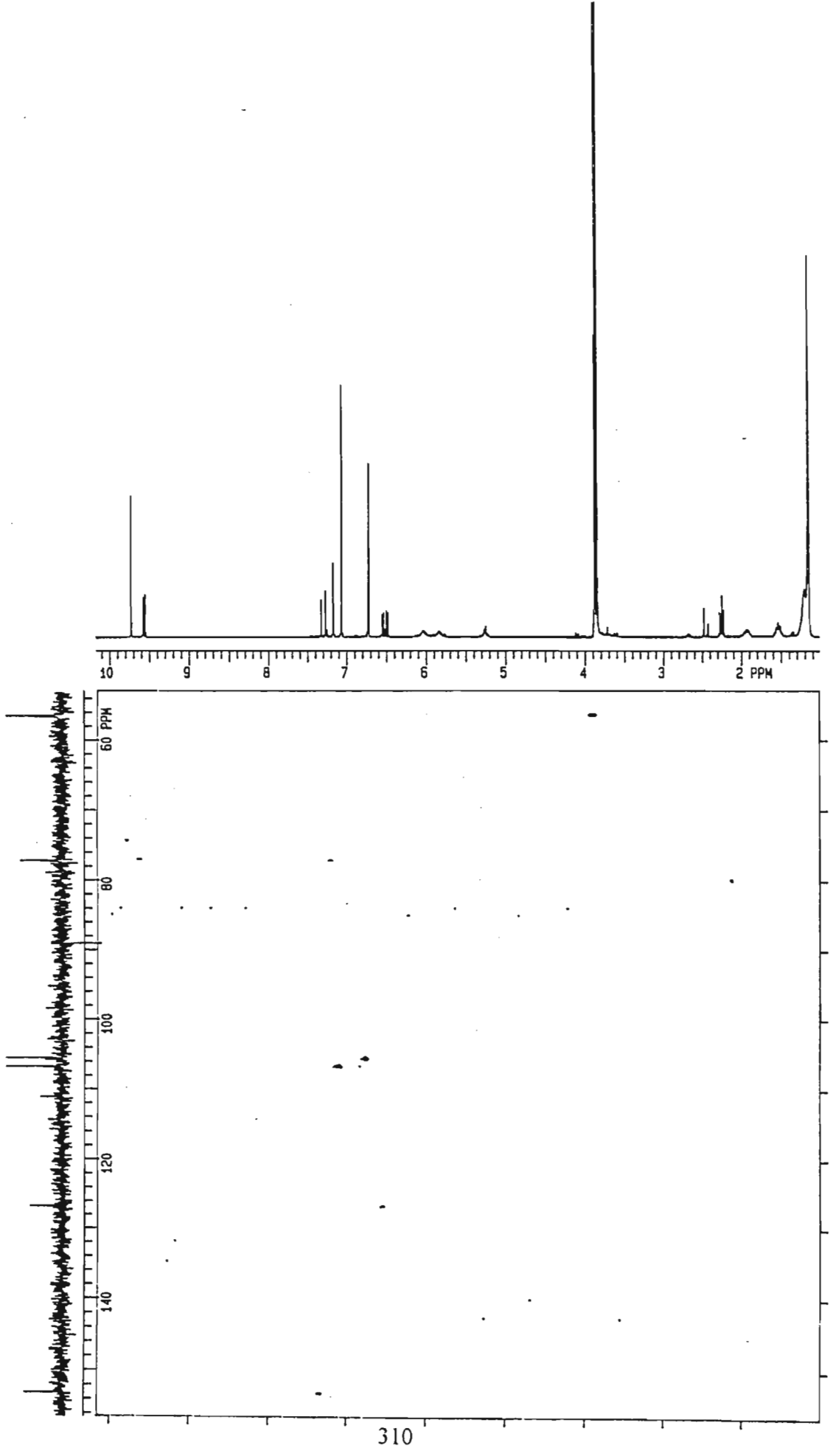


Spectrum 9b: Infrared spectrum of [9]

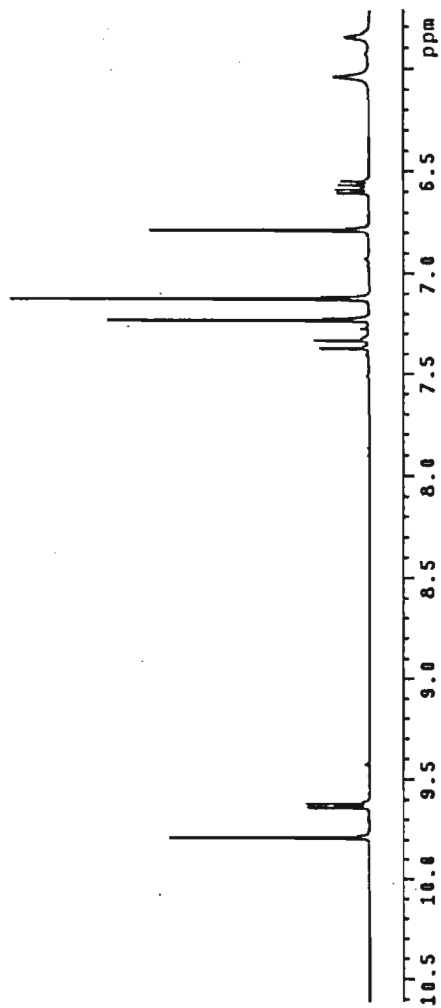
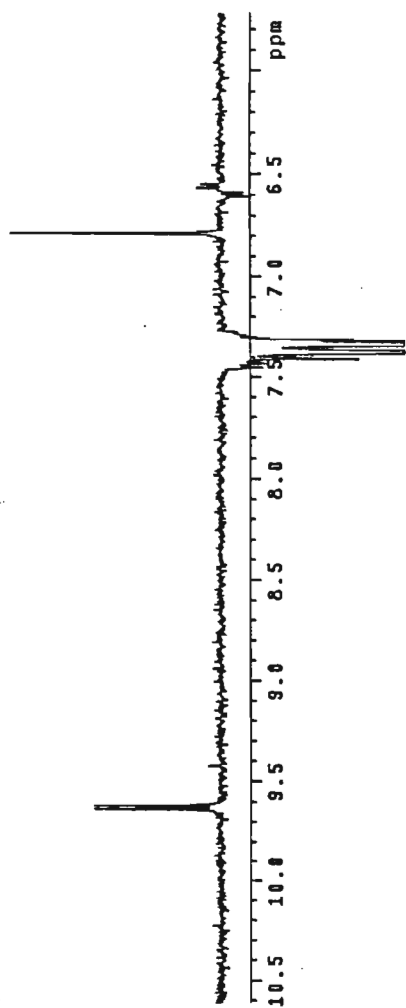


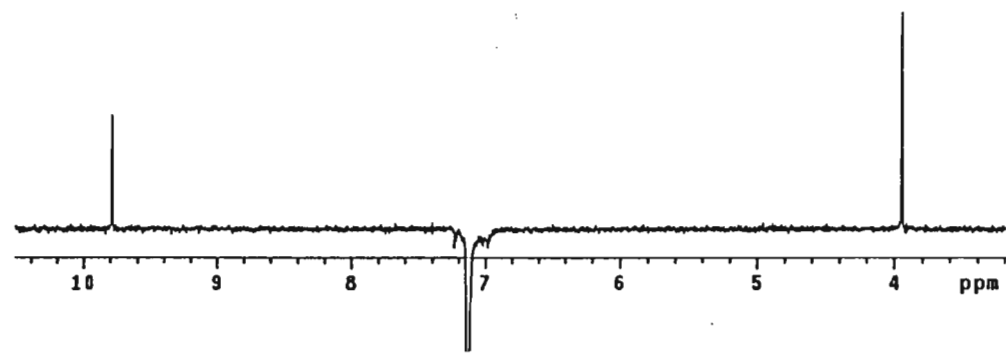
Spectrum 9c: ^1H NMR spectrum of [9]



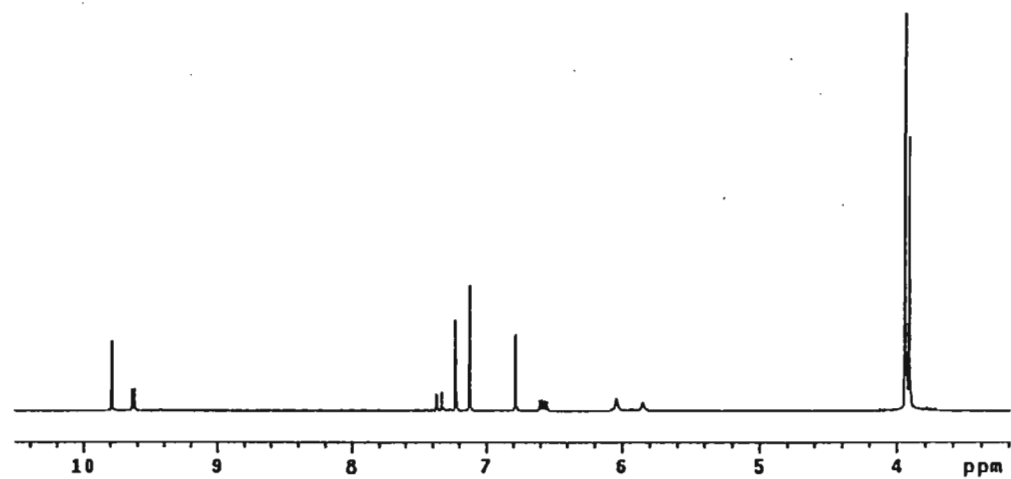


Spectrum 9e: HETCOR spectrum of [9]





312



Spectrum 9g: NOE spectrum of [9] showing irradiation of chemically equivalent H-3' and H-5'